Dopamine neurotoxicity, oxidative stress and schizophrenia - in vitro and in vivo studies of peroxisomal reactions to increased dopamine

Inauguraldissertation

zur Erlangung des Doktorgrades der Naturwissenschaften (Dr. rer. nat.) am Fachbereich Psychologie und Sportwissenschaften der Justus-Liebig-Universität Gießen

vorgelegt von Phillip Grant, Dipl. Psych., geb. am 07.05.1979 in Köln

1. Gutachter: Prof. Dr. Dr. Jürgen Hennig,

Abteilung für Differentielle Psychologie und Persönlichkeitsforschung, Fachbereich Psychologie und Sportwissenschaften, JLU Gießen

2. Gutachterin: Prof. Dr. Eveline Baumgart-Vogt,

Institut für Anatomie und Zellbiologie, AG Medizinische Zellbiologie, Fachbereich Humanmedizin, JLU Gießen

Gießen, im August 2011

„But who knows what she spoke to the darkness, alone, in the bitter watches of the night, when all her life seemed shrinking, and the walls of her bower closing in about her, a hutch to trammel some wild thing in?"

John Ronald Reuel Tolkien, The Return of the King

I dedicate this doctoral thesis to Marion Krey-Leiden, without whom I would have never ventured on the path that ultimately lead me to where and who I am today and therefore, inexorably, without whom this thesis would never have been written.

You are, without doubt, the best teacher I have ever had and certainly the one dearest to me. You were the first person ever to teach me about psychology in general and about schizophrenia in particular. But, most of all, you managed to inspire a young teenager to do things with his life he would never have even considered otherwise. Thank you! I will always remember you fondly.

Acknowledgements

My first thanks go out to Jürgen Hennig, not only for supervising my thesis, but also for having faith in me and my work for all these years. Out of all the people involved in my academic career I have known you the longest, and looking back I cannot ever think of a time when your ear was not open for me. You are genuinely interested in the ideas, innovations and achievements of your students and associates and are always interested in interdisciplinarity in all of its forms. Finally, I would like to thank you for being an excellent boss, who values the independence and self-reliance of the members of his team, but is always there whenever one feels the need for creative thought or input of any kind. Thank you; it's been fun and I'm sure it will continue to be fun!

I would also like to thank Eveline Baumgart-Vogt for giving me the possibility to learn a vast multitude of experimental methods and to gain experience and expertise in fields of research that are usually very uncommon for psychologists. I would also like to thank you for allowing me to gain an immense amount of anatomical knowledge not only through teaching me yourself (and I will never again forget the deep muscles of the neck), but even more so by allowing me to teach in a number of lectures, courses and seminars by myself. I thank you especially for the great independence you gave me both in my capacity as a lecturer and as a researcher. I am aware that the topics of my academic interest are slightly removed from your personal research questions, wherefore I am particularly indebted to you for allowing me the freedom to investigate these issues anyway.

Very special thanks go out to Robert Snipes, whom I consider a mentor, an academic father figure and most importantly a dear friend. Thank you for believing in me, supporting me when things got rough and for sometimes pushing me over those boundaries I would normally not have crossed and thereby showing me that the grass really can be greener on the other side. And most of all, thank you for calling me "one of the best anatomists they have", especially in a time when I had started to doubt myself and my justification for working as an anatomist altogether.

Thank you to Moni Wimmer for never wanting to learn that I am not really all that much into chocolate and instead always offering it (alongside some partly excruciatingly awful teas) as comfort food alongside very many valuable words of advice and

encouragement. Your door was always open for me and others in need a kind ear and reassuring words.

I thank Klaus-Peter Valerius for his help in perfusion and injection of the animals, especially the one that repeatedly bit me the one time I actually tried to inject it myself. I also thank you for your refreshing cynicism and your special humour and most of all for the many hours of discourse on the finer aspects of the workings of the human brain.

The latter thanks I would also like to extend to Wieland Stöckmann, Peter Langer and Hans-Rainer Duncker for helping me with those questions which were so crazy that only I could ask them and nobody apart from you could answer.

I would like to thank Barbara Ahlemeyer for her assistance in all matters cell cultural, not only for me personally, but also for the help supervising the work of Annika for her diploma thesis. But even more I would like to thank you for being one of the most kind-hearted persons I have ever met. You were always helpful and sincerely interested in aiding all those around you, while at the same time allowing others to help you in return. This always gave me a feeling of being accepted as a peer, even though your academic standing is far higher than that of most of the people around you.

To Bianca Heß/Petterson/Pfeiffer I only say on thing, which means more than all other things I could say: The dream of the “C4-TA” will never die!

I thank Andrea Klein/Textor for being a good friend and colleague and especially for saying those things that I very often did not want to, but definitely had to hear.

To Magdalena Gottwald for taking in a young guy “from the street” and teaching him the basis of what then became this magnum opus, even though you never did show me the humid chamber in the cellar where all the spiders live.

Elke Richter I thank for her enthusiasm and her willingness to help wherever and whenever she could as well as her (at least in Hessen) exceptional command of the German language… may these qualities in you never go “sur neige”.

Thank you Gaby Thiele for always smiling, always being friendly, always being helpful and for always making one feel liked, even in the tensest of situations… you have a true gift.

I offer my thanks to Susanne Pfreimer and Tamara Papadakis for taking me with them on the long and difficult journey to silver-colored ultracryo-sections. I wish we could have continued on that path a lot longer.

My thanks also go out to Elke Rodenberg-Frank for performing the IHC-stainings with nickel-enhacement and introducing this method to the group.

Apart from being the right hand of the boss in all administrative issues and being an excellent secretary and always performing her job with a friendly smile, I thank Silvia Heller for being not only a dear colleague, but also a true friend. You were always someone I could come to with my worries and you showed great faith in my person by confiding some of your own personal worries in me.

This thesis would not be complete without the individual work of Annika Fischer, whom I had the great fortune of supervising during her undergraduate research. I am very thankful to you and exceptionally proud of the work you did and the final result you achieved in your diploma thesis. Alongside her I would also like to thank Ingra Weßel, Timm Tristan Berg, Eva Hesselbach and Anca Nenicu for donating specimen samples of their own individual work for my big Pex14p-marathon as well as Klaus Kuchelmeister for the donation of human brain samples.

I would also like to thank all other colleagues at the Institute of Anatomy and Cell Biology for the time we spent together. Additionally, I thank all of my new colleagues from the Department of Differential Psychology and Personality Research for making me feel more than welcome and integrating me into their team the way they did.

Last, but proverbially all but least, I would like to thank my family and friends, for just about everything they have done to help me during the time they have shared my life; especially my parents and their spouses, my grandparents and of course Kim. You were always there when I needed you most and you let me be there for you, when you needed me. Thank you for sharing my life, marrying me and for being who you are. I love you with all my heart! Please don't change… except of course for the things about you I find annoying ☺

Table of contents

Page

Acknowledgements

Table of contents

Abbreviations

Abstract

1. Introduction **1**

1.1 Schizophrenia 1

1.1.1: Epidemiology and societal consequences 1

1.1.2: Signs and symptoms 3

1.1.3: Diagnostic guidelines 4

1.1.4: Neurodegeneration in schizophrenia 6

1.1.5: Proposed causes of schizophrenia 7

1.1.5.1 Genetic risk factors 7

1.1.5.2 Environmental risk factors 10

1.1.5.3 Neurochemical mechanisms 13

1.2 Reactive oxygen species and antioxidant defense systems 19

1.2.1 Oxygen chemistry, radicals and reactive oxygen species formation 19

1.2.2 Antioxidant defense mechanisms and oxidative stress 23

1.2.3 Pro- and antioxidant metabolism in the brain 27

1.3 Dopamine - Metabolism, transmission and neurotoxicity 30

1.3.1 Dopamine metabolism - synthesis and degradation 30

1.3.2 The dopaminergic synapse 32

1.3.3 Dopaminergic pathways in the mammalian brain 34

1.3.4 The mesolimbic dopamine pathways - Specific motivation and Incentive Salience 35

1.3.5 The dopamine hypothesis of schizophrenia 37

1.3.6 Dopamine neurotoxicity and dopamine induced oxidative stress 41

1.3.7 Oxidative stress in schizophrenia 43

1.3.7.1 NMDAR blockage leads to an increase in mesolimbic dopamine release 44
1.3.7.2 Oxidative stress in pharmacological models of schizophrenia using NMDAR-antagonists 46

1.4 Peroxisomes 48
1.4.1 Peroxisomal ontogeny 48
1.4.2 Peroxisomal metabolism 51
1.4.3 Peroxisomes in the nervous system 55
1.4.4 Peroxisomal disorders 60
1.4.5 Problems in labeling peroxisomes 61

1.5 Aims and schematic overview 65

2. Materials and Methods 67
2.1 Animal treatment with MK-801 67

2.2 Tissue preparation for morphological methods 68
2.2.1 Tissue acquirement 68
2.2.1.1 Mouse tissue 68
2.2.1.2 Rat tissue (liver) 68
2.2.1.3 Cat and Sacred Baboon 68
2.2.1.4 Human tissue 68
2.2.2 Embedding and processing for light and fluorescence microscopy 69
2.2.3 Embedding and processing for electron microscopy 69

2.3 Cell culture 69
2.3.1 Mixed primary murine neuronal cultures 69
2.3.1.1 Preparation of primary neuronal cultures of the medial neocortex of newborn mice 69
2.3.1.2 Peroxisome proliferator (ciprofibrate) treatment of primary neuronal cultures 70

2.3.1.3 Dopamine and haloperidol treatment of murine primary neuronal cultures 70
2.3.2 Primary astrocytes cultures 70
2.3.2.1 Preparation of primary astrocyte cultures of the neocortex of newborn mice 70
2.3.2.2 Dopamine treatment of murine primary astrocyte culture 70
2.3.3 Mouse and human hepatoma cells 70

2.4 Morphological staining techniques 71
2.4.1 Histological staining 71
2.4.1.1 Modified Kluver-Barrera staining 71
2.4.1.2 Sudan Black B (SBB) staining 71
2.4.2 Indirect Immunohistochemistry (IHC), Immunofluorescence (IF) and ImmunoGoldLabeling (IGL) 71
2.4.2.1 IHC on paraffin-embedded tissue sections 71
2.4.2.2 IF on paraffin-embedded tissue sections 71
2.4.2.3 Multiplex IF on human and murine brain tissue sections 72
2.4.2.4 Multiplex IF on murine primary neuronal and astrocyte cultures 72
2.4.2.5 IF using QuantumDots® on mouse and human hepatoma cells 72
2.4.2.6 IGL for electron microscopy 72

2.5 Reverse transcription polymerase chain reaction (RT-PCR) 72
2.5.1 RNA extraction protocols 73
2.5.1.1 RNA extraction from animal tissues 73
2.5.1.2 RNA extraction from primary murine astrocyte cultures 73
2.5.1.3 RNA extraction from animal whole blood 73
2.5.2 RNA denaturation, quantification and quality control 73
2.5.2.1 DNase digestion 73
2.5.3 First Strand Synthesis (FSS) 74
2.5.4 Primer Design 74
2.5.5 Polymerase Chain Reaction (PCR) 75

2.5.5.1 Nested PCR 75
2.5.5.2 Agarose-Gel Electrophoresis 75

2.6 Imaging 76

2.7 Statistical Analyses 76

3. Results 77
3.1 Establishing Pex14p as the optimal peroxisomal marker for comparative and experimental morphology 77
3.1.1 Specificity of the self-created antibodies against catalase and Pex14p 77
3.1.2 Specificity of secondary antibodies and peroxidase substrate reaction 79
3.1.3 Peroxisomes in epithelial cells of mesodermic and endodermic origin 80
3.1.3.1 Kidney 81
3.1.3.2 Endocrine pancreas 83
3.1.3.3 Exocrine cells of mouse pancreas and submandibular gland 83
3.1.3.4 Exocrine cells of the human submandibular gland 85
3.1.3.5 Duodenum 86
3.1.4 Follicular development in the ovary 87
3.1.5 Steroid hormone producing cells 91
3.1.5.1 Ovary and testis 92
3.1.5.2 Adrenal cortex 93
3.1.6 Peroxisomes in cells originating from the neural tube and crest 94
3.1.6.1 Adrenal medulla 94
3.1.6.2 Primary neurons before and after treatment with a peroxisome proliferator 94
3.1.6.3 Peroxisomes in the human brain 95
3.1.6.4 Overview of the microscopic anatomy of the human hippocampal formation 99
3.1.7 Labeling of peroxisomes with QuantomDots (QDots®) 102

3.2 Analyzing peroxisomal reactions to increased dopamine 103
3.2.1 Morphological analyses of Pex14p and catalase in the hippocampus of schizophrenic patients vs. controls 103
3.2.2 Effects of increased dopamine and haloperidol on primary murine neuronal cultures 104
3.2.3 Effects of increased dopamine on primary murine astrocyte cultures 107
3.2.3.1 Morphological analyses 108
3.2.3.2 Analyses of gene expressions 110
3.2.4 Effects of MK-801-treatment in male pubescent C57Bl/6J mice 114
3.2.4.1 Analyses of gene expressions 115
3.2.4.2 Morphological analyses 120

4. Discussion, summary and conclusions 125
4.1 Peroxisomal localization with Pex14p as a novel marker protein 125

4.2 Dopamine neurotoxicity, schizophrenia and peroxisomal metabolism 131
4.2.1 Effects of dopamine treatment on primary murine neuronal and astrocyte cultures 131
4.2.2 Effects of treatment of male pubescent C57Bl/6J-mice with the NMDAR-antagonist MK-801 138

4.3 Summary, conclusions and implications for further research 143
4.3.1 Implications for further research 145

5. References 147
5.1 Figure references 164
5.3 Online references 165

Appendix A - Materials and methods: Detailed descriptions I
A.1 Cell culture I
A.1.1 Mixed primary murine neuronal cultures I
A.1.2 Primary astrocytes cultures I

A.2 Morphological staining techniques II
A.2.1 Histological staining II
A.2.1.1 Modified Kluver-Barrera staining II
A.2.2 Indirect Immunohistochemistry (IHC), Immunofluorescence (IF) and ImmunoGoldLabeling (IGL) III
A.2.2.1 Principle of indirect immunolabeling III
A.2.2.2 IHC on paraffin-embedded tissue sections VII
A.2.2.3 Multiplex IF on human and murine brain tissue sections VII
A.2.2.4 Multiplex IF on murine primary neuronal and astrocyte cultures VIII
A.2.2.5 IF using QuantumDots® on mouse and human hepatoma cells VIII
A.2.2.6 IGL for electron microscopy IX

A.3 Reverse transcription polymerase chain reaction (RT-PCR) X
A.3.1 Pinciple of RT-PCR X
A.3.2 RNA extraction protocols XIV
A.3.2.1 RNA extraction from animal tissues XIV
A.3.2.2 RNA extraction from animal whole blood XIV
A.3.3 RNA denaturation, quantification and quality control XV
A.3.3.1 DNase digestion XVI
A.3.4 First Strand Synthesis (FSS) with SuperScriptTM II reverse transcriptase XVI
A.3.5 Polymerase Chain Reaction (PCR) XVII
A.3.5.1 Agarose-Gel Electrophoresis XVII

Appendix B - Recipes and Primers **XVIII**
B.1 Recipes XVIII
B.2 Primers XXIV

Abbreviations

‘	minute
‘’	second
18S rRNA	ribosomal ribonucleic acid, small component (*Eukaryotae*)
28S rDNA	gene encoding for ribosomal ribonucleic acid, large component, 28S (*Mus musculus*)
28S rRNA	ribosomal ribonucleic acid, large component (*Eukaryotae*)
3-MT	3-methoxytyramine
3NP	3-nitropropionic acid
4-HNE	4-hydroxynonenal, aka HNE
5-HT	5-hydroxytryptamine, aka serotonin
5-HT_{2A}	5-hydroxytryptamine receptor 2A, aka serotonin receptor 2A
5-HTT	5-hydroxytryptamine transporter, aka serotonin transporter, solute carrier family 6, member 4
A	adenine
AAI	aqua ad iniectabilia
ABC	avidin-biotin complex
ABCD1	ATP-binding cassette sub-family D member 3, aka ALDP
ABCD2	ATP-binding cassette sub-family D member 2
ABCD3	(gene encoding for) ATP-binding cassette sub-family D member 3, aka PMP70
AC	adenyl cyclase
AD	aldehyde dehydrogenase
ADP	adenosine diphosphate
ALDP	adrenoleukodystrophy protein, aka ABCD1
AMPA	2-amino-3-(5-methyl-3-oxo-1,2- oxazol-4-yl)propanoic acid
AMV	avian myeloblastosis virus
AOE	antioxidant enzyme
APA	American Psychiatric Association
APOE	gene encoding for apolipoprotein E (*Homo sapiens*)
ARE	antioxidant response element

ATP	adenosine triphosphate
ATPase	adenosine triphosphatase
BAS	behavioural activation system
β-ME	β-mercaptoethanol
BioBPS	Bio Gene Portal System (biogps.org)
BLAST	basic local alignment search tool
bp	base pair
BSA	bovine serum albumin
BSA-c	bovine serum albumine, negatively charged acetylated (Aurion)
C	cytosine
C57Bl/6J	C57 black 6J inbred mouse strain, aka black 6 inbred mouse strain
CA(1-4)	Cornu ammonis, aka Amun's horn (sector 1-4)
CaM kinase	calcium/calmodulin dependent kinase
cAMP	cyclic adenosine monophosphate
CAT	(gene encoding for) catalase (*Homo sapiens, Mus musculus*)
cDNA	complementary (to mRNA) deoxyribonucleic acid, single stranded
CGL	Corpus geniculatum laterale, aka lateral geniculate body
CNS	central nervous system
C*O*MT	catechol-*O*-methyl transferase
COMT	gene encoding for catechol-*O*-methyl transferase (*Homo sapiens, Mus musculus*)
CRE	cAMP response element
CREB	cAMP response element binding protein
CSF	liquor cerebrospinalis, aka cerebrospinal fluid
CuZnSOD	copper and zinc-containing superoxide dismutase, two isozymes SOD1 and SOD3
D	specific hydrogen peroxide detoxification constant
DAAO	(gene encoding for) D-amino acid oxidase (*Homo sapiens, Mus musculus*)
DAB	3,3'-diaminobenzidine
DALY	disability-adjusted life years
DAO	gene encoding for D-amino acid oxidase (*Homo sapiens, Mus musculus*)

D-AspOx	D-aspartate oxidase
DAT	(gene encoding for) dopamine active transporter, aka solute carrier family 6, member 3 (SLC6A3), neurotransmitter dopamine
DBH	(gene encoding for) dopamine-β-hydroxylase
DDC	(gene encoding for) DOPA-decarboxylase
DG	Gyrus dentatus, aka dentate gyrus
DLP	dynamin-like guanosine triphosphatase
DMEM	Dulbecco's modified Eagle's medium
DNA	deoxyribonucleic acid
DNase	deoxyribonuclease
DNMT	DNA methyltransferase, aka DNA MTase
DNPH	2,4-dinitrophenylhydrazine
dNTP	deoxyribonucleotide triphosphate
DOPA	3,4-dihydroxyphenylanlanine, aka L-DOPA
DOPAC	3,4-dihydrophenyl acetic acid
DRD1-DRD5	genes encoding for dopamine receptors D_1-D_5 (*Homo sapiens, Mus musculus*)
DSM-IV-TR	Diagnostic and Statistical Manual of Mental Disorders, 4th Edition, Text Revision
DSM-V	Diagnostic and Statistical Manual of Mental Disorders, 5th Edition
dT	thymidine
DTNBP1	gene encoding for dystrobrevin binding protein 1 (*Homo sapiens*)
DTT	dithiothreitol, aka Cleland's reagent
e^-	electron
EDTA	ethylenediaminetetraacetic acid
ELISA	enzyme linked immunosorbent assay
EM	electron microscopy/microscope
eNOS	endothelial nitric oxide synthase
EPSP	excitatory postsynaptic potential
ER	endoplasmic reticulum
EtBr	ethidium bromide
F20	schizophrenia

Fab (domain)	immunoglobin fragment, antigen binding
FBS	fetal bovine serum
Fc (domain)	immunoglobin fragment, crystallizable
FCS	fetal calf serum
FFPE	formalin-fixed paraffin-embedded
fig.	figure
fis1	fission 1 protein
FSS	first strand synthesis, aka reverse transcription
g	acceleration, 9.80665 m/s^2
g	gram
G	gauge, outer hypodermic needle diameter
G	guanine
GABA	gamma-aminobutyric acid
GABRB2	gene encoding for gamma-aminobutyric acid A receptor, beta 2 (*Homo sapiens*)
GAPDH	glyceraldehyde 3-phosphate dehydrogenase
GDA	glutardialdehyde
GFAP	(gene encoding for) glial fibrillary acidic protein
GOE	great oxygenation event
GPx	glutathione peroxidase
GR	glutathione reductase
GRIN2B	gene encoding for glutamate receptor, ionotropic, N-methyl-D-aspartate 2B (*Homo sapiens*)
GSH	glutathione
GSSG	glutathione disulfide
GWAS	genome-wide association study
GxE	gene X environment
HBSS	Hank's balanced salt solution
HBV	hepatitis B virus
HDA	helicase dependent amplification

Hepa 1-6	perpetual hepatocellular carcinoma cell line, *Mus musculus (C57L)*
HepG2	perpetual hepatocellular carcinoma cell line, *Homo sapiens*
HIST1H2BJ	gene encoding for histone cluster 1, H2bj (*Homo sapiens*)
HIV	human immunodeficiency virus
HP	gene encoding for haptoglobin (*Homo sapiens*)
Hp	Hippocampus proper, aka hippocampal formation
hr	hour
HVA	homovanillic acid
i.p.	intraperitoneal
ICD-10	International Statistical Classification of Diseases and Health Related Problems, 10th Revision
ICSS	intracranial self-stimulation
IF	(indirect) immunofluorescence
Ig(G)	immunoglobin (G)
IGL	(indirect) immunogold labeling
IHC	(indirect) immunohistochemistry
IL1B	gene encoding for interleukin 1, beta (*Homo sapiens*)
iNOS	inducible nitric oxide synthase
IQ	intelligence quotient
IUGR	intrauterine growth retardation
kb(p)	kilo base (pair)
kDA	kilodalton
Keap1	kelch-like ECH-associated protein 1
LI	latent inhibition
LTP	long term potentiation
M_1G	pyrimido[1,2-*a*]purin-10(*3H*)-one
MAO	monoamine oxidase
MAOA	(gene encoding for) monoamine oxidase, isozyme A, aka monoamine oxidase A
MAOB	(gene encoding for) monoamine oxidase, isozyme B, aka monoamine oxidase B

MAP kinase	mitogen-activated protein kinase
MAP2	microtubule associated protein 2
MDA	malondialdehyde
MFB	median forebrain bundle
MFP	multifunctional protein
mGlu2/3R	metabotropic glutamate 2/3 receptor
mGluR	metabotropic glutamate receptor
MK.	MK-801-treated
MK-801	(5*S*,10*R*)-(+)-5-Methyl-10,11-dihydro-5*H*-dibenzo[*a*,*d*]cyclohepten-5,10-imine maleate, aka dizocilpine
MMLV	Moloney murine leukaemia virus
MnSOD	manganese-containing superoxide dismutase, aka SOD2
MOPS	3-(N-morpholino)propanesulfonic acid
mPFC	medial prefrontal telencephalic neocortex/isocortex
mPTS	peroxisomal membrane targeting signal
mRNA	messenger ribonucleic acid
MTHFR	gene encoding for methylenetetrahydrofolate reductase (*Homo sapiens*)
NAcc	Nucleus accumbens, aka accumbens nucleus
NAD^+	nicotinamide adenine dinucleotide, oxidized form
NADH	nicotinamide adenine dinucleotide, reduced form
NCBI	National Center for Biotechnology Information
NET	norepinephrine transporter, aka noradrenaline transporter
nLE	negative life event
NMDA	N-methyl-D-aspartate
NMDAR	glutamate receptor, ionotropic, N-methyl-D-aspartate
nNOS	neuronal nitric oxide synthase
NO	nitric oxide
NOTCH4	gene encoding for notch 4 (*Homo sapiens*)
NPP	negative predictive power

Nrf2	(gene encoding for) nuclear factor (erythoid-derived 2)-like 2
$O_2^{\circ-}$	superoxide radical anion
OH°	hydroxyl radical
$ONOO^-$	peroxynitrite
PB	phosphate buffer
PBD	peroxisomal biogenesis disorder
PBS	phosphate buffered saline
PBSA	bovine serum albumin in phosphate buffered saline
PCA	principal component analysis
PCP	phencyclidine, aka “angel dust”
PCR	polymerase chain reaction
PED	peroxisomal enzyme deficiency
PET	positron emission tomography
PEX1-PEX19	genes encoding for peroxins (peroxisomal biogenesis factors) 1 through 19 (*Homo sapiens, Mus musculus*)
Pex1p-Pex19p	peroxins (peroxisomal biogenesis factors) 1 through 19
PFA	paraformaldehyde
PFC	prefrontal telencephalic neocortex/isocortex
P_i	inorganic phosphate group
PKA	protein kinase A, cAMP dependent
PLXNA2	gene encoding for plexin A2 (*Homo sapiens*)
PMP	peroxisomal membrane protein
PMP70	peroxisomal membrane protein, 70 kDA, aka ABCD3
PNMT	phenylethanolamine N-methyltransferase
PPAR	peroxisome proliferator-activated receptor
PPI	prepulse inhibition
PPP	positive predictive power
PTS	peroxisomal targeting signal
PUFA	polyunsaturated fatty acid

Qdot	quantum dot
qRT-PCR	quantitative reverse transcription polymerase chain reaction
RBT	proteinase K buffer (Qiagen RNA extraction Kits)
RCDP1	rhizomelic chondrodysplasia punctata, type 1
RDD	DNase buffer (Qiagen RNA extraction Kits)
rDNA	ribosomal deoxyribonucleic acid
REB	elution buffer (Qiagen RNA extraction Kits)
rER	rough endoplasmic reticulum, aka Nissl bodies
RLT	lysis buffer (Qiagen RNA extraction Kits)
RNA	ribonucleic acid
RNase (H)	ribonuclease (H)
RNS	reactive nitrogen species
ROH	organic alcohol
ROS	reactive oxygen species
RPE	washing buffer (Qiagen RNA extraction Kits)
rpm	rotations per minute
rRNA	ribosomal ribonucleic acid
RSB	resuspension buffer (Qiagen RNA extraction Kits)
RT	room temperature
RT-PCR	reverse transcription polymerase chain reaction
RW1	washing buffer (Qiagen RNA extraction Kits)
SAGE	serial analysis of gene expression
SAH	S-adenosyl homocysteine
SAM	S-adenosyl-L-methionine
SBB	Sudan black B
SLC18A2	solute carrier family 18, member 2, neurotransmitter dopamine, aka VMAT2
SLC6A3	solute carrier family 6, member 3, neurotransmitter dopamine, aka DAT
SLC6A4	gene encoding for solute carrier family 6, member 4 (neurotransmitter serotonin, aka 5-HTT) (*Homo sapiens*)
SNARE	soluble N-ethylmaleimide-sensitive factor attachment protein receptor

SOD	superoxide dismutase
SOD2	(gene encoding for) manganese-containing superoxide dismutase, aka MnSOD
SPECT	single-photon emission computer assisted tomography
SPSS	Statistical Package for the Social Sciences
SzGene	Schizophrenia Gene database, szgene.com
T	thymine
TAE	tris acetate EDTA
Taq	*Thermus aquaticus*
TBARS	thiobarbituric acid reactive substances
TH	tyrosine hydroxylase
TP53	gene encoding for tumor protein p53 (*Homo sapiens*)
TPH1	gene encoding for tryptophan hydroxylase 1 (*Homo sapiens*)
UK	United Kingdom of Great Britain and Northern Ireland
US(A)	United States of America
veh.	vehicle-treated
VLCFA	very long chain fatty acid
VMAT2	vesicular monoamine transporter 2, aka solute carrier family 18, member 2 (SLC18A2), neurotransmitter dopamine
VTA	Area tegmentalis ventralis, aka ventral tegmental area
WHO	World Health Organization
X-ALD	X-linked adrenoleukodystrophy
XOx	xanthine oxidase
YLD	years lost to disease
ZNF804A	gene encoding for zinc finger protein 804A (*Homo sapiens*)

Abstract

Signs of neurodegeneration are commonly found in schizophrenic patients, albeit still unclear, why they occur and whether they are a cause or rather an effect of schizophrenia. Although there are numerous studies supporting either theory, the working hypothesis of this thesis is that an overactivity of mesolimbic dopaminergic pathways leads to dopamine neurotoxicity in terms of an increased production of reactive oxygen species (ROS), in time leading to oxidative stress and thereby to so-called atypical neurodegeneration. This in turn negatively influences i.a. frontal glutamate neurotransmission, thereby linking the proposed schizophrenia-models of hyperdopaminergia and hypoglutamatergia.

A key player in the body's antioxidant capacity is the peroxisome. This cell organelle is involved in both enzymatic (e.g. through the H_2O_2-degrading enzyme catalase) as well as non-enzymatic antioxidant metabolism. Its role in schizophrenia has, however, only been poorly examined, even though peroxisomes additionally are the only known source to-date of major enzymes for the degradation of cofactors of NMDA-receptors (including NMDA itself). Changes in peroxisomal metabolism and abundance therefore influence both the brain's capacity to degrade ROS as well as the functionality of its NMDA receptors and vice versa. This thesis therefore examines the reactions of peroxisomes to increased dopamine.

Since peroxisomes are involved in a number of other metabolic functions apart from antioxidant defense, their enzyme content is highly heterogeneous. Catalase and ABCD3 are generally used as markers for peroxisomes. Their abundance is, however, highly dependent on metabolic demands and therefore varies extremely between as well as within different organs, tissues and cells. Especially in the brain, both catalase and ABCD3 are barely detectable, thereby leading to a marked underestimation of true peroxisomal abundance and distribution.

In the first part of this thesis it was therefore attempted to establish a new peroxisomal marker, peroxin 14 (Pex14p), which is part of a docking complex on the peroxisomal membrane relevant for import of all matrix proteins and therefore independent of individual peroxisomal metabolism.

Using various morphological methods in a large variety of organs, tissues and cell types from a number of different species it could be shown that Pex14p is indeed present in

the membrane of every healthy peroxisome and is expressed in similarly high levels in tissue sections and cell cultures of different organs and species.

As Pex14p is also highly suited as a peroxisomal marker in all neuronal tissue, post mortem brain sections of schizophrenic patients and controls were analyzed regarding the abundance and distribution of peroxisomes as well as catalase. The results were, however, inconclusive, wherefore the reactions of peroxisomes to increased dopamine were analyzed under more controllable conditions within the second part of this thesis. The effects of dopamine in vitro were examined using primary murine neuronal and astrocyte cell cultures and the in vivo-effects in a pharmacological mouse model (through subchronic systemic administration of the selective, non-competitive NMDAR-antagonist MK-801).

Analyses of gene expression patterns from the brains of the animals show i.a. an activation of antioxidant pathways in MK-801-treated animals compared to vehicle-treated controls as well as an increase in mRNA copies of enzymes involved in NMDAR-cofactor degradation.

Morphological experiments show that dopamine changes peroxisomal reactions and neuronal morphology specifically and only in intact neuron-astrocyte interactions, mimicking the atypical neurodegeneration found in schizophrenic patients. Additionally, increased levels of selected antioxidant enzymes were found to be increased in the brains of MK-801-treated animals.

It can therefore be concluded that dopamine does indeed lead to increased ROS production in the brain, which is, however, initially still countered by an increase in antioxidant defense mechanisms. This strengthens the initial hypothesis that oxidative stress (i.e. the state of disequilibrium between ROS production and antioxidant defense) is an effect rather than a cause of schizophrenia.

Finally, the dopamine-related increase in the expression of genes encoding for enzymes degrading NMDAR-cofactors, thereby leading to a decrease of NMDAR-mediated neurotransmission, shows that hyperdopaminergia and hypoglutamatergia in schizophrenia are not separate entities, but rather influence, uphold and even exacerbate each other. This led to the proposition of a new integrative model of the etiopathogenesis of schizophrenia, linking both hyperdopaminergia and hypoglutamatergia together.

1. Introduction

1.1 Schizophrenia

In the current version of the International Statistical Classification of Diseases and Related Health Problems, 10th Revision (ICD-10), subsection F (Classification of Mental and Behavioural Disorders) (World Health Organization, WHO, 2007, p. 78) schizophrenia is described as "characterized in general by fundamental and characteristic distortions of thinking and perception, and by inappropriate or blunted affect. Clear consciousness and intellectual capacity are usually maintained, although certain cognitive deficits may evolve in the course of time." The latter aspect of the WHO definition has particularly been scrutinized since increasingly more findings report cognitive dysfunction as a major symptom in schizophrenic patients (Kuperberg & Heckers, 2000; Mueser & McGurk, 2004; Ongur et al., 2006; van Os & Kapur, 2009) often even in the prodromal phase of first episode patients before the emergence of psychotic symptom (Addington, Brooks & Addington, 2003; van Os & Kapur, 2009). Cognitive deficits are widely accepted to be more enduring than psychotic symptoms (Vinogradov, 2003; Mueser & McGurk, 2004; van Os & Kapur, 2009) and are considered a better predictor for clinical outcome than response to treatment. The current development presents a resurgence of interest regarding the cognitive alterations and decline over the course of the disorder as originally proposed by the *dementia praecox* model of Emil Kraepelin and refuted by the diagnostic model based on the concept of *schizophrenia* by Eugen Bleuler. Some schizophrenia researchers even suggest the idea that cognitive symptoms (rather than psychosis) may actually be the core feature of schizophrenia.

1.1.1 Epidemiology and societal consequences

Reports in prevalence and incidence of schizophrenia are extremely heterogeneous (Goldner et al, 2002). The average incidence is reported between 0.02 and 0.2% per year. Due to the often chronic course of schizophrenia the prevalence is higher, being reported between 0.34 and 1%. The life time prevalence is estimated around 1% (Goldner et al., 2002; Mueser & McGurk, 2004; Austin, 2005; Picchioni & Murray, 2007; van os & Kapur, 2009). Data by the WHO estimated over 26 million cases of schizophrenia worldwide in 2004, 16.7

million of which were classified as a disabling condition. Schizophrenia therefore belongs to the most severe disability class (VII), alongside severe depression, severe migraine, quadriplegia and terminal cancer (WHO, 2008). Üstün et al. (1999) place schizophrenia third in their rank of disabling effect of health conditions by severity behind quadriplegia and dementia. The disorder causes 8.3/8.0 million years lost to disease (YLD), making up for 2.8/2.6% of total YLD with values for males and females respectively (WHO, 2008). Compared to other diseases of similar disabling effects, but far higher prevalence, schizophrenia is one of, if not the major burden to society, requiring a disproportionate share of mental health services and leading to significant work place drop out. Approximately 25% of beds in psychiatric care facilities are occupied by schizophrenic patients, who also account for 50% of hospital admissions. The total costs of treating schizophrenia are high, estimated to be 44.9 billion dollars in the USA for the year 1994, 2.6 billion pounds in the UK for 1996 and 2.35 billion Canadian dollars in Canada for the same year (Mueser & McGurk, 2004). The total direct and indirect economic annual burden caused by schizophrenia is estimated at roughly 1.2 trillion dollars in the US (Austin, 2005) The combined economic and social costs of schizophrenia place it among the world's top ten causes of disability-adjusted life-years (DALY), accounting for an estimated 2.3% of all burdens in developed countries and 0.8% in developing economies (Mueser & McGurk, 2004). The disorder is slightly more common in males than females (ratio approximately 1.4:1), but has a definitive pattern of earlier onset, combined with more negative symptoms, worse clinical outcome and lower chance of full recovery in men compared to women (Hafner et al., 1993; Picchioni & Murray, 2007). Patients usually present with their first schizophrenic episode during late puberty to early adolescence.

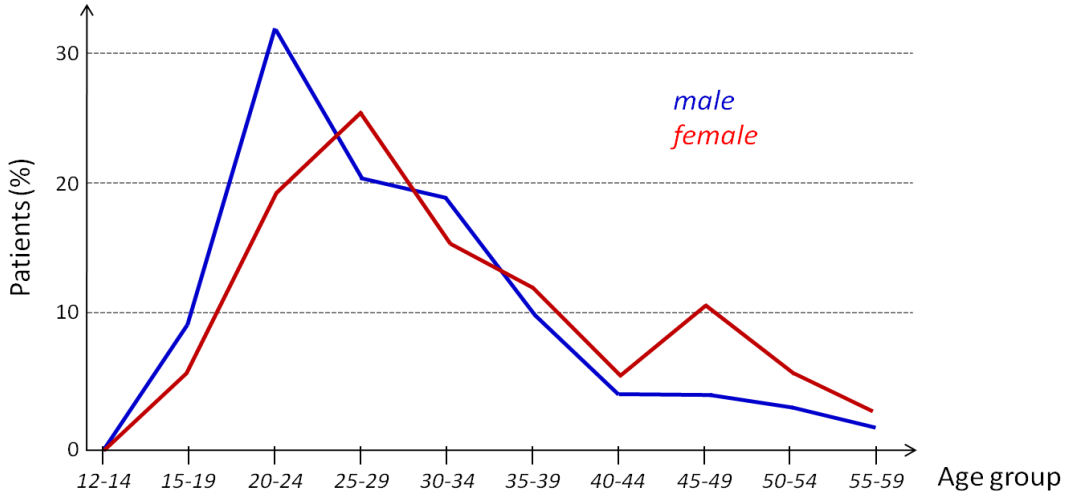

Fig. 1.1_1: Gender differences in age of onset of schizophrenia (*modified from Hafner et al., 1993*)

Schizophrenia is also recognized (directly and indirectly) as a cause of excessive mortality in patients. Reasons here fore are often due to social withdrawal, lack of personal care, well-balanced eating habits and physical activity (e.g. inducing circulatory, digestive, endocrine, neurological and or respiratory diseases), side effects of antipsychotic medication as well as a significant increase in smoking-related deaths (Brown, Inskip & Barraclough, 2000; Evins & Goff, 2008). The rate of successful as well as attempted suicides is also uncommonly high in schizophrenic patients (Caldwell & Gottesman, 1990; Radomsky et al., 1999, Tandon, 2005).

1.1.2 Signs and symptoms

Schizophrenic symptoms can generally be grouped into four categories: Positive, negative, cognitive and affective. Positive symptoms include delusions, hallucinations, thought and speech disorders and bizarre behavior. Negative symptoms are characterized by a reduction in normal psychophysical processes, e.g. alogia, avolition, asociality (not to be mistaken for antisociality) and catatonia. Cognitive deficits are common in schizophrenic patients and often predate the first florid psychotic episode (see introductory remarks to this chapter). Schizophrenic patients on average perform one standard deviation below the norm in various trials testing attention, processing speed, working and long-term memory, executive function and social cognition (van Os & Kapur, 2009) and their premorbid IQ, years before the onset of psychosis, is estimated on average at one-half of a standard deviation below that of healthy controls (Woodberry et al., 2008). Finally, affective disorders can range in both extremes from the norm (blunted affect & anhedonia vs. manic symptom) or involve so-called inappropriate affect, during which patients show affective responses not only incoherent with the socially accepted emotional expression (e.g. laughing upon receiving of bad news), but also sometimes not matching the emotion the patient “wants” to express (Davison & Neale, 1998). The model currently being able to best describe the congregation of such a broad array of (in part) seemingly unrelated symptoms is that of aberrant salience (Kapur, 2003). The inability of patients to discriminate between relevant and irrelevant stimuli at first leads to delusional ideas, which may then mature into full-blown positive and affective symptoms. Aberrant salience can also directly cause cognitive symptoms since patients will be incapable of adequate attention, sensorimotor gating including processing speed, stimulus perception and recognition as well as stimulus generalization, which is an

integral part of many learning processes. The added advantage of this proposed mechanism is that it also offers an explanation for the early onset as well as persistence of cognitive deficits, the ongoing mental decline observed in many patients as well as the high prediction value of cognitive impairment regarding the outcome of the disorder. Finally, aberrant salience may also present as lack of salience (because, in essence, all stimuli being processed as equally salient means that no stimulus is more salient than the others) thereby leading to negative symptoms, including blunted affectivity, anhedony and even post-schizophrenic depression. This can be illustrated nicely by a patient quotation from McGhie & Chapman, (1961, p. 106): "*I can't concentrate on television, because I can't watch the screen and listen to what is being said at the same time. I can't seem to take in two things like this at the same time, especially when one of them means watching and the other means listening. On the other hand I always seem to be taking in too much at the one time and then I can't handle it and can't make sense of it.*"

1.1.3 Diagnostic guidelines

Two major diagnostic manuals exist for psychiatric disorders, the aforementioned ICD-10 (mostly used in Europe) and the Diagnostic and Statistical Manual of Mental Disorders, 4th Edition, Text Revision (DSM-IV-TR) (American Psychiatric Association, APA, 2000). The agreement between diagnoses derived from either system is reported to be very high (Jakobsen et al., 2005) (q.v. table 1.1_1).

Both manuals share the subdivisions paranoid schizophrenia, hebephrenic or disorganized schizophrenia, catatonic schizophrenia, undifferentiated schizophrenia and residual schizophrenia, whereby the developers of the DSM-V are contemplating on dropping these sub-classifications (www.dsm5.org). The ICD-10 additionally defines a post-schizophrenic depression and simple schizophrenia, a slowly progressive form of the disorder consisting solely of negative symptoms and without any history of hallucinations, delusions or any other manifestations of an earlier psychotic episode.

Table 1.1_1: Diagnostic guidelines according to DSM-IV-TR and ICD-10

Diagnostic criterion	Description	DSM-IV-TR	ICD-10
Characteristic symptoms (*two or more during 1 month or more*)	Delusions – thought echo/insertion/withdrawal/ broadcasting	+ (one during 1 month if delusion is bizarre)	+ (one during 1 month, if very clear)
	Delusions – control/influence/passivity/ perception (referred to body, actions, sensations or thoughts)	+ (one during 1 month if delusion is bizarre)	+ (one during 1 month, if very clear)
	Delusions – persistent, culturally inappropriate and completely impossible	+ (one during 1 month if delusion is bizarre)	+ (one during 1 month, if very clear)
	Hallucinations - auditory	+ (one, if running commentary or two or more conversing voices)	+ (one during 1 month, if very clear)
	Hallucinations – persistent, of any other modality	+	+
	Incoherent/disorganized speech (resulting from breaks or interpolations in the train of thought)	+	+
	Catatonic or grossly disorganized behavior (incl. negativism, mutism or stupor)	+	+
	Negative symptoms	+	+
	Significant and consistent changes in personal behavior (loss of interest, aimlessness, idleness, self-absorbed attitude, social withdrawal)	only if leading to social/ occupational dysfunction (see below)	only for Simple Schizophrenia (duration of at least one year)
Duration		at least 6 months (including prodrome and residual)	at least 1 month
Social/occupational dysfunction		+	possibly subclinical during prodrome
Exclusion	Affective/schizoaffective disorder	+	+
	Direct effects of substance intoxication/withdrawal	+	+
	Direct effects of general medical condition (includes brain disease/disorder, epilepsy, hyper-/hypoglycemia etc.)	+	+

1.1.4 Neurodegeneration in schizophrenia

Although not mentioned in either of the commonly used diagnostic manuals, schizophrenia is closely associated with neurodegenerative processes. Progressive reduction of brain total volume, enlargement of ventricles and loss of cortical as well as subcortical gray matter have been found in chronic and first-episode schizophrenic patients, whereby the exacerbation of neurodegeneration through antipsychotic pharmacotherapy cannot be excluded. The amount of neurodegeneration and loss of brain connectivity correlate with the severity of positive symptoms (Suzuki et al., 2005; Lui et al., 2009). The cause of neurodegeneration is still not clear, but could likely be due to oxidative damage caused by dopamine neurotoxicity (personal communication by Prof. Nancy Andreasen). Interestingly, the neurodegenerative processes appear to differ from those found in primary neurodegenerative disorders like Alzheimer's disease, as there is no evidence of significantly increased neuronal death or reactive gliosis (Lieberman, 1999). It appears rather that schizophrenic patients show signs of atypical neurodegeneration, namely reduction of neuronal size resulting in secondary pathological features including loss of dendritic arborization and synaptic density, altered synaptic plasticity and increases in neuronal density (Benes et al., 1991a; 1991b; Browning et al., 1993; Daviss & Lewis, 1995; Selemon, Rajkowska & Goldman-Rakic, 1995; Arnold et al., 1996; Perrone-Bizzozero et al., 1996; Glantz & Lewis, 1997, Goldman-Rakic & Selemon, 1997; Zaidel, Esiri & Harrison, 1997; Rajkowska, Selemon & Goldman-Rakic, 1998).

1.1.5 Proposed causes of schizophrenia

Although the list of possible causes of schizophrenia is extensive, recent studies suggest a gene-environment interaction model (GxE), under which most of the commonly described ethiopathogenetic mechanisms can be subsumed (van Os & Kapur, 2009).

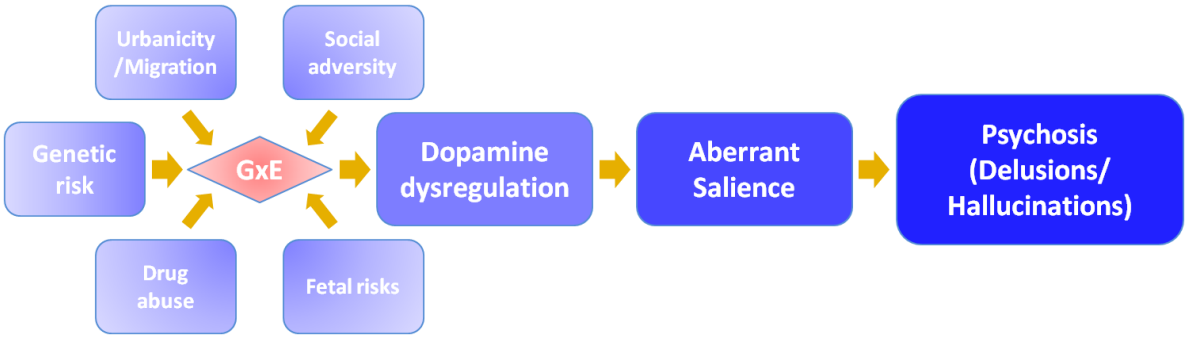

Fig. 1.1_2: GxE-model of schizophrenia and related psychoses

Many findings indeed show a significantly higher risk for schizophrenia as a result of environmental risk factors in patients carrying risk-alleles (van Os, Kenis & Rutten, 2010).

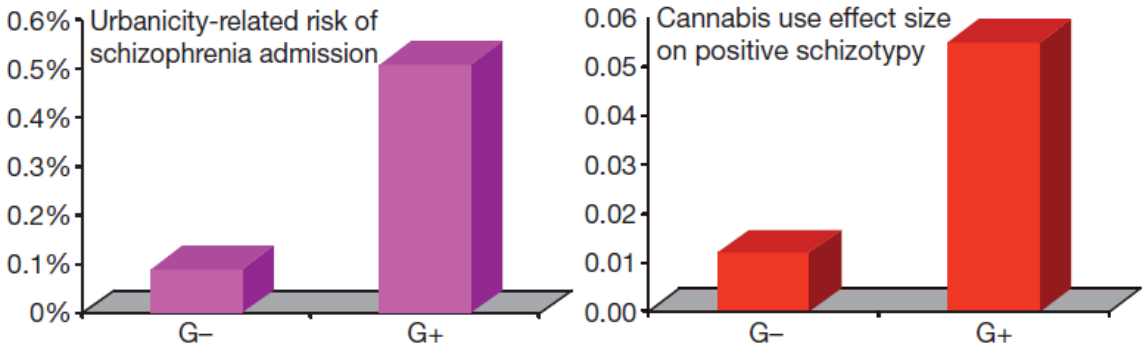

Fig. 1.1_3: Carriers of "risk alleles" for schizophrenia (G+) are influenced more by environmental factors regarding schizophrenia-related symptoms and clinical admissions than non-carriers (G-). (*modified from van Os, Kenis & Rutten, 2010*)

The following section shall therefore be divided into three aspects: (a) genetic risk factors, (b) environmental risk factors and (c) neurochemical mechanisms or alterations.

1.1.5.1 Genetic risk factors: The genetic basis of schizophrenia is widely acknowledged. The risk of schizophrenia is extremely high in first degree relatives of schizophrenics, especially in monozygous twins (this effect is exacerbated due to common in-utero environment), very

high in second degree relatives and still considerably higher in third degree relatives than in the general population:

Table 1.1_1: Rates of schizophrenia among relatives of schizophrenic patients

Familial relationship	**Schizophrenia rates among relatives of schizophrenic patients**		
	Tsuang & Vandermey, 1980 (approx. values)	*Gottesman, 1991*	*Rowe, 1994*
Siblings	9%	9%	7.3%
Monozygotic twins	58%	48%	44.3%
Dizygotic twins		17%	12.1%
Siblings - neither parent schizophrenic	8.5%		
Siblings - one parent schizophrenic	14%		
Same sex siblings	12%		
Opposite sex siblings	6%		
Half-siblings	3.5%	6%	2.9%
Nieces or nephews	2.5%	4%	2.7%
Children	12%	13%	
Children - both parents schizophrenic	37%		36.6%
Children - one parent schizophrenic			9.4%
Grandchildren	3%	5%	2.8%
Parents	5%	6%	
Uncles or aunts	2.5%	2%	
First cousins	3%	2%	1.6%
General population/spouses	1%	1%	1%

The number of association studies published on potential genetic risk factors for schizophrenia borders on 2000, unfortunately with highly heterogeneous and often inconsistent results. In order to help with the interpretation of this wide array of results, Allen et al., created a regularly updated and publicly accessible online database (*SzGene,* www.szgene.org) of all genetic association studies for schizophrenia published in peer

reviewed journals and written in English (Allen et al., 2008). For eligible polymorphisms with genotype data in at least four case-control samples, continuously updated random-effects meta-analyses are presented. In the initial paper on the SzGene-database a total of 24 genetic variants were found in 118 meta-analyses within 16 different genes (*APOE, COMT, DAO, DRD1, DRD2, DRD4, DTNBP1, GABRB2, GRIN2B, HP, IL1B, MTHFR, PLXNA2, SLC6A4, TP53 and TPH1*) that showed nominally significant effects with average summary odds ratios of approximately 1.23. By 2011 SzGene lists a total of 1727 eligible studies performed on 1008 genes with 8788 polymorphisms in question. The number of meta-analyses is currently 287. SzGene also currently incorporates the findings of 14 genome-wide association studies (GWAS) and 12 other large-scale studies (mostly fine-mapping studies and GWAS re-analyses/follow ups). In all these studies, merely three protein-coding genetic loci were found in more than one study: *ZNF804A* and *HIST1H2BJ* (in two studies each) and *NOTCH4* (in three studies). As of 2009, Taylor et al. reviewed 63 mouse models with mutations or complete knockouts of various considered risk genes for schizophrenia. The validity of these mouse models is very heterogeneous. Any inferences from knockout animals should be drawn with great care, since the dysfunction of an entire gene does not represent the actual underlying genetic component found in schizophrenic patients. Even more so, the lack of any protein missing through the genetic knockout during ontogeny may have influences and repercussions on a wide variety of (neuronal) functions not directly involved with the protein/gene that has been knocked out, e.g. neuronal migration and growth, synaptogenesis, myelination or glial (especially astrocyte) development. Finally, the vast interconnectivity between neuronal pathways and transmitter systems and their interdependence during brain maturation and ontogeny may lead to false interpretations regarding immediate causality, e.g. a gene knockout in transmitter system A may lead to alterations in the development of basal activity of transmitter systems B which in turn influences systems C and D, whereof only D is involved in the etiopathogenesis of the disorder in question. Drawing the conclusion from the exemplary knockout that alterations in transmitter A activity in humans causes the disorder would therefore be highly questionable. The issue of critical time periods for the etiopathogenesis of schizophrenia will therefore be addressed in the following section.

In humans allelic variants of many schizophrenic candidate genes have also been shown to have an impact on schizotypy or endophenotypes of schizophrenia in the general population (Stefanis et al., 2007; Billino, Hennig & Gegenfurtner, 2011a; 2011b).

1.1.5.2 Environmental risk factors: Amongst the more commonly discussed environmental factors or negative life events (nLEs) that are discussed as being causally involved in the development of schizophrenia are intra-uterine and perinatal complications (e.g. intra-uterine growth retardation, viral infections, hypoxia, malnourishment), physical, psychological and sexual abuse, high expressed emotions in the family, social adversity, double bind relationships, migration, urbanicity, stress and drug abuse (especially cannabinoids, cocaine, amphetamine and phencyclidine/ketamine).

Two concepts appear to be of major importance regarding the influences of nLEs on the outbreak of schizophrenia: Sensitization and critical time periods. The concept of sensitization refers to the observation that multiple exposure to environmental risk factors (either multiple single exposures to different factors or repeated exposure to similar factors or a combination of both) leads to a greater increase in the development of phenotypical symptoms, eventually resulting in lasting schizophrenia (Collip et al., 2008)

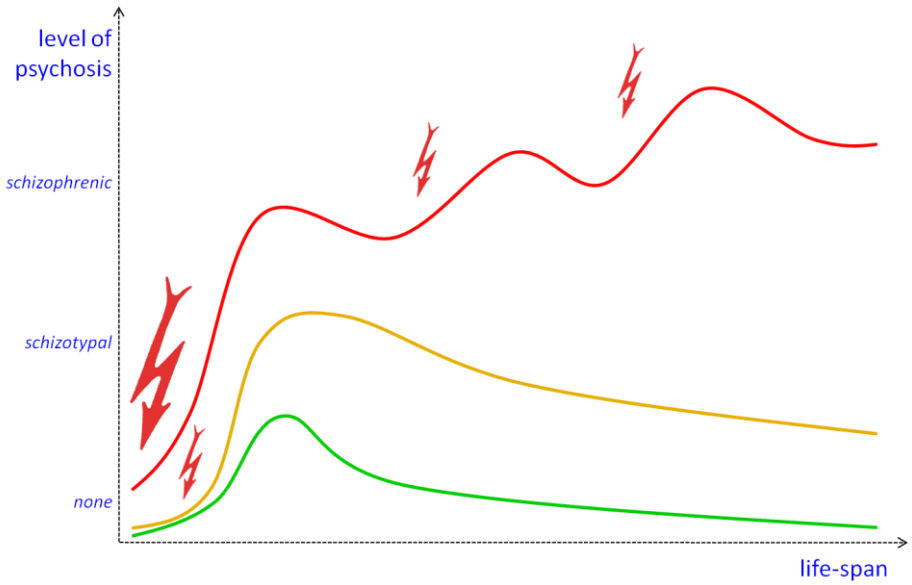

Fig. 1.1_4: The concept of sensitization; Person A (green) has ‘‘normal’’ developmental expression of subclinical psychotic experiences that are mild and transient. Person B (yellow) has similar expression but longer persistence due to additional but mild environmental exposure. Person C (red) has prolonged persistence due to severe and/or repeated environmental exposure and subsequent transition to clinical psychotic disorder, which can be repeatedly and easily triggered again at later time-points by relatively mild stressors. (*based on Collip et al, 2008*)

Evidence for the validity of this concept could be shown i.a. in an animal study on intra-uterine growth retardation induced through low-protein diet of the pregnant mother C57Bl/6J mice (Vucetic et al., 2010). Results showed significant alterations in dopamine metabolism in the offspring in comparison to pups of mice fed with a control diet (in essence, increase in dopaminergic neurons in the midbrain, higher levels of mRNA expression of genes related to dopamine metabolism, altered methylation patterns of same genes, increase in dopamine abundance in combination with reduced dopamine degradadation etc.). In regards to behavioral patterns (locomotion patterns as commonly used as schizophrenia-phenotypical symptom expression in rodents), however, mice did not show differences compared to control animals. When a second environmental risk factor was introduced (high fat diet or cocaine administration), experimental animals did show a clear phenotype.

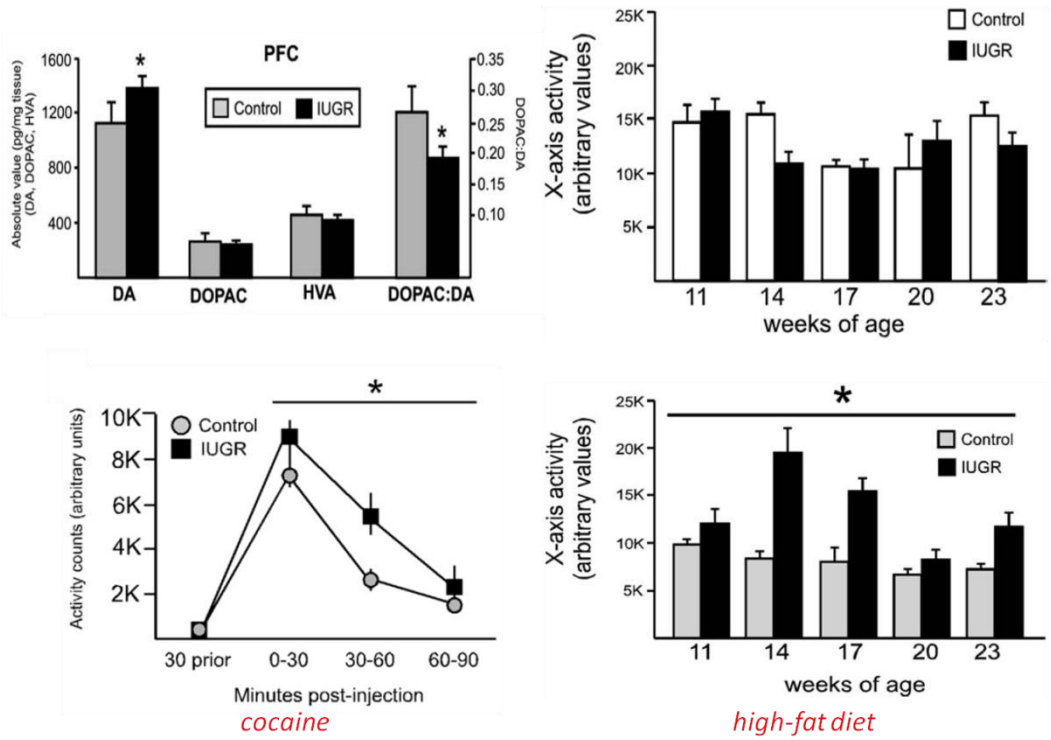

Fig. 1.1_5: Animals with intrauterine growth retardation (IUGR) initially show no schizophreniform phenotype, despite various significant epigenetic, morphological and neurochemical alterations, until exposed to an environmental stressor like cocain or high-fat diet. (*modified from Vucetic et al., 2010*)

Similar results regarding sensitization were found in a large national cohort study performed on all children born in Sweden between 1963 and 1983 (n = 2.1 million). Among other results the authors showed that the risk of admission for schizophrenia rose with the

number of adverse social variables, leading them to attribute 20% of cases of schizophrenia to adverse social exposure (Wicks et al., 2005).

Various other animal models with a wide range of validity exist for schizophrenia that involve environmental challenges, including brain lesions, induced metabolite deficiencies, intra-uterine, peri- and postnatal physical or social stress, viral infections of the pregnant mother animal etc. (Taylor et al., 2009; published on schizophreniaforum.org).

Many of the inconsistencies regarding environmental influences on the outbreak of psychosis can be explained through critical life or time periods. These are sensitive periods of neuronal development during which the basal activities and the interconnections within and between neuronal pathways/transmitter systems are established. In this context it is important to note that, apart from primary intrauterine neural development, the brain continues to mature long after birth with significant changes in synaptic plasticity and neurotransmission occurring during puberty, most likely due to the influences of sex steroids. Gestational brain maturation studies comparing the consequences of maternal viral infections show significant correlations between schizophrenia and influenza during the second to early third, but not the first trimester (Mednick et al., 1988; Sham et al., 1992; Kunugi et al., 1995). Vice versa, maternal nutritional deprivation was fund to be a major risk factor during the first, but not the second or third gestational trimester (Susser & Lin, 1992; Susser et al., 1996; Hoek, Brown & Susser, 1998; StClair et al., 2005; Xu et al., 2009). Also, maternal stress during pregnancy, especially during months 3-5 and 9, was shown to be associated with increased risk of schizophrenia compared to paternal loss during the first year of life (Huttunen & Niskanen, 1978). Similar results regarding critical time periods can be found for the influences of drug abuse during puberty, whereof especially cannabis is considered a major risk factor. A vast number of animal and human studies using different methods conclude that schizophrenia is associated to cannabis use during puberty, but not in adults. This can be explained through several interconnections: (a) external stimuli are important for unique brain development. (b) Dopaminergic systems undergo critical refinement during adolescence. (c) Dopaminergic, glutamatergic and GABA-ergic system interact in the mature and developing brain with each other as well as the endocannabinoid system. (d) The immature brain contains many silent glutamatergic synapses, which have NMDA receptors, but lack AMPA receptors (see section on glutamate transmission). These silent synapses are converted into functional ones during critical time periods due to the

incorporation of AMPA receptors. (e) Neuronal activity during critical time periods changes the composition of NMDA receptors, which are made up of different subunits, whereby immature NMDA receptors are more sensitive to glutamate and therefore to glutamate excitotoxicity. Therefore binding of glutamate as well as influencing the NMDA receptor indirectly through cannabinoids during critical periods will have long-lasting effects (for an extensive review on brain maturation and cannabinoids, see Bossong & Niesink, 2010). Over all it can be said that there is a vast amount of evidence that the influence of environmental factors on the development of schizophrenia is not only dependent on repetitive events as shown through studies on sensitization, but also that the brain undergoes significant periods during which it is sensitive to the influence of specific life events but not others. Therefore the risk of schizophrenia being exacerbated through negative life events is not only inter-, but also intraindividually different, meaning the same life event may or may not lead to an outbreak of psychosis between as well as within persons.

The common link between genes, environment and neurochemistry is believed to be active methylation and/or demethylation of genes (especially within promoter regions). During DNA methylation a methyl group is transferred from S-adenosyl-L-methionine (SAM) to (preferably) cytosine bases/deoxycytidine nucleosides through the enzyme DNA methyltransferase (DNA MTase, DNMT). The alterations of DNA methylation interfere with binding of transcription factors to promoter regions of genes, thereby altering their expression patterns.

1.1.5.3 Neurochemical mechanisms: Two major theories regarding alterations in neurotransmission have been proposed as causally related to schizophrenia: The dopamine and the glutamate hypotheses of schizophrenia. The dopamine hypothesis as well as the possibility of interactions between both theories shall be discussed in more detail in the following chapter on dopamine.

The theory of glutamate hypofunction in schizophrenia was first proposed by Kim et al. in 1980, due to findings of low glutamate levels in the cerebrospinal fluid (CSF) of schizophrenic patients. These results were fortified through findings that schizophreniform symptoms could be induced acutely through blockage of glutamatergic N-methyl-D-aspartate receptors (NMDARs) in healthy controls (Javitt & Zukin, 1991; Krystal et al., 1994). The same groups of substances were also shown to induce longer (8-24 hrs) episodes of

psychosis in schizophrenic patients strikingly resembling symptoms during florid episodes of their illness (Lahti et al., 1995). Unlike other pharmacological substances, NMDAR blockers are able to induce both positive and negative symptoms of schizophrenia (Bowers & Freedman, 1966; Krystal et al., 1994) as well as cognitive symptoms and thought disorders similar to schizophrenic patients (Oye, Paulsen & Maurset, 1992; Malhotra et al., 1996; Adler et al., 1999).

Post mortem studies on schizophrenic patients show changes in glutamate metabolism and NMDAR subunit composition (Tsai et al., 1995; Clinton & Meador-Woodruff, 2004), and a pilot SPECT-study found reduced NMDAR binding in the hippocampus of medication-free schizophrenic patients (Pilowsky et al., 2006).

Double-blind, placebo-controlled studies have shown significant improvement in positive and negative symptoms comparable to control groups treated with olanzapine in patients treated with an agonist of the metabotropic glutamate 2/3 receptor (mGlu2/3R), however, with prolactin levels, extrapyramidal motor symptoms and weight gain comparable to placebo-treated controls (Patil et al., 2007; Mosolov et al., 2010). Due to the nature of the NMDAR, being both ligand- and voltage-gated (see below), agonists of other glutamate receptors, like the mGLU2/3R, could enhance post-synaptic membrane depolarization and thereby NMDAR transmission.

Based on the aforementioned indication of glutamatergic involvement in the etiopathogenesis of schizophrenia many animal models have been established using selective non-competitive NMDAR blockers (reviews by Bubeníková-Valesová et al., 2008 or Carpenter & Koenig, 2008) - alternatively mouse models were established with mutations or knockouts of various genes encoding for proteins involved in NMDAR-transmission. The most common pharmacological models of NMDAR blocking use phencyclidine (PCP, street name “Angel Dust”), ketamine (street name “Special K”) or dizocilpine (MK-801). Ketamine is still used across the world, including Germany, during full anesthesia, but usually only in cases where patients present with risk of peri-operative circulatory collapse, as they often report vivid and frightening sensory perceptions and/or nightmares during anesthesia (personal communication from Dr. Andrea Mietens, anesthesiologist, Giessen, Germany). In this thesis the pharmacological MK-801 model was chosen in male pubescent C57Bl/6J mice.

Table 1.1_2: Some animal correlates of schizophrenia symptoms *(modified from Arguello & Gogos, 2006*)

Symptom type	Clinical manifestation	Preclinical model/ animal correlate
Positive	Psychomotor agitation	Hyperlocomotion in response to novelty or stress
	Psychostimulant supersensitivity	Enhanced locomotor response to psychostimulants
Negative	Social withdrawal	Decreased interaction with conspecifics
	Anhedonia	Decreased reinforcing properties of drugs of abuse und natural rewards
Cognitive	Memory deficits	Delayed nonmatch to sample tasks, serial odor span
	Attentional deficits	Latent inhibition, 5-choice serial reaction time tasks
	Executive dysfunction	Attention set-shifting task

Glutamate is the major excitatory neurotransmitter found in the mammalian central nervous systems, especially in the forebrain. It is stored in synaptic vesicles and released into the synaptic cleft upon Ca^{2+}-dependent exocytosis, when an action potential reaches the presynaptic button. Apart from the aforementioned metabotropic glutamate receptors (mGluRs) three major ionotropic receptors are known. They are named according to their major agonists: AMPA (2-amino-3-(5-methyl-3-oxo-1,2- oxazol-4-yl)propanoic acid), kainate and NMDA (N-methyl-D-aspartate) receptors. AMPA and kainate receptors are ligand-gated ion channels involved in fast excitatory synaptic transmission and lead to depolarization of the postsynaptic membrane (excitatory postsynaptic potential, EPSP). NMDA receptors, however, are blocked through a Mg^{2+}-ion within the channel and are therefore not only ligand-, but also voltage-gated, as the Mg^{2+} only dissociates from within the pore, if the postsynaptic membrane has been sufficiently depolarized. Apart from the binding sites for NMDA/glutamate and Mg^{2+} the NMDAR also has several other binding sites for cofactors,

like D-serine, D-cycloserine and glycin, and antagonists like ketamine, PCP and MK-801. The open NMDAR is a channel for sodium, potassium and, importantly, also for calcium ions.

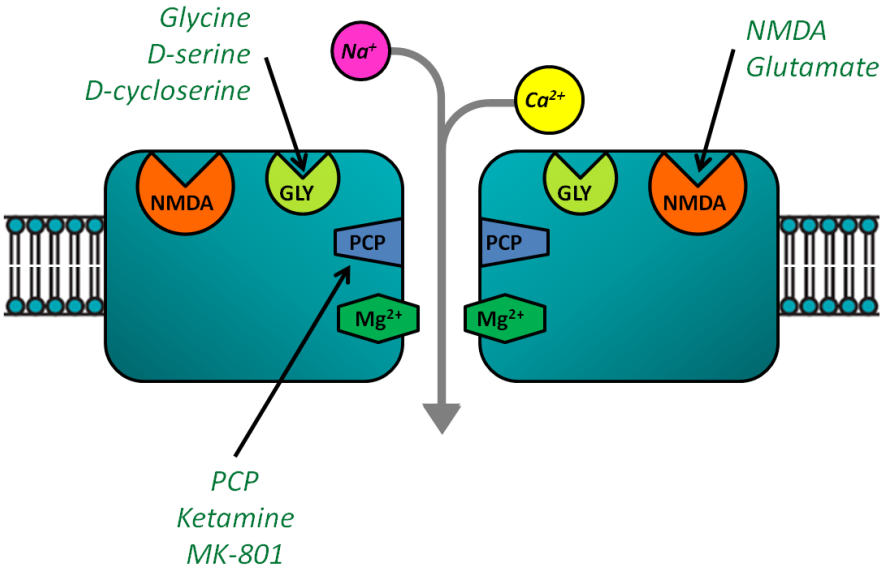

Fig. 1.1_6: N-methyl-D-aspartate receptor (NMDAR); *Gly: binding site for glycine, D-serine, D-cycloserine; NMDA: binding site for glutamate, D-aspartate, NMDA; PCP: binding site for phencyclidine (PCP), ketamine, dizocilpine (MK-801) (modified from Javitt, 2006*)

Influx of calcium through the NMDAR pore leads directly and indirectly to the activation of various kinases, including Ca2+/calmodulin dependent (CaM) kinases, mitogen-activated protein (MAP) kinases, tyrosine kinase and protein kinases A and C. This complex signal transduction cascade leads to the phosphorylation of a cyclic adenosine monophosphate (cAMP) response element binding protein (CREB), which then binds to the cAMP response element (CRE) in the promoter regions of various genes, e.g. for the expression of proteins for new AMPA receptor formation, thereby leading to alteration of the synaptic strength (synaptic plasticity). This process of neurotransmitter-induced gene expression, referred to as long term potentiation (LTP), is known for other transmitter receptors (e.g. dopamine receptors of the D_1-family or the serotonin receptor 5-HT_{2A}), but is best studied in NMDA receptors.

For NMDAR activation to work, a complex interplay between neurons and astrocytes is necessary, since both glutamate metabolism as well as the production of cofactors involve astrocytes. The important cofactor D-serine, for example, is produced in astrocytes from L-serine through the enzyme serine racemase. It has been shown to effectively reduce positive, negative as well as cognitive symptoms in antipsychotic-resistant schizophrenia patients (Tsai et al., 1998; Heresco-Levy et al., 2005). Upon Ca^{2+}-influx into the postsynaptic

neuron neuronal nitric oxidide synthase (nNOS) is activated producing NO, which then diffuses through the neuronal and astrocyte membranes and deactivates serine racemase, thereby functioning as negative feedback mechanism for NMDAR transmission. It has also been shown that NMDAR blockage using MK-801 leads to a rapid increase in expression of serine racemase mRNA (Yoshikawa et al., 2004a). In this thesis serine racemase expression induction was therefore chosen as an internal positive control for the action of MK-801.

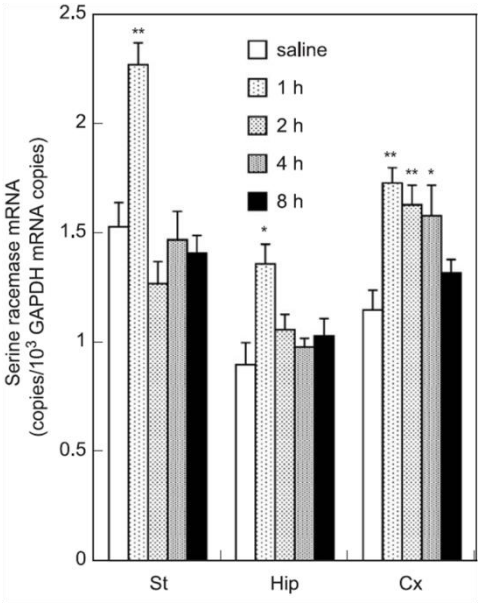

Fig. 1.1_7: Time course of changes in the levels of serine racemase mRNA in several brain areas of rat after systemic administration of MK-801 (0.4 mg/kg); *St: striatum, Hip:hippocampus, Cx: cortex (modified from Yoshikawa et al., 2004a*)

The alternative mechanism of termination of NMDAR transmission is through enzymes degrading amino acids of D-chirality, such as NMDA, D-serine and D-aspartate (which is also an NMDAR agonist). The currently only known enzymes to perform this function are the peroxisomal enzymes D-amino acid oxidase (DAAO) and D-aspartate oxidase (D-AspOx). Both enzymes have therefore also been discussed in the context of schizophrenia. Findings regarding the involvement of D-AspOx are few, but Errico et al. (2008) showed a reduction of a commonly used schizophrenic phenotype (prepulse inhibition, PPI) as well as an increase in hippocampal learning through unphysiological D-aspartate increases in an MK-801 mouse model both after oral D-aspartate administration as well as in mice with a targeted deletion of the D-AspOx gene.

DAAO, on the other hand, is currently on 40th place on SZGene's Top Results list since many studies have proposed links between polymorphic variations of the encoding gene and

schizophrenia (Chumakov et al., 2002; Liu et al., 2004; Schumacher et al., 2004; Wood, Pickering & Dechairo, 2007). Post-mortem studies show elevated DAAO activities and expression rates in brains from schizophrenic patients (Burnet et al., 2008; Madeira et al., 2008), and increased levels of D-serine were found in patients' CSF and serum (Hashimoto et al., 2003; 2005; Bendikov et al., 2007).

Interestingly, Yoshikawa et al. (2004b) found that inhibition of NMDAR trafficking through MK-801 leads to significant increases in DAAO mRNA expression. This process is, however, markedly slower than the aforementioned induction of serine racemase expression. A possible explanation is that the increase in D-serine would also lead to an increase in DAAO expression. Alternatively, sequences homologous to cAMP response elements (CREs) were found in the 5'-flanking region of the DAAO gene (Fukui & Miyake, 1992). It is therefore possible that the increase in DAAO activity found in patients is not primarily the cause of schizophrenic symptoms, but could also be a side effect of transmitter system interactions (e.g. through activation of dopamine release and binding to certain D_1-like receptors involved in CREB phosphorylation). This side effect would in turn exacerbate rather than cause a schizophrenia phenotype. This is speculative, but other interactions between the glutamatergic and dopaminergic systems are better established, wherefore this argumentation would fit in line with a proposed model of hyperdopaminergia as a bottleneck within the etiopathogenesis of schizophrenia (q.v. the appropriate section in the next chapter).

1.2 Reactive oxygen species and antioxidant defense systems

Interestingly, oxygen was not originally found freely in earth's atmosphere. Free oxygen, released from early obligate anaerobic prokaryotes during photosynthesis, was absorbed by minerals. Approximately 2.4 billion years ago, after the minerals had become saturated with oxygen, it began to accumulate freely in the atmosphere, thereby killing off a large portion of obligate anaerobics, an event known as the Great Oxygenation Event (GOE). Survival of organisms in this new toxic atmosphere made an evolutionary step necessary, which took place approximately 2 billion years ago through the endosymbiosis of what were to become mitochondria. These organelles are not only capable of enzymatically reducing and thereby detoxifying ROS, but also allowed archaebacteria, that had previously obtained their energy through glycolysis and fermentation, to use oxygen for respiration, thereby not only giving an evolutionary advantage, but ultimately allowing for life outside the ocean. Other theories state, that mitochondria were actually not the first endosymbionts, but were preceded by actinobacterial ancestors, which would then evolve into peroxisomes (Duhita et al., 2010). These indigestible parasitic invaders were also capable of degrading ROS, but could not generate energy through redox metabolism.

Even though oxygen now is an element vital for the survival of aerobic organisms, mainly during the generation of energy in form of adenosine triphosphate (ATP) through mitochondrial respiratory chain activity (ca. 80% cellular oxygen), it is also a highly reactive and potentially toxic molecule. The result of these reactions (removal of electrons from other molecules; oxidation) can lead to the formation of reactive oxygen species (ROS), which can be briefly divided into radicals and non-radicals. Accumulation of ROS can alter the intracellular redox balance and may lead to oxidation of cellular macromolecules like lipids, proteins or even nucleic acids. ROS are therefore usually combated by antioxidant defense mechanisms of the cells, which consist of enzymatic and non-enzymatic antioxidant mechanisms. A state of disequilibrium between pro- and antioxidant mechanisms is referred to as oxidative stress (Reddy & Yao, 1996).

1.2.1 Oxygen chemistry, radicals and reactive oxygen species formation

Oxygen is the element with the atomic number 8 in the periodic table. It is represented by the abbreviation O and has an atomic weight of 15.994 u (Da; g/Mol). It has

eight protons in its core and eight electrons, whereof six are in its valence shell, making oxygen a potent electron acceptor (hence the term oxidization/oxidizing agent). Its major function in eukaryotes is therefore that of the being the most electronegative of all electron acceptors in the electron transport chain of mitochondrial respiration.

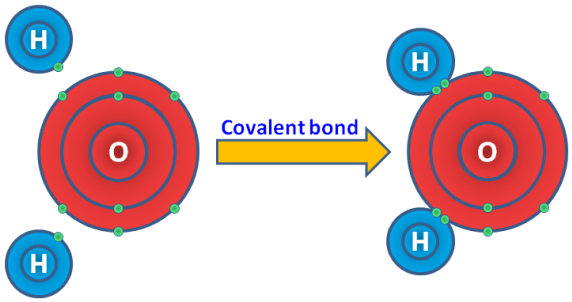

Fig. 1.2_1: Illustration of a single oxygen atom undergoing a covalent bond with two hydrogen atoms to form molecular oxygen. Hereby the highly reactive oxygen receives two electrons to its outer shell transferring it into a non reactive state. (*modified from Encyclopaedia Britannica*)

The most common oxygen-allotrope, dioxygen (O_2), usually exists in its ground state (triplet oxygen), since this form is least reactive. Of the eight electrons involved in the double bind between two oxygen atoms, two each occupy a molecular orbital alone. This makes dioxygen a diradical. In triplet oxygen, as opposed to the alternative state called singlet oxygen, however, both of these unpaired electrons have equal spins, wherefore triplet oxygen could only accept electrons from another reaction partner with two unpaired electrons of opposite spin to its own (Halliwell, 2006). Other electrons involved in double bonds are paired in an orbital with another electron of opposite spin, wherefore they would not be accepted by triplet oxygen. Through energy input it can occur that one of the unpaired electrons inverts its spin, thereby changing triplet oxygen into the highly reactive singlet oxygen, which can occur during photosensitization reactions or during lipid peroxidation (Halliwell et al., 2006) as is also used by the immune system amongst other reactive oxygen species for killing of bacteria (Wentworth et al., 2002). Singlet oxygen exists in two possible configurations: either both opposing electrons continue to occupy one molecular orbital each or they pair up in one molecular orbital leaving the other completely empty.

Since dioxygen has both the character of a double bound molecule (as shown through the skeletal formula <O=O>) as well as that of a radical (as shown through the skeletal formula ·O̲-O̲·) the most accurate description of the molecules nature through a

skeletal formula would be <O÷O>. It can be reduced through either receiving 4 electrons alongside 4 protons, as is the case during mitochondrial respiration, to form water (O_2 + 4 H^+ + 4 e^- > 2 H_2O) or, receive only 2 electrons and 2 protons to form hydrogen peroxide (O_2 + 2 H^+ + 2 e^- > H_2O_2). This step is often a byproduct of enzymatic activity (e.g. during degradation of dopamine through monoamine oxidases). Although dioxygen is not a primary cause of oxidative damage in its triplet state, it can lead to autoxidation of other molecules. Especially in the brain, reaction of O_2 with several aromatic neurotransmitters and their precursors or metabolites leads to the formation of quinones and semiquinones. These strong oxidizing agents consist of cyclic dione structures with two double bonded oxygen atoms. They no longer have aromatic character and can react with neutrophilic macromolecules to form other ROS.

Fig. 1.2_2: Formation of a quinone through autoxidation of dopamine (*modified from Stokes et al., 1999*)

Dioxygen is, however, not directly the major font of intracellular ROS formation. Most oxidative damage comes from electron leakage during mitochondrial respiratory chain activity. Under physiological circumstances, electrons are transported along the inner mitochondrial membrane through a series of redox reactions, whereby the electrons are always passed on to a more electronegative redox-partner. The most electronegative molecule is dioxygen, which is reduced as described above by cytochrome c oxidase (complex IV) to water. Approximately 80% of the bodies inhaled oxygen is used in this pathway, which is therefore also referred to as cellular respiration (Halliwell, 2006). Through the energy won through these redox reactions protons are pumped from the mitochondrial matrix into the intermembrane space, thereby causing a proton gradient over the membrane, which in turn powers an ATP synthase.

Even under physiological conditions, however, there is a leak of electrons from this transport chain, mainly at complexes I and III. These free electrons then react with dioxygen within the mitochondrial matrix as well as the intermembrane space to form the superoxide radical (full name: superoxide radical anion; $O_2^{\bullet-}$). Since these electrons come one at a time,

molecular dioxygen can accept them even as triplet oxygen. The rate of leakage is usually less than 5 %, but can increase during hyperoxia (Halliwell, 2006).

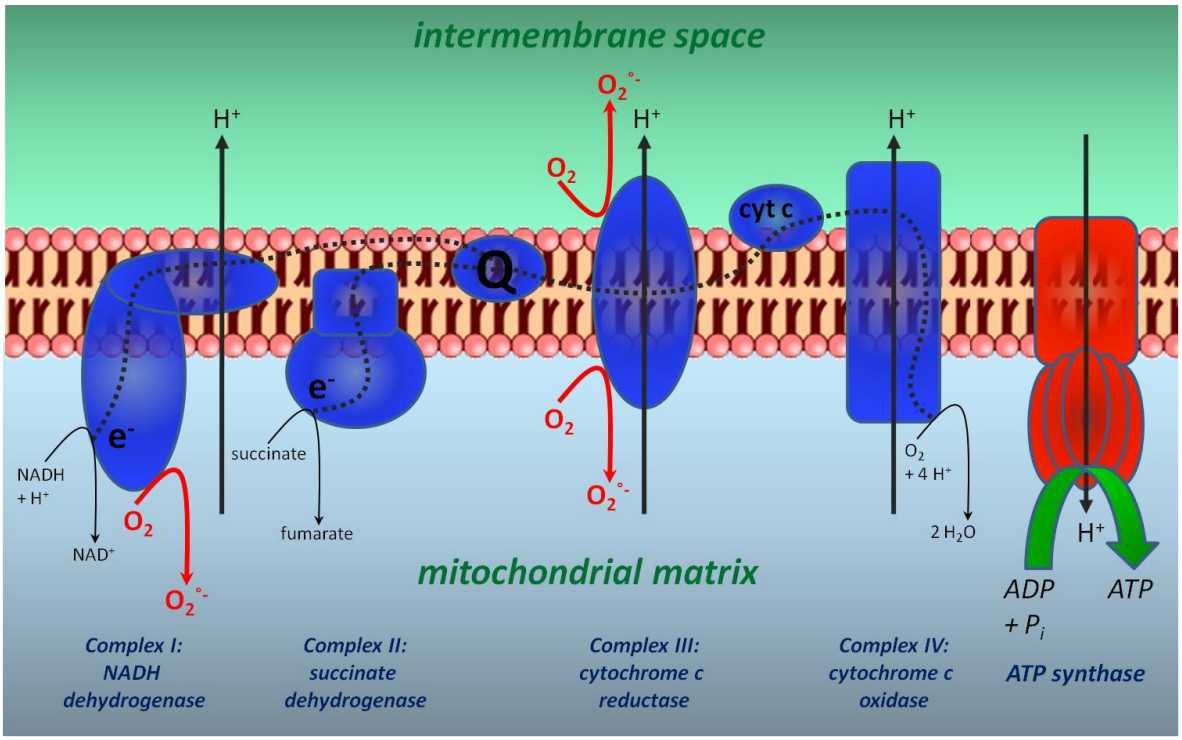

Fig. 1.2_3: Schematic illustration of the electron transport chain along the inner mitochondrial membrane showing common sites of electron leakage and superoxide radical anion ($O_2^{\bullet-}$) formation

The superoxide radical is usually not highly reactive, despite its "super" name, as it has only one unpaired electron left compared to dioxygen (Halliwell, 2006). It is usually reduced through the so called dismutation reaction ($2\ O_2^{\bullet-} + 2\ H^+ > H_2O_2 + O_2$), which can occur spontaneously or be enzymatically catalyzed through superoxide dimutases (SODs; see section on antioxidant enzymes) (Maier & Chan, 2002), but also reacts with nitric oxide ($NO^{\bullet}$) to form peroxynitrite ($ONOO^-$), linking the production of ROS to equally toxic reactive nitrogen species (RNS). The resulting hydrogen peroxide from the dismutation is then often broken down during Fenton reaction ($H_2O_2 + Fe^{2+} > Fe^{3+} + OH^{\bullet} + OH^-$), whereby the hydroxyl radical ($OH^{\bullet}$) is formed. $OH^{\bullet}$ is one of the most reactive chemical species known and can damage cellular macromolecules by oxidizing them (Maier & Chan, 2002).

Another major source of hydrogen peroxide and potential hydroxyl radicals is as a byproduct of enzymatic oxidation (e.g. through xanthine oxidase, NADPH oxidases or cythochromes P450). Especially relevant thereof in this context is the enzymatic degradation of monoamines through monoamine oxidases (MAOs). Hereby the monoamine is converted

into an aldehyde with H_2O_2 and ammonia as byproducts (**R**$CH_2NH_2 + O_2 + H_2O$ > **R**$CHO + H_2O_2 + NH_3$) (Halliwell, 2006).

Apart from the aforementioned, other molecules can turn into ROS, often through contact with another ROS (radical chain reaction) or as a byproduct of enzymatic catalyzation.

Table 1.2_1: List of common reactive oxygen species (ROS) (*modified from Halliwell, 2006*)

Free radicals	Non-radicals
Superoxide $O_2^{\bullet-}$	Hydrogen peroxide H_2O_2
Hydroxyl OH°	Hypobromous acid HOBr
Hydroperoxyl $HO_2^{\bullet}$	Hypochlorous acid HOCl
Carbonate $CO_3^{\bullet-}$	Ozone O_3
Peroxyl $RO_2^{\bullet}$	Singlet oxygen $^1\Delta g$
Akloxyl RO°	Organic peroxides ROOH
Carbon dioxide radical $CO_2^{\bullet-}$	Peroxynitrite $ONOO^-$
Singlet oxygen $O_2\ ^1\Sigma g^+$	Peroxynitrate O_2NOO^-
	Peroxynitrous acid ONOOH
	Peroxomonocarbonate $HOOCO_2^-$
	Nitrosoperoxycarbonate $ONOOCO_2^-$

1.2.2 Antioxidant defense mechanisms and oxidative stress

The primary defense mechanisms of aerobic organisms against oxidative damage can be divided into two categories: antioxidant enzymes (AOEs) or non-enzymatic reducing agents. Both systems act in synergy with each other and overlap at the glutathione system. Additionally it is discussed, whether a subgroup of ether lipids (plasmalogens) could be involved in antioxidant defenses by acting as radical scavengers within cellular membranes. Antioxidant defense is mainly carried out within the cytoplasm, but also in cellular organelles; mainly in mitochondria and peroxisomes. The main group of AOEs consists of superoxide dismutases (SODs), catalase (CAT) glutathione peroxidase (GPx) and its synergist glutathione reductase (GR). The expression of genes encoding for most antioxidant enzymes is regulated through the transcription factors nuclear factor (erythroid-derived 2)-like 2 (Nrf2) and peroxisome proliferator-activated receptors (PPARs).

There are, however, a variety of other enzymes that are important in antioxidant pathways, such as different peroxidases, oxidases and reductases (Matés, 2000). A group of

peroxidases that have been the center of attention regarding brain antioxidant defenses are peroxiredoxins, which reduce both molecular hydrogen peroxide as well as organic peroxides (**R**O=O**R**), by offering a reducing SH group which is oxidized by the peroxide to sulfenic acid (SOH), thereby turning the organic peroxide into an alcohol. Some peroxiredoxins (2-Cys) have two SH groups, whereby the other reacts with the SOH groups forming a disulfide bond which in turn is now reduced by thioredoxin. Peroxiredoxins have a lower catalytic rate compared to other peroxide reducing enzymes, like CAT or GPx, although this is compensated for by large concentrations and low Michaelis constant for H_2O_2. A problem with peroxiredoxin pathways is that the enzymes are inhibited and also readily oxidized by hydrogen peroxide, whereby low levels of H_2O_2 can be cleared by peroxiredoxins, but increasing amounts will inhibit the detoxifying enzymes. This is probably due to the fact that H_2O_2 is also used in cellular signaling as well as in the immune system, wherefore acute increases in intracellular concentrations of hydrogen peroxide should not necessarily be degraded immediately. H_2O_2 then activates the expression of various antioxidant genes, including peroxiredoxin coding genes, leading to an increase in enzyme production to make up for the inhibited and oxidized base content, whereby H_2O_2 can now be degraded after having "done its job". This mechanism, however, backfires during excessive and prolonged hydrogen peroxide increases, making the peroxiredoxin defense mechanism suboptimal during oxidative stress (Halliwell, 2006).

The bulk of ROS is degraded through SODs, CAT and GPx, whereby SODs form the first of a two step degradation and CAT and/or GPx the second. SODs are metalloproteins and are classified depending on the metal ion in their active centers. Manganese- containing superoxide dismutases (MnSOD; SOD2) are found within the mitochondrial matrix, whereas SODs with copper and zinc (CuZnSODs) are found either in the cytoplasm and mitochondrial intermembrane space (SOD1) or in the interstitium (SOD3). SODs have also been reported in peroxisomes of rats (Wanders & Denis, 1992; Kira, Sato & Inoue, 2002) and humans (Kira, Sato & Inoue, 2002), while other papers refute these findings in both species (Kobayashi et al., 1993; Liou et al., 1993). In plants the results are clearer, since many species appear to have peroxisomal SODs, like peas (del Río et al., 2003), peppers (Mateos et al., 2003), tomatoes (Kuzniak & Sklodowska, 2005) and watermelons (Sandalio et al., 1997; Rodríguez-Serrano et al., 2007).

As mentioned before the action of SODs is to enzymatically combine superoxide radicals in order to form hydrogen peroxide (dismutation reaction), thereby converting one reactive oxygen species into another. It is therefore necessary for healthy antioxidant capacities that cells have SODs as well as hydrogen peroxide degrading enzymes. Out of these catalase is limited only to H_2O_2 degradation and does not peroxidize organic peroxides (Aebi, 1984). It is one of the most efficient enzymes known to exist, being able to catalyze over 40 million molecules each second (Goodsell, 2004) and therefore being unable to be saturated with its substrate (Lledías et al., 1998). Catalase is a homoquadromer heme-containing metalloprotein which converts hydrogen peroxide into dioxygen and water ($2\ H_2O_2 > 2\ H_2O + O_2$). This two-step reaction starts with a reduction of the first hydrogen peroxide molecule to water, whereby the second O-atom is transferred to the heme-containing region of the enzyme. Hereby the Fe^{3+} is converted through the loss of its electron and the addition of O to Fe^{4+}=O, wherefore the heme is now a cation radical, which may now oxidize the second H_2O_2 molecule, turning over the O-atom and being reduced back to its original state in the progress.

The alternative mechanism of H2O2-degradation is the glutathione system, which also degrades organic peroxides. Hereby the tripeptide glutathione (GSH) functions as a reducing agent and is reduced itself in a second enzymatic reaction to its original state. The reduction of glutathione to glutathione disulfide (GSSG) through a donation of an electron to the peroxide substrate is catalyzed through selenium-dependent glutathione peroxidase (GPx) and produces water or an alcohol (**R**OH). GSSG is then reduced back to GSH through glutathione reductase (GR), whereby an electron is transferred from NADPH (Dringen, Pawlowski & Hirrlinger, 2005).

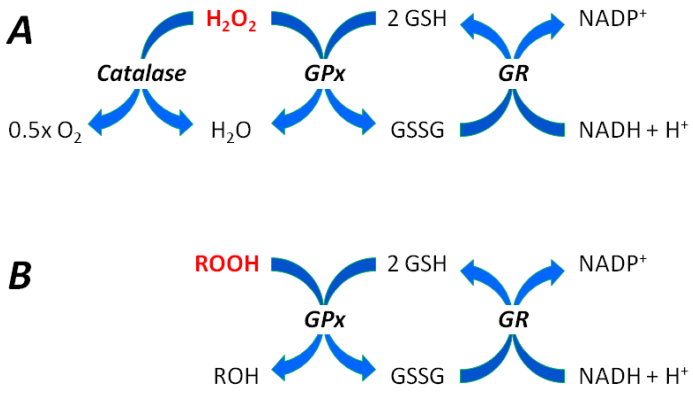

Fig. 1.2_4: Degradation of hydrogen peroxide (A) and organic peroxides (B) through catalase and the glutathione system; *GR: glutathione reductase, GPx: glutathione peroxidase, GSH: glutathione, GSSG: glutathione disulfide (modified from Dringen, Pawlowski & Hirrlinger, 2005*)

Apart from enzymatic antioxidant defense, many reducing agents exist in most cells. Major examples hereof are vitamins A (retinol), C (ascorbic acid) and E (α-tocopherol), b-carotene, melatonin, uric acid, NADPH and coenzyme Q_{10} (ubiquinol) as well as metallothionein, polyamines, adenosine, urate, polyphenols, flavonoids, phytoestrogens, cysteine, homocysteine, taurine, methionine, *s*-adenosyl-L-methionine, resveratrol, nitroxides & plasmalogens (Matés, 2000). The role of plasmalogens in this list is insofar extraordinary as they are not soluble molecules, but rather a group of etherlipids which make up between 20 % and 55% (tissue dependent) of biological membranes. They contain a vinyl ether at the *sn*-1 position of their glycerol backbone and are therefore highly targeted by ROS. It has been argued that this functions as a radical scavenging system to protect the integrity of membranes as well as membrane proteins. This interpretation is, however, highly controversial, since a reduction of plasmalogens through ROS does not break the chain of oxidative damage, but rather leads to the formation of other highly toxic ROS. It is therefore not clear, whether or not plasmalogens actually have antioxidant properties (Lessig & Fuchs, 2009).

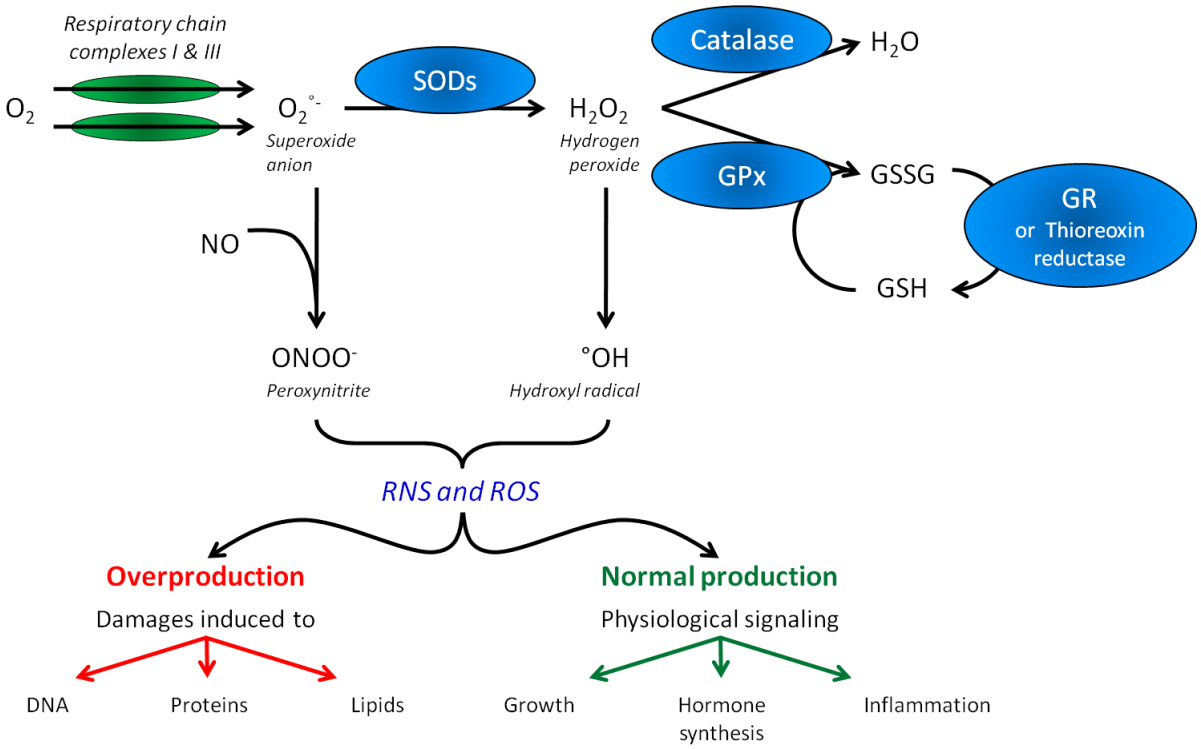

Fig. 1.2_5: Overview of the major ROS generating and degrading pathways (*based on Bellance, Lestienne & Rossignol, 2009*)

Under normal physiological circumstances there is a constant production of ROS, which are degraded through cellular antioxidant mechanisms. If this equilibrium is, however, shifted in a way that either the ROS production overcomes the antioxidant systems, the latter underfunction and cannot cope with "normal" intracellular ROS-levels or elevated ROS levels lead to an underfunction of antioxidant defense, in any case the result is a chronic shift towards prooxidant conditions in the body. This state of disequilibrium is referred to as oxidative stress (Reddy & Yao, 1996; Matés et al., 2000; Emerit, Edeas & Bricaire, 2004; Dringen, Pawlowski & Hirrlinger, 2005). Oxidative stress is assessed through the measurements of (by)product of peroxidation of lipids, proteins and/or DNA. Lipid peroxidation is classically measured through quantification of malondialdehyde (MDA) through a ThioBarbituric Acid Reactive Substances (TBARS) assey during which the resulting red fluorescent derivative is detected spectrophotometrically. Aldehydes like MDA or 4-hydroxynonenal (4-HNE) often react with proteins leading to the formation of protein carbonyl groups. These are made to react to hydrazones in a 2,4-dinitrophenylhydrazine (DNPH) assey, which can be quantified through fluorescence measurements or using spectrophotometry (Castegna, et al. 2003). Finally DNA also reacts with MDA which leads to the adduction of the carcinogenic molecule pyrimido[1,2-*a*]purin-10(*3H*)-one (M_1G). Different assays for M_1G can be performed based on mass spectrometry or immunochemical techniques (Marnett, 1999a; 1999b).

1.2.3 Pro- and antioxidant metabolism in the brain

Since the mammalian brain is by far the most extremely oxygenated of all organs it is highly susceptible to oxidative damage. Making up only approximately 2% of the body's weight in humans, the cells of brain utilize 20% of the consumed oxygen (Clarke & Solokoff, 1999). The main reason for this high oxygen turnover is the extraordinary amount of ATP needed for the regulation of cellular membrane potentials via Na^+/K^+-ATPases. As previously mentioned, ATP is won primarily through mitochondrial respiratory chain activity. In neurons this means that a high risk for the formation of superoxide radicals through electron leakage exists. Since all areas of the brain contain SODs, the superoxide radicals can be dismutased leading to the production of H_2O_2. But also others of the aforementioned fonts of ROS are of high importance in neuronal tissue. First of all, since neurons and astrocytes are metabolically very active cells, they produce a major amount of intracellular hydrogen and organic peroxides through enzymatic activity. On the one hand there are neurotransmitter-

degrading enzymes like monoamine oxidases, which produce both H_2O_2 as well as aldehydes. On the other hand enzymes like cyclooxygenases or lipoxygenases produce specific organic peroxides (Dringen, Pawlowski & Hirrlinger, 2005). High oxygenation also leads to increased levels of autoxidation of aromatic compounds to quinones (Stokes et al., 1999).

Apart from these previously mentioned mechanisms of ROS production the brain also has specific risks which make it especially vulnerable to oxidative stress: (a) Brain tissue is highly saturated in polyunsaturated fatty acids (PUFAs) which are common targets of membrane tissue peroxidation (Kuhn & Borchert, 2002). (b) Neurons suffer from the neurotransmission-linked Ca^{2+}-influx, both in presynaptic buttons, where Ca^{2+} enters the neurons due to voltage-gated channels that open upon an action potential in order to allow for Ca^{2+}-dependent fusion of vesicular and presynaptic membranes during exocytosis, as well as postsynaptically in NMDAR-expressing neurons, since the NMDAR is also a Ca^{2+}-channel. Ca^{2+} activates neuronal nitric oxide synthase (nNOS). Aditionally the brain produces NO° through endothelial NOS (eNOS) as well as inducible NOS (iNOS) from activated microglia. NOS and superoxide radicals from the highly toxic ROS peroxynitrite ($ONOO^-$) (Emerit, Edeas & Bricaire, 2004). (c) Some areas of the brain, like substantia nigra, caudate, putamen and pallidum, are rich in metal ions like iron, which increase the risk of ROS formation (Schenck & Zimmerman, 2004). Also many brain proteins contain iron, such as hemoglobin, cytochromes, ferritin, aconitases, non-heme iron proteins in the mitochondrial electron transport chain, cytochromes P450, and tyrosine and tryptophan hydroxylases (Halliwell, 2006).

In contrast, the antioxidant capacities of the brain are relatively poorly developed. Neurons have extremely low levels of catalase (Arnold & Holtzman, 1978; Holtzman, 1982), which even decrease with maturation (Ahlemeyer et al., 2007). Most catalase in the brain is located in astrocytes which play an important part in maintaining the brain's redox homeostasis (Ahlemeyer et al., 2007; Fisher, 2010). The brain's most common mechanism of enzymatic peroxide degradation appears to be through peroxi- and thioredoxins, which are, however, probably not suited for detoxification of severely increased H_2O_2 levels as may occur in the brain (see above; Halliwell, 2006). The degradation of H_2O_2 through GSH/GpX/GR appears to be the major means of preventing oxidative stress under normal brain-physiological conditions, but is has been shown that, as is the case for catalase,

neurons contain relatively low amounts of GSH, which is mainly found in astrocytes (Halliwell, 2006). Over all, calculation of a specific H_2O_2-detoxification rate constant ($D = p^{-1} \times t_{1/2}^{-1}$; p, protein content in mg; $t_{1/2}$, half-time in min; calculated for the detoxification of 100 μM H_2O_2) showed that neurons have the lowest peroxide disposal rate compared to other cells in the nervous system (Dringen, Pawlowski & Hirrlinger, 2005).

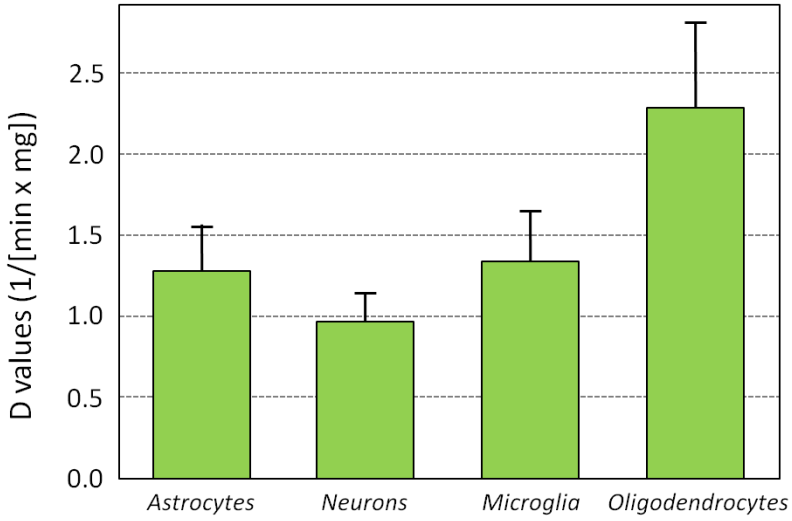

Fig. 1.2_6: Comparison of specific H_2O_2-detoxification rate constants (D) between different cell types in nervous tissue; *A: astrocytes, N: neurons, M: microglia; O: oligodendrocytes (modified from Dringen, Pawlowski & Hirrlinger, 2005*)

Due to this high vulnerability for redox disequilibrium in the brain, oxidative stress has been reported in a number of neurodegenerative diseases. Examples hereof are Parkinson's (Jenner, 2005; Chinta & Andersen, 2008), Huntington's (Emeric, Edeas & Bricaire, 2004), Alzheimer's diseases (Moreira et al., 2005a; 2005b; 2005c; 2005d) and schizophrenia (see following chapter).

1.3 Dopamine - Metabolism, transmission and neurotoxicity

Since dopamine trafficking is widely considered to play an important role in the aethiopathogenesis of schizophrenia and since it is elemental to the argumentative line of this thesis, it as well as several aspects of its neurochemistry, -anatomy and -(patho)physiology shall be discussed in the following chapter. Aim of the chapter is to build argumentative bridges between the metabolism and neurotransmission of dopamine and possible neurotoxic effects of (hyper)dopaminergia as well as interactions with the glutamatergic system.

1.3.1 Dopamine metabolism - synthesis and degradation:

The biogenic monoamine dopamine was first described as a proper neurotransmitter, rather than only a precursor to noradrenalin, under the name of 3-hydroxy-tyramine by Arved Carlsson in 1958 (Carlsson et al., 1958) as was reaffirmed shortly after as an endogenous neurochemical agonist independently distributed of its derivative noradrenalin (Bertler & Rosengren, 1959a; 1959b).

Dopamine is mainly synthesized in the CNS and to a lesser extent in the postganglionic neurons of the sympathetic nervous system, including the chromaffine cells of the adrenal medulla, from the aromatic amino acid tyrosine. Like noradrenaline/norepinephrine and adrenaline/epinephrine it therefore belongs the group of catecholamines. The pseudo-essential amino acid tyrosine can either be taken up into the body through food or can be synthesized in the liver from the essential amino acid phenylalanine by the enzyme phenylalanine hydroxylase. It is taken up into catecholaminergic neurons and chromaffine cells and then converted through cytoplasmic tyrosine hydroxylase (TH) to 3,4-dihydroxyphenylalanine (DOPA). This is the rate-limiting step in catecholamine synthesis. It is very common to refer to DOPA, slightly more accurately, as L-DOPA or levodopa. Since, however, all biologically active enantiomers of the catecholamine synthesis (as well as most other bioactive substances in humans) share the L-chirality, for reasons of simplicity, unless otherwise stated, e.g. as in D-serine, all enantiomers are of L-chirality.

DOPA, unlike dopamine, is able to cross the blood brain barrier and is therefore commonly used in the pharmacotherapy of Parkinson’s disease. It is, whether if given as a

supplement or synthesized endogenously, converted in the cytoplasm into mature dopamine through the enzyme DOPA-decarboxylase (DDC). Dopamine is then taken up into synaptic vesicles through the amine/proton antiporter vesicular monoamine transporter 2 (VMAT2), also known as solute carrier family 18, member 2 (SLC18A2) (Eiden et al., 2004). In dopaminergic neurons, and also to a low percentage in the sympathetic nervous system and adrenal medulla, it is stored here and secreted during action potential controlled Ca^{2+}-dependent exocytosis. In (nor-)adrenergic cells it is converted further through the vesicular emzyme dopamine-β-hydroxylase (DBH) into noradrenaline.

Apart from the conversion into noradrenaline through DBH, dopamine is degraded in homovanillic acid (HVA) through a two-step reaction by the enzymes catechol-*O*-methyltransferase (C*O*MT) and monoamine oxidase (MAOA and MAOB) in synergy with aldehyde dehydrogenase (AD). Hereby enzymatic degradation first through C*O*MT leads to the intermediate product 3-methoxytyramine (3-MT), whereas MAOs/AD convert dopamine into 3,4-dihydroxyphenyl acetic acid (DOPAC) (Eisenhofer, Kopin & Goldstein, 2004).

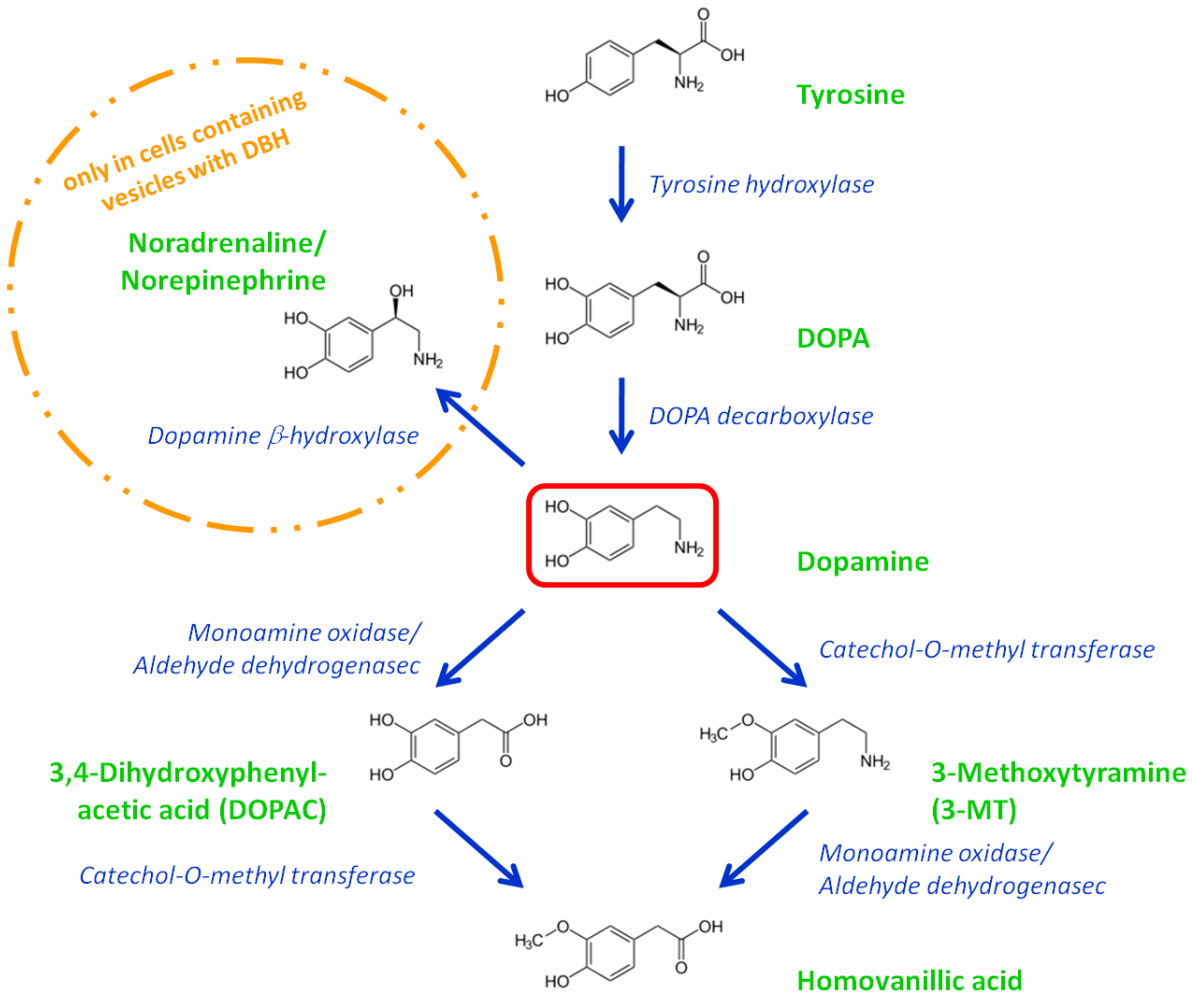

Fig. 1.3_1: Enzymatic dopamine metabolism

1.3.2 The dopaminergic synapse

The storage of dopamine within synaptic vesicles is mainly regulated through VMAT2, which is essential for the stability of the transmitter as well as the health of the dopaminergic neurons due to reduced toxicity of dopamine within the vesicle (Miyazaki & Asanuma, 2008; Sulzer & Zecca, 1999), whereby there is a constant equilibrium between dopamine uptake and diffusion into the cytoplasm (Eisenhofer et al., 2004; 2008). The disruption of this equilibrium is thought to be involved in increased dopamine neurotoxicity and shall be discussed in a later chapter.

Upon an action potential reaching the axonic terminal button (or the chromaffine cell through a *pre*ganglionic sympathetic cholinergic neuron) there is an influx of Ca^{2+} through voltage-gated channels which leads to the fusion of the vesicular and the target SNAREs (**s**oluble **N**-ethylmaleimide-sensitive factor **a**ttachment protein **re**ceptors) which in turn allows for the exocytotic fusion of the vesicular membrane to the presynaptic membrane of the terminal button (Drenckhahn, 2003) and the release of dopamine into the synaptic cleft.

Dopamine binds to one of five types of dopamine receptors (numbered D1 through D5 and encoded for by the genes DRD1 through DRD5), whereby the dopamine receptors D_1 and D_5 form the D_1-like family and the receptors D_2 through D_4 form the D_2-like family (Girault & Greengard, 2004). All dopamine receptors are G-protein coupled metabotropic transmembrane proteins working through the adenyl cyclase (AC), cyclic adenosine monophosphate (cAMP) & protein kinase A (PKA) second messenger system, whereby D_1-like receptors activate AC through the G_s alpha subunit and the D_2-like receptors inhibit AC through the G_i alpha subunit (Civelli et al., 1991a; 1991b; Neves at al., 2002). Most dopamine receptors are found postsynaptically, however, the D_2-receptor has two isoforms - a long and a short form, differentiated through a sequence of 29 amino acids - (Civelli et al., 1991b), whereby the short form acts as a presynaptic autoceptor (Castellano et al., 1993; Elsworth & Roth, 1997; Jomphe et al., 2005).

Dopamine action is terminated primarily through removal of the transmitter from the synaptic cleft through the dopamine active transporter (DAT), also known as the solute carrier family 6, member 3 (SLC6A3). It is a Na^+ and Cl^- (2:1 per dopamine molecule) co-transporter powered through an ion concentration gradient generated through a Na^+/K^+-ATPase. After reuptake into the presynaptic neuron via the DAT dopamine is either restored into vesicles through VMAT2 or enzymatically degraded through MAOs/AD (Eisenhofer,

Kopin & Goldstein, 2004). In the postsynaptic neuron dopamine is degraded by both COMT and MAOs/AD into homovanillic acid, whereas remaining dopamine in the synaptic cleft is katabolised through postsynaptic membrane-bound COMT (Elsworth & Roth, 1997). In the prefrontal cortex (PFC) neurons express significantly less DAT in comparison to those in the nucleus accumbens (NAcc) or the striatum. In these cases it has been shown in knockout mice that dopamine is taken up into postsynaptic neurons by the norepinephrine [noradrenalin] transporter (NET) (Morón et al., 2002).

An important part of the dopaminergic synapse is the astrocyte, since astrocytes have been repeatedly shown to express DAT, COMT and both MAOs (Fisher, 2010).

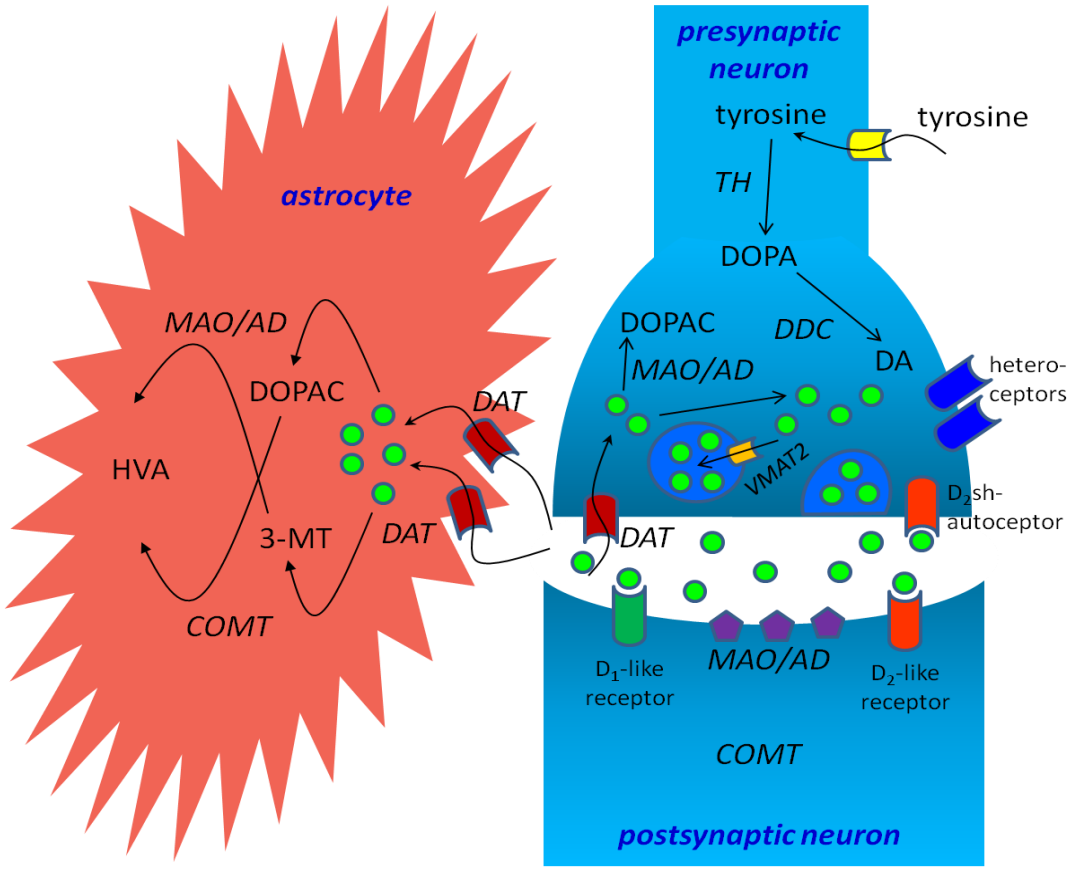

Fig. 1.3_2: Dopaminergic synapse; *3-MT: 3-methoxythyramine, AD: aldehyde dehydrogenase, COMT: catechol-O-methyl transferase, DA: dopamine, DAT: dopamine active transporter, DDC: DOPA decarboxylase, DOPA: 3,4-dihydroxyphenylalanine, DOPAC: 3,4-dihydroxyphenylacetic acid, HVA: homovanillic acid, MAO: monoamine oxidase, TH: tyrosine hydroxylase, VMAT2: vesicular monoamine transporter 2*

1.3.3 Dopaminergic pathways in the mammalian brain

Dopamine synthesis not only occurs in terminal buttons of dopaminergic neurons, but also in their somata, where it is stored into vesicles which are then anterogradely transported by kinesine along axonal microtubules to the synaptic terminals. These long axon bundles form the dopaminergic neuronal pathways. The exact number of these pathways depends upon different nomenclatures, but most authors consider two to three major systems in which dopamine acts as a neurotransmitter (nidrostriatal and mesolimbic [sometimes divided into mesolimbic and mesocortical]) and one in which it has hormonal function (tuberoinfundibular) (Civelli et al., 1991a; Van den Heuvel & Pasterkamp, 2008).

The tuberoinfundibular system is very clearly defined as a group of hypothalamic neurons in the arcuate nucleus of the tuber cinereum that project to the median eminence and infundibulum where they secrete dopamine into the hypophyseal portal vein. It is transported via the bloodstream to the mammotropic acidophilic cells of the anterior pituitary and here inhibits the secretion of the somatotropic hormone prolactin, wherefore dopamine in this pathway is also referred to as prolactin inhibiting hormone (PIH).

The first of the classical dopamine neurotransmitter systems is the nigrostriatal (sometimes called mesostriatal) pathway, which consists of different subpathways emanating from the paranigral and retrorubral nuclei and mainly the substantia nigra pars compacta, running in the median forebrain bundle (MFB) and terminating in the caudate and putamen (dorsal striatum) (Standring (ed.), 2008, *Gray's Anatomy*). It is involved in the modulation of striatal gating and is underfunctioning in patients suffering from Parkinson's disease.

The mesolimbic and mesocortical (sometimes referred to as mesolimbocortical or just mesolimbic) dopamine pathways begin in the ventral tegmental area of the midbrain (VTA) and terminate inter alia in the nucleus accumbens (NAcc) and the prefrontal cortex (PFC) respectively. Since they are both considered essentially dysregulated in patients suffering from schizophrenia (*dopamine hypothesis of schizophrenia*) (Howes & Kapur, 2009), they shall be discussed in more detail in the following section.

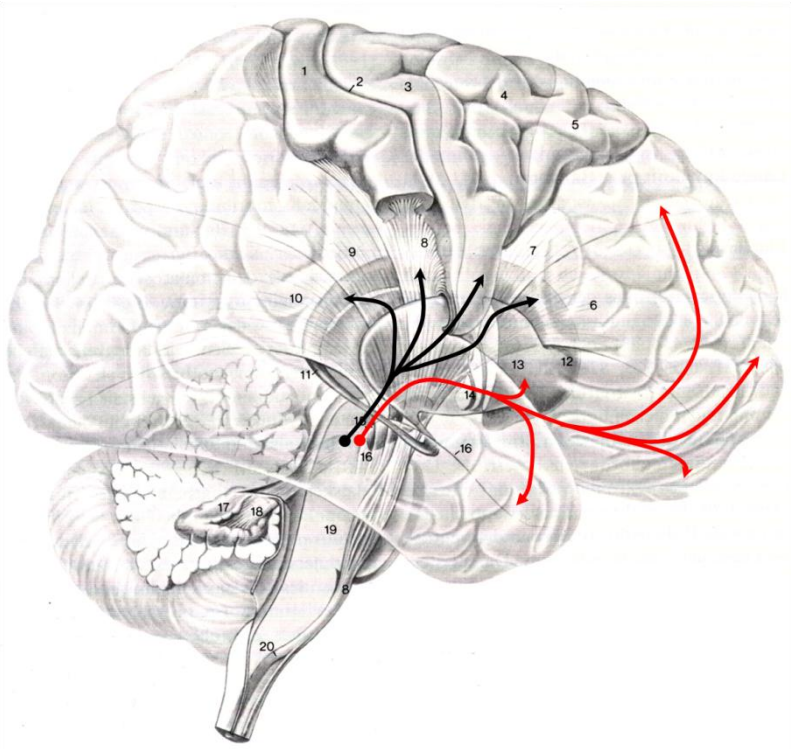

Fig. 1.3_3: Schematic illustration of the nigrostriatal (black) and mesolimbic (red) dopamine systems *(modified from Nieuwenhuys, Voogd & van Huijzen, 2007*)

1.3.4 The mesolimbic dopamine pathways - Specific motivation and Incentive Salience

The mesolimbic and mesocortical dopamine pathways connect the mesencephalic ventral tegmental area (VTA) with structured of the limbic lobe or the areas of the neocortex involved in limbic functions, expressiv verbis the accumbens nucleus (NAcc), amygdala, hippocampus (Hp) and the prefrontal cortex (PFC) (Van den Heuvel & Pasterkamp, 2008). Since the discovery of specific rodent behavior shown when given the opportunity of electrically stimulating their own mesolimbic structures, intracranial self-stimulation, ICSS (Olds & Milner, 1954), it has often been described as the reward pathway of the mammalian brain. Mapping the rat midbrain by using electric self-stimulation revealed that most of the neurons giving rise to ICSS-behavior when stimulated were located in the VTA. Their axons travel into the lateral hypothalamus, form part of the medial forebrain bundle and terminate within a variety of structures of the forebrain. Self-stimulation was described as a rate of at least 500 responses per h for 15 minutes in different trials (Crow, 1972).

Fundamentally in the field of neuroscience these findings clearly established the NAcc and the mesolimbic dopamine pathway as involved in appetitive or specific motivation and positive reinforcement (Salamone, 1994). The specificity of this stimulus-dependent reward pathway sets it apart, both anatomically and functionally, from the unspecific

motivation system ascending from the nucleus basalis MEYNERT within the substantia innominata of the basal forebrain. While the nucleus basalis MEYNERT projects diffusely into the entire cortex and is responsible for curiosity, drive and showing behavior out of one's own volition (Duncker, 1999), the mesolimbic system consists of distinct pathways involved in the positive reinforcement of and approach towards specific conditioned stimuli.

The NAcc is located bilaterally of the septal area and forms part of the ventral striatum. It can morphologically and functionally clearly be distinguished as consisting of two regions - NAcc core and NAcc shell, each with distinctive chemoarchitectural properties as well as different afferent and efferent connections. The NAcc core merges dorsally with the caudate nucleus and the putamen and bears morphological resemblance to these regions. It has therefore been suggested by Haber et al. (1990) that the nucleus accumbens cannot be distinguished from other parts of the striatum. This does not, however, seem to be corroborated by the fact that the dorsal and ventral parts of the striatum receive individual dopaminergic input from different regions within the midbrain (Niewenhuys, Voodg & van Huijzen, 2008).

The main efferents of the NAcc include projections to the PFC via the ventral pallidum and the dorsal thalamus. It also has decending connections to the striatum and substantia nigra and the pontine aspects of the reticular formation, thereby leading to disinhibition of approach behavior. The mesolimbic dopamine system has therefore been described as the Behavioral Activation System (BAS) within the Reinforcement Sensitivity Theory of personality by Jeffery Gray et al. (1982; 1987; Gray & McNaughton, 2000, Pickering & Gray, 2001; McNaughton & Corr, 2004) alongside projections to the PFC from the NAcc and directly from the midbrain (Depue and Collins, 1999; Pickering and Gray, 2001; Knutson and Cooper, 2005). It has also been associated with drug seeking behavior and with both positive as well as negative reinforcement during the development and the maintenance of addiction, since almost every recreational drug has been shown to lead to an increase of DA-signaling to the NAcc (Di Chiara et al., 2004). Since the NAcc also communicates directly with the amygdala and the hippocampus it is apparently involved in emotional learning and positive as well as negative reinforcement during operant learning in a sense of association formation regarding the prediction of future rewards. This was shown in studies on learning in rats with destroyed VTA and NAcc. These animals were still capable

of learning, but showed a lack in motivation to perform reward-bringing behavior (Berridge, 2007).

Importantly, however, during learning a shift in the firing pattern of the nucleus accumbens neurons occurs. Initially the NAcc is activated by unpredictable rewards. If these rewards are however coupled with a specific stimulus, the NAcc will be activated by the now conditioned reward-predicting stimulus, but no longer upon receiving the reward. This reflects the acquired incentive salience of the conditioned stimulus. If the reward-predicting stimulus is presented (and the NAcc activated), but is not followed by a reward, the firing rate of the NAcc is reduced exactly at the time the reward was expected to occur (Schultz, Dayan & Montague, 1997).

Finally it has been shown that repeated stimulation of the NAcc through the same or strongly similar stimuli (e.g. during addiction behavior) leads to a decrease of DA release as well as post-synaptic activation, explaining the so called b-process of hedonic dynamics and, in the clinical context, many of the various symptoms associated with withdrawal. This also leads to an increase in wanting or craving for a specific stimulus of growing incentive salience (Young, Gobrogge & Wang, 2011).

The consequences of mesolimbic hyperfunction will be discussed further under the aspect of the dopamine hypothesis of schizophrenia.

1.3.5 The dopamine hypothesis of schizophrenia

According to Oliver Howes and Shitij Kapur (2009) the evolution of the dopamine hypothesis of schizophrenia underwent three distinct evolutionary steps. The first involvement of the dopaminergic system was suggested as a result of pharmacological studies showing the discovery of antipsychotic drugs (Delay, Deniker & Harl, 1952) and their effects on dopamine metabolism (Carlsson & Linqvist, 1963). The fact that dopamine antagonists alleviated psychosis (Carlsson, Linqvist & Magnusson, 1957; Seeman & Lee, 1975; Creese, Burt & Snyder, 1976; Seeman et al., 1976), whereas dopamine agonists, like amphetamine, could induce psychotic symptoms (Lieberman, Kane & Alvir, 1987), suggested an underlying hyperactivity at dopaminergic synapses in patients suffering from schizophrenia. This first dopaminergic hypothesis focused on the dopamine receptor (Snyder, 1976), but did not link hyperdopaminergia to specific regions of the brain. It could also not explain differences between positive or negative symptomatology or explain the

mechanism, by which an increase of dopaminergic activity could lead to the symptoms observed in schizophrenia (Howes & Kapur, 2009).

A "modified dopamine hypothesis of schizophrenia" was published in 1991 by Davis et al. addressing various issues that had been at odds with the dopamine receptor hyppothesis. Firstly it was shown in many schizophrenic patients that metabolites of dopamine in the cerebrospinal fluid were not generally elevated. Secondly, the fact that clozapine, a drug that has rather low affinity for and occupancy at the D_2-receptor, was superior in treating psychotic symptoms in some patients, combined with post-mortem and PET-studies on D_2- and D_3-receptors in humans, conflicted heavily with the receptor-centered model. Thirdly, findings on differential distribution of various dopamine receptor subtypes, namely higher levels of D_1-receptors in the cortex compared to higher levels of D_2-receptors in the striatum and NAcc, suggested regional differences in erroneous dopamine signaling. The final straw were PET studies showing decrease of prefrontal blood flow and its correlation to schizophrenic symptoms. Davis therefore proposed that schizophrenia resulted as a combination of cortical hypodopaminergia and subcortical hyperdopaminergia, a model that was suggested to explain the occurrence of positive (through striatal hyperfunction) as well as negative (through frontal hypofunction) symptomatology. This model therefore no longer focused on the causal involvement of dopamine receptors, but rather on the transmitter itself. The hypothesis did not, however, explain the origins of dopaminergic abnormalities (Davis et al., 1991).

A third version of the dopamine hypothesis was proposed by Howes and Kapur in 2009 and was called the "final common pathway"-hypothesis by the authors. Instead of focusing singularly on the mesolimbic pathway the authors propose that schizophrenia results from dysfunctions of multiple neuronal systems that lead to cognitive deficits and negative symptoms on the one hand and to hyperactivity of the mesolimbic pathway on the other, this being the cause of psychosis. It has been noted by the authors that this hypothesis should therefore more poignantly be called the "dopamine hypothesis of psychosis-in-schizophrenia".

The underlying idea behind the "final common pathway"-model is that mesolimbic hyperactivity will lead to a state of aberrant salience, namely that the VTA neurons would fire not only with respect to incentively salient stimuli, but rather indiscriminately to a variety of (often completely irrelevant) stimuli. The human mind's need to make sense of

these abnormally salient stimuli or combination of stimuli would then lead to either delusions or hallucinations, whereby the latter would be interpreted as reflection of actual experiences with regard to the aberrant salience. “Thus, dopamine, which under normal conditions is a mediator of contextually relevant saliences, in the psychotic state becomes a creator of saliences, albeit aberrant ones” (Kapur, 2003, page 15). During early onset of schizophrenic episodes (the prodromal phase) patients will often describe noticing stimuli in their environment as more clearly or keenly or with greater awareness. Alternatively this beginning psychosis is often described as an increase in sensory sharpness or brain activity. Colors are described as brighter and more saturated, music is perceived as more meaningful and patients often describe feelings of anticipation, foreboding or even premonition. Finally, irrelevant stimuli are explained cognitively in a “top-down” fashion dependent on the experiences and psychologically relevant themes of each individual, thereby explaining the cultural differences in delusion and hallucination types as well as contents. As soon as an individual has come up with his or her “psychotic explanation” of the aberrantly salient stimuli, new information will be integrated into the preexisting fabrication and new stimuli confirming this fabrication will be specifically sought out according to the patient’s frame of mind. Through this, a patient may experience entire theoretical buildings of aberrant conclusions and fabrications. In many cases these are perceived as acoustic phenomena either in the own voice or in a third voice (Kapur, 2003; Kapur, Mizrahi & Li, 2005). The latter situation is found in extremis in patients who report thought disorders like thought removal, disruption or inputting.

Subclinical disinhibition of incentive salience and mesolimbic dopaminergic action could likely explain early onset cognitive impairment in patients long before the first schizophrenic episodes, but also endophenotypes that focus on failures in sensorimotor gating, e.g. reduction of prepulse or latent inhibition (PPI, LI) or deficiencies in oculomotor efficiency.

In an attempt to integrate many of the various models of the aethiopathogenesis of schizophrenia with the dopaminergic systems and the hypothesis of aberrant insentive salience, the author proposes another dopamine hypothesis of schizophrenia, that, rather than place mesolimbic hyperdopaminergia at the end of the pathogenetic cascade, puts it in the middle and could therefore be coined the “mesolimbic bottleneck theory” of schizophrenia. This model depends upon a number of assumptions:

- Risk factors or vulnerabilities (like genes, substance abuse, social adversity, obstetric complications or infant viral infections etc.) can cause mesolimbic hyperactivity via mechanisms that are both unknown and most likely relatively idiosyncratic.
- Mesolimbic hyperactivity causes cognitive deficits, endophenotypes and full blown psychotic symptoms in schizophrenia through the mechanism of aberrant incentive salience as proposed by the "final common pathway"-model.
- Hyperdopaminergia leads to dopamine neurotoxicity (in form of oxidative stress).
- Dopamine neurotoxicity in turn exacerbates cognitive deficits and causes structural deficits on the molecular, cellular and macroscopic levels (like loss of dendritic arborisation, reduced synaptic connectivity, atypical neurodegeneration, changes in laterality, loss of gray matter volume and cortical glutamate hypofunctionality).
- The reduced glutamatergic activity (primarily through NMDAR hypofunction or even loss of NMDAR transmission in certain neurons or populations of neurons) will in turn lead to further disinhibition of the mesolimbic dopamine pathway turning the neuronal impairments to a self-sustaining vicious cycle.

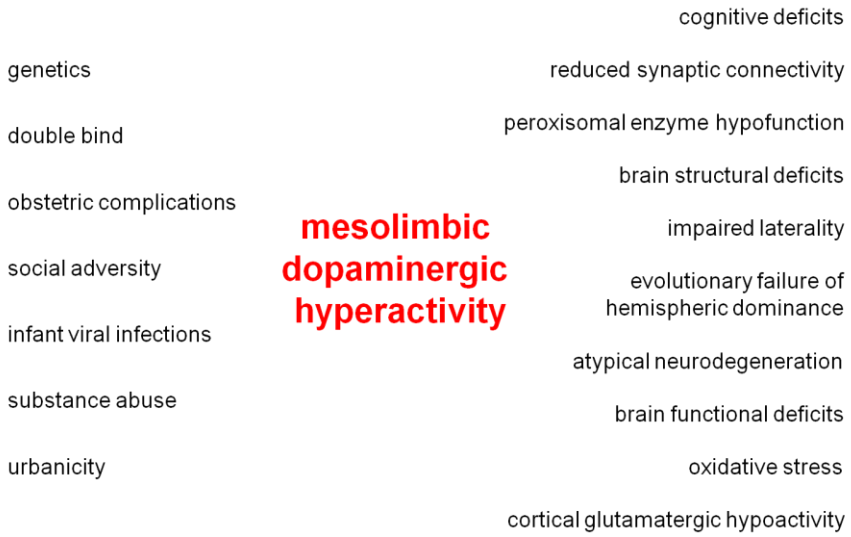

Fig. 1.3_4: Integrative "mesolimbic bottleneck theory" of schizophrenia; *left hand side: possible GxE-interactions leading to mesolimbic hyperdopaminergia; right hand side: signs and symptoms caused by hyperdopaminergia, in some cases sustaining mesolimbic hyperactivity*

Since the proposed model hinges mainly on the latter aspects, namely that hyperdopaminergia leads to dopamine neurotoxicity and dopamine induced oxidative stress and that reduced NMDAR activity in the forebrain in term leads to mesolimbic hypodopaminergia, they shall be discussed in more detail in the following sections.

1.3.6 Dopamine neurotoxicity and dopamine induced oxidative stress

Dopamine neurotoxicity depends widely on dopamine stability and abundance. While dopamine is prone to auto-oxidation in the intra- and extracellular spaces, it appears relatively stable within the presynaptic storage vesicles (Riddle, Fleckenstein & Hanson, 2006). This mechanism is due to differential pH inside the vesicles (pH ca. 5.5) as compared to outside (pH ca. 7.5) (Rudnick & Clark, 1993; Eiden & Weihe, 2011). Substances belonging to the amphetamine family act as potent dopamine releasers from both the synapse and the vesicles, by interacting with both the DAT and VMAT2, being taken up into the presynaptic terminal and vesicles and then reversing the flow-direction of both transporters (Sulzer & Rayport, 1990; Fleckenstein et al., 2007). Dopamine is therefore found in large abundance in the cytoplasm and the synaptic cleft, where is begins to form reactive oxygen species (ROS) not only through auto-oxidation (Riddle, Fleckenstein & Hanson, 2006), but also through enzymatic degradation. The brains of humans or other mammals abusing or treated with amphetamines can therefore be considered as pivotal in vivo models for neurotoxicity and oxidative stress caused by hyperdopaminergia. The ability of amphetamines to release dopamine in the human brain has been shown in methamphetamine users (Laruelle et al., 1995, Wilson et al., 1996; Moszczynska et al., 2004). And indeed, post-mortem gas chromatography-mass spectrometry studies showed significantly elevated levels of malondyaldehyde and 4-hydroxynonenal, both products of oxidative damage, in the caudate, frontal cortex and cerebellum of chronic methamphetamine users compared to controls (Fitzmaurice et al., 2006). The direct connection between these two findings has been examined in animal studies. Reviews suggest that methamphetamine leads to damage of dopaminergic synaptic terminal buttons caused by excessive oxidative stress possibly related to the formation on dopamine-derived oxidation products (Davidson et al., 2001).

Dopamine-induced oxidative stress was also reported in astrocyte cultures (Hirrlinger, Schulz & Dringen, 2002). In vitro neuronal cultures exposed to dopamine show oxidative stress as well as a significant decrease in dendritic spines (Grima et al., 2003).

The activation of antioxidant genes through treatment with 6-Hydroxydopamine in vitro and in vivo was demonstrated in mice by Jakel et al. (2005), whereas more recent studies have shown dopamine to induce activity of Nrf2 (nuclear factor 2), a transcriptional factor that activates the expression of various antioxidant defense pathways by binding to the

antioxidant response element (ARE) in the promoter regions of antioxidant genes, through formation of ROS (Shih, Erb & Murphy, 2007).

The neurotoxicity of dopamine injections into the rat striatum, as measured through death of tyrosine hydroxylase-positive neurons as well as measurements of oxidation products of dopamine, were attenuated by equimolar injections of antioxidants like ascorbic acid or glutathione, which makes the oxidative capacity of excess dopamine more than likely (Hastings, Lewis & Zigmond, 1996).

In a pharmacological model of chronic Parkinson's disease, part of the symptoms of which are generally considered to be caused by dopamine neurotoxicity and dopamine-induced oxidative stress (Chinta & Andersen, 2008), even showed significant reduction of morphological, biochemical and behavioral Parkinson's markers, when mice were pretreated with rosiglitazone, a PPARγ (peroxisome proliferator active receptor γ)-agonist and activator of antioxidant transduction pathways (Schintu et al., 2009). PPAR-agonists have since been suggested as therapeutic targets in the treatment of Parkinson's (Chaturvedi & Beal, 2008). Similar results were found when Parkinson's animals were treated with various cannabinoids of different receptor selectivity, also suggesting that the antioxidant capacity of these plant-derived agents protect neurons against dopamine neurotoxicity (Lastres-Becker et al., 2005).

The biochemical mechanisms of dopamine neurotoxicity are auto-oxidation on the one hand and formation of ROS byproducts during enzymatic degradation on the other.

Dopamine has been shown to form highly reactive quinones through enzymatic action, presence of metal ions and spontaneous auto-oxidation, thereby causing damage to intracellular macromolecules like lipids, proteins or even nucleic acids (Stokes et al., 1999, Sulzer & Zecca, 1999). The quinone formation and therefore the cytotoxic potential is higher in dopamine compared to other catecholamines, due to the fact that dopamine oxidizes to quinones faster and reduces back more slowly (Graham, 1978; Graham et al., 1978).

Dopamine degradation through MAOs leads to the formation of the byproduct H_2O_2 (Maker et al., 1981), which has high potential of producing ROS like hydroxyl radicals (OH°) through the Fenton reaction (Stokes et al., 1999). These in turn increase the rate of auto-oxidation of dopamine to dopamine-quinone (Nappi et al., 1995) creating a vicious cycle of positive reinforcement between these two pathways of dopamine neurotoxicity through ROS formation.

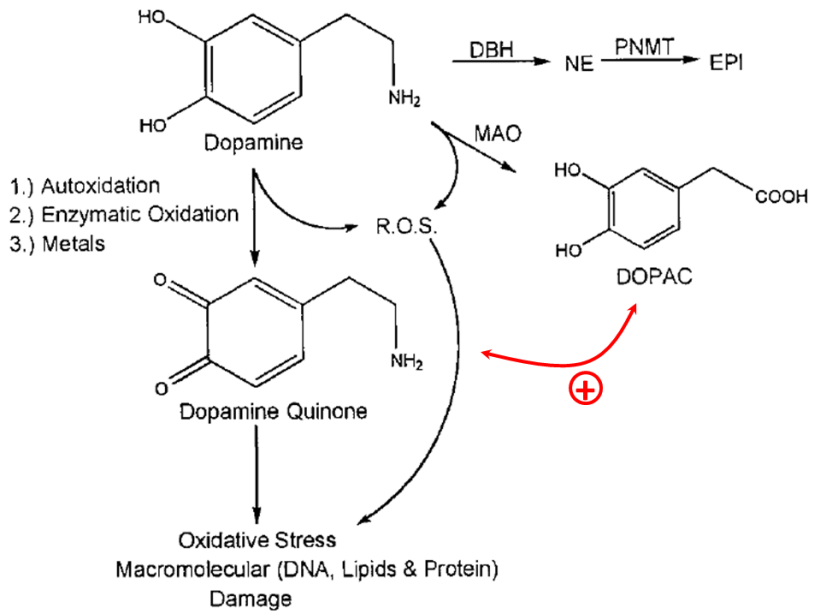

Fig. 1.3_5: Biochemical mechanisms of dopamine neurotoxicity and dopamine induced oxidative stress (*modified from Stokes et al., 1999*)

1.3.7 Oxidative stress in schizophrenia

Albeit prone to fall victim to oxidative damage, not only through dopamine neurotoxicity, the brain is poorly equipped with antioxidant defense mechanisms (Halliwell, 1992, 2006). It is therefore not overly surprising that many researchers attribute various neuropathologies to oxidative stress. Especially for Parkinson's disease and schizophrenia countless papers have linked these disorders of dopaminergic neurotransmission to dopamine neurotoxicity and oxidative stress.

Several studies have been published over the last thirty to forty years showing alterations of antioxidant enzyme levels and activities in blood cells of patients suffering from chronic schizophrenia (Glazov & Mamzev, 1976; Golse et al., 1978; Abdalla et al., 1986; Reddy et al., 1991; Mukherjee et al., 1996) as well as increases in plasma lipid peroxidation products (Prilipko, 1984; Peet at al., 1993; Mahadik et al., 1995; 1998) or both (Ranjenkar et al., 2003; Zhang et al., 2006). More recent studies even found significant correlations between antioxidant enzyme activities and levels of lipid peroxidation products in the blood of schizophrenic patients and measures of psychopathology (Li et al., 2006; Zhang et al., 2006).

Addressing the issues of inferences of blood data on CNS metabolism, these findings have been corroborated through studies on post-mortem brain samples taken from schizophrenic patients and compared to matched controls. Results show membrane

phospholipid abnormalities, altered glutathione redox state and increased nitric oxide radicals (Yao, Leonard & Reddy, 2000; 2004; 2006) and overall impairments of the fatty acid composition (Horrobin et al., 1991; McNamara et al., 2007). Examinations of levels of thiobarbituric acid reactive substances (TBARS), another harmful lipid peroxidation product, also revealed elevated levels in the CSF of schizophrenic patients (Pall et al., 1987; Lohr et al., 1990).

Overall, although there are many findings that suggest significant oxidative damage or oxidative stress in schizophrenic patients, there are major confounding factors like typical vs. atypical neuroleptical therapy, schizophrenia type, age of onset and duration since onset. It is therefore difficult to find clear correlations between schizophrenic symptoms and oxidative stress. Furthermore the question of causal relationship - the chicken and the egg issue - cannot be answered through status quo analyses of schizophrenic patients.

Research therefore calls for different approaches to this topic, like endophenotype research in healthy and/or subclinical subjects or animal studies in which schizophreniform phenotypes can be induced specifically and controlled regarding the emergence of oxidative damage or antioxidant responses.

The two most common pharmacological models for schizophrenia in rodents are the amphetamine- and NMDAR-antagonist-models. Since the mechanism of amphetamine-induced hyperdopaminergia (as described above) is less representative of likely metabolic alterations in the human schizophrenic brain, the model of NMDAR-antagonists seems the more internally and externally valid, since it appears to lead to an increase in endogenous dopamine pathway activity. Furthermore it mirrors the concept of schizophrenia being described as “dopaminergic noise and glutamatergic silence” (conference statement by Bernd Gallhofer, 2010), thereby allowing for a possible combination of two of the major described schizophrenia-theories into one conjoint model. The advances of this model and the most-likely connection between the glutamatergic and dopaminergic systems shall therefore be described in the next paragraph.

1.3.7.1 NMDAR blockage leads to an increase in mesolimbic dopamine release: The associations of the glutamatergic system, especially the NMAR linked neurotransmission, to schizophrenic symptoms are observed clearly in humans, non-human primates and other mammalian species. Firstly, drugs blocking the NMDAR, like Ketamin, Phencyclidin

(Phenylcyclohexylpiperidin, PCP) and Dizocilpine (MK-801) lead to a specific schizophreniform phenotype both observed in overt behavior and in endophenotypical research (e.g. PPI-inhibition) (Luby, 1959; Long, Malone & Taylor, 2006). Secondly, patients with a past history of schizophrenia exhibit pronounced and sustained relapses after taking NMDAR-blockers (Domino and Luby, 1981; Braff, Geyer & Swerdlow, 2001; Yui et al, 1999a; 1999b; 1999c).

This does not, however, answer the question whether this is an independent mechanism or whether there is a neuronal connection between NMDAR-transmission and mesolimbic dopamine release in a direction that blocking the NMDAR leads to an increase in dopamine in the striatum (especially the NAcc) and other regions of the forebrain.

PCP was shown to be a potent blocker of the NMDAR in the early 1980s, by when it had become a major recreational drug since its availability for this purpose under the name “angel dust” in the 1960s (Lodge & Anis, 1982). MK-801 was identified as another NMDAR-antagonist shortly thereafter (Coan, Saywood & Collingridge, 1987).

An increase of dopamine was observed in microdialysis studies after NMDAR-blocking using MK-801 in different regions of the rat brain, namely the striatum and the NAcc (Loscher, Annies & Hönack, 1991; Mathé et al., 1996) as well as the medial PFC (Kuroki et al., 1999). Apart from its role in NMDAR-antagonism, PCP was also shown to block dopamine reuptake (Pechnick, Bresee & Poland, 2006), although it was shown clearly that the increase of dopamine in the medial PFC, unlike in the striatum, is not mediated through blocking of dopamine reuptake, but rather through increasing dopamine flow to the mPFC from subcortical or even subprosencephalic regions (Nishijima et al., 1996). A similar conclusion, namely that the mechanism of dopamine increase is independently of reuptake-inhibtion was drawn for MK-801 (Wolf et al., 1994). It can therefore be assumed that NMDAR-antagonists activate the mesolimbic and mesocortical dopamine pathways, rather than only inhibit the reuptake of dopamine in the forebrain. These findings from animal studies are also observed in imaging studies performed on human subjects (Kegeles et al., 2000; Laruelle, Kegeles & Abi-Dargham, 2003; Narendran et al., 2005).

Pharmacological influences on PCP- or MK-801 induced hyperdopaminergia as well as disruption of PPI and LI have been described for α_1-adrenoceptor ligands (Mathé et al., 1996; Takahashi, Horikomi & Kato, 2001), 5-$HT_{2A/2C}$-receptor agonists and antagonists (Kuroki et al., 1999), lithium carbonate (Umeda et al., 2006) as well as cannabidiol (Long,

Malone & Taylor, 2006). Unpublished data from PsychoGenics showed attenuation of PCP- or MK-801 induced schizophreniform symptoms in rodents through olanzepine, clozapine, haloperidol and aripiprazole (www.psychogenics.com/pdf/Psychosis.pdf).

It is commonly suggested that neuronal pathways involved in mesolimbic disinhibition through blocking of NMDARs would have to be modulated through GABAergic interneurons which attenuate dopamine production in the VTA as well as release in the NAcc, when activated through the glutamatergic efferents. Upon blockage of NMDARs on these glutamatergic neurons, GABAergic neurons projecting onto mesolimbic dopaminergic neurons would no longer be activated, leading to a disinhibition of the mesolimbic pathway.

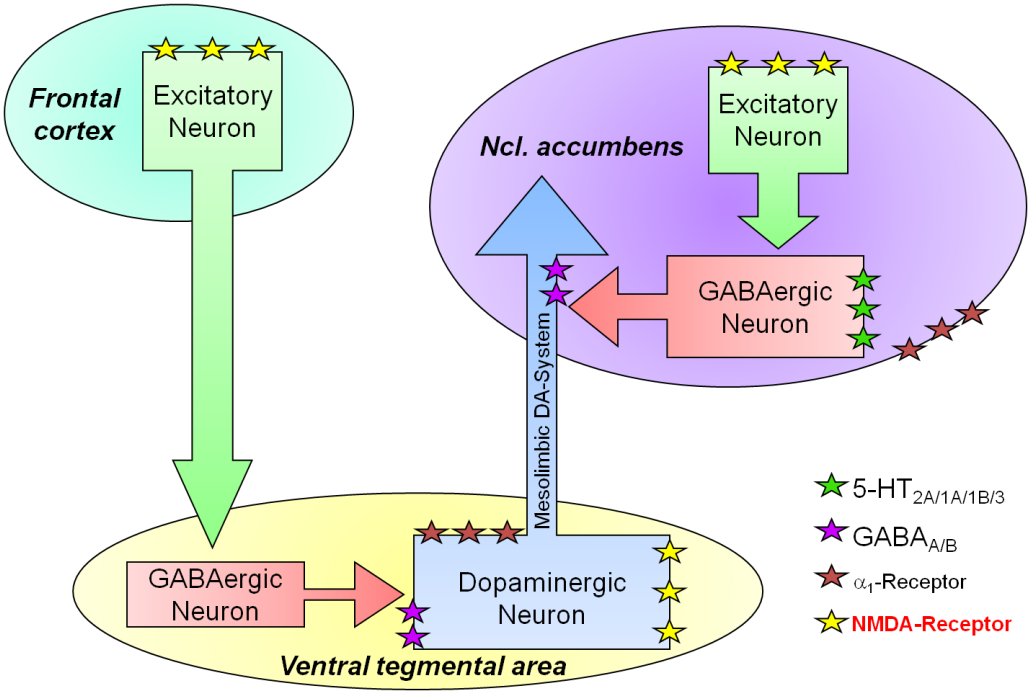

Fig. 1.3_6: Interactions between the (frontal) glutamatergic and the mesolimbic dopamine system showing the mechanism of NMDAR-antagonist induced mesolimbic hyperdopaminergia; inhibition of NMDA-receptors leads to a reduction of GABAergic attenuation and thereby to disinhibition of dopaminergic neurons in the VTA and their axon terminals in the NAcc.

1.3.7.2 Oxidative stress in pharmacological models of schizophrenia using NMDAR-antagonists: Results regarding the influences of selective NMDAR-antagonists are few, but ambiguous. Some studies report antioxidant effects of treatment with NMDAR-blockers in cases of otherwise induced oxidative stress (Drian et al., 1991; Kalonia et al., 2009; da Cunha et al., 2011; Noh et al., 2011), probably through inhibition of glutamatergic excitotoxicity (Gao et al., 2007; Cheng et al., 2008; Sun et al., 2010). Other groups showed that MK-801

could enhance activity of antioxidant enzymes (Harkany et al., 1999; Selakovic, Janac & Radenovic, 2010), which can be interpreted in line with the argumentation that NMDAR-blocking has alternative prooxidant effects which in turn would activate antioxidant defenses, since no direct interaction between NMDAR-antagonists and antioxidant signal transduction has been reported. A study by Bondy & Guo (1996) strengthens this hypothesis by showing that protective effects of MK-801 could not be attributed to antioxidant substance effects.

Experiments in which NMDAR-blockers were given not in combination with other prooxidant treatments showed that these drugs actually induce oxidative damage when given alone (Sharma et al., 1997; Rajdev, Fix & Sharp, 1998; Alva, Palomeque & Carbonell, 2006; Zuo et al., 2007; de Oliveira et al., 2009; da Silva et al., 2010; Radonjic et al., 2010; Wang et al., 2010). These studies often also report subsequent increases in antioxidant defense mechanisms and are therefore in agreement with the interpretation that possible protective mechanisms of NMDAR-blockers are not only mediated through inhibition of glutamate excitotoxicity, but also induce antioxidant systems through their own prooxidant capacities. This supposition is strengthened further by showing that oxidative damage from MK-801 could be attenuated through antioxidant supplements (Ozyurt et al., 2007a; 2007b; Willis & Ray, 2007). Finally, Nasr, Carbery & Geddes (2009) found that NMDAR-antagonists had moderate to no protective effects on striatal degeneration induced through 3-nitropropionic acid (3NP) injections, but rather exacerbated motor deficits caused by 3NP administration. Taken into account that ketamine, PCP and MK-801 are known to decrease sensorimotor gating and induce motor deficits, most likely through mesolimbic dopamine release, these findings seem so support the argumentation on the pro- vs. antioxidant effects of selective NMDAR-blocking.

Taken together, the ambiguity of results could be explained through the assumed interaction between the glutamatergic and dopaminergic systems. It can therefore be assumed that NMDAR-antagonists activate the mesolimbic and mesocortical pathways and thereby induce oxidative damage, which in turn leads to increases in antioxidant defense mechanisms. The MK-801-model of psychosis in animals and the activation of antioxidant metabolism as a measure for the extent of dopamine neurotoxicity can therefore be considered internally valid and shall be used in this thesis.

1.4 Peroxisomes

Peroxisomes are single lipid bilayer membrane organelles found in almost all eukaryotic cells including plant cells. They were first described by Rhodin (1954) in the proximal tubule of the mouse kidneys and referred to by him as microbodies. The name "peroxisome" was given by Christian de Duve (de Duve & Baudhuin, 1966), who was the first to isolate peroxisomes from rat liver and identify them as cell organelles (de Duve, 1969). The name was chosen due to his findings of various oxidases as well as a peroxidase (catalase) within the peroxisome. The phylogenic origins of peroxisomes are still unclear, although the fact that peroxisomal proteins are mostly formed on free ribosomes and imported into the organelles post-translationally, fully folded, oligomeric and co-factor-bound directly from the cytoplasm (Léon, Goodman & Subramani, 2006) suggests a certain degree of (semi)autonomy as found in endosymbionts like mitochondria and chloroplasts. The fact that peroxisomes have no DNA and only a single membrane could be explained by the theory that peroxisomes preceded mitochondria in the phylogenic timeline, which could also explain why, unlike mitochondria, peroxisomes have the capability of degrading ROS and very long chain fatty acids (VLCFAs), but cannot generate ATP (q. v. chapter 1.2). These suggestions have been criticized (Gabaldón & Capella-Gutiérrez, 2010) and other mechanisms of peroxisomal biogenesis involving the ER have been discussed (Hoepfner et al., 2005; Kim et al., 2006; Titorenko & Mullen, 2006). Studies on peroxisomal ontogeny suggest that these finding do not, however, necessarily exclude the possibility of endosymbiotic peroxisomal origins (see following section).

1.4.1 Peroxisomal ontogeny and metabolism

Out of the over 80 genes encoding for peroxisomal proteins found in *Homo sapiens*, roughly three quarters encode for metabolic enzymes, whereas the other 20 are involved in peroxisomal ontogeny, proliferation and maintenance (Schrader & Fahimi, 2008). The group of proteins expressed from these genes is referred to as peroxins and numbered continuously (e.g. peroxin 1, Pex1p; encoded by the PEX1 gene).

Preperoxisomal vesicles are generated both through division of existing peroxisomes as well as through budding off of the ER (South & Gould, 1999, Kim et al., 2006; Titorenko & Mullen, 2006).

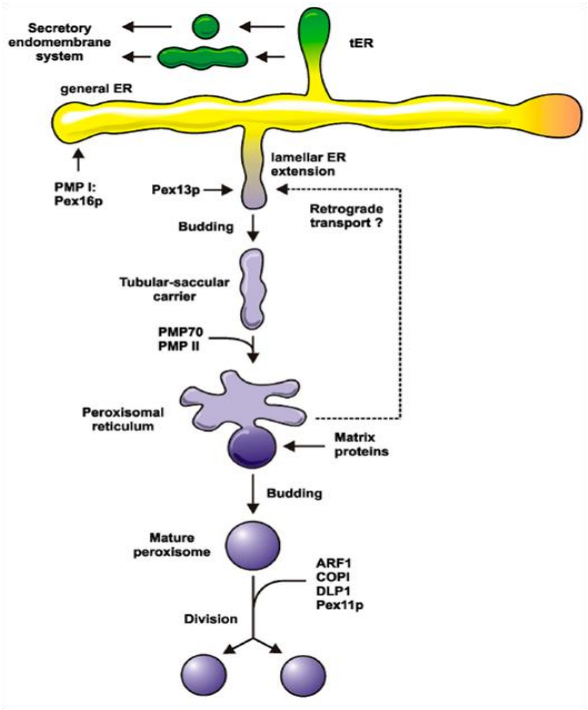

Fig. 1.4_1: Peroxisomal biogenesis in plants and mammals (*modified from Titorenko & Mullen, 2006*)

The import of Pex16p into the membrane of this organelle precursor then turns the vesicle into a nascent peroxisome, which may then, upon import of members of the peroxin 11 family, divide further to form new nascent peroxisomes. This mechanism is also relevant during the duplication of mature peroxisomes (South & Gould, 1999). Thereby new peroxisomes may proliferate both from pre-existing peroxisomes or be synthesized de novo.

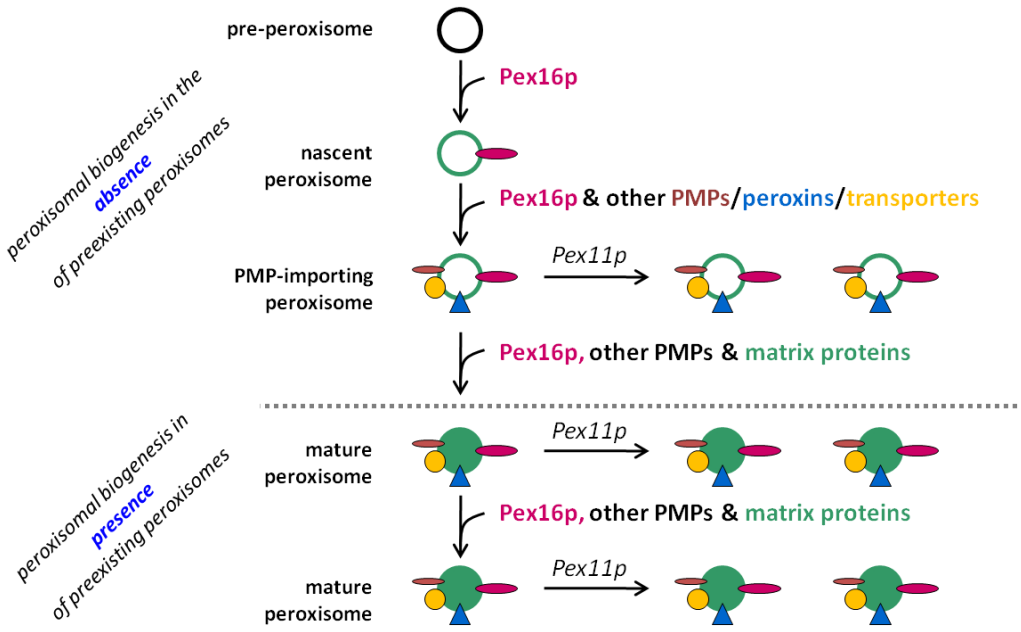

Fig. 1.4_2: A model of peroxisome biogenesis in the absence (top) and presence (bottom) of preexisting peroxisomes (*adapted from South & Gould, 1999*)

Apart from Pex16p other perosisomal membrane proteins (PMPs) are then imported through mechanisms that are not clearly understood. PMPs that are synthesized on free polyribosomes contain a membrane targeting signal (mPTS) and are bound and shuttled to the nascent peroxisome by Pex19p and recruited into the membrane through binding to Pex3p. Pex16p is required for this machinery in mammals, although its exact function is not clear. Lack of all or either of these proteins therefore leads to complete absence of detectable peroxisomes (Schrader & Fahimi, 2008).

Peroxisomal progeny from preexisting parent organelles includes three steps: Elongation of parent peroxisomes, constriction leading to a "pearls on a string" appearance and, finally, fission into new daughter organelles. Elongation is thought to be controlled through members of the Pex11p family, fission through dynamin-like GTPases (DLPs), which are recruited from the cytosol to the dividing peroxisome through fission 1 protein (Schrader & Fahimi, 2008).

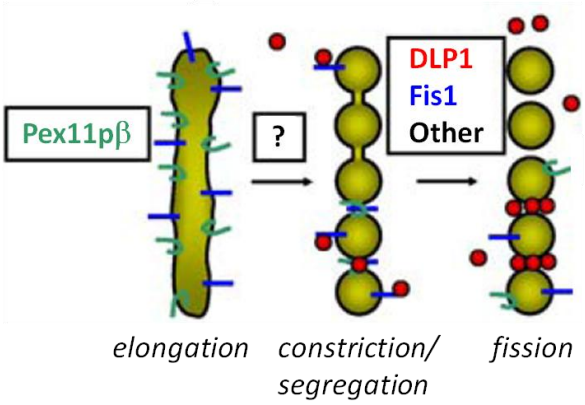

Fig. 1.4_3: Pex11p-dependent peroxisomal proliferation (*modified from Schrader & Fahimi, 2008*)

Import of enzymes into the peroxisomal matrix requires the presence of a docking complex within the peroxisomal membrane. This complex is made up of the peroxins 13, 14 and 17. Matrix proteins contain specific targeting signals (sequences of amino acids) either at the C-terminus (peroxisomal targeting signal 1, PTS1) or the N-terminus (PTS2) which are bound by Pex5p and Pex7p respectively and shuttled through these to the nascent peroxisome, where they interact with the docking complex described above. The actual dissociation and translocation into the matrix probably involves peroxins 2, 8, 10 and 12, leaving Pex5p and Pex7p to be recycled back into the cytoplasm. The exact method of transport through the peroxisomal membrane is unclear, since peroxisomes do not have pores unlike the nucleus, through which matrix proteins could be imported (Schrader & Fahimi, 2008).

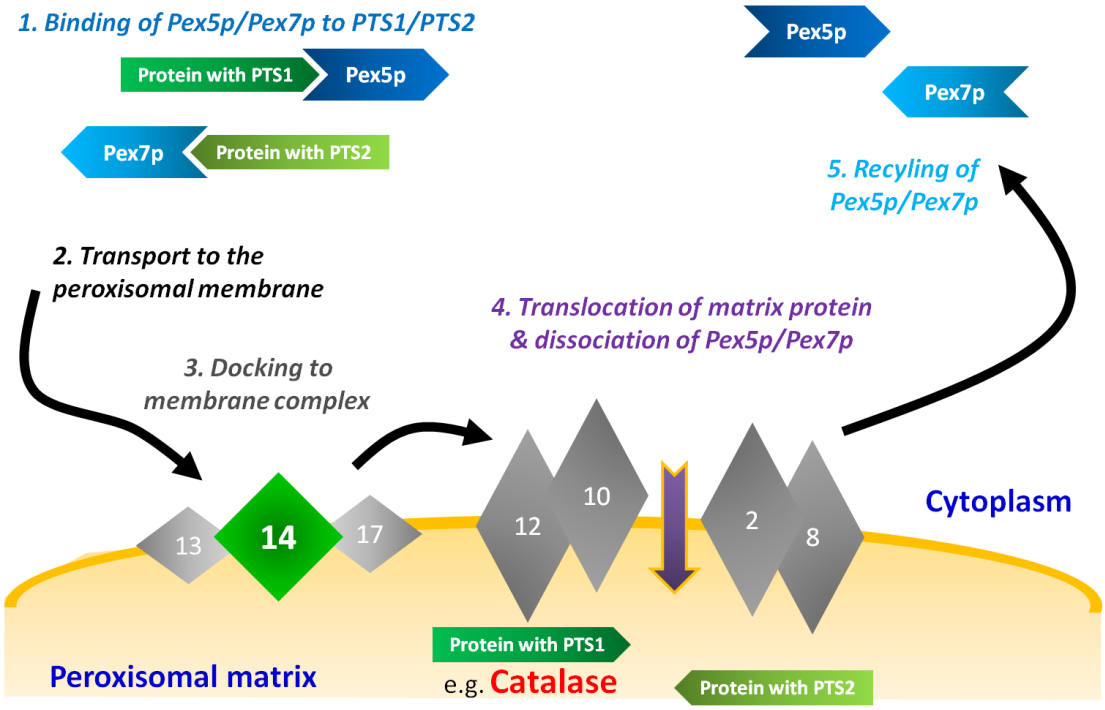

Fig. 1.4_4: Peroxisomal matrix protein import

1.4.2 Peroxisomal metabolism

Peroxisomes are involved in a majority of metabolic pathways, including ROS metabolism, β-oxidation of VLCFAs, α-oxidation of branched chain fatty acids, ether lipid synthesis and D-amino acid degradation. In the context of this thesis emphasis shall only be laid on ROS- and D-amino acid-metabolism. For a full list of peroxisomal functions see table 1.4_1 (from Schrader & Fahimi, 2008).

Table 1.4_1: List of peroxisomal functions (*modified from Schrader & Fahimi, 2008*)

Peroxide metabolism (catalase and H2O2-generating oxidases), ROS/NOS metabolism
Lipid biosynthesis (i.a. ether phospholipids/plasmalogens, bile acids & cholesterol)
Fatty acid β-oxidation (i.a. VLFCAs, branched chain fatty acids, unsaturated fatty acids)
Fatty acid α-oxidation
Long chain and VLCFA activation
Regulation of acyl-CoA/CoA ratio
Protein/amino acid metabolism (i.a. D-amino acid degradation, transamination, proteases)
Catabolism of purines
Glyoxylate and dicarboxylate metabolism
Hexose monophsphate pathway
Glycerol synthesis
Nicotinate and nicotinamide metabolism
Retinoid metabolism

Peroxisomes contain a number of enzymes that generate as well as others that degrade ROS, mainly in the form of hydrogen peroxide. The importance of peroxisomal antioxidant defense can be shown through incubation of cultured cells in UV radiation or with H_2O_2, whereby peroxisomes are shown to elongate, which is the first step in peroxisomal progeny. This effect is clearly linked to the detoxification of ROS as it could be attenuated through pre-incubation with the antioxidant N-acetylcysteine (Schrader, Wodopia & Fahimi, 1999). Cells successively adapted to increasing levels of dioxygen where shown to not only be able to survive in excessive O_2-concentrations (99%), but also shown twice the amount of peroxisomes, both compared to control cells (van der Valk et al., 1985). H_2O_2-incubation has also been shown to increase the expression of various peroxin-encoding genes (Lopez-Huertas et al., 2000; Desikan et al., 2001). Finally, ROS induction also increases activity of peroxisomal AOEs (van der Valk et al., 1985; Dhaunsi et al., 1993). A full overview of peroxisomal ROS-metabolism is described in Schrader & Fahimi (2004; 2006).

Table 1.4_2: List of ROS-producing and -degrading peroxisomal enzymes (*modified from Schrader & Fahimi, 2006*)

Enzymes in peroxisomes that generate ROS		
Enzyme	**Substrate**	**ROS**
Acyl-CoA oxidases	Long chain fatty acids, methyl brachend fatty acids, bile acid intermediates	H_2O_2
Urate oxidase (not in hominoids)	Uric acid	H_2O_2
Xanthine oxidase	Xanthine	H_2O_2, $O_2^{\bullet -}$
D-amino acid oxidase	D-amino acids	H_2O_2
Pipecolic acid	L-pipecolic acid	H_2O_2
D-aspartate oxidase	D-aspartate, NMDA	H_2O_2
Sarcosine oxidase	Sarcosine, pipecolate	H_2O_2
L-alpha-hydroxy acid oxidase	Glycolate, lactate	H_2O_2
Poly amine oxidase	*N*-Acetyl spermine/spermidine	H_2O_2
Nitric oxide synthase	L-Arginine	H_2O_2
Plant sulfite oxidase	Sulfite	H_2O_2
Enzymes in peroxisomes that degrade ROS		
Enzyme	**Substrate**	**Enzyme also present in**
Catalase	H_2O_2	Cytoplasm (e.g. erythrocytes) and nucleus
Glutathione peroxidase	H_2O_2	All cell compartments
MnSOD	$O_2^{\bullet}$	Mitochondria
CuZnSOD	$O_2^{\bullet}$	Cytoplasm
Epoxide hydrolase	Epoxides	ER and cytoplasm
Peroxiredoxin 1	H_2O_2	Cytoplasm, mitochondria, nucleus
PMP20	H_2O_2	
Plant ascobate-glutathione cycle	H_2O_2	plants only

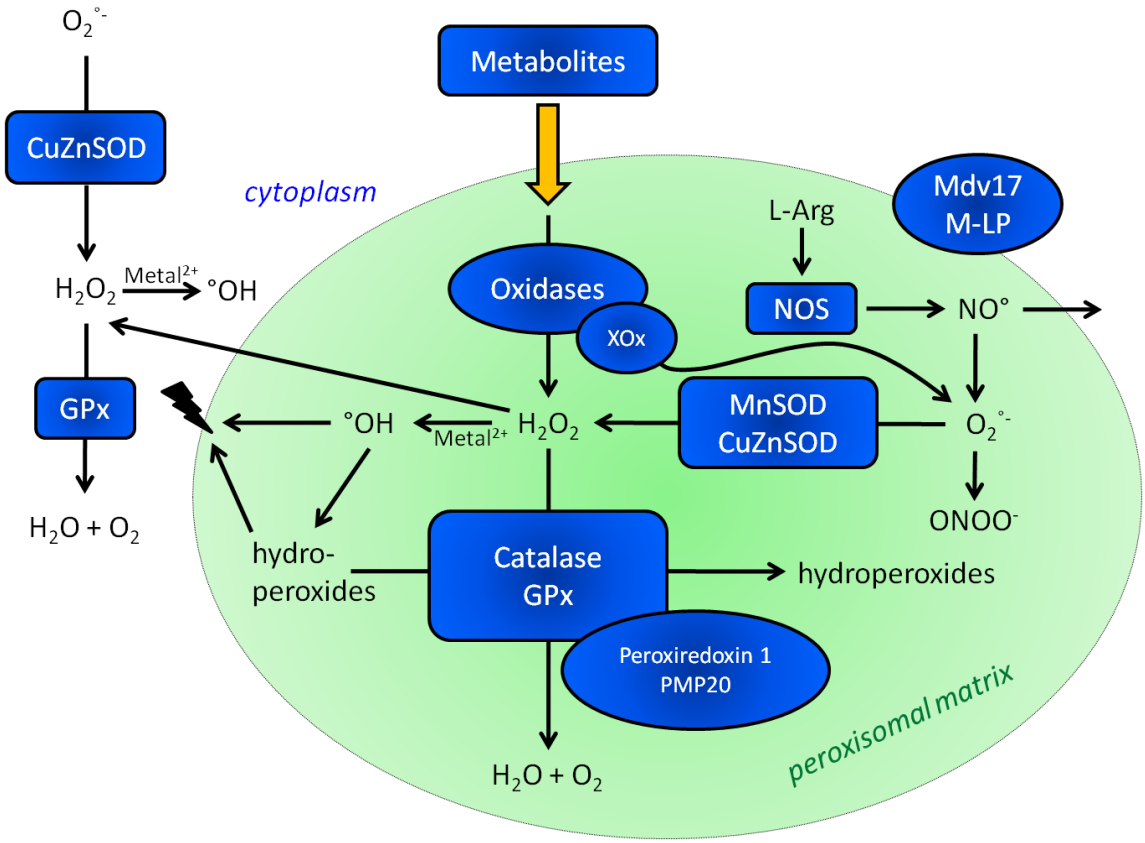

Fig. 1.4_5: Schematic overview of peroxisomal ROS metabolism (adapted from Schrader & Fahimi, 2006)

A noteworthy aspect of peroxisomal enzymatic content and metabolism is the phylogenic and inter-species difference in the activity of pathways involved in purine metabolism. Important peroxisomal enzymes hereof are xanthine oxidase and urate oxidase (aka uricase). Compared to other mammals certain primates, namely prosimians and Old World monkeys (*Catarrhini*), have generally lower levels of urate oxidase activity. In extremis, all genera of hominoids (comprised of hominids (*Hominidae*): *Pongo*, *Gorilla*, *Pan* and *Homo,* and gibbons (*Hylobatidae*): *Hylobates, Hoolock, Nomascus* and *Symphalangus*) as well as a few species of New World monkeys (*Platyrrhini*) express absolutely no urate oxidase due to several mutations found in various regions of the encoding gene (Oda et al., 2002). Although there appears to be an adaptive decrease in the activity of xanthine oxidase (Xu, LaVallee & Hoidal, 2000), which produces uric acid, the substrate of urate oxidase, especially in humans the amount of uric acid in the body is substantially elevated compared to that of other primate and mammalian species (Johnson et al., 2005). These differences have been suggested as essential in hominid and especially human evolution, since the antioxidant and anti-inflammatory capacity of uric acid is believed to be responsible for these species' longevity, increased brain complexity and therefore intelligence. Since

intelligence and cognitive capacity are closely linked to the form of phenotypical symptoms of schizophrenia, this mutation may play a pivotal role in explaining the differences between expressed behavioral, cognitive and perceptional abnormalities in various animal models of the disorder. The inability to degrade uric acid is also the cause of gout, a disease which is only found in the aforementioned primate species.

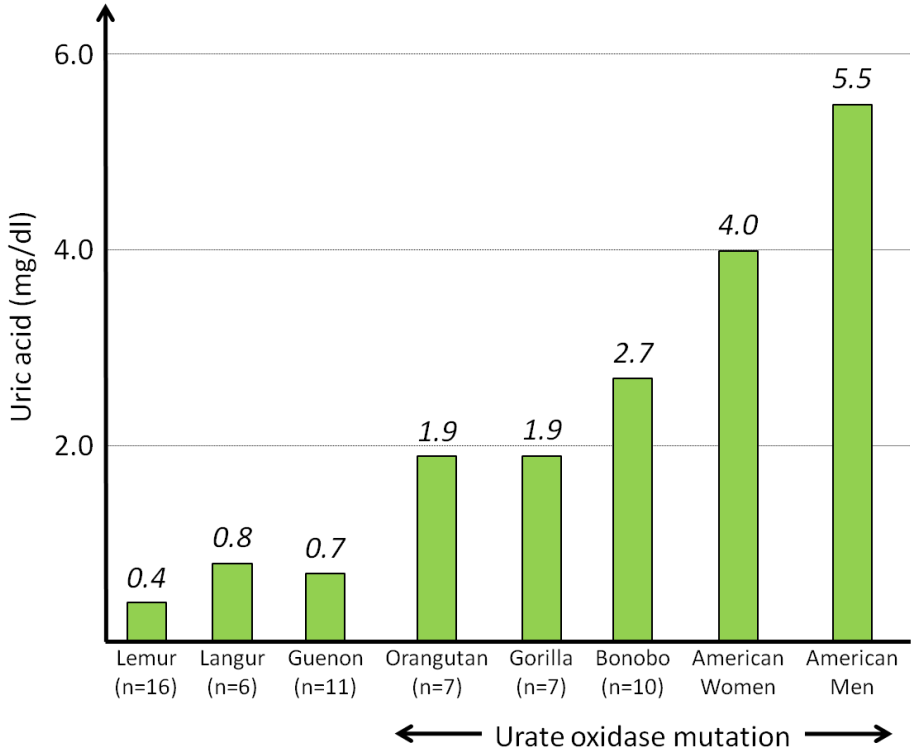

Fig. 1.4_6: Uric acid levels in primates (*adapted from Johnson et al., 2005*)

1.4.3 Peroxisomes in the nervous system

The role of peroxisomes in the brain and other neuronal tissues is but poorly examined. A first description of the organelle's abundance and distribution in nervous tissue was published by Gail Arnold and Eric Holtzman (Arnold & Holtzman, 1978; Holtzman, 1982), who found different populations of peroxisomes dependent on enzyme content. One population was rich in catalase and poor in D-amino acid oxidase (DAAO), whereas the other was oxidase-poor and catalase-rich. These populations of peroxisomes were differentially distributed between neuronal cells, in essence between neurons and glial cells, as well as between different brain regions. In general, both groups were found both in higher abundance and of larger size in glial cells compared to neurons. Largest quantities of peroxisomes were found in astrocytes and oligodendrocytes as well as in ependyma, suggesting the neuroprotective functions of these cells with regard to ROS metabolism.

Within neurons, peroxisomes were most abundant in the perikarya and the large dendrites and only very sparse in axons and synaptic terminals.

Regarding differential distribution between various brain regions, Holtzman emphasizes the lack or low abundance of catalase-containing peroxisomes in Purkinje cells, cerebrocortical neurons as well as dorsal root ganglion cells. In contrast he found relatively larger populations of catalase-positive bodies in catecholaminergic cells, with the exception of the adrenal medulla. He does, however, warn about the overinterpretation of negative cytochemical results.

Apart from differences between cells and regions, Holtzman also described ontogenetic differences within the same cells and regions. Whereas catalase is found in relatively high levels in developing neurons, including in synaptic terminals, as well as in oligodendrocytes during myelination, the amount of catalase is reduced drastically during the later stages of ontogeny. This is explained by a possible involvement of peroxisomes in membrano- and myelogenesis, which would be in line with previously described findings that peroxisomes are involved in ether lipid synthesis, of which there is a large concentration in neuronal and glial membranes.

Further investigations regarding the distribution of D-aspartate oxidase (D-AspOx) were performed by Kurt Zaar and coworkers (Zaar et al., 2002) on rat and human brain sections using immunohistochemistry, immunoelectronmicroscopy and in-situ hybridization. Findings indicate that D-AspOx is located solely in peroxisomes, widely distributed in the CNS and mainly localized in neurons and astrocytes.

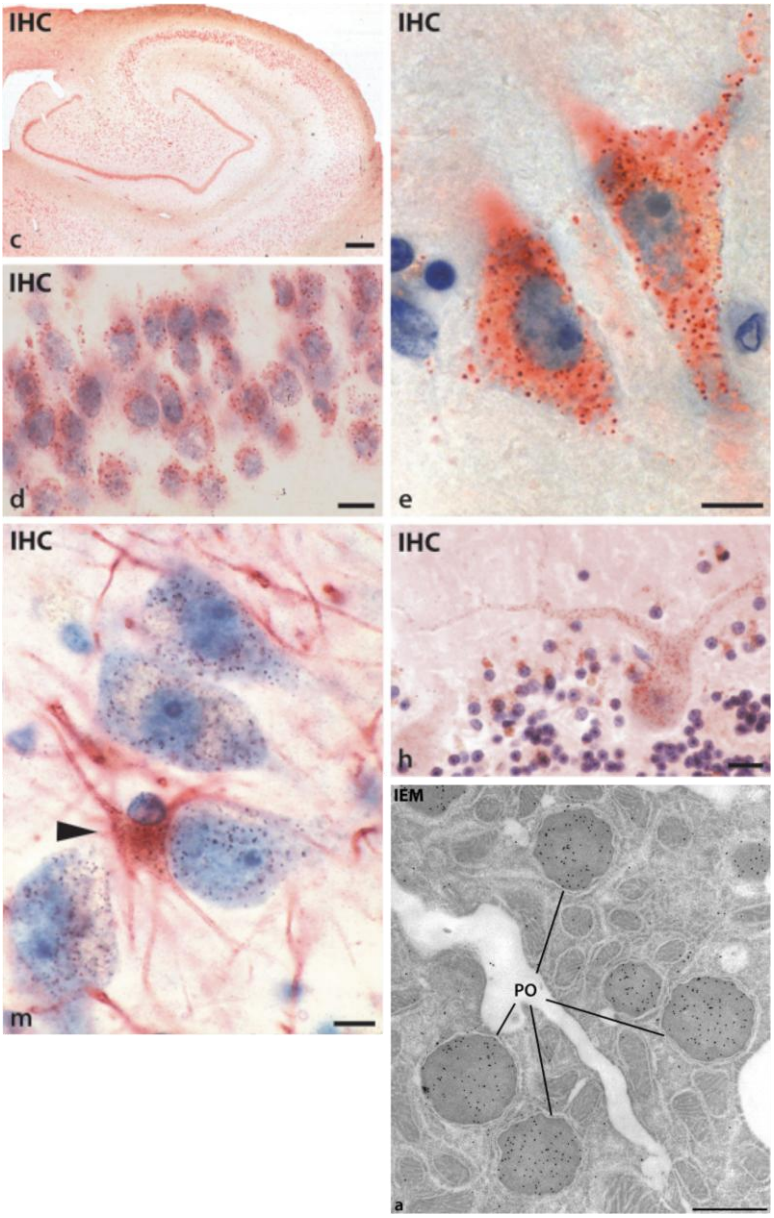

Fig. 1.4_7: Cellular and subcellular distribution of D-aspartate oxidase in (a) rat kidney, (c) human hippocampal overview, (d) granule cells and (e) multipolar cells of the human dentate dyrus, (m) interneurons and astrocytes in the stratum lacunosum-moleculare of the human cornu ammonis and (h) Purkinje cell of the human cerebellar cortex; *IEM: immunoelectron microscopy, IHC: immunohistochemistry, PO: peroxisome (modified from Zaar et al., 2002)*

A study using indirect immunofluorescence on mouse brain sections showed similar findings to Holtzman in that a significant down-regulation of catalase abundance and immunoreactivity was observed between postpartum days 2 and 38 and that catalase immunoreactivity was markedly different between neurons and glial cells with highest levels found in astrocytes. Moreover peroxisomal abundance was evaluated independently of enzymatic content through the usage of a novel peroxisomal marker protein, peroxin 14

(Pex14p, q.v. section on problems in labeling peroxisomes), which showed that the decrease in catalase immunoreactivity was not mirrored by the decrease in peroxisomal abundance (Ahlemeyer et al, 2007). These findings were corroborated through examination of various other peroxisomal proteins, catalase-activity assays and through Western blotting. The latter also clearly showed that, while catalase content decreases continuously throughout early ontogeny, Pex14p-levels remain stable after a global reduction of peroxisomal protein levels between postpartum days 2 and 15. These findings stress the importance of peroxisomes in the developing brain, not only during neuronal growth and myelination, but also during the transition from the hypoxic environment in utero to postnatal hyperoxia.

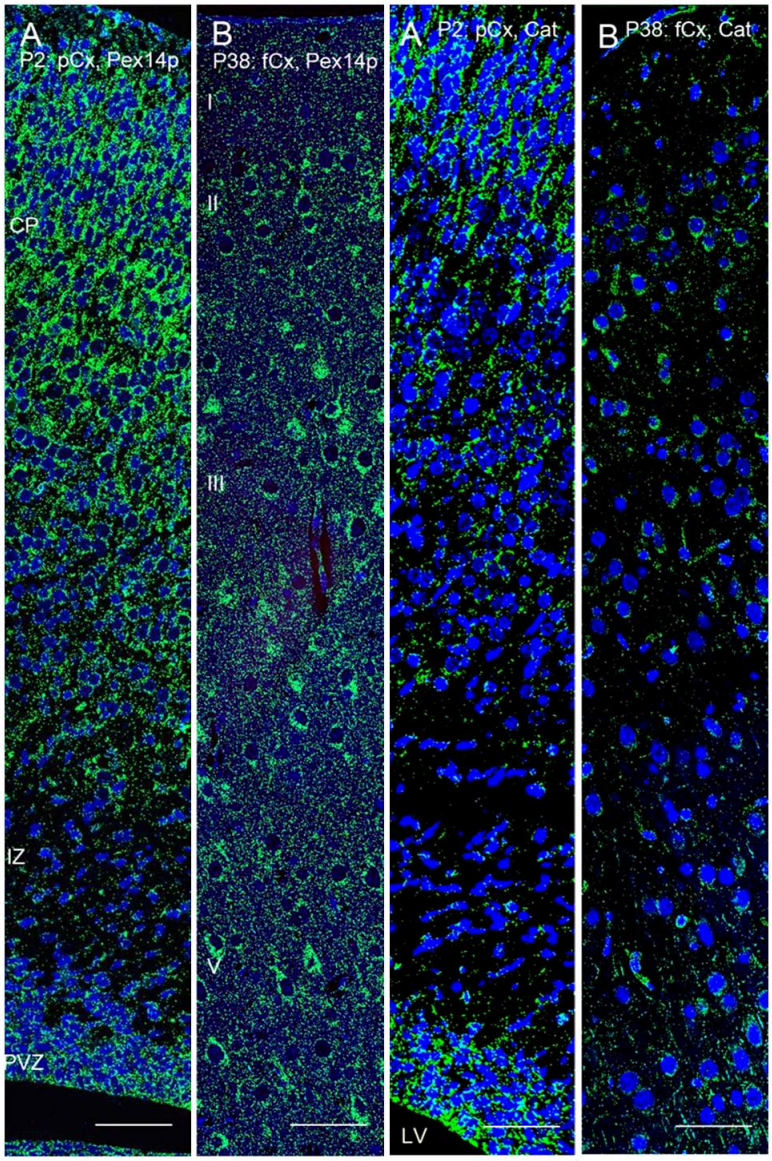

Fig. 1.4_8: Distribution of Pex14p and catalase in the early and late developing mouse neocortex; *I-V: neocortical laminae, CP: cortical plate, fCx: frontal cortex, IZ: intermediate zone, LV: lateral ventricle, P2/38: postpartum days, pCx: parietal cortex, PVZ: periventricular zone (modified from Ahlemeyer et al., 2007*)

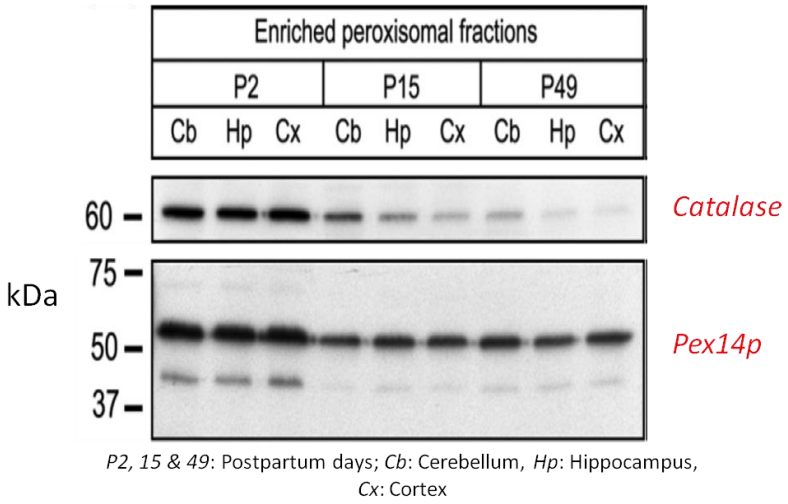

Fig. 1.4_9: Western blotting shows differential regulation of catalase and Pex14p during murine brain development (*modified from Ahlemeyer et al., 2007*)

The importance of intact peroxisomal function is also shown through marked neurological deficits, neuronal migration retardation and abnormal neurogenesis in all different knockout-models of various peroxisomal biogenesis proteins and metabolic enzymes (Baes et al., 1997 [Pex5p KO]; Faust et al., 1997; 2001; 2003 [Pex2p KO]; Li et al., 2002 [Pex11βp KO]; Maxwell et al., 2003 [Pex13p KO]; Huyghe et al., 2006 [peroxisomal multifunctional protein 2, MFP-2 KO]).

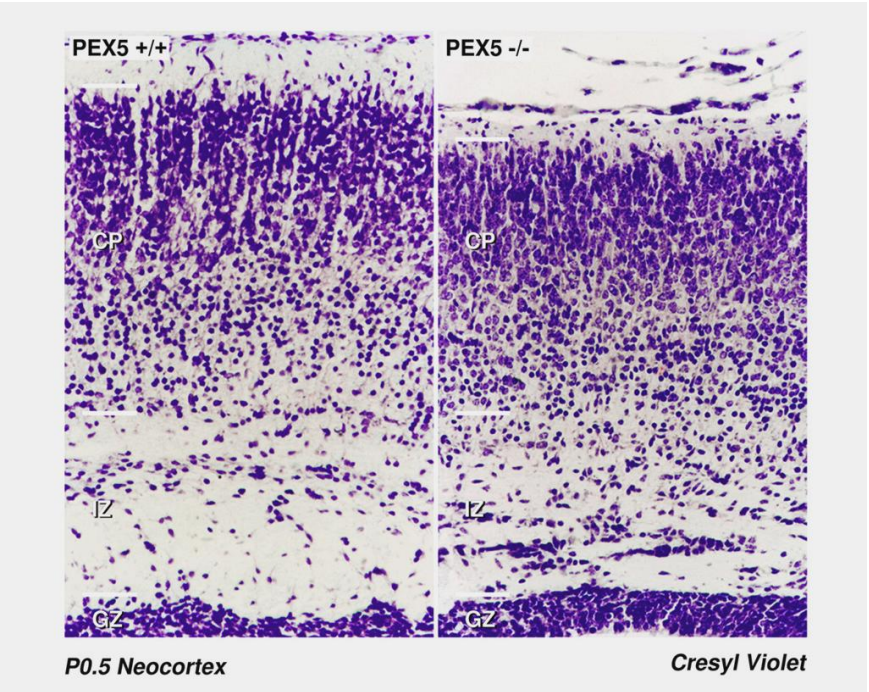

Fig. 1.4_10: Retardation of neuronal migration in the neocortex of the PEX5 knockout mouse; *CP: cortical plate, GZ: germinative zone, IZ: intermediate zone (modified from Baes et al., 1997*)

Since these animals all show signs of a storage disease as is found in the human peroxisomal disorder “Zellweger syndrome” (see section on peroxisomal disorders) and neural migration is dependent on more than functional peroxisomes solely in the brain (Janssen et al., 2003; Krysko et al., 2007), owing to multiorgan peroxisomal dysfunction in these mouse models, they are not well suited for analysis of intrinsic roles of peroxisomes in the brain. This unsuitability is further underlined by the obvious conclusion that peroxisomal function in the developing brain is not equal to that in the adult brain.

1.4.4 Peroxisomal disorders

Peroxisomal disorders can be divided into two groups: Peroxisomal biogenesis disorders (PBDs) on the one hand and single peroxisomal enzyme deficiencies (PEDs) on the other. The PBDs consist of rhizomelic chondrodysplasia punctata, type 1 (RCDP1), which is caused by a mutation in the PEX7 gene and the disorders of the so-called Zellweger spectrum, which include infantile Refsum disease, neonatal adrenoleukodystrophy and Zellweger syndrome. Disorders of the Zellweger spectrum, of which Zellweger syndrome is the most severe, are usually caused by multiple genetic mutations in a variety of PEX genes. The disorders are named after Hans Zellweger, who first described the disorder as cerebrohepatorenal syndrome, due to the multi-organ involvement. Patients exhibit symptoms of a storage disorder since their lack of functional peroxisomes inhibits degradation of VLCFAs and branched chain fatty acids. Patients also show decreased levels of plasmalogens and hypomyelination. This accompanied by neuronal migration and neurogenesis defects accounts for severe muscular hypotonia, seizure, apnea and inability to swallow. For a full description of the syndrome see Zellweger et al., 1988. There is currently no known curative treatment for Zellweger syndrome. Palliative measures involve pneumonia and asphyxiation prophylaxis as well as artificial nutrition. Patients usually die within their first year of life (Steinberg et al., 2006).

Peroxisomal enzyme deficiencies are far more numerous and can affect any of the peroxisomal metabolic pathways (see table 1.4_3). The most commonly known PED is probably X-linked adrenoleukodystrophy (X-ALD), a dysfunction of the peroxisomal fatty acid transporter ABCD1. The palliative treatment, Lorenzo’s oil, is a 4:1 mixture of glycerol trioleate and glycerol trierucate, developed and named by Augusto and Michaela Odone after their son Lorenzo, who suffered from X-ALD.

Table 1.4_3: List of the single peroxisomal enzyme deficiencies (*modified from Wanders & Waterham, 2006*)

Peroxisomal pathway affected	Defect enzyme	Disease
Ether phospholipid synthesis	DHAPAT	Rhizomelic chondrodysplasia punctata Type 2 (DHAPAT deficiency)
Peroxisomal beta-oxidation	ADHAPS	Rhizomelic chondrodysplasia punctata Type 3 (alkyl-DHAP synthase)
	ABCD1	X-linked adrenoleukodystrophy
	ACOX1	Acyl-CoA oxidase deficiency
	DBP	D-bifunctional protein deficiency
	AMACR	2-MethylacylCoA racemase deficiency
	SCPx	Sterol carrier protein X deficiency
Peroxisomal alpha-oxidation	PHYH/PAHX	Refsum disease (phytanoyl-CoA hydroxylase deficiency)
Glyoxylate detoxification	AGT	Hyperoxaluria Type 1
H2O2-metabolism	CAT	Acatalasaemia

1.4.5 Problems in labeling peroxisomes

The most common marker for the localization of peroxisomes in morphological or cell culture studies is catalase, an enzyme endogenous to peroxisomes and commonly found in eukaryotes. Its function is the decomposition of hydrogen peroxide to water and oxygen, thereby protecting the cell from oxidative damage. This organelle-specific cytochemical staining became available for light and electron microscopy due to the introduction of the alkaline 3,3'-diaminobenzidine (DAB) reaction for endogenous catalase (Fahimi, 1968; 1969; Novikoff & Goldfisher, 1969). It was originally believed that catalase was ubiquitously expressed in all animal cells (Hruban et al, 1972), but since catalase has the highest turnover numbers in all enzymes, it is therefore not present in all cell types and tissues in equal amounts at the same time, since one molecule of catalase can decompose millions of hydrogen peroxide molecules per second (Goodsell, 2004). Although all of the mechanisms for the Nrf2-dependent induction of catalase-expression are not yet completely understood, it is shown to be dependent on different factors like maturation (Ahlemeyer, 2007) or the amount of reactive oxygen species (ROS) in the respective cell. ROS are produced during subcellular metabolism, e.g. in mitochondrial respiratory chain, wherefore intracellular catalase-concentration is directly dependent on specific cellular ROS metabolism and only indirectly on peroxisomal abundance. Since a major part of ROS is produced during mitochondrial respiration, ROS-release and thereby mitochondrial amounts of manganese-

superoxide dismutase (SOD2) also influence the levels of catalase. In general it can therefore be ascertained that the enzyme content of peroxisomes is highly heterogeneous, not only between cell types or tissues, but also within cell types and tissues depending on the stage of ontogeny (Baumgart, 1997, Baumgart et al, 2003, Luers et al., 2006). In the brain, for example, it has been shown that catalase is highly expressed in neurons during the embryonic development of the mouse central nervous system, but is then significantly downregulated and can, in adult animals, mainly be found only in glial cells (Arnold & Holtzman, 1978; Ahlemeyer et al. 2007). Similar intercellular differences in catalase-concentration between male germ cells, different somatic cell types of the testis or the cells of the alveolar epithelium could be shown in mice (Nenicu et al, 2007; Karnati & Baumgart-Vogt, 2008). Therefore positive peroxisomal localization by using antibodies against catalase or by the cytochemical alkaline 3,3'-diaminobenzidine- (DAB)-reaction (Fahimi et al., 1976) turns out to be imprecise and heavily dependent on the metabolism of the respective cell type.

The supposed low abundance of peroxisomes in neurons was shown to be incorrect by staining morphological samples from rat and human brain for other enzymes known to be found only in peroxisomes, namely D-amino acid oxidase (Holtzman, 1982) or D-aspartate oxidase (Zaar et al., 2002). Since these enzymes are, however, common to neuronal tissue, their capabilities as peroxisomal markers in other tissues and organs are limited.

A similar statement can be made about another commonly used peroxisomal marker, namely adenosine triphosphate-binding cassette sub-family D member 3 (ABCD3), a 70-kDa peroxisomal membrane protein (formerly PMP70). This ABC-transporter is a major component of the peroxisomal membrane and is involved in transport of lipid derivatives through the peroxisomal membrane (Kamijo et al, 1992). ABCD3 expression is also highly dependent on cell metabolism. Due to its involvement in the initial steps of peroxisomal lipid metabolism, namely the bringing of the metabolites into the peroxisome, its expression pattern differs highly in some tissues from that of catalase.

It is therefore necessary to find another peroxisomal marker, which is capable of labeling peroxisomes in all tissues and cell types independently of metabolic changes. The likelihood of finding an optimal ubiquitous peroxisomal marker is highest within the group of peroxisomal biogenesis proteins (peroxins) that are part of the organelle membrane such as the members of the docking complex for the import of matrix proteins are ideal for this

purpose. First attempts were done with antibodies against peroxin 13 (Pex13p) and peroxin 14 (Pex14p: Distel et al., 1996) in testis and lung (Nenicu et al., 2007; Karnati & Baumgart-Vogt, 2008), whereof Pex14p showed better and more uniform results, probably due to the better accessibility of the antigen compared to that of Pex13p.

In this thesis the peroxin 14 is therefore presented as the optimal peroxisomal marker. Pex14p is a peroxisomal biogenesis protein (peroxin) involved in the docking of both PTS1- and PTS2-linked peroxisomal matrix enzymes (Albertini et al, 1997), present within every intact peroxisomal membrane and found in similarly high levels in distinct cell types and organs. To show this, a large variety of tissues and organs as well as primary cultured neurons and mouse and human hepatoma cells were compared regarding their distinct and individual abundance of catalase, ABCD3 and Pex14p. In order to compare levels of catalase with those of antioxidant enzymes in other organelles parallel tissue sections were also stained for SOD2. In addition to standard localization of the anti-Pex14p antibody with immunofluorescence, peroxidase-based immunohistochemistry and immunogold-labeling QuantumDots (Qdots) were used for localization of peroxisomes in cultured cells. The unique capabilities of this new peroxisomal marker for morphometric purposes can furthermore be shown through experiments on cells treated with the peroxisome-proliferator ciprofibrate.

Apart from the cell biological advantages of Pex14p as a peroxisomal marker, the temporal stability of the epitope, its sensitivity to different fixation techniques as well as the cross-species applicability of our self-created antibody were also examined. For this purpose labeling of peroxisomes in tissues from mouse, cat, Sacred Baboon (*Papio hamadryas*) and human was attempted, using samples from freshly perfused animals, samples taken from field studies almost 15 years ago, human autopsy samples as well as biopsies from body donors to the gross anatomy course of the Institute for Anatomy and Cell Biology (JLU Giessen). These samples were fixed in aqueous formaldehyde (formalin), pH-buffered formaldehyde solution (Lilie's formol), pH-buffered paraformaldehyde- (PFA)-solution or in Bouin's fixative.

This is additionally the first attempt of localizing Pex14p in the human brain, which in and of itself makes localization of peroxisomes especially problematic. In classical immunohistochemical staining peroxisomes is complicated by diffusion artifacts of the reaction products into the surrounding cytosol. Since neuronal tissue is known to have very

few and exceptionally small peroxisomes this method is definitely inferior to immunofluorescence staining. This approach will be shown to work more than adequately in cultured cells and animal tissues, but comes with its own setbacks in the human brain, due to the accumulation of lipofuscin granules, which fill almost the entire cytoplasm of neurons. Since lipofuscin is made up of various lipid-containing residues of lysosomal digestion it autofluoresces in all emission wavelengths and brightly outshine specific immunofluorescence signals. Therefore, attempts were made to quench lipofuscin autofluorescence through pre-staining with a lipid staining agent (Sudan Black B), which in turn, however, also reduces the signal of the fluorochromes and leads to unspecific background fluorescence.

Nevertheless, this thesis suggests that Pex14p is the ideal standard marker protein for the localization of peroxisomes, allowing for reliable studies regarding abundance and distribution of peroxisomes, thereby giving accurate numerical values which would not be obtainable through catalase or ABCD3 stainings due to strong intra- and intercellular differences.

1.5 Aims and schematic overview

The primary aim of this thesis is to examine the role of oxidative stress and dopamine neurotoxicity in the etiopathogenesis of schizophrenia and attempt to integrate many preexisting models into one. Since the role of peroxisomes has not been researched extensively a special emphasis shall be laid on the involvement of this organelle.

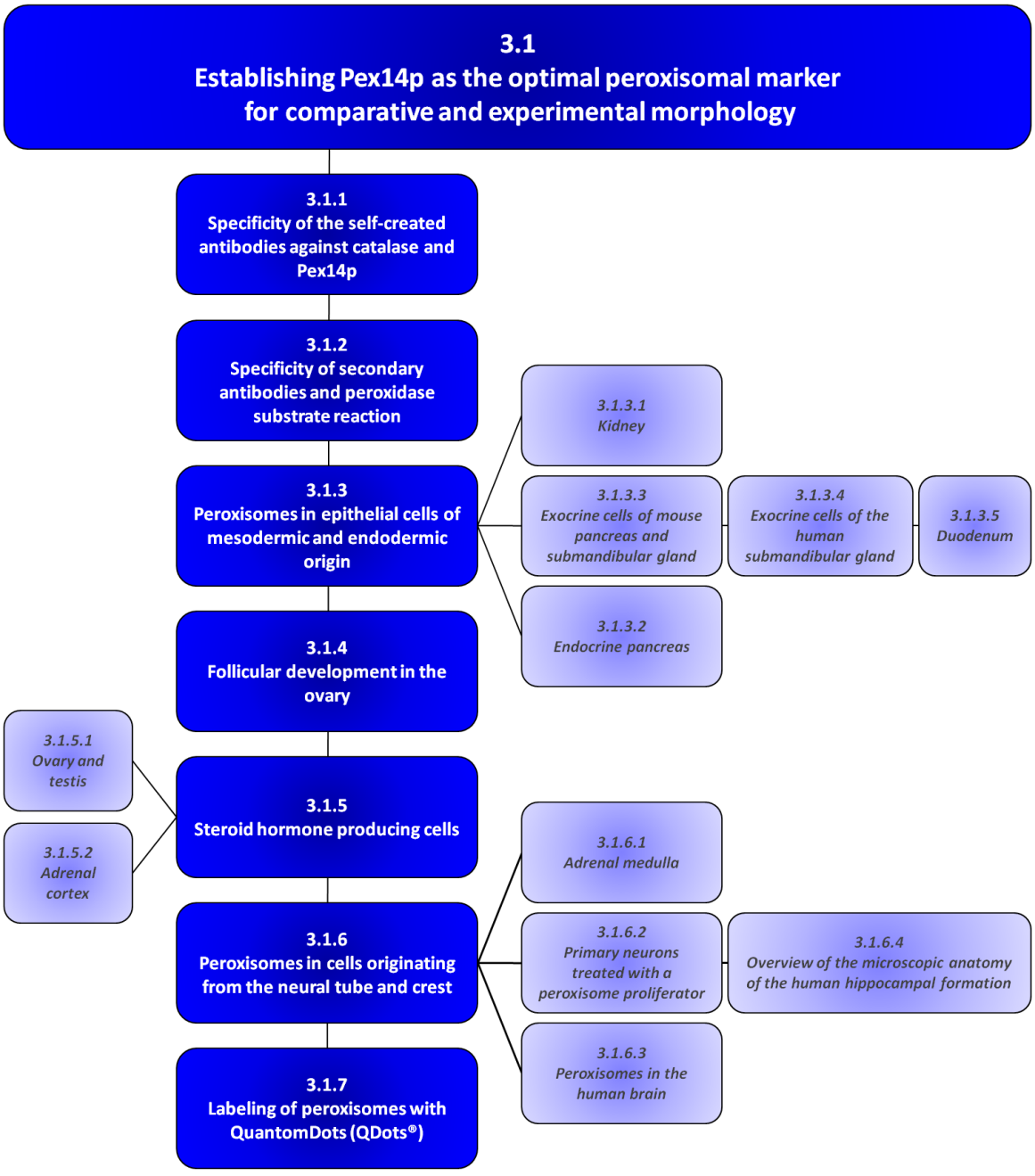

Fig. 1.5_1: Flow chart of the experiments performed within the first part of the thesis

The first part of this thesis shall therefore be an attempt of localizing peroxisomes ubiquitously and independently of metabolism and enzyme content using a new marker protein, peroxin 14 (Pex14p). Labeling of peroxisomes shall be attempted in various tissues and cell types of different species, including human (with special emphasis on human brain), through different methods, including immunohistochemistry, immunofluorescence and immunoelectronmicroscopy (see fig. 1.5_1).

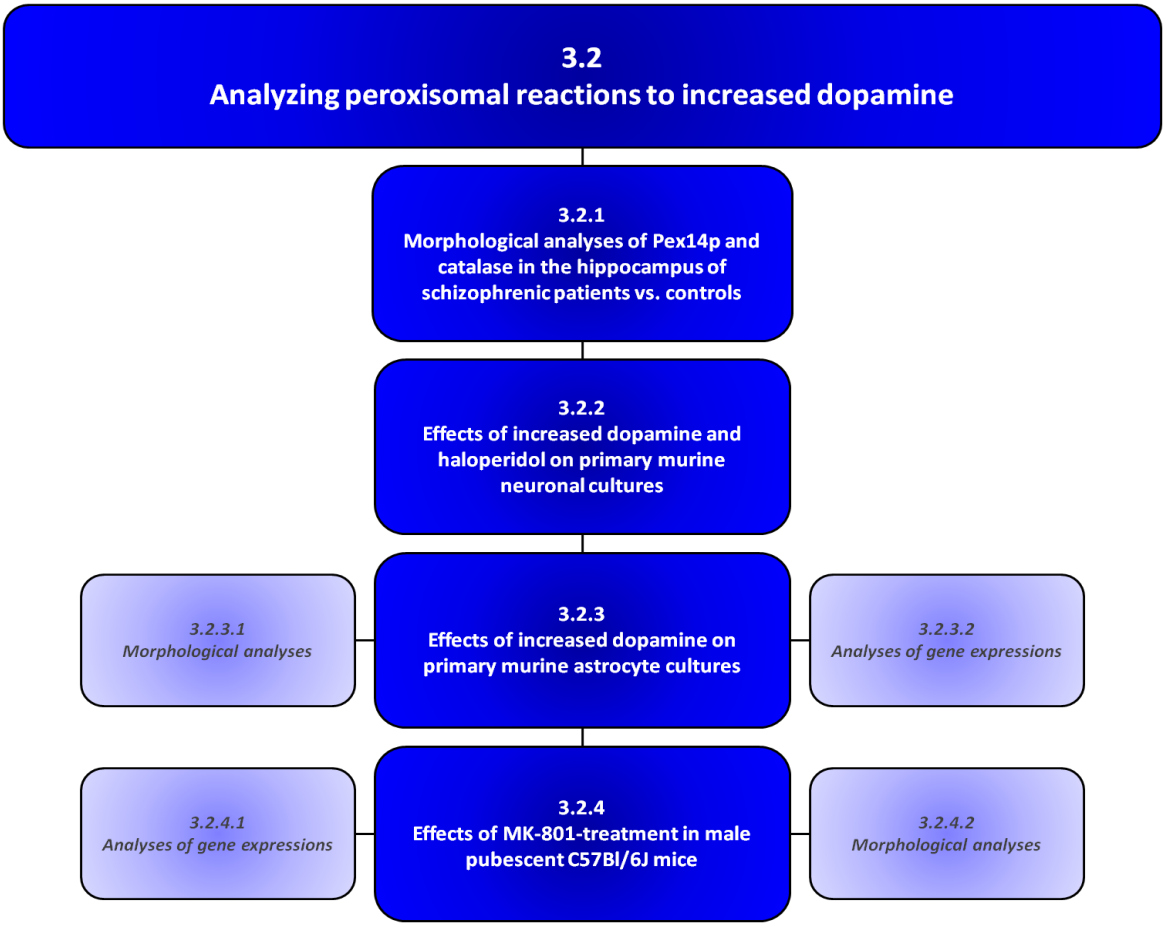

Fig. 1.5_2: Flow chart of the experiments performed within the second part of the thesis

In the second part, the newly established marker shall be used to measure peroxisomal reactions to increased dopamine in vivo and in vitro. Additionally the expression levels and protein content of various enzymes involved in antioxidant defense and dopamine metabolism shall be analyzed alongside selected proteins believed to be relevant for the interaction between dopamine and glutamate neurotransmission and peroxisomal metabolism, e.g. D-amino acid oxidase, D-aspartate oxidase and serine racemase. Analyses shall be performed on post-mortem brain sections from schizophrenic patients, cultured murine astrocytes and neurons as well as male pubescent C57Bl/6J mice treated with the selective non-competitive NMDAR antagonist dizocilpine (MK-801) (see fig 1.5_2).

2. Materials and methods

All experiments were performed in accordance to international ethical standards of the Justus-Liebig-University, Giessen (Germany). Human tissues were taken from donors who testamentarily donated their bodies to the Institute of Anatomy and Cell Biology (JLU Giessen). Animal testing was approved through the regional board (animal research proposal "MK-801 und (anti-)oxidativer Stoffwechsel", Geschäftszeichen V 54 - 19 c 20-15 (1) GI 20/23 Nr. 05/2010, Feb. 25 2010), in accordance with § 8 paragraph 1, German Protection of Animals Act (TSchG).

For reasons of conciseness, the methods performed in this thesis shall only be described briefly in this section. For detailed information see appendix A.

2.1 Animal treatment with MK-801

Animals used were male pubescent wild type C57Bl6/J mice, obtained from Charles River, Germany. Each experiment consisted of three animals, whereof one was treated with a vehicle (0.9% saline) and the other two with MK-801. The selective NMDAR-antagonist MK-801 (dizocilpine, (5S,10R)-(+)-5-Methyl-10,11-dihydro-5*H*-dibenzo[a,d]cyclohepten-5,10-imine maleate, Tocris Bioscience) was given in a final concentration of 0.5 mg per 1 g body weight. A 20x stock solution was prepared by dissolving 10 mg MK-801 (337.37 g/Mol) in 5 ml sterile 0.9% saline solution. Aliquots of 10 ml were stored at -80°C, thawed prior to use and 190 ml of sterile 0.9% saline solution were added, where after the solution was sterilized using a sterile filter. Each animal was weighed and 5 ml of the MK-801 solution or a vehicle per g body weight were injected intraperitoneally to reach the final treatment amount of 0.5 mg per 1 g body weight.

Animals were either treated once and sacrificed after 1 h or were treated once every 24 hrs and sacrificed one hour after the final injection. Treatment durations were 25 hrs (2 treatments), 49 hrs (3 treatments) or 73 hrs (4 treatments). Method of sacrifice was cervical dislocation.

2.2 Tissue preparation for morphological methods

2.2.1 Tissue acquirement

2.2.1.1 Mouse tissue: Animals used for the comparative morphological analyses were anaesthetized with isoflurane and subsequent intraperitoneal injection of a mixture of ketamine/xylazine/Sedastress®. After a short rinse with 0.9% NaCl to remove blood cells, animals were perfused anterogradely via the left ventricle with 4% depolymerized paraformaldehyde (PFA) in phosphate buffered saline (PBS, pH 7.4) containing 2% sucrose for light and immunofluorescence analyses or with 4% PFA in 0.1% phosphate buffer (PB) for electron microscopy, after which organs were individually removed and immersion fixed over night in the respectively same fixative.

Animals used in the studies on MK-801-induced dopamine neurotoxicity were sacrificed through cervical dislocation.

2.2.1.2 Rat tissue (liver): Tissues were obtained with kind permission of Dr. Wiebke Moebius (MPI Göttingen, Germany), fixed in 4% PFA and 0.2% glutardialdehyde (GDA) in 0.1% PB.

2.2.1.3 Cat and Sacred Baboon: Sections were taken from paraffin blocks which were prepared for use in our histology course up to 20 years ago. Fresh tissue was dissected from the cadavers and fixed in Lilie's formol. Samples were then refixed in Bouin's fixative over night in the same fixative.

2.2.1.4 Human tissue: Brain samples were taken from human autopsy-materials, kindly provided by Prof. Dr. Klaus Kuchelmeister (at that time: Department of Neuropathology, University of Giessen, Germany). Brains were removed from the bodies during postmortem and, after initial inspection, immersion fixed in 4% formaldehyde in tap water for at least three weeks. After thorough fixation, brains were dissected and small samples (ca. 2x2cm) were cut for paraffin embedding.

Samples from human submandibular glands were acquired from body donors to the Institute for Anatomy and Cell Biology's gross anatomy course. Bodies were cooled over night and perfused retrogradely via the femoral artery with a fixation solution containing 5% phenoxytol, 66% ethanol 9% formaldehyde and 20% water.

2.2.2 Embedding and processing for light and fluorescence microscopy

Samples were dehydrated through a graded alcohol series (50%, 70%, 80%, 96% and 2x99%) and embedded in paraffin in an automated vacuum infiltration tissue processor (Leica TP 1020). Two micron sections were cut on a standard rotation microtome (Leica RM 2135) with a block cooling system and collected on precoated SuperFrost Plus microscope slides (Menzel).

2.2.3 Embedding and processing for electron microscopy

Samples were recut into approximately 1x1x1mm blocks. Some of the blocks were then embedded in either LR White resin (polymerization at 50°C) or in Unicryl resin (UV-polymerization at 4°C). Blocks were neither refixed in glutardialdehyde nor in osmium tetroxide in order to preserve maximum antigenicity. Semithin and ultrathin (silver to gray interference colored) sections were cut with glass and diamond knives (Diatome ultratrim) on a Reichert Ultracut ultramicrotome. Ultrathin sections were collected on 100 mesh nickel grids coated with 1% formvar and dried at room temperature.

Other blocks were not embedded into synthetic resins, but infiltrated with 2.3M sucrose in 0.1% phosphate buffer (PB) according to the Tokuyasu method for cryo-ultramicrotomy (Tokuyasu, 1973). After infiltration, blocks were mounted on T-pins and quick-frozen in boiling liquid nitrogen. Blocks were introduced into a Reichert Ultracut-S ultramicrotome with a Reichert FC R cryo-chamber and trimmed into a mesa with a glass knife at -80°C. Ultrathin sections (gold to gray interference colored) were then cut with a cryo-diamond (Diatome cryo immuno) at between -80 and -120°C (according to tissue consistency) and picked up onto formvar-coated nickel grids using a mixture of 2.3M sucrose and 2% methyl cellulose.

2.3 Cell culture

2.3.1 Mixed primary murine neuronal cultures

2.3.1.1 Preparation of primary neuronal cultures of the medial neocortex of newborn mice:

Primary cultures from the medial neocortex of newborn C57BL/6J mice were prepared as previously described (Ahlemeyer and Baumgart-Vogt, 2005). For a detailed description see appendix A, section A.1.1.

2.3.1.2 Peroxisome proliferator (ciprofibrate) treatment of primary neuronal cultures: Ciprofibrate was added to primary cortical neurons 4 h after seeding until day 6 at a final concentration of 100 µM, whereas controls received vehicle only.

2.3.1.3 Dopamine and haloperidol treatment of murine primary neuronal cultures: On the seventh day of cultivation 20 ml of a vehicle (medium) or a sterile dopamine or haloperidol solution of defined concentration (100x of final concentration) were added to reach final concentrations of 0 (vehicle), 10, 25, 50, 100 or 200 mM. Cells were treated with dopamine or haloperidol for 24 hrs, where after the solution was removed by pipetting. Cells were then washed three times briefly with warm PBS and then fixed in 4% PFA in PBS for indirect immunofluorescence labeling.

2.3.2 Primary astrocytes cultures

2.3.2.1 Preparation of primary astrocyte cultures of the neocortex of newborn mice: Astrocytes were cultivated using the neocortices of entire litters of newborn C57Bl/6J mice. For a detailed description see appendix A, section A.1.2.

2.3.2.2 Dopamine treatment of murine primary astrocyte cultures: On the third day after passaging the medium was changed and 60 ml of a vehicle (medium) or a sterile dopamine solution of defined concentration (100x of final concentration) were added to reach final concentrations of 0 (vehicle), 0.1, 1, 10, 50, 100, 200, 500 mM. Cells were treated for either 24, 48 or 72 hrs, resulting in a 3x8-design.

2.3.3 Mouse and human hepatoma cells

Hepa 1-6 cells (from DSMZ, Braunschweig, Germany) were cultured on Petri dishes containing a coverslip in DMEM supplemented with sodium pyruvate and 20% FCS. Semi-confluent cultures at passages 13-15 were used for the experiments.

HepG2 cells (from ATCC, HB-8065, delivered by Promochem, Wesel, Germany) were cultured on collagen-coated Petri dishes containing a coverslip in DMEM supplemented with sodium pyruvate, non-essential amino acids and 20% FBS. Semi-confluent cultures at passages 98-100 were used for the experiments.

2.4 Morphological staining techniques

2.4.1 Histological staining

2.4.1.1 Modified Kluver-Barrera staining: Sections were stained for 1.5-2 hrs at 60°C in luxol fast blue and differentiated in 0.1% NaOH (aq). Counterstaining with acidophilic cresyl violet was performed at RT for 8-15'. Kluver-Barrera stains myelin sheaths blue, nuclei, nucleoli and Nissl bodies (rER) violet and neuropil cyan. For a detailed description see appendix A, section A.2.1.1.

2.4.1.2 Sudan Black B (SBB) staining: SBB staining was used in combination with subsequent indirect immunofluorescence staining in order to quench unspecific fluorescence from lipofuscin granules (Schnell, Staines & Wessendorf, 1999).

Sections were incubated over night at 60°C followed by 3 changes of xylene (5' each) to remove the paraffin. Afterwards sections were rehydrated through a descending series of ethanol (2 x 99%, 1 x 96°; 90%, 80%, 70%; 5' each) and then introduced into a solution of 0.1% SBB in 70% ethanol for 10'. Thereafter rehydration of sections was continued using 50% ethanol and ultrapure water for 5' each. Hydrated sections were then used for indirect immunofluorescence labeling (see below).

2.4.2 Indirect Immunohistochemistry (IHC), Immunofluorescence (IF) and ImmunoGoldLabeling (IGL)

2.4.2.1 IHC on paraffin-embedded tissue sections: Stainings for Pex14p, catalase, ABCD3 as well as mitochondrial Mn-superoxide dismutase (SOD2) were carried out according to a standardized protocol for indirect immunofluorescence on formalin-fixed paraffin-embedded (FFPE) tissues (based on Grabenbauer et al., 2001 and Baumgart et al., 2003). For a detailed description see appendix A, section A.2.2.2.

2.4.2.2 IF on paraffin-embedded tissue sections: The protocol was similar to that for IHC-labeling (see above), but without H_2O_2-incubation or adding of avidin and biotin to the respective solutions. Secondary donkey antibodies against rabbit were coupled with AlexaFluor 488 fluorophore (Molecular Probes/Invitrogen) and diluted 1:300 in 1% PBSA with 0.05% Tween 20. Nuclei were counterstained with Hoechst 33342 (Sigma) and TOTO-3

iodide (Molecular Probes) diluted in PBS. All washing steps and incubation procedures (except for antigen retrieval) were performed at room temperature. Slides were mounted with Mowiol mounting medium (Polysciences) mixed two parts to one with n-propylgallate (Sigma) as fading agent.

2.4.2.3 Multiplex IF on human and murine brain tissue sections: Main steps were the same as described above. Apart from a primary rabbit antibody against Pex14p, catalase or ABCD3 further primary antibodies against MAP2 (neuronal marker) and GFAP (astrocyte marker), raised in different animals) were used simultaneously and visualized with respective secondary antibodies carrying green (for Pex14p, catalase, SOD2), red (for GFAP) and blue (for MAP2) fluorophores. For a detailed description see appendix A, section A.2.2.3.

2.4.2.4 Multiplex IF on murine primary neuronal and astrocyte cultures: Labeling protocols were similar to those described above for human and murine brain sections. For a detailed description see appendix A, section A.2.2.4.

2.4.2.5 IF using QuantumDots® on mouse and human hepatoma cells: Labeling cells and tissues with secondary antibodies coupled to QuantumDots® was performed using the standard protocols described above and in appendix A, however, without success. The labeling protocol was therefore carefully adapted stepwise by the author, until satisfactory results were obtained. For a detailed description of the final protocol for IF on cells using QuantumDots® see appendix A, section A.2.2.5.

2.4.2.6 IGL for electron microscopy: All washing and incubation steps were performed on drops pipetted onto a specially cast rubber panel. Primary antibodies against Pex14p and catalase were visualized through nanogold-Fab'-probes with silver or gold enhancement. For a detailed description see appendix A, section A.2.2.6.

2.5 Reverse transcription polymerase chain reaction (RT-PCR)

Prior to RNA extraction all surfaces and gloves were treated with chaotropic agents (RNaseZap, Sigma) to avoid RNase contamination. Metal tools (scissors, tweezers and

scalpels) were incubated for 60’ in 70% ethanol. RNA extraction were performed using appropriate kits from Qiagen (RNeasy Mini Kit for cells and tissues; RNeasy Protect Animal Blood Kit for blood samples), wherefore buffer compositions cannot be described. Buffer names are those given by Qiagen.

2.5.1 RNA extraction protocols

2.5.1.1 RNA extraction from animal tissues: Excised organs were immediately placed into a stabilizing agent and flash frozen in liquid nitrogen for storage. RNA extraction was performed according to the RNeasy Mini Kit (Qiagen) protocol. For a detailed description see appendix A, section A.3.2.1.

2.5.1.2 RNA extraction from primary murine astrocyte cultures: Dopamine- or vehicle-containing medium was removed by pipetting and cultures were washed in cold RNase free PBS (4°C). Each Petri dish was incubated with 350 µl buffer RLT + 3.5 µl β-ME for 30’ at room temperature to lyse the cells and reduce protein disulfide bonds. The cell lysate was then pipetted onto the QIAshredder spin column and centrifuged for 2’ at >8000 *g*. The subsequent steps were identical to those described for tissues in appendix A, section A.3.2.1. In the final step RNA was eluted with 43 µl RNase-free water.

2.5.1.3 RNA extraction from animal whole blood: After collection blood was mixed with an appropriate volume of RNA Protect Animal Blood Reagent (Qiagen), incubated for 2 hrs at RT and frozen in liquid nitrogen for storage. RNA extraction was performed according to the RNeasy Protect Animal Blood Kit (Qiagen) protocol. For a detailed description see appendix A, section A.3.2.2.

2.5.2 RNA denaturation, quantification and quality control

All RNA eluates were denatured through incubation for 5’ at 65°C and quantified using a spectrophotometer (BioRad Smart Spec™ 3000). RNA-integrity was additionally controlled through a denaturing agarose-MOPS/FA-gel electrophoresis. For a detailed description see appendix A, section A.3.3.

2.5.2.1 DNase digestion: DNase digestion was either performed on column or prior to First Strand Synthesis. For a detailed description see appendix A, section A.3.3.1.

2.5.3 First Strand Synthesis (FSS)

FSS was performed according to the SuperScript™ II reverse transcriptase (Invitrogen) protocol. For a detailed description see appendix A, section A.3.4.

2.5.4 Primer Design

Primers for cDNAs of the mRNAs of 28S rDNA, PEX14, CAT, SOD2, ABCD3 & GFAP were taken from the primer stock of the Division of Medical Cell Biology (Institute for Anatomy and Cell Biology, JLU Giessen). All other primers were self-designed using the Primer Basic Local Alignment Search Tool (Primer-BLAST) online program (NCBI, www.ncbi.nlm.nih.gov/tools/primer-blast*). Primers were designed to be separated by at least one intron on the corresponding genomic DNA so that possible amplification products of contaminating genomic DNA could be detected and differentiated from the intended cDNA amplificates. Primers were only searched for in the species Mus musculus. PCR product size was set at default (70-1000 base pairs). Optimum primer melting temperatures were initially set at 59°C-61°C.* Primer specificity stringency was set at at least 4 mismatches to unintended targets, including 4 mismatches within the last 7 base pairs at the 3'end. Maximum self complementarity and maximum 3' end complementarity was set at 4 and 2 respectively.

In cases were no primers matched the aforementioned criteria, these were loosened progressively until suitable primers were found. For a complete list of primers used for PCRs and nested PCRs see appendix B.

Primers were ordered as lyophylisates from Operon and diluted with PCR clean water (aqua ad iniectabilia, AAI, Braun) for 10' at 37°C on a thermo-shaker set at 700 rpm to create stock solutions (100 pmol/µl), which were stored at -20°C. Before use, portions of the stock solutions were diluted 1:10 with AAI in RNase- and DNase-free reaction tubes. Ready-to-use primer solutions were also stored at -20°C.

Several primer-pairs for each template were tested in temperature graded PCRs (5 temperature steps) with various numbers of PCR cycles until the best primers and the optimal conditions for each template (regarding cDNAs transcribed from cell-, tissue- or whole blood-RNA) and each primer pair were found (see appendix B).

2.5.5 Polymerase Chain Reaction (PCR)

PCRs were pipetted and run in DNase-free PCR-softstrips (0.2 ml, Biozym). Pipetting steps were all carried out either on crushed ice or PCR cool blocks. PCRs were run in an iCycler thermal cycler (BioRad).

PCR single reaction volume was 25 μl, consisting of 5.2 μl master mix, 1 μg (0.5 μg for samples taken from whole blood) cDNA (X μl) and an appropriate volume of AAI (19.8-X μl). For each primer pair a control samples was run containing just 5.2 μl master mix and 19.8 μl of AAI with the omission of cDNA.

For detailed information on the composition of master mixes as well as PCR protocols see appendix A, section A.3.5.

2.5.5.1 Nested PCR: In the cell culture experiments the expression of specific templates (DAO, DRD1, DRD2, DRD3, DRD4, DRD5, COMT1t3 and DAT) appeared to be very low, wherefore the signal/noise-ratio of the PCR products was considered insufficient. In these cases nested PCRs were run. Here for a second (nested) primer pair was designed, whereby the nested primers lay farther towards the 3'-end of the amplicon in comparison to the original primers. The product of the first PCR run with the respective first primer pair was then amplified again, but using the nested primer pair. Thereby the target template was amplified even more, whereas unspecific noise was reduced simultaneously. For nested primer pairs see appendix B.

2.5.5.2 Agarose-Gel Electrophoresis: PCR amplification products were mixed with 2ml DNA loading dye (Blue/Orange 6x loading dye, Promega) and analyzed through electrophoresis using a 1% agarose-gel. For detailed descriptions see appendix A, section A.3.5.1.

2.6 Imaging

Light and fluorescence microscopical images were taken with a Leica fluorescence microscope (Leica DMRD with a Leica DC 480 digital camera) and a confocal laser scanning microscope (Leica TCS SP2, setting at airy 1, average of 16 scans).

Gel pictures were taken in a BioRad GelDoc 2000 with QuanityOne® software (version 4.3.0, BioRad)

EM pictures were taken at 80 kV with a LEO906 electron microscope (Zeiss, Wetzlar).

All ex post facto modifications of images were performed with Adobe® Photoshop® CS2 version 9.0 or Adobe® Photoshop® Elements version 9.

2.7 Statistical Analyses

All statistical analyses were performed with the Statistical Package for the Social Sciences (SPSS), different versions.

3. Results

In order to find an optimal ubiquitous marker for peroxisomes independently of metabolism, cell and tissue type or species the general abundance and distribution of catalase, ABCD3 and Pex14p was compared in a large variety of organs, tissues and cell types of different embryonic origin. Results show that a more accurate picture of the abundance as well as inter- und intracellular distribution of peroxisomes is given through Pex14p rather than catalase, which is the generally used maker enzyme (Hruban et al., 1972). Catalase and ABCD3 are metabolically dependent enzymes which are present in many cell types, but vary strongly regarding their abundance and distribution, whereas Pex14p is found in every healthy and intact peroxisomal membrane and can therefore be used as a general marker.

With the new Pex14p-labeling it is therefore possible to localize peroxisomes in various species, different tissues and distinct cell types in all different stages of ontogeny.

3.1 Establishing Pex14p as the optimal peroxisomal marker for comparative and experimental morphology

3.1.1 Specificity of the self-created antibodies against catalase and Pex14p

Western blotting for catalase and Pex14p performed and published by co-workers shows the specificity of both antibodies. The specificity of the catalase antibody was also further established through preabsorption with bovine liver catalase. The incubated antibody was centrifuged and the supernatant was used for immunostaining on formalin fixed and paraffin embedded (FFPE) sections as described above for the IF technique. In these control experiments no signal for catalase could be detected (Ahlemeyer et al., 2007).

Additionally, the specificity of both antibodies was examined in immunogold-EM experiments, showing specific binding of both antibodies with a negligible amount of unspecific background. Pex14p-staining in electron microscopy has not been achieved before and could not be performed successfully on epoxy resins, even after etching with H_2O_2 or 70% ethanolic sodium hydroxide (data not shown here). In acrylic resins immunogold labeling of Pex14p was achieved, but labeling densities and signal/noise ratios were considered relatively unsatisfactory. Therefore labeling was attempted in cryo-ultrathin sections with markedly better results.

Pex14p as a membrane protein can be clearly shown around the perimeter of peroxisomes comparable to immunogold-labeling for ABCD 3 (Baumgart, 1997), whereas the functional enzyme catalase is located in the peroxisomal matrix (Fig. 3.1_1). The abundance of catalase is striking, especially in comparison to other matrix enzymes like acyl-CoA oxidase, enoyl-CoA hydratase (Litwin & Beier, 1988), D-amino acid oxidase, multifunctional protein 1 (Baumgart, 1997) or D-aspartate oxidase (Zaar et al., 2002). The density of catalase labeling is also markedly increased in cryo-ultrathin sections compared to resin ultrathin sections (both in rat liver, e.g. Baumgart, 1997) showing that immunogold labeling using cryo-ultramicrotomy is far superior even than acrylic resin embedding, albeit more difficult during cutting and handling. The ultrastructural tissue preservation is, however, obviously superior in resin-embedded ultrathin sections.

As peroxisomes are less abundant and smaller in the brain compared to the liver, enhancement times for the immunogold particles was increased, wherefore the particles surrounding two peroximes (probably in axons) are not round, but unevenly shaped. The areas devoid of catalase in the two larger peroxisomes are most likely caused by urate oxidase crystals, which are present in peroxisomes of most mammalian species, but not in hominoids (q.v. chapter 1.4.2).

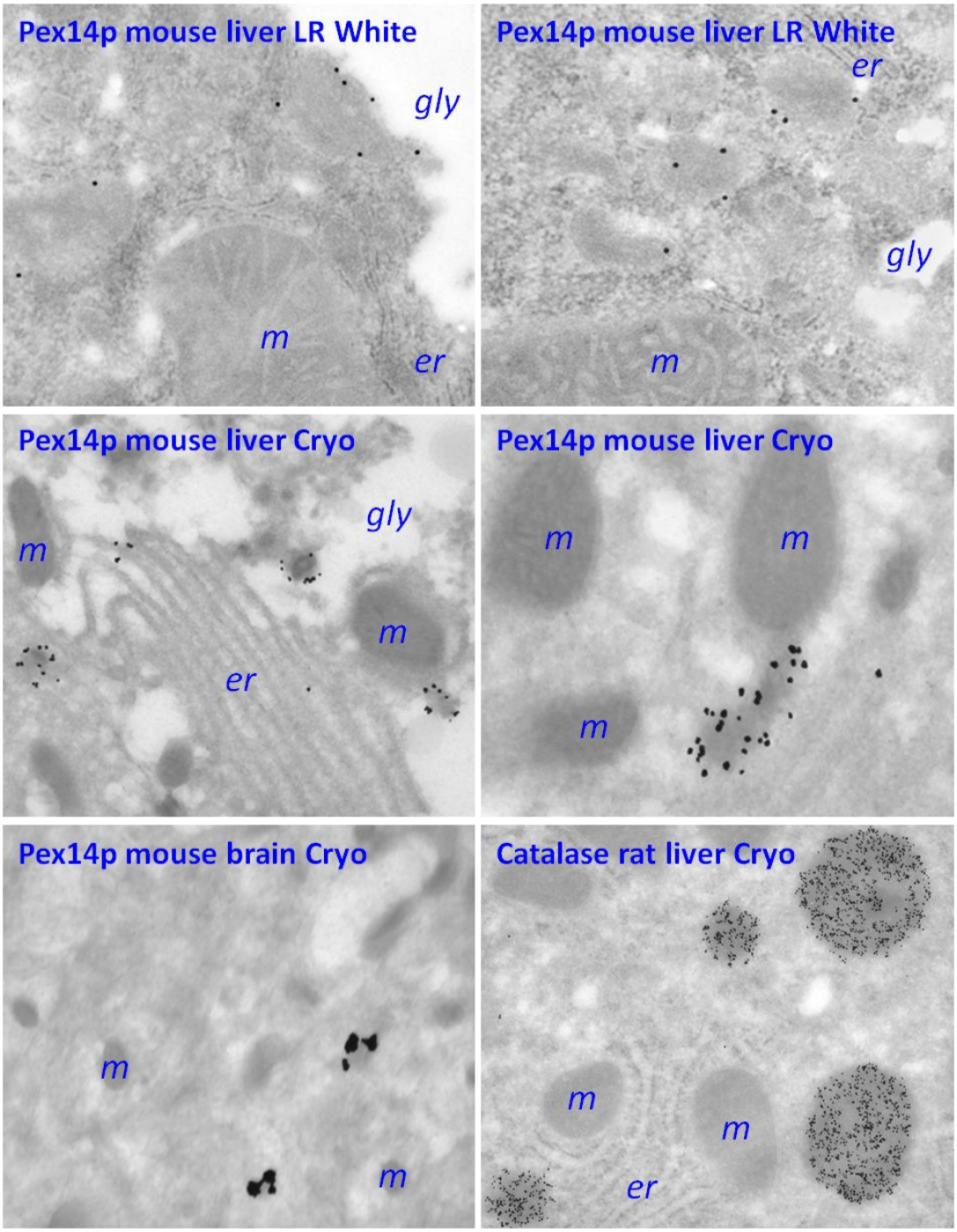

Fig. 3.1_1: Immunogold labeling of Pex14p in acrylic resin (top row) and cryo (bottom rows) ultrathin sections; *er: rough endoplasmic reticulum, gly: glycogen fields, m: mitochondria*

3.1.2 Specificity of secondary antibodies and peroxidase substrate reaction

Unspecific binding of secondary antibodies or unspecific reaction of the peroxidase substrate as well as adequate quenching of endogenous peroxidases was control for through sections which were incubated parallel to and in the same fashion as regular sections, but with omission of the primary antibodies. In these control sections no signal was ever observed. An example shall be given of catalase, Pex14p and the appropriate negative control

in the developing murine abdomen. Not only can the differential distribution of catalase and peroxin 14 be illustrated, but it can also be shown that the specificity of secondary antibodies and the peroxidase substrate reaction is given in all different tissues and organs (Fig. 3.1_2).

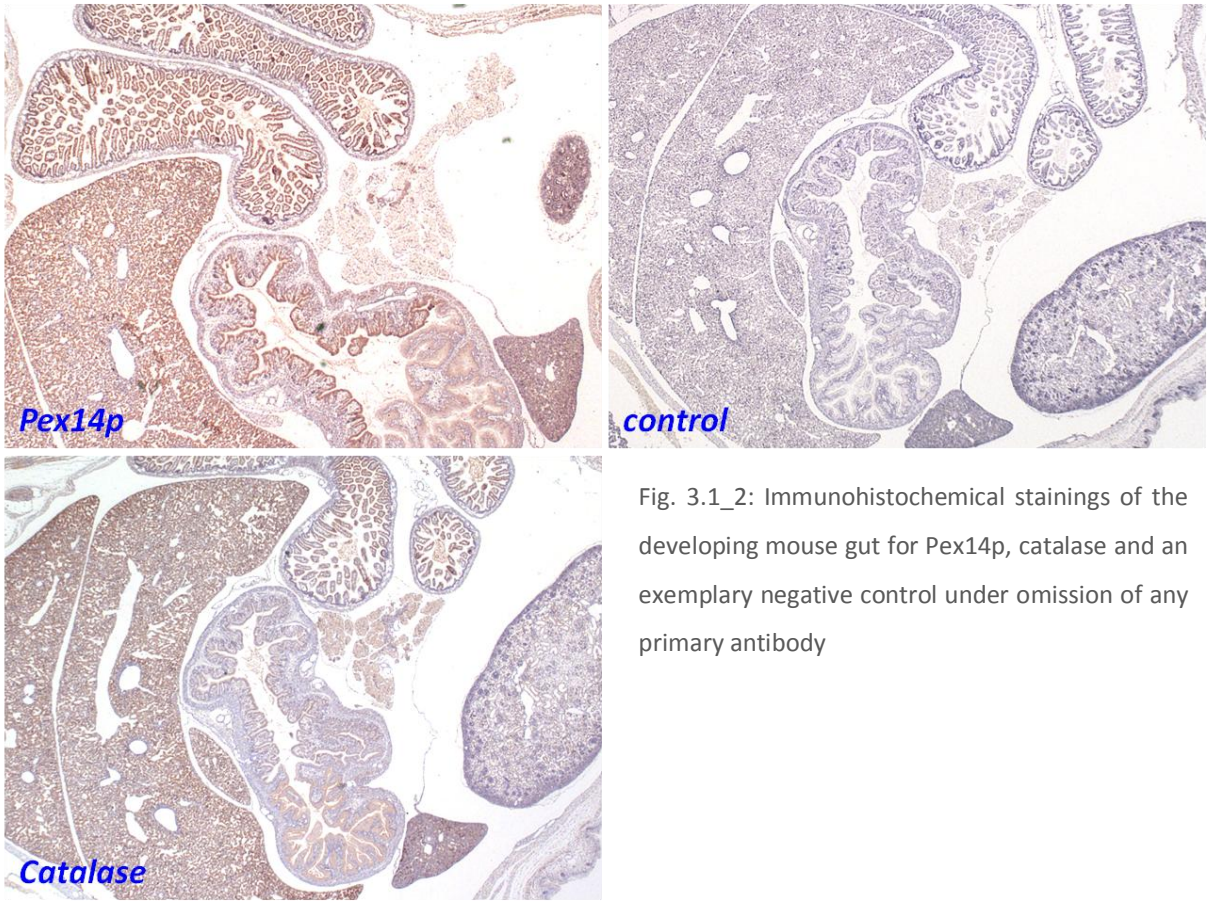

Fig. 3.1_2: Immunohistochemical stainings of the developing mouse gut for Pex14p, catalase and an exemplary negative control under omission of any primary antibody

3.1.3 Peroxisomes in epithelial cells of mesodermic and endodermic origin

Epithelia are known for their functional, structural and metabolic diversity. Their major functions are the lining of the body, the forming of a barrier to the outside world (also within the respiratory, gut and urinary organs) as well the endo- and exocrine secretion.

The epithelia of different organs with distinct functions were therefore examined regarding their peroxisome content and the differences in abundance and distribution of catalase (CAT), ABCD3 and Pex14p. Duodenum and kidney were chosen as examples for epithelial lining of different parts of the viscera with endodermic and mesodermic origin respectively. Epithelia serving a glandular function were investigated in the endocrine and exocrine pancreas as well as the serous, mucous and duct cells of the submandibular gland.

Due to the findings of coworkers in testis (Nenicu et al, 2007) epithelial cells involved in steroid hormone production were also examined more closely.

3.1.3.1 Kidney (Fig. 3.1_3): The distribution of peroxisomes within the different parts of the renal nephron is dichotomous. Pex14p is found in all cells of the renal corpuscle, the distal (marked by the macula densa) and intermediary tubules as well as the collecting ducts in similar abundance. There is, however, a marked increase in peroxisomal density within the proximal tubules, identifiable through the urinary pole. This dichotomy in the expression patterns is also found in ABCD3- and catalase-stainings. Both of the latter stainings, however, do not show peroxisomal distribution consistent to the staining for Pex14p. In ABCD3-labeling, the renal corpuscle has less positive signals within the glomerulum and the parietal layer of Bowman's capsule is completely negative. This would allow the supposition that the signals within the glomerulum are found within the endothelial cells of the blood vessels, while the podocytes of the visceral layer of Bowman's capsule and maybe also the intraglomerular mesangial cells show no signal for ABCD3, which would explain the weaker and not as evenly distributed signal for ABCD3 compared to Pex14p.

Catalase is found in high abundance within the proximal tubules, which is concurrent with findings in electron microscopy and in situ hybridization (Baumgart, 1997), but catalase is found only very sparsely within the glomerulum. Again, similar to the staining for ABCD3, the parietal layer of Bowman's capsule appears negative for catalase, wherefore it is again likely that the sporadic signals within the glomerulum are also within endothelial peroxisomes. The distal tubules are hardly stained for catalase. The distribution of catalase was therefore compared to that of mitochondrial SOD2, in order to assess whether catalase is expressed in high amounts within cells with high mitochondrial antioxidant activity. As expected, SOD2 is found in all cells of the renal duct system, but with markedly higher levels within the proximal tubules, whereas the renal corpuscle is mainly devoid of signal. This difference can also be seen in standard fluorescence microscopy in serial sections of the same renal corpuscle and macula densa in stainings for Pex14p and catalase.

The results from the FFPE-sections taken from a freshly perfused mouse were replicable in sections from the kidney of a Sacred Baboon, immersion fixed in Lilies's formol and refixed in Bouin's fixative in the year 1984 as part of our regular histology course for medical and dentistry students.

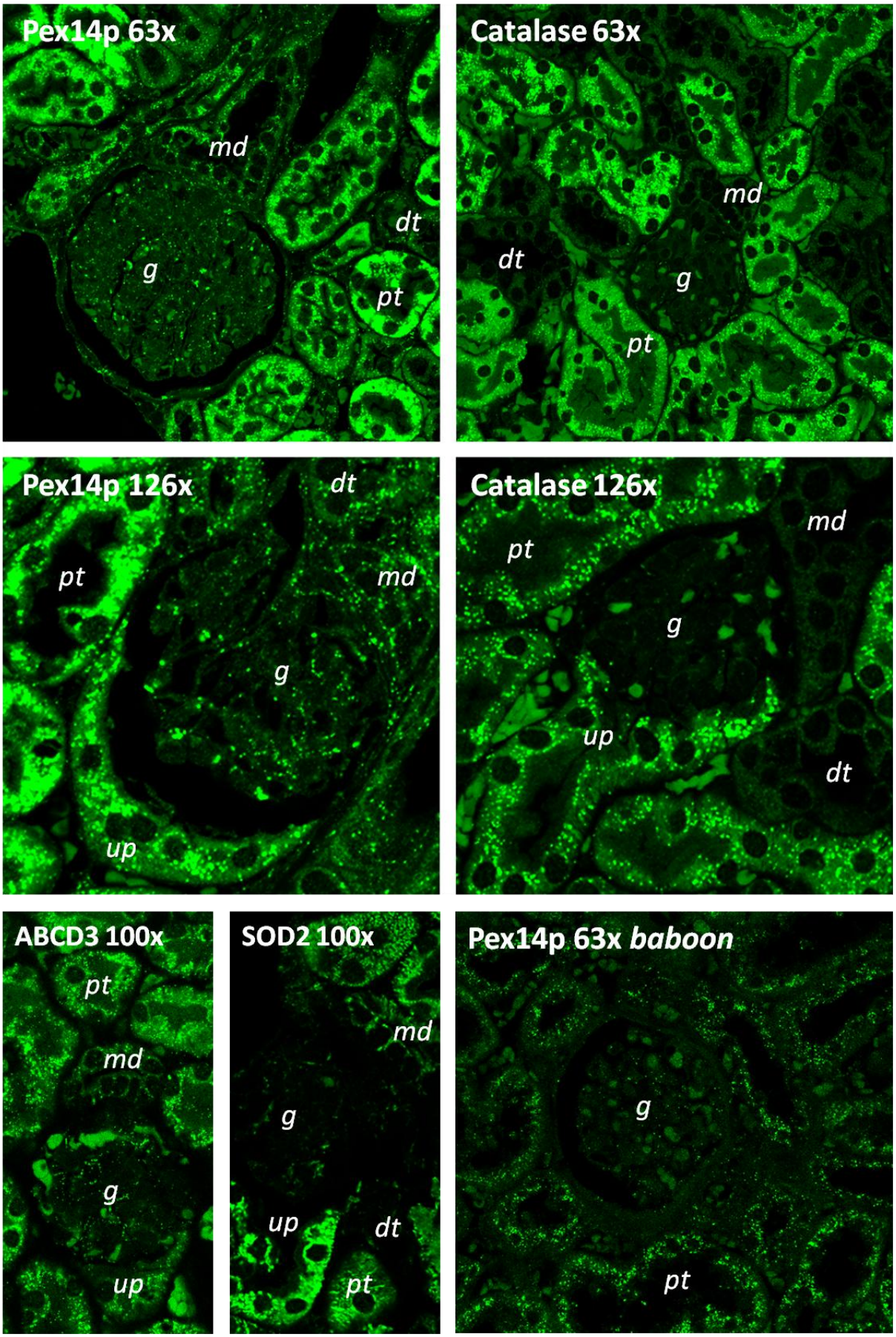

Fig. 3.1_3: Immunofluorescence labeling of Pex14p, catalase, ABCD3 and SOD2 in sections of mouse and baboon kidney; *dt: distal tubule, g: glomerulum, md: macula densa, pt: proximal tubule, up: urinary pole*

3.1.3.2 Endocrine pancreas: Whereas the exocrine pancreas shows a similar distribution of Pex14p as well as catalase as is found in other exocrine glands of endodermic origin (see next section), the exocrine cells in the islets of Langerhans differ markedly regarding both peroxisomal as well as catalase abundance. While the number of peroxisomes is extremely high within the exocrine cells, catalase appears to be almost absent and only traceable in what appear to be peroxisomes of endothelial cells (Fig 3.1_4). This would suggest a role of peroxisomes in pancreatic hormone metabolism that is independent of H_2O_2-degradation.

Multivariate analyses of the morphometric quantification of various parameters of fluorescence signal intensity (ratios signal/area, signal/nucleus and signal area/whole area) for Pex14p and catalase immunolabelings (n=29) showed significant differences between protein content ($F = 21.76$, $p < .001$; $F = 25.42$, $p < .001$; $F = 10.00$, $p = .004$) as well as between endocrine and exocrine pancreas ($F = 24.25$, $p < .001$; $F = 63.9$, $p < .001$; $F = 6.78$, $p = .016$). A principle component analysis (PCA with Varimax-rotation and Kaiser-normalization) of all items measuring the ratios signal/area & signal area/whole area revealed a two-factor solution (factor 1: endocrine pancreas, factor 2: exocrine pancreas) explaining for 76.1% of variance. The ratio signal/nucleus was excluded from PCA, due to the fact that the size and abundance of cells differ substantially between endocrine and exocrine pancreas, wherefore the aforementioned ratio was considered unsuitable in this context.

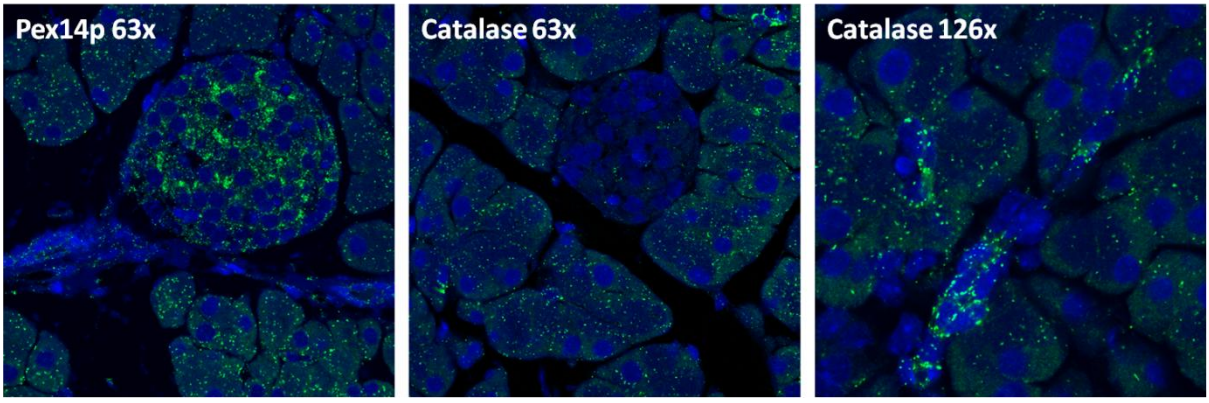

Fig. 3.1_4: Immunofluorescence labeling for Pex14p and catalase in the mouse pancreas; left and middle images show an endocrine islet surrounded by exocrine acini. The right image shows an excretory duct in the exocrine part of the pancreas.

3.1.3.3 Exocrine cells of mouse pancreas and submandibular gland (Figs. 3.1_4 & 3.1_5): The distribution of peroxisomes in the serous glandular cells of both the submandibular gland and the pancreas is quite comparable. Peroxisomes are found in moderate abundance throughout

the cytoplasm. In the serous part of the gland the abundance of peroxisomes in duct cells is markedly higher as is their distribution herein clearly perinuclear. Mucous cells of the submandibular gland exhibit higher numbers of peroxisomes within their cytoplasm, even higher than the adjacent duct cells. They appear to be displaced to the basal part of the cell.

Catalase is found in similar distribution within the serous cells of the submandibular gland and the pancreas, albeit in lesser amount. In duct cells, however, catalase is significantly increased both in pancreas and in the submandibular gland. In the larger ducts of the submandibular gland an unexpected catalase-pattern was found, which was not punctuate as usual, but appeared in the basal cell layer to be evenly distributed throughout the entire cytoplasm. This phenomenon was observed in different ducts, different sections and through different labeling techniques, suggesting that basal cells of the submandibular duct truly possess physiologically cytoplasmic catalase.

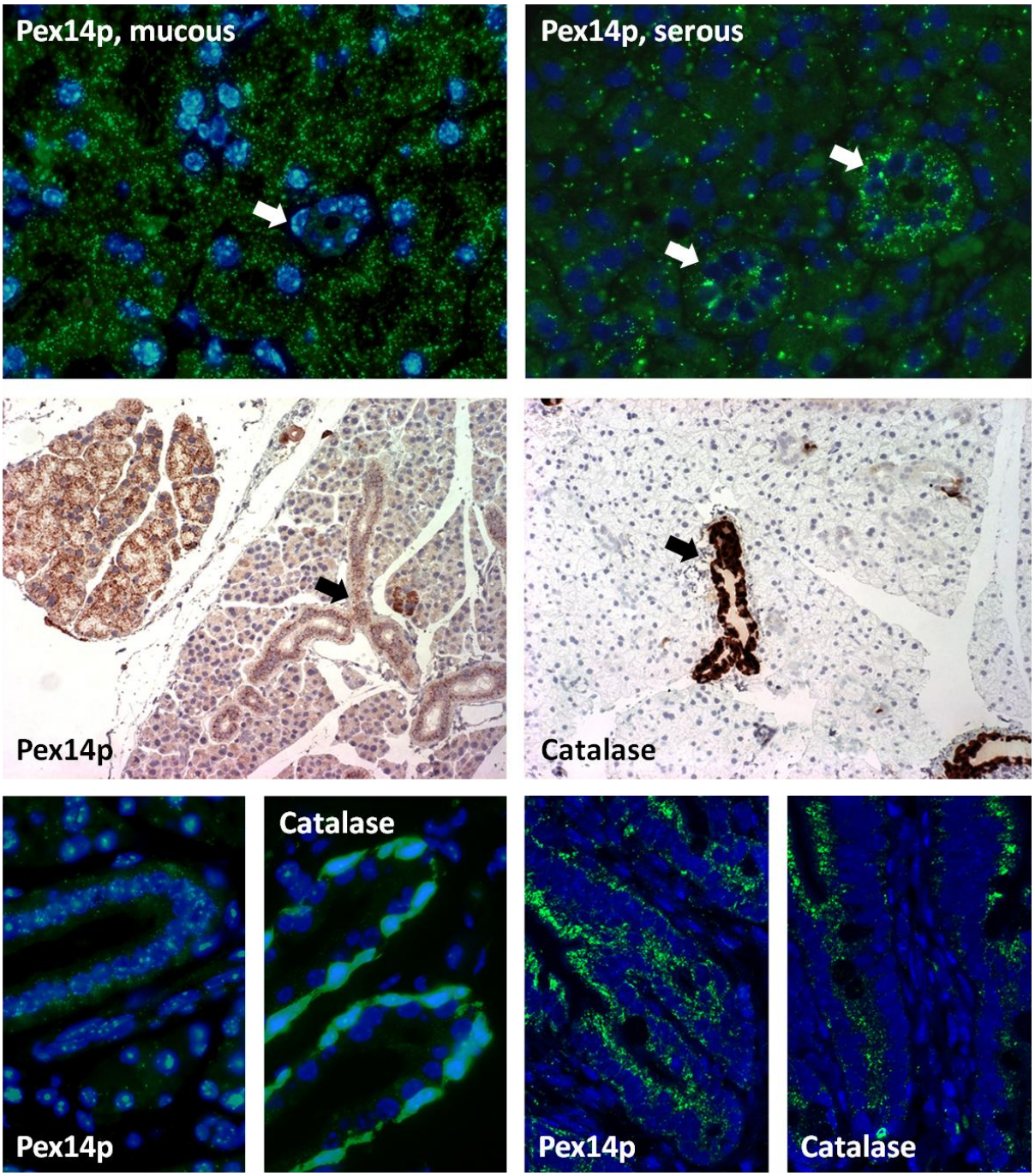

Fig. 3.1_5: Immunolabeling of Pex14p and catalase in serous, mucous and duct cells (arrows) of the mouse submandibular gland and in the duodenum (bottom two images on the right). In the middle left image the mucous part is on the left hand and the serous part on the right hand side of the image. The bottom two images on the left show higher magnifications of excretory ducts.

3.1.3.4 Exocrine cells of the human submandibular gland (Fig. 3.1_6): Apart from the question of conservation of peroxisomal membrane protein expression and abundance between mouse and human, another question regarding this tissue sample was also, whether the protein was still detectable in samples that had not been prepared specifically for

laboratory research, thereby giving insight into the stability of the Pex14p-antigen as well as the sensitivity of the Pex14p-antibody.

Tissue was taken from body donors to the gross anatomy course and was therefore already in a state of beginning decay, as can be seen by the beginning autolysis of the glandular tissue. The labeling for Pex14p, however, is consistent with that achieved in samples taken from freshly perfused animals that had immediately been transferred into immersion fixation solution. Apart from the identical localization of the signals in the glandular ducts and parenchyma, the excellent quality of the staining (albeit in relatively poor quality of tissue preservation) shows the advantages of both the Pex14p-antigen as well as the high quality of the antibody.

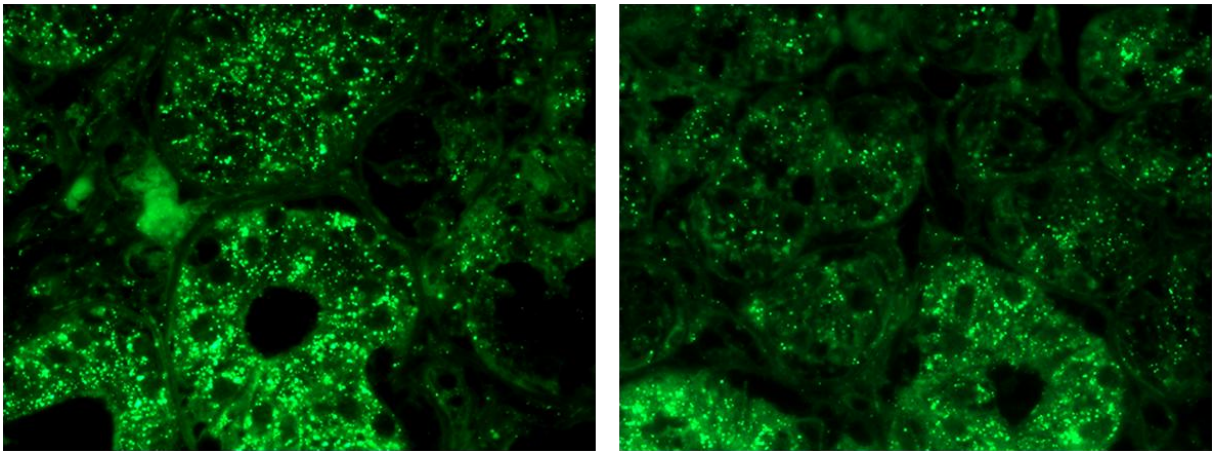

Fig. 3.1_6: Two sections of a human submandibular gland in an advanced stage of autolysis stained for Pex14p

3.1.3.5 Duodenum (Fig. 3.1_5): Catalase-staining clearly allows a distinction between the epithelia of the villi and those of the krypts, as the positive signals on both sides of the nuclei of krypt-cells are markedly reduced in comparison to those of the villi. The amount of catalase within the lose connective tissue of the lamina propria is also highly reduced and barely detectable. Pex14p-staining, however, shows that peroxisomes are actually more or less evenly distributed in the epithelia of both villi and crypts. They are found around the nucleus and towards both ends of the cell with, however, relatively larger amounts towards the luminal/apical side of the duodenal epithelium. Peroxisomes are also found randomly throughout the lose connective tissue of the lamina propria within the villus.

3.1.4 Follicular development in the ovary (Figs. 3.1_7 & 3.1_8)

Oxidative stress is one of the key mechanisms in X-linked adrenoleukodystrophy (X-ALD) (Powers et al., 2005; Fourcade et al., 2008), a rare inherited disorder leading not only to adrenal dysfunction, but in 80% of male patients to impairment of testicular functions (Powers, 1985). Male germ cells have just recently been shown to contain a large number of small peroxisomes, whereof some have very low levels of catalase. Additionally it was also shown in the same paper that the peroxisomal compartment undergoes drastic alterations and clustering in the cytoplasm of elongated spermatids during spermiogenesis (Nenicu et al., 2007).

The peroxisomal abundance and distribution during the maturation of the oocyte within follicular development was therefore examined. Similarly to male germ cells (Nenicu et al., 2007) oocytes show little to no signal for catalase. Also the amount of traceable catalase in the surrounding corona radiata and granulosa epithelia is quite low, albeit that theca cells and cells of the corpus luteum exhibit extremely high levels of catalase.

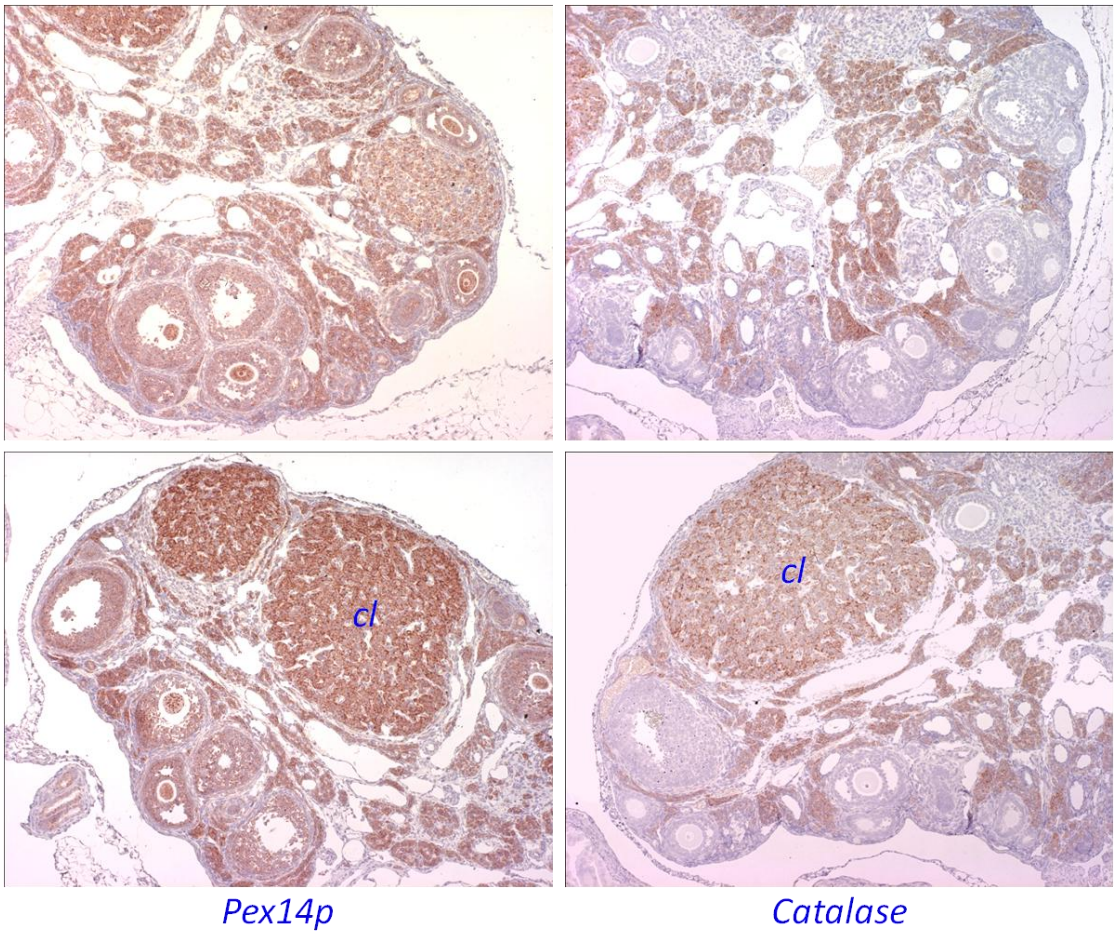

Fig. 3.1_7: Immunohistochemical stainings of a mouse ovary for Pex14p (left column) and catalase (right column); *cl: corpus luteum*

To evaluate possible differences in the content of antioxidant enzymes between the various cells of the ovary a labeling for mitochondrial SOD2 was performed, showing a similar pattern of the enzyme to that of catalase, however with higher intensity in each instance. Low levels of SOD2 are found within the oocyte, medium levels in the follicular epithelia and the highest levels in the theca cells. ABCD3 and Pex14p are distributed in a comparable manner in the ovary, as can be seen by differential staining of the same tertiary follicle.

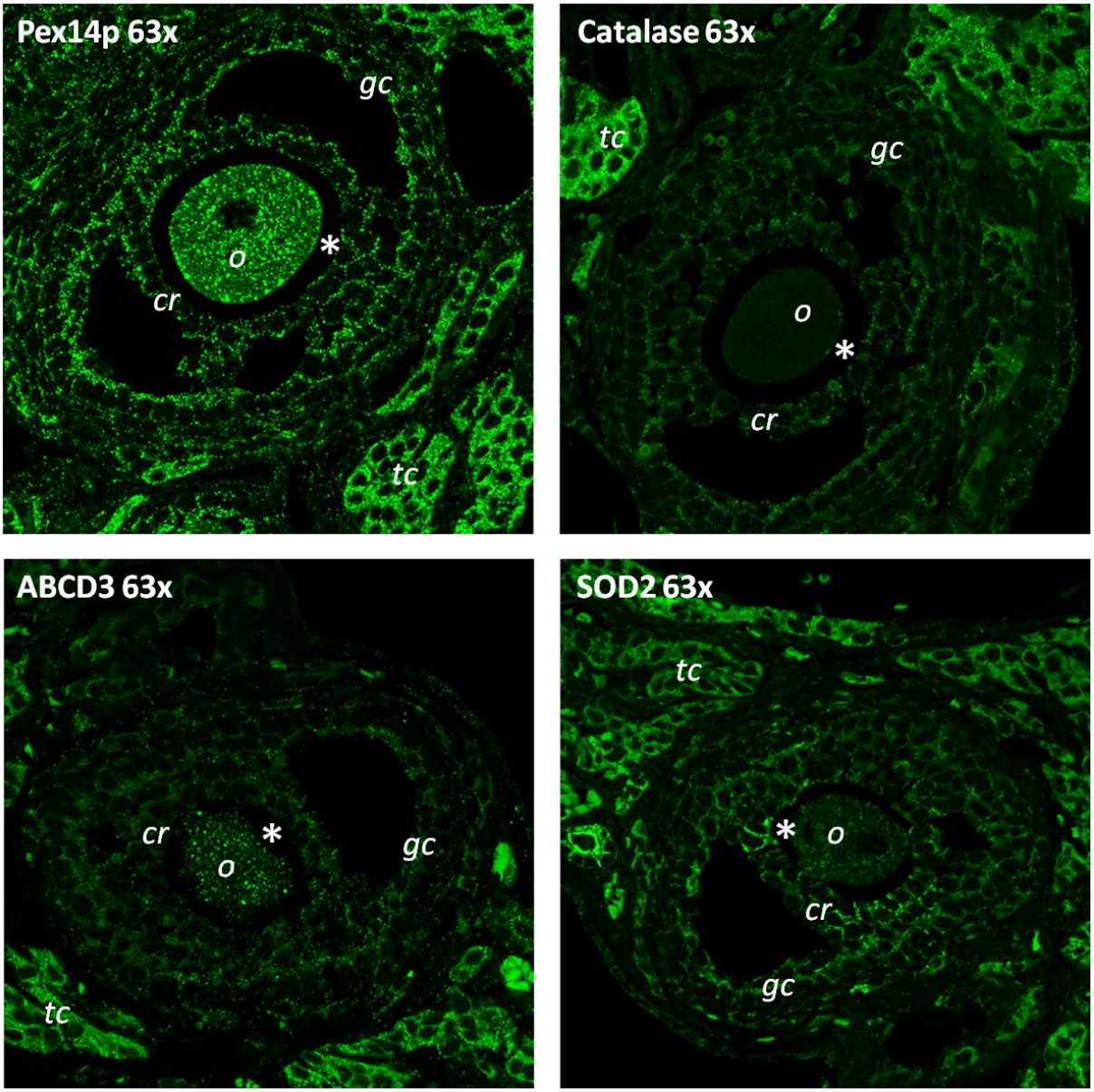

Fig. 3.1_8: Immunofluorescence labeling of serial sections of the same tertiary follicle for Pex14p, catalase, ABCD3 and SOD2; *cr: corona radiata, gc: granulosa cells, o: oocyte, tc: theca cells, asterisks mark the zona pellucida*

It can clearly be shown that peroxisomes are present in very high abundance not only in the endocrine cells of the ovary, but also in the oocyte itself. This observation holds true for all stages of follicular development and oocyte maturation. Primordial follicles are very small and enclose even smaller oocytes, whereof the cytoplasm is extremely small. The primordial follicle is in a dormant or quiescent state and biologically almost inactive, which makes the low number of peroxisomes not surprising. As the follicle develops into a primary follicle and the oocyte matures and increases in size, the cytoplasm becomes densely populated with peroxisomes of various sizes. This development continues through the secondary to the tertiary Graafian follicle. The specificity of all stainings can hereby clearly be seen through the obvious void surrounding the secondary and tertiary follicles, which marks the zona pellucida, a glycoprotein polymer capsule surrounding the oocyte and containing no cellular organelles. In several oocytes Pex14p-positive structures were found similar in shape compared to those described by Nenicu et al. (2007) in late spermatids (Fig. 3.1_10). They are significantly larger in size than those in late spermatids and can be viewed without the necessity of electron microscopy. It is most likely that they are indicative of the oocyte within an atretic follicle and represent the rearrangement of the peroxisomal compartment during cytoplasmic restructuring while the cell undergoes apoptosis.

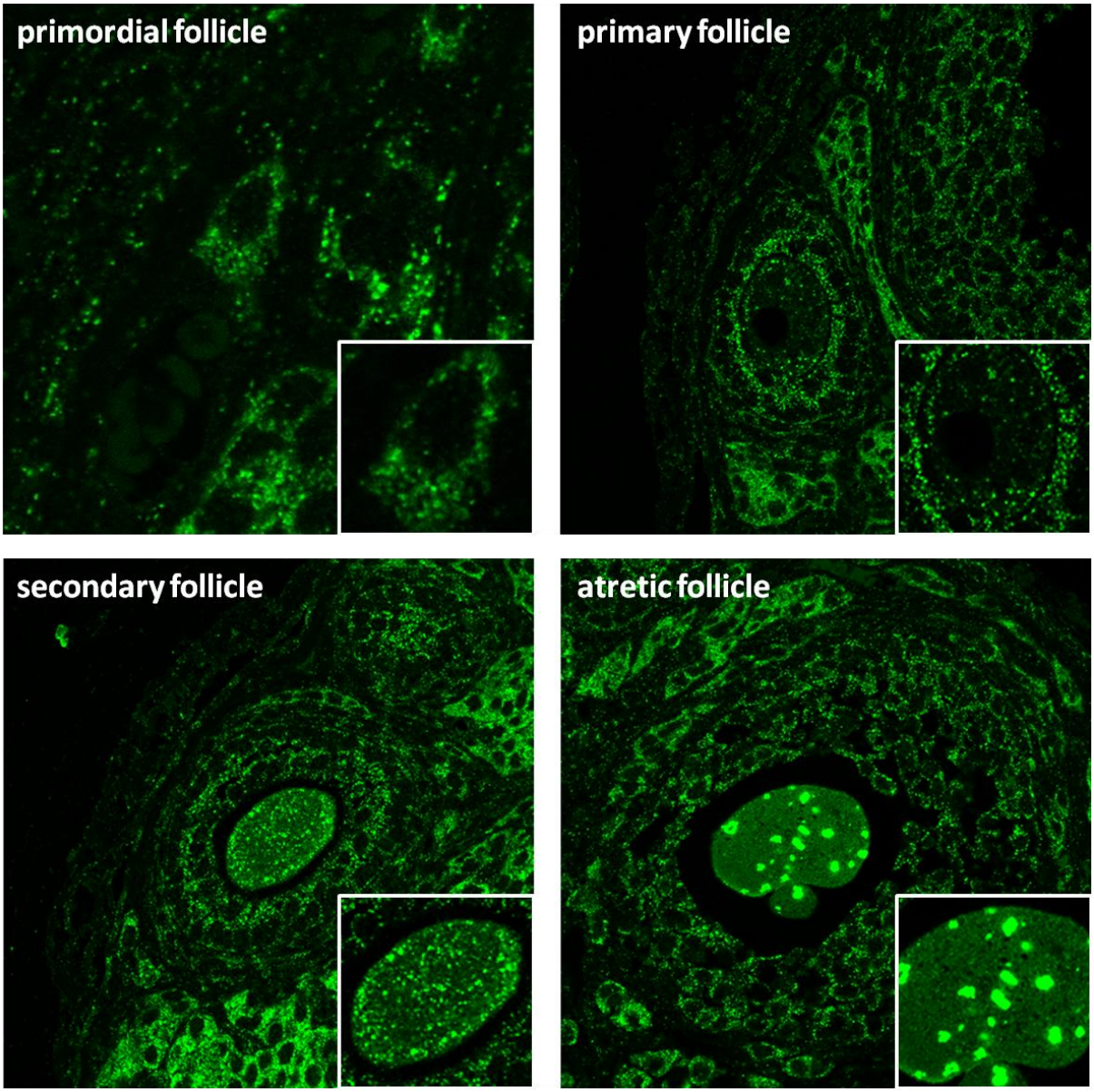

Fig. 3.1_9: Immunofluorescence labeling of Pex14p in various stages of follicular development. All images were taken at 63x magnification, inserts of the oocytes are in 126x magnification.

The structures found in late spermatids before phagocytosis of the cytoplasmic droplet by Sertoli cells were described by light as well as electron microscopy and characterized as catalase-positive double membrane loops. They can also be shown through staining against Pex14p and are also present in seminiferous tubules from a male cat (Fig. 3.1_10). These images also show the quality and sensitivity of the new Pex14p-staining method, as the paraffin blocks of the cat testis are over-20-year-old specimens from our regular histology course. The tissue was immersion fixed in Lilie's formol and refixed in Bouin's fixative rather than taken from animals freshly perfused with PFA. This also goes for sections taken from cat ductus epididymidis (Fig. 3.1_10).

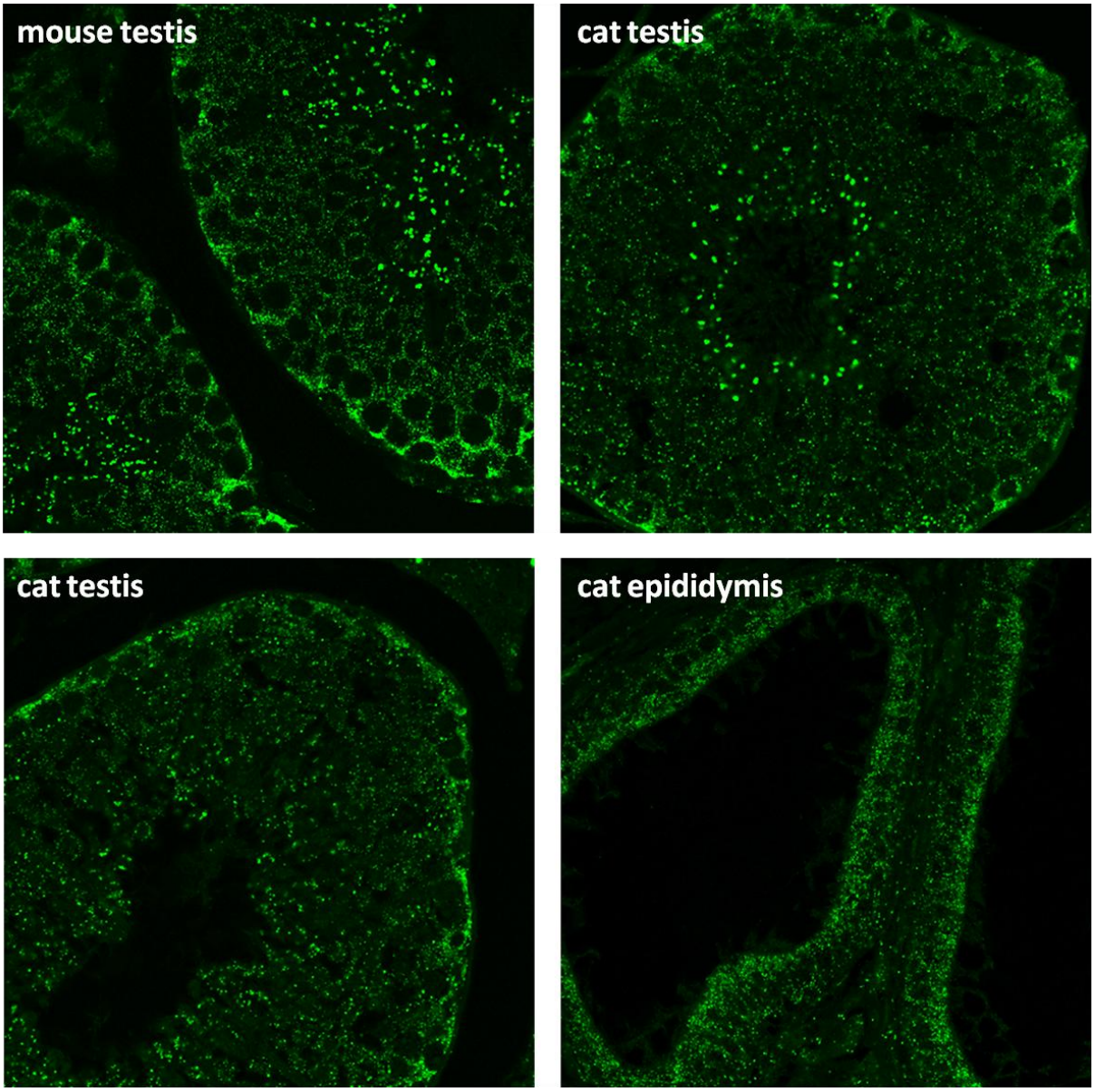

Fig. 3.1_10: Pex14p in mouse and cat testis during different stages of spermatogenesis as well as in the cat epididymis; all images were taken at 63x magnification

3.1.5 Steroid hormone producing cells

Peroxisomes are highly abundant in all cells involved in steroid hormone synthesis, albeit with interindividual differences in density. Most of these peroxisomes are also extremely rich in catalase, in some cases leading to more intense signals than in Pex14p-staining (Fig. 3.1_11). This is probably due to high mitochondrial activity, namely side-chain cleavage during steroid synthesis as well as necessary for protection of steroidogenesis against H_2O_2. Interestingly, peroxisomes in many steroid secreting cells do not exhibit a punctuate pattern, but rather a tubular one at higher magnification (Fig. 3.1_11).

3.1.5.1 Ovary and testis: As previously shown by Nenicu et al. (2007), peroxisomes are present in Leydig cells of the testis as well as in the basal compartment of the germinal epithelium and in peritubular myoid cells (Fig. 3.1_11). Catalase signals are extremely high within Leydig cells (Fig. 3.1_11).

These results are mirrored by the analogous cells of the female gonad, namely the theca and granulosa cells within the ovary. Pex14p can be clearly seen in both the granulosa and the corona radiata epithelium. The signal is highest in the apical parts of the superficial layers of the granulosa cells. Outside the follicle, however, the signal is even more intense within the cells of the theca organ (Fig. 3.1_8).

The signal distribution for catalase is similar to that of Pex14p, however with clearly visible differences regarding intensity. While the signal within granulosa and corona radiata cells is slightly weaker than in stainings for Pex14p, the signal intensity within the theca cells, on the other hand, surpasses that of Pex14p.

The theca cells also clearly show the tubular peroxisomal pattern found in most steroid hormone producing cells (Fig. 3.1_11).

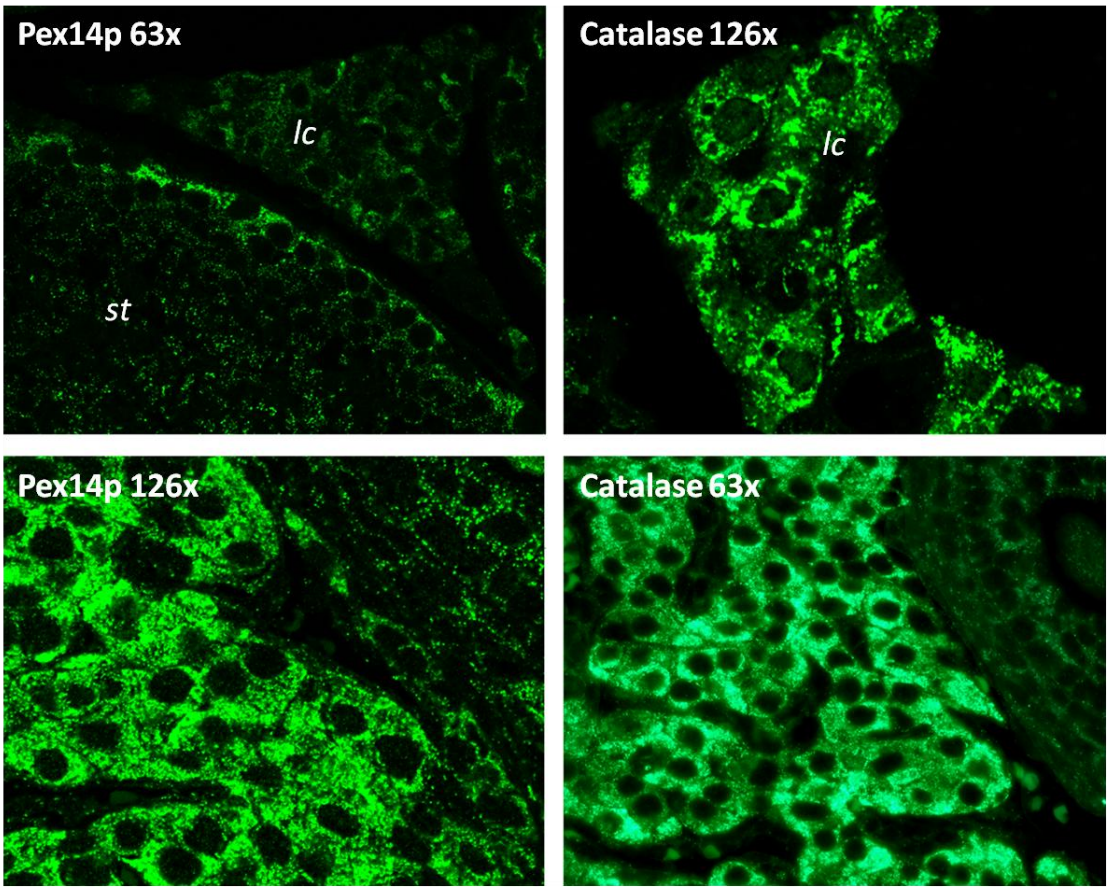

Fig. 3.1_11: Pex14p and catalase in steroid hormone producing cells of the mouse testis (top row) and ovarian theca organ (bottom row); *lc: Leydig cell, st: seminiferous tubule*

3.1.5.2 Adrenal cortex (Figs. 3.1_12 & 3.1_13): The differences in peroxisomal distribution between the three layers of the adrenal cortex can already be seen at low magnification in both Pex14p- and Catalase-stainings. Levels are lowest within the zona fasciculata, slightly higher in the zona reticularis and markedly higher in the zona glomerulosa. These differences can also be seen at higher magnifications as well as in the staining for ABCD3, which is similarly distributed to Pex14p in the adrenal cortex. Higher magnifications of the zona glomerulosa also show the presence of peroxisomes in the cells of the surrounding adrenal fibrous capsule. Comparable to the layers of Bowman's capsule in the kidney, catalase- and ABCD3-stainings were negative within the adrenal fibrous capsule (not shown here). Finally, the tubular pattern of peroxisomal distribution can also be seen at higher magnifications, similar to ovary and testis.

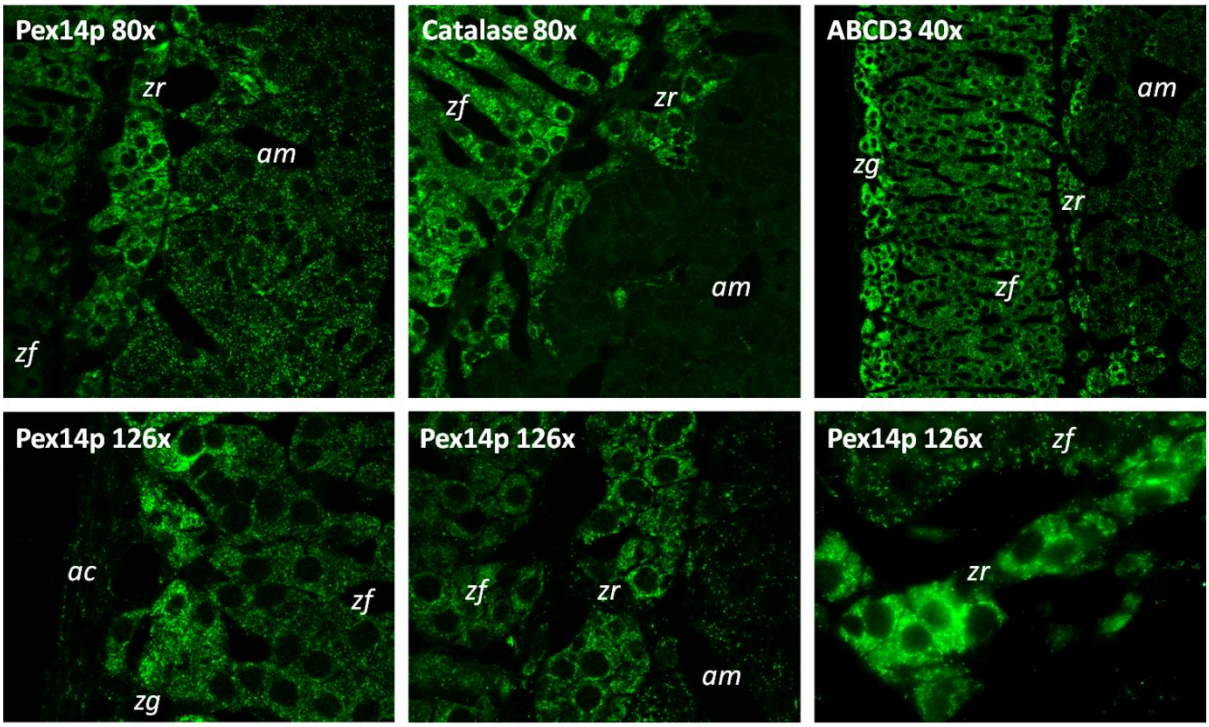

Fig. 3.1_12: Immunofluorescence labeling of Pex14p, catalase and ABCD3 in the mouse adrenal gland; *ac: adrenal capsule, am: adrenal medulla, zf: zona fasciculate, zg: zona glomerulosa, zr: zona reticularis*

The extreme difference between Pex14p- and catalase-signals of the cells of the adrenal medulla shall be described together with the differences in other cells originating from the neural tube and crest.

3.1.6 Peroxisomes in cells originating from the neural tube and crest

The differential distribution of Pex14p and catalase within the developing mouse CNS as well as between primary cultured neurons and astrocytes was recently reported by co-workers (Ahlemeyer et al., 2007). Furthermore, the sharp contrast between catalase-positive bodies in the developing nervous system and lack thereof in corresponding areas of the adult brain has also been described by Arnold and Holtzman (1978) and Holtzman (1982).

3.1.6.1 Adrenal medulla (Figs. 3.1_12 & 3.1_13): Apart from cells of the central and peripheral nervous system, the chromaffine cells of the adrenal medulla originate from the neural crest and can be viewed upon as somewhat analogous to catecholaminergic cells of peripheral sympathetic ganglia, including their being supported by Schwann cells. They also share the extremely high dissonance of neurons regarding the number of peroxisomes labeled with Pex14p compared to the nearly undetectable amounts of catalase. The few positive catalase signals within the adrenal medulla (Fig. 3.1_12) are likely to come from peroxisomes in either endothelial cells of the large medullary vessels or from Schwann cells surrounding the adrenergic chromaffine cells.

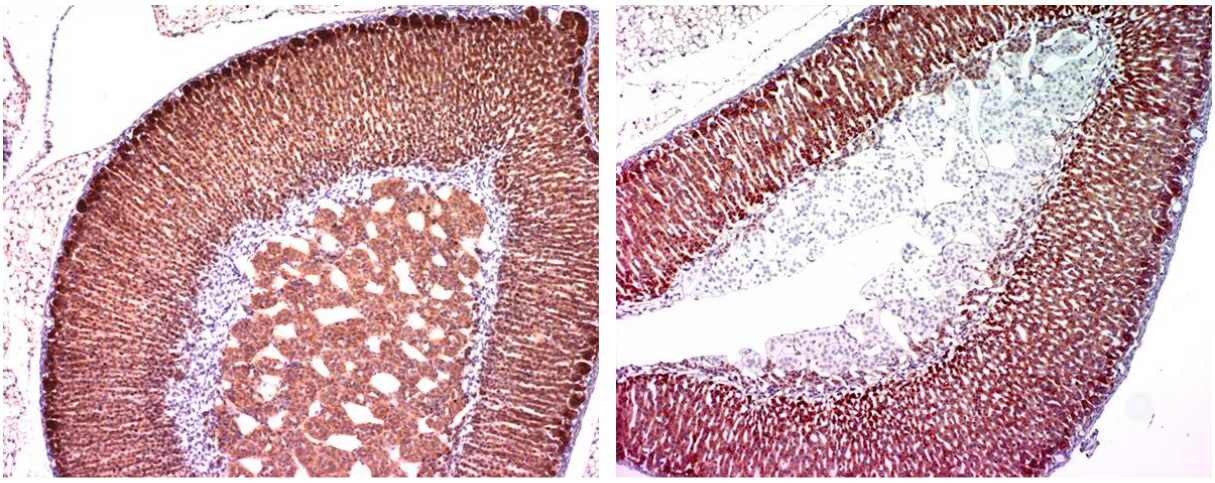

Fig. 3.1_13: Immunohistochemical overview of the mouse adrenal gland

3.1.6.2 Primary neurons before and after treatment with a peroxisome proliferator (Fig. 3.1_14): On the basis of the aforementioned, the reactions of Pex14p (as indicator of total number of peroxisomes) and catalase to the treatment of primary neurons from mouse neocortex with a peroxisome proliferator were examined. It is obvious that baseline catalase-

signals are lower compared to those for Pex14p. Interesting, however, is the fact that catalase does not increase linearly to Pex14p upon treatment with ciprofibrate. This means that not only is catalase less abundant at baseline, but also that peroxisome proliferation in neurons does not lead to a proportionate increase in catalase-containing peroxisomes.

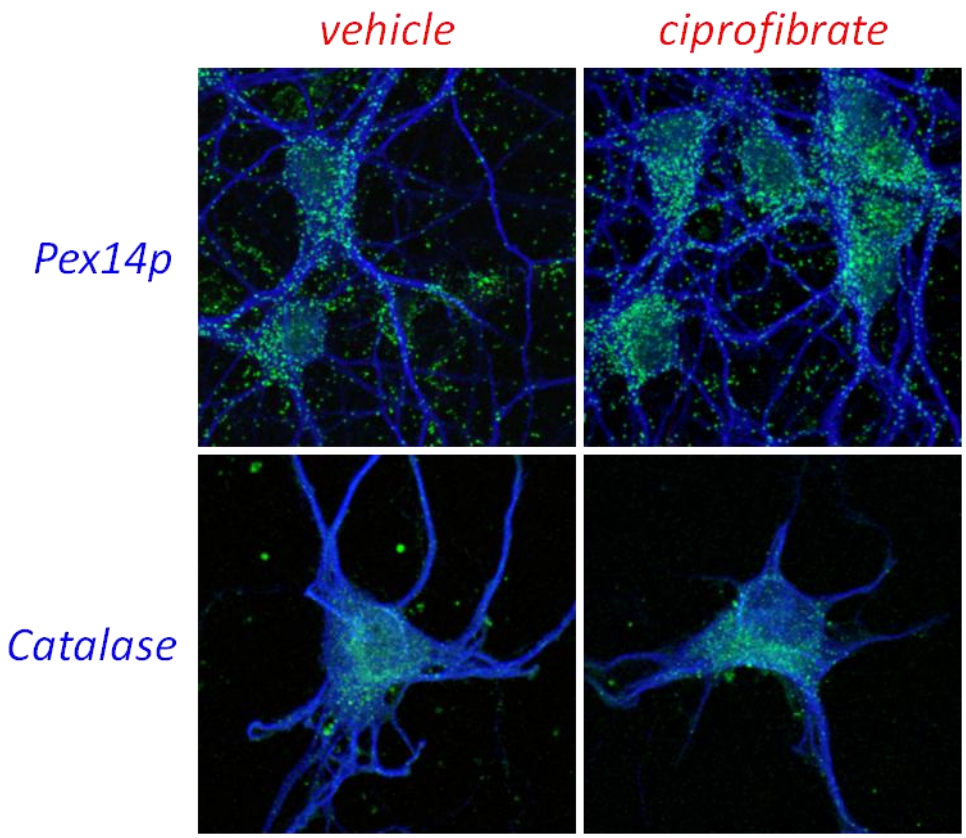

Fig. 3.1_14: Primary cultured neurons from the mouse neocortex treated for 24 hrs with a vehicle (left column) or the peroxisome proliferator ciprofibrate (right column)

3.1.6.3 Peroxisomes in the human brain: To further examine the distribution of peroxisomes in the central nervous system as well as to establish the value of the novel Pex14p marker, an attempt at labeling of peroxisomes in the human brain was made. This was done on samples taken from human autopsies. It has to be mentioned that human brain autopsy material is notoriously difficult to process, firstly, due to the brains tendencies for fast and early autolysis and, secondly, due to the accumulation of larger lipofuscin granules within the cytoplasm of the neurons (arrows in Fig. 3.1_15). Lipofuscin is a yellow brown pigment composed of lipid-containing residues lysosomal digestion, which begins to accumulate in neurons during aging. It seriously complicates explorative immunostaining of aged neuronal tissue due to its filling out great part of the neuronal cytoplasm. In cases of direct or indirect immunofluorescence, lipofuscin also hinders the signaling in that it is comprised of various different lipid

derivatives, in turn containing a large amount of unconjugated pi-electrons and therefore strongly fluoresces at every excitation wavelength, outshining the fluorochromes of interest.

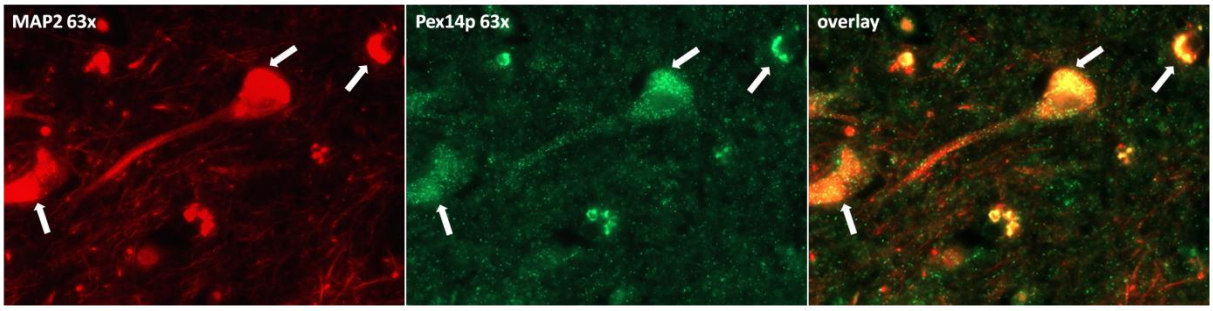

Fig. 3.1_15: Lipofuscin granules in a human CA neuron fluorescing at different excitation wavelengths

Lipofuscin is not susceptible to photobleaching, but can be quenched by staining with Sudan Black B (SBB) (Schnell et al., 1999), which, however, also seriously reduces the intensity of the signal of the respective flourochromes and often leads to unspecific background (Fig. 3.1_16, q.v. Materials & Methods).

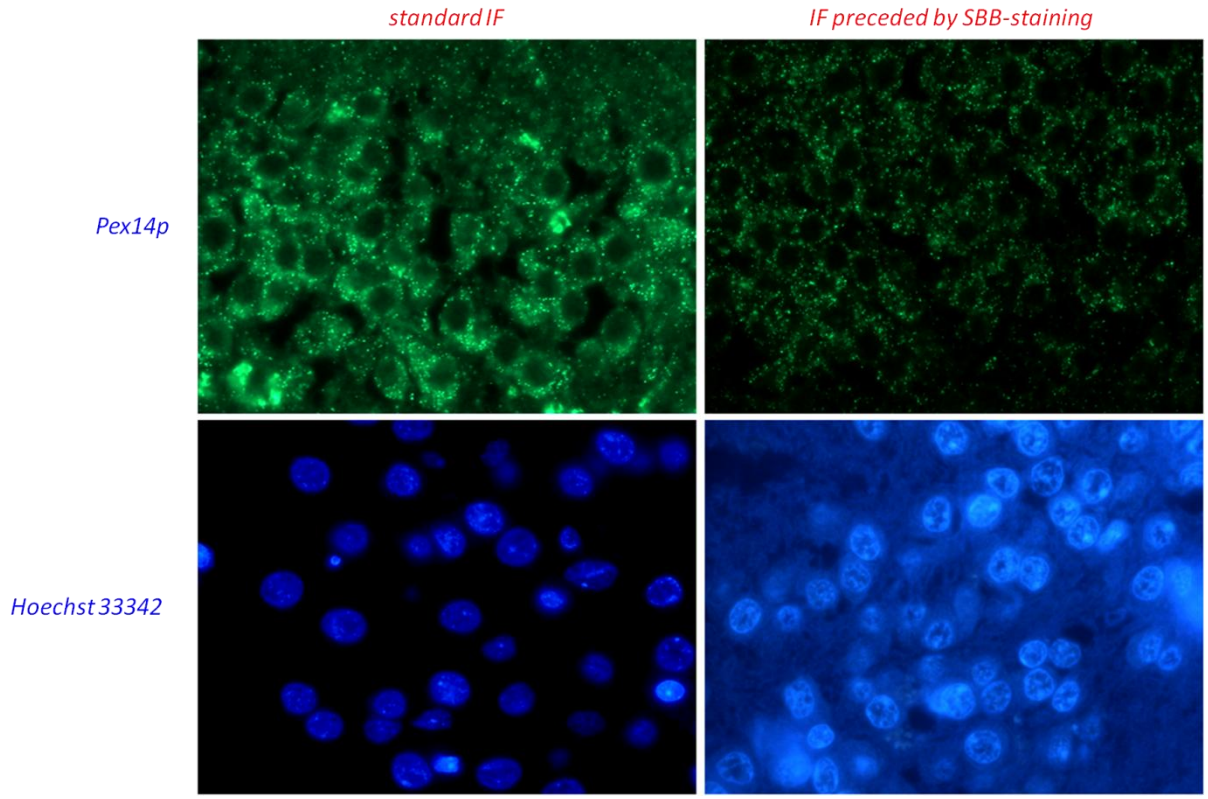

Fig. 3.1_16: Granule cells from a human hippocampus showing specific and unscpecific (lipofuscin) fluorescence signals with and without SBB-pretreatment

By carefully adapting the staining protocol and maximizing antigen retrieval, as well as through careful reduction of exposure times during photography and through ex post facto augmentation of the images with Adobe® Photoshop® peroxisomes in the human brain could successfully be labeled using IF and IHC procedures, but without significant contortion or falsification of the images (Fig. 3.1_17).

It could herefore be shown that peroxisomes are definitely present in neurons of the human cerebellum, hippocampal formation and lateral geniculate body (CGL) of the thalamus.

Notice the proportionality of peroxisomes to the sizes of the respective neurons. This can be shown in granule cells of the dentate gyrus compared to pyramidal cells from the cornu ammonis or a neuron from one of the magnocellular layers of the CGL. The same phenomenon can be used to distinguish the relatively larger Golgi cells within the granule cell layer of the cerebellar cortex (Fig. 3.1_17, asterisks).

It is also noteworthy that peroxisomes appear in distinctively larger number in places of dendritic fission, as shown by Purkinje cells from the cerebellar cortex (Fig. 3.1_17, arrows). This is in accordance with the supposition of Arnold and Holtzman (1978) that peroxisome content is related to cellular enlargement and the formation of neuronal processes. Finally, the Pex14p-staining can also be used to show that, although peroxisomes appear to be relatively sparsely distributed in the actual axons, their number is markedly increased within the initial axonal segment or axon hillock (Fig. 3.1_17, arrowhead).

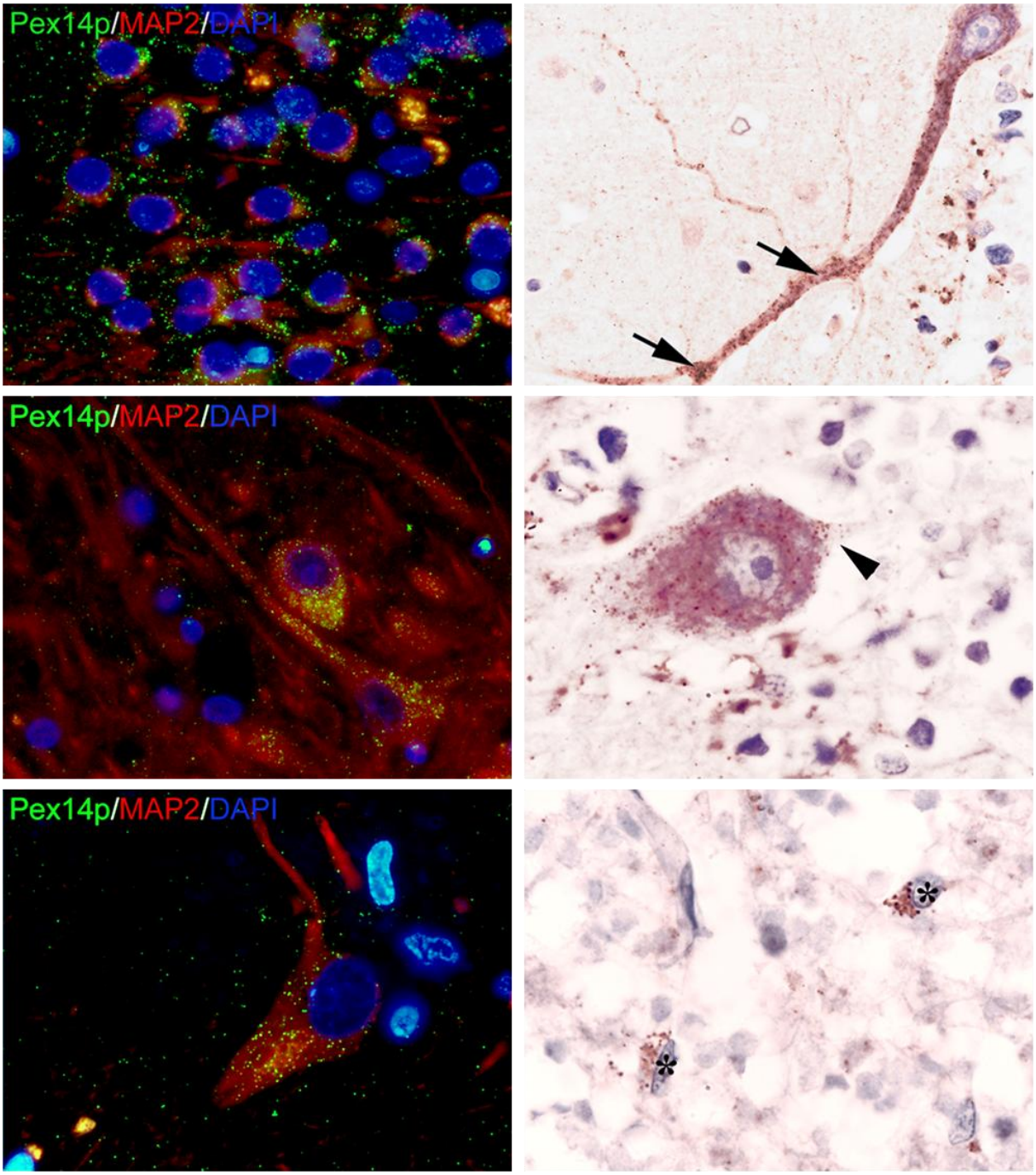

Fig. 3.1_17: Immunofluorescence and immunohistochemical labeling of Pex14p in various cell types and regions of the human brain; top left: granule cells from the hippocampal dentate gyrus, middle left: CA neurons from the hippocampal cornu ammonis, bottom left: neuron from the magnocellular region of the lateral geniculate body (CGL), top left: Purkinje cell perikaryon and larger dendrites from the cerebellar cortex (arrows show peroxisomal clusters at sites of dendritic branching), middle right: Purkinje cell perikaryon (arrow head shows peroxisomes in the initial axon segment/axon hillock), bottom right: Golgi cells (asterisks) in the granule cell layer of the cerebellar cortex

3.1.6.4 Overview of the microscopic anatomy of the human hippocampal formation: Since the human hippocampal formation is extremely large and intra- as well as interindividually diverse and the various sectors are difficult to differentiate in staining methods not specifically developed for brain, parallel sections were stained with the modified Kluver-Barrera method. The microscopic anatomy of the human and mouse hippocampal formation share certain similarities, wherefore it shall be exemplarily illustrated here (Figs. 3.1_18 & 3.1_19).

Due to the hemispheral rotation during brain ontogeny the human hippocampus in its entirety is roughly C-shaped reaching from the septal area (hippocampus precommissuralis) via the stria of the induseum griseum (hippocampus supracommissuralis) to the hippocampus proper (hippocampus retrocommissuralis). The first to parts of the hippocampus will not be discussed here. The hippocampal formation is comprised of two intertwined inverse archicortices, namely the dentate gyrus (DG) and Amun's horn (cornu ammonis, CA), whereby the latter continues seamlessly into the subiculum. The cornu ammonis was divided by Rafael lorente de Nó into four fields, CA1 through CA4, whereby CA1 follows the subiculum and CA4 was described as laying in the hilum of the dentate gyrus (Lorente de Nó, 1934). Studies by David Amaral and Ricardo Insausti, however, showed that the field CA4 does in fact not belong to Amun's horn, but is the plexiform layer of the dentate gyrus (Amaral, 1978; Insausti & Amaral, 2004). This new nomenclature has, unfortunately, not yet been incorporated into all revisions of standard anatomy text books.

Since the cornu ammonis is an inverse cortex, the pyramidal cells have their apices away from the surface, wherefore the white matter lies directly beneath the external glial limiting membrane and is referred to as the alveus. It condenses into fringe-like structures, the fimbriae, which continue in the fornix, one of the major output pathways of the cornu ammonis. The major input into the hippocampal formation is comprised of myelinated axons from the entorhinal cortices, the perforant path (tractus perforans).

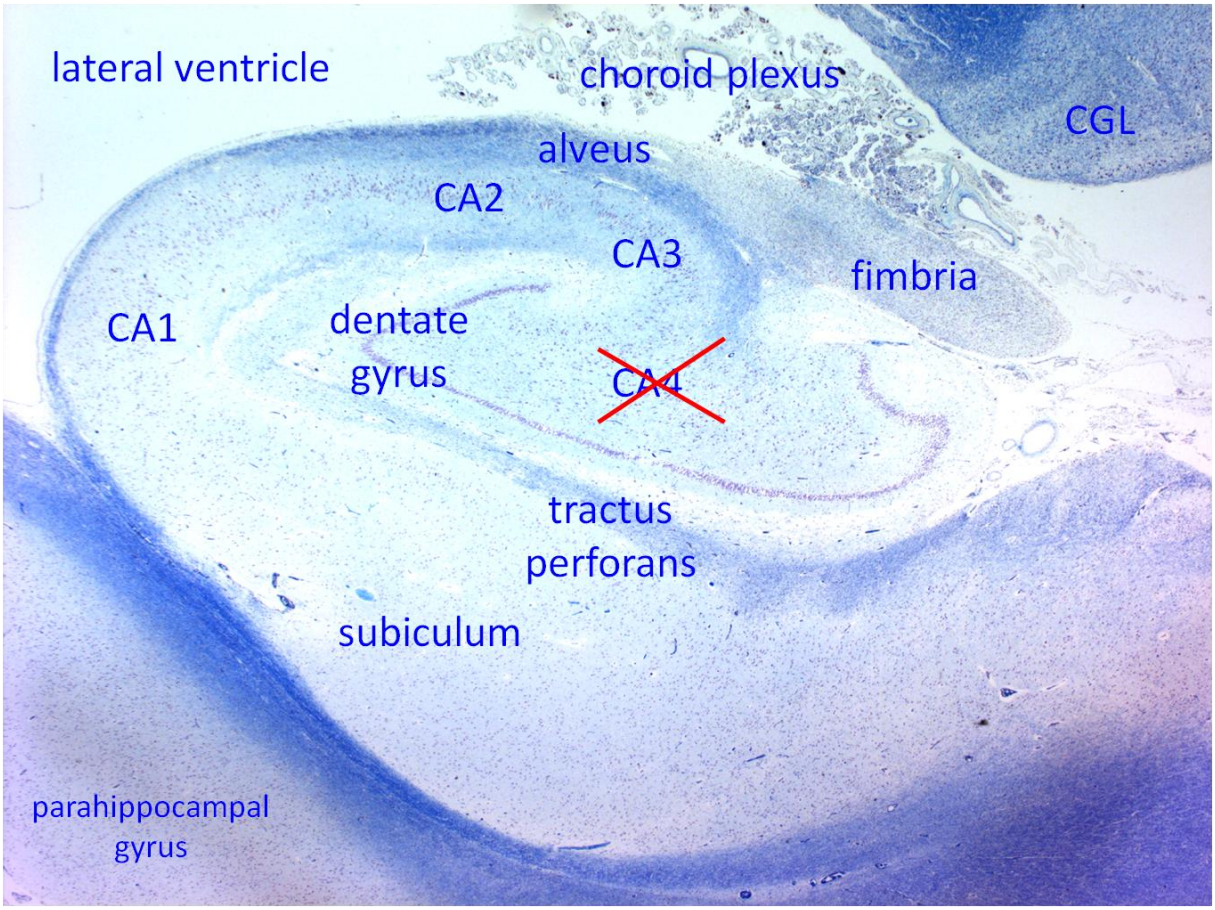

Fig. 3.1_18: Modified Kluver-Barrera staining of the human retrocommissural hippocampal formation; *CA: cornu ammonis, CGL: lateral geniculate body*

Being archicortical, both the dentate gyrus and the cornu ammonis are trilaminar in nature, whereby the cornu ammonis features efferent pyramidal cells and the dentate gyrus, as the primary input part of the hippocampal formation features spiny stellate cells. Additionally both cortices are comprised of a vast variety of interneurons. The dentate gyrus is also relatively inverse, wherefore its molecular layer borders directly on the perforant path, which lies within the molecular layer of the cornu ammonis. The granular layer of the dentate gyrus is followed by the plexiform layer, sometimes referred to as the hilum of the denate gyrus. In general, all fields of the cornu ammonis share the same stratification, with the exception of the field CA3. Beneath the alveus is the stratum oriens, followed by the pyramidal layer. The axons of the pyramidal cells mainly of fields CA3 give of so-called Schaffer collaterals on their way to the alveus, thereby forming the stratum radiatum. Since these collaterals terminate mostly in the field CA1, the end of the stratum radiatum marks the border between the cornu ammonis and the subiculum. The deepest layer (originally the most superficial layer in hippocampal ontogeny) is the stratum lacunosum-moleculare with

the perforant path. In addition hereto, the field CA3 features a small stratum between the pyramidal cell layer and the stratum radiatum, which is comprised mainly of unmyelinated mossy fibres from the granule cells of the dentate gyrus and is therefore called the stratum lucidum. The borders between the fields of the cornu ammonis are not sharp, but can be differentiated approximately through the morphology of the pyramidal layer. Whereas the field CA2 features a single band of densely packed pyramidal cells, both CA3 and CA1 have more loosely distributed pyramidal neurons, which make up two distinguishable layers within the field CA1. The border between CA3 and the plexiform layer of the dentate gyrus (formerly CA4) is marked by the end of the stratum lucidum. The fuzzy transition between CA1 and the subiculum, as described above, can be distinguished through the gradual disappearance of the stratum radiatum (Insausti & Amaral, 2004).

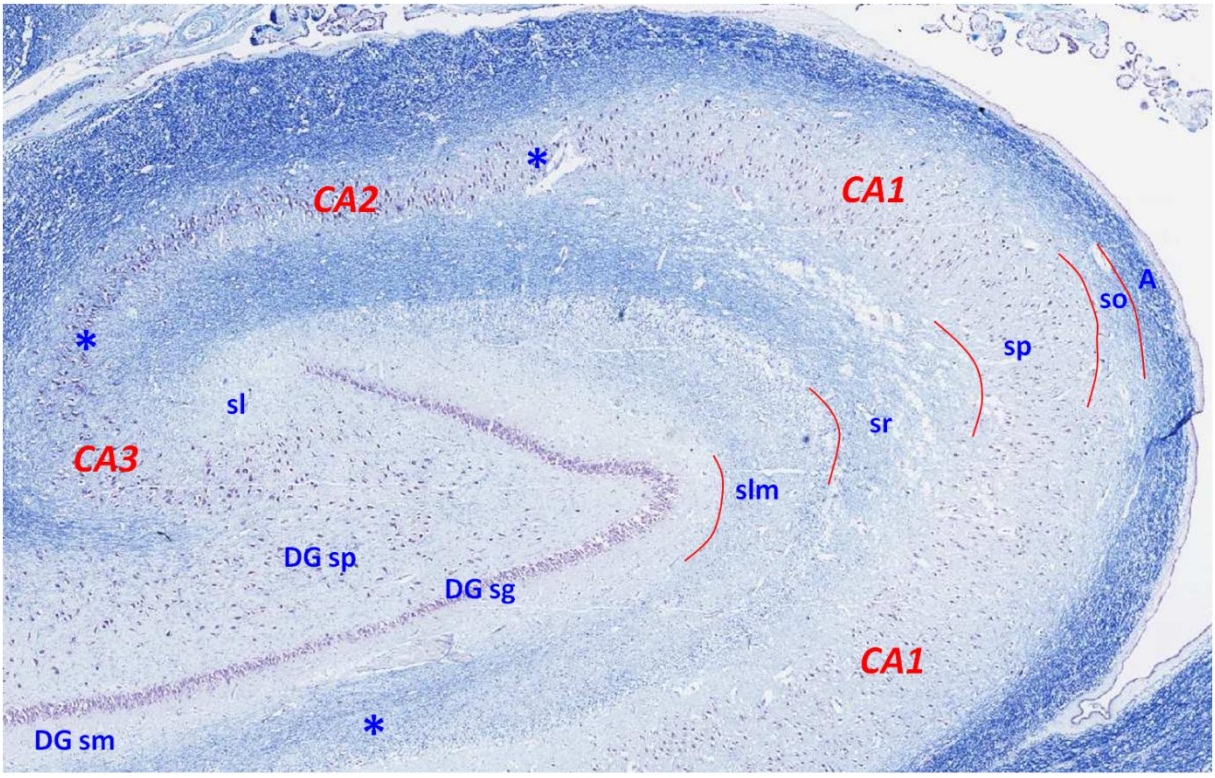

Fig. 3.1_19: Modified Kluver-Barrera staining showing the microscopic anatomy of the human hippocampal formation; *A: alveus, CA: cornu ammonis, asterisks show the approximate borders between the CA fields, DG sg: granule cell layer of the dentate gyrus, DG sm: molecular layer of the dentate gyrus, DG sp: plexiform layer of the dentate gyrus, sl: stratum lucidum of the CA, slm: stratum lacunosum-moleculare of the CA; so: stratum oriens of the CA, sp: stratum pyramidale of the CA, sr: stratum radiatum of the CA*

3.1.7 Labeling of peroxisomes with QuantomDots (QDots®) (Fig. 3.1_20)

The usually rather small size of peroxisomes makes it better for morphometric purposes to use IF-techniques rather than IHC, as the spatial resolution of an IF fluorochrome signal is usually higher than that of an organic dye or substrate like DAB commonly used in IHC. The disadvantage of fluorochromes for morphometry, however, is (a) the sometimes insufficient strength of the signal (in IHC this could be remedied by extending the development time of the color-dye reaction) and (b) the susceptibility to photobleaching of the fluorochromes, even though this has become easier thanks to fading and bleaching agents as well as to the new generation of AlexaFluor® fluorochromes.

Even so, the possibility of labeling peroxisomes with a fluorescent marker with a signal yield higher than that of AlexaFluor®, which is also unsusceptible to photobleaching, is offered by nanocrystal technology in the form of QDots.

QDots are significantly more difficult to handle and markedly larger in size than classical fluorochromes (q.v. Materials & Methods), wherefore labeling was performed on mouse (Hepa 1-6) and human (HepG2) hepatoma cell lines. QDots are all excited by UV-light and differ in size and therefore in the wavelength of their emitted photons, for which they are also denominated. Both small Qdot 525 as well as significantly larger QDot 655 nanocrystals were successfully established for labeling of Pex14p in Hepa 1-6 and in HepG2 cells.

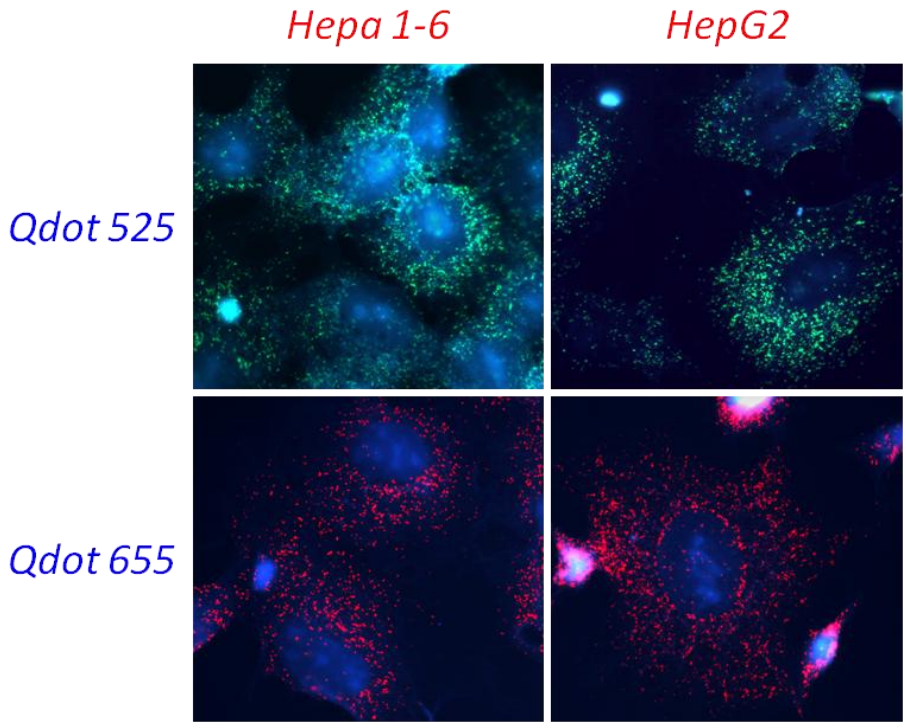

Fig. 3.1_20: Labeling of Pex14p in mouse (Hepa 1-6) and human (HepG2) hepatoma cell lines using different sized QuantomDot nano-crystals

3.2 Analyzing peroxisomal reactions to increased dopamine

3.2.1 Morphological analyses of Pex14p and catalase in the hippocampus of schizophrenic patients vs. controls (Fig. 3.2_1):

Labeling of catalase in hippocampal sections taken from different brains of patients diagnosed with schizophrenia showed no detectable signal for catalase as was the same in sections from control patients. As expected, catalase is not present in high enough abundance in the adult brain to detect through immunohistochemistry. Since many results report decreased amounts and activity levels of catalase in schizophrenics it is not surprising that no differences can be detected between schizophrenia and control cases. The differences between Pex14p signals are also very subtle, albeit that the number as well as size of peroxisomes appear to be slightly reduced in schizophrenic patients compared to controls. The remaining peroxisomes do, however, seem to be a little more densely packed in proximity to the nucleus, which would be in line with atypical neurodegeneration, wherein neuronal processes become stunted thereby also leading to a reduced number of organelles in the cells with remaining organelles located in the perikaryon.

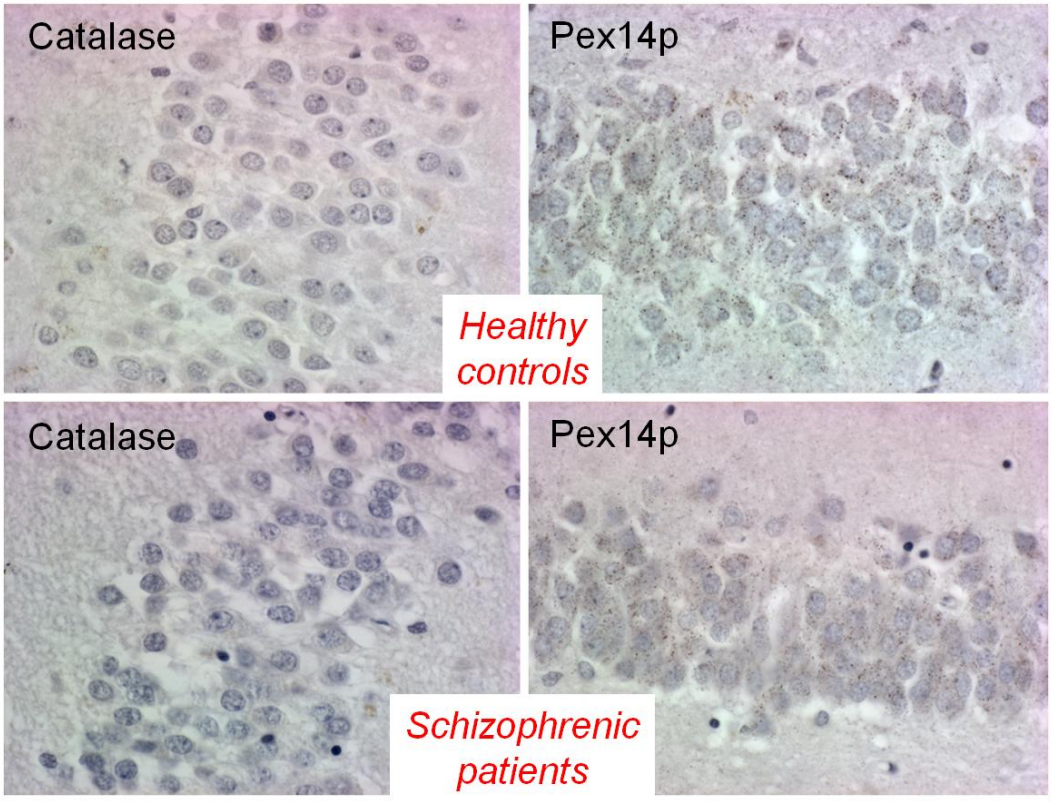

Fig. 3.2_1: Immunohistochemistry using DAB with nickel-enhancement of Pex14p and catalase in the dentate gyrus of post-mortem brain sections of schizophrenic patients and controls

Unfortunately no information was available regarding the subtype or duration of schizophrenia or the (especially pharmaceutical) therapy regimens in the patients from whom the samples were obtained, wherefore these results were interpreted with great care and not many inferences could be drawn regarding the differences and lack thereof between groups.

3.2.2 Effects of increased dopamine and haloperidol on primary murine neuronal cultures

To examine the effects of increased extracellular dopamine on peroxisomal abundance and catalase levels in a more controlled fashion, primary murine neurons were cultured and treated with different concentrations of dopamine for 24 hours. Unlike in the human brain sections, the differences in catalase levels are striking, especially in the few astrocytes that are present in these cultures. Catalase appears to be increased in a dose-dependent fashion in dopamine-treated cultures compared to vehicle-treated controls (Fig. 3.2_2).

Peroxisomal abundance and distribution changes in a fashion similar to that hypothesized from literature reports on atypical neurodegeneration as well as the findings from human hippocampal sections. Peroxisomes appear to be smaller in size, less abundant and distributed closer to the nucleus. They appear almost absent in both neuronal and astrocyte processes in comparison to vehicle-treated controls. Although the amount of MAP2 signal (blue) appears similar in the 100 μM dopamine culture to the vehicle-treated cells, the reduced signal density between the labeled neuronal processes indicates a loss of smaller dendritic processes that usually form a fine network in culture, which can be visualized through increasing the intensity of the appropriate laser. The reduction of these smaller processes, that were shown to express various synaptic proteins in experiments performed in another context (data is therefore not shown here), and the loss of peroxisomes therein as well as in the larger dendrites through incubation with dopamine is again in accordance with the model of atypical neurodegeneration caused by excess dopamine.

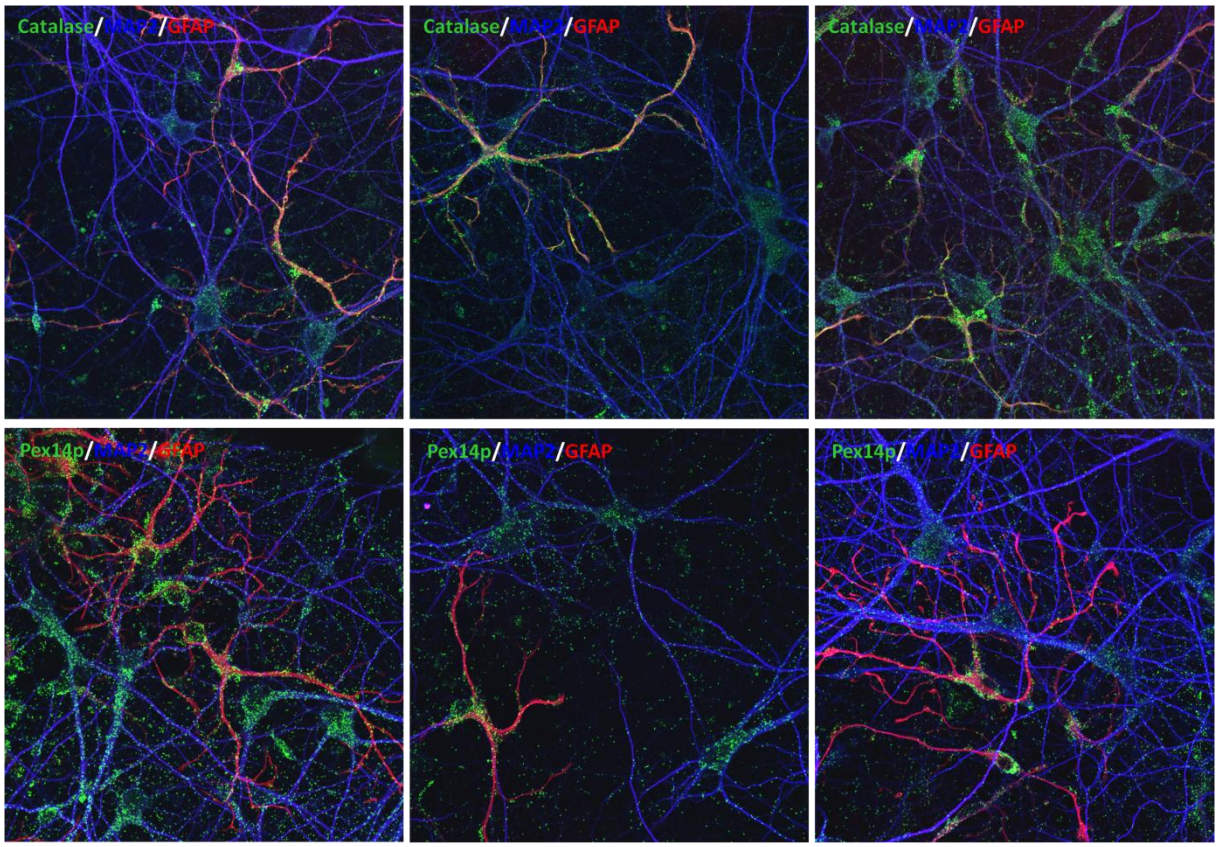

Fig. 3.2_2: Triple IF staining for MAP2 (neurons), GFAP (astrocytes) and Pex14p or catalase in primary murine cortical cultures treated for 24 hrs with different concentrations of dopamine or a vehicle

To further examine this, neuronal survival was measured in all cultures, showing that dopamine leads to a slight increase in cell death. This increase is, however, neither significant nor dose-dependent considering the high concentrations of dopamine some cultures were exposed to (Fig. 3.2_3). It can therefore be assumed that dopamine cultivation may lead to the death of a certain basal amount of cells, but that the majority of cells do not undergo apoptosis even if dopamine levels are increased tremendously.

In contrast hereto, parallel incubations of cells with haloperidol causes a dose-dependent increase in cell death that reaches around 90% in the highest concentrations (Fig. 3.2_3).

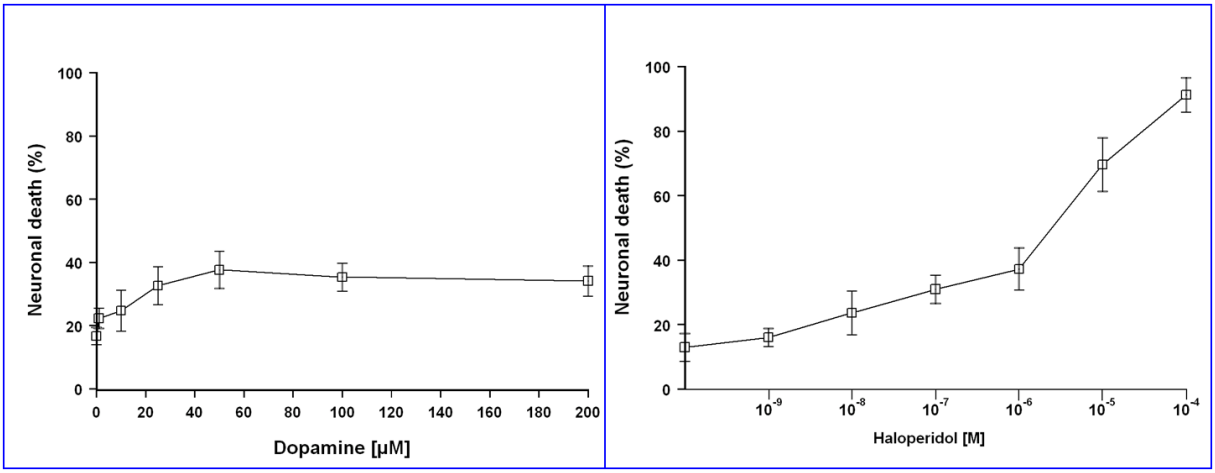

Fig. 3.2_3: Neuronal death in primary murine cortical cultures after 24 hrs of incubation with increasing dosages of dopamine or haloperidol

In morphological staining this can also be seen clearly in higher dopamine concentrations. Additionally, haloperidol leads to a marked dose-dependent increase in catalase content in the surviving cells, especially in astrocytes (Fig. 3.2_4). This increase is higher than that found in dopamine-treated cells. The abundance of peroxisomes decreases in the few surviving neurons, but increases in astrocytes. The remaining peroxisomes in neurons appear to be larger in size compared both to vehicle- as well as dopamine-treated cultures (Fig. 3.2_2). It therefore can be held that the effects of (typical) neuroleptics on the nervous system are pronouncedly different to those of dopamine, wherefore findings from pharmacologically treated patients should be interpreted with great care.

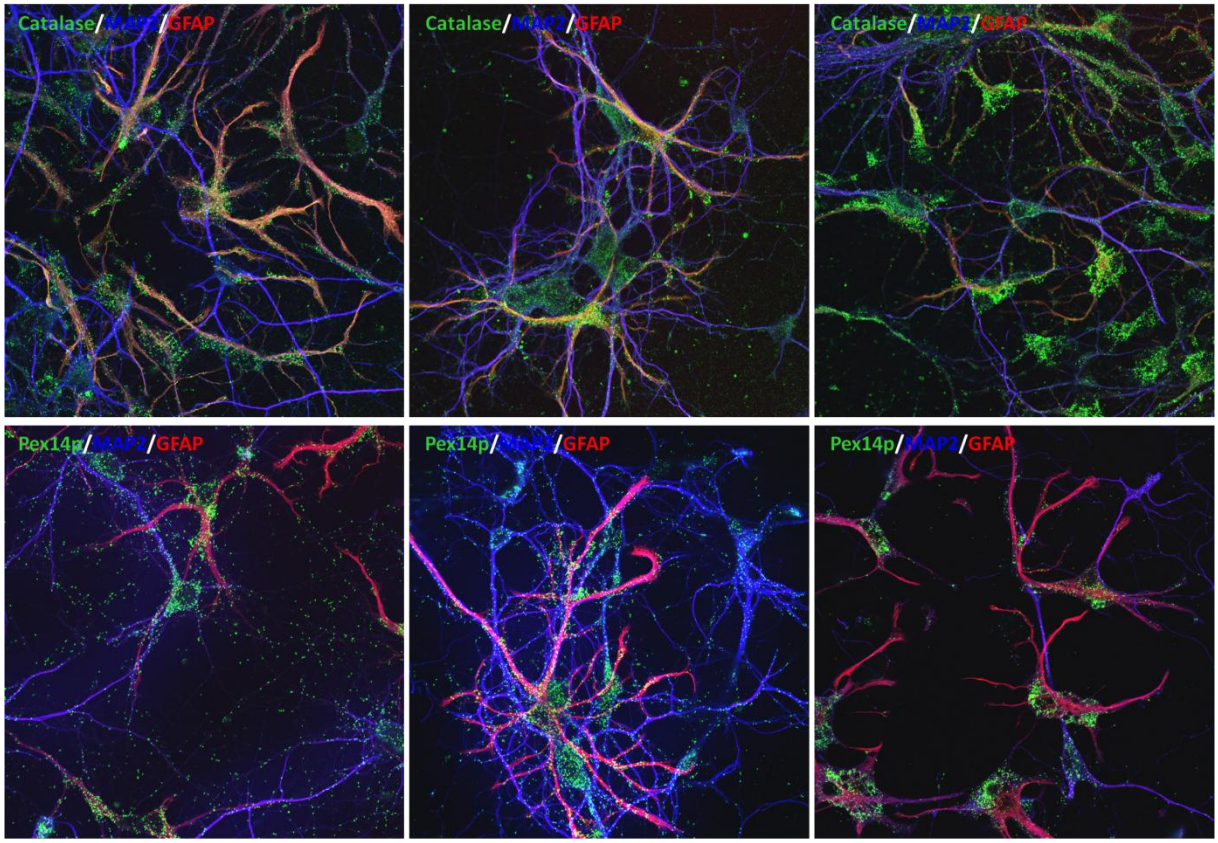

Fig. 3.2_4: Triple IF staining for MAP2 (neurons), GFAP (astrocytes) and Pex14p or catalase in primary murine cortical cultures treated for 24 hrs with different concentrations of haloperidol or a vehicle

3.2.3 Effects of increased dopamine on primary murine astrocyte cultures

Since the influences of dopamine (and haloperidol) on both Pex14p and catalase were different between neurons and astrocytes, with astrocytes generally showing more pronounced reactions to either substance, the question emerged whether these findings were inherent to astrocyte metabolism or dependent on neuron-astrocyte interaction. From the general function of astrocytes as important factors i.a. in maintaining homeostases important for neuronal survival, it would be expectable that the reactions of astrocytes are dependent on signaling from neurons and should therefore be less pronounced, if not absent in cell cultures containing no neurons.

To examine the verisimilitude of these expectations, cultures of pure murine astrocytes were established and treated with different concentrations of dopamine for 24, 48 and 72 hrs. For reasons of conciseness, the results from the cultures treated for 48 hrs shall not be shown here. For more detail see Fischer, 2010.

3.2.3.1 Morphological analyses: The absence of neurons was controlled through immunolabeling for GFAP, MAP2 and nuclear counterstaining (Fig. 3.2_5). Apart from the high amount of GFAP-positive cells, no signal was detected for MAP2, wherefore it can be assumed that no neurons survived the cultivation procedure. The nuclei not belonging to GFAP-positive cells are likely to belong to fibroblasts which survive from (mainly) remnants of the pia mater and, unlike neurons, survive and multiply under the cultivation conditions. The effects of the fibroblasts on the validity of results are discussed extensively in Fischer (2010). It is considered unlikely that these connective tissue cells have a greatly falsifying effect.

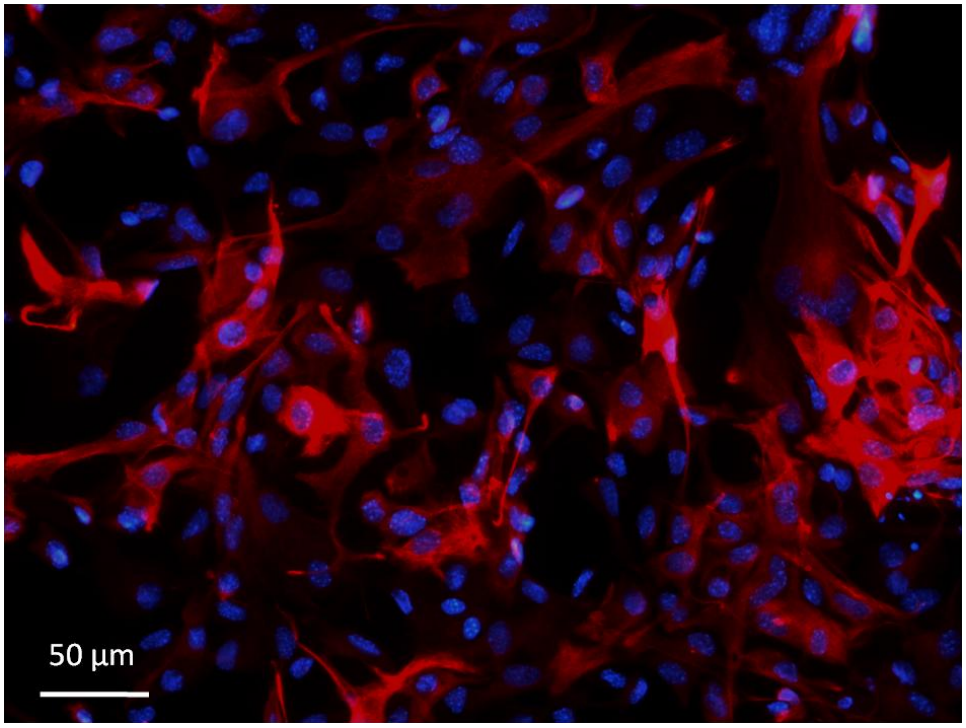

Fig. 3.2_5: Double IF labeling for MAP2 and GFAP in primary murine astrocyte cultures with nuclear counterstaining. Red cells are astrocytes. The lack of blue cells shows that no neurons are present in the culture. Nuclei outside of red cells belong to fibroblasts.

The effects of dopamine-incubation can be seen clearly through a distinct dose-dependent discoloration of the medium even after 24 hrs (Fig. 3.2_6). This discoloration, due to changes in pH of the medium, is most probably caused by autoxidation of dopamine, dopamine metabolism of the cultivated cells and/or both.

Fig. 3.2_6: Dose-dependent discoloration of the medium of primary murine astrocytes after 24 or 72 hrs of incubation with dopamine

The effects of dopamine-treatment on astrocyte viability were negligible with on average only 3 % of cells undergoing apoptosis in all cultures, even those treated with a vehicle (Fig. 3.2_7). The range of nuclei with apoptotic morphology is slightly shifted from 2,5 – 3,2 % (vehicle) to 2,8 – 3,6 % (dopamine), whereby this difference is neither significant nor dose-dependent. It can therefore be assumed that, even more so than in cultures containing neurons, dopamine does not induce apoptosis.

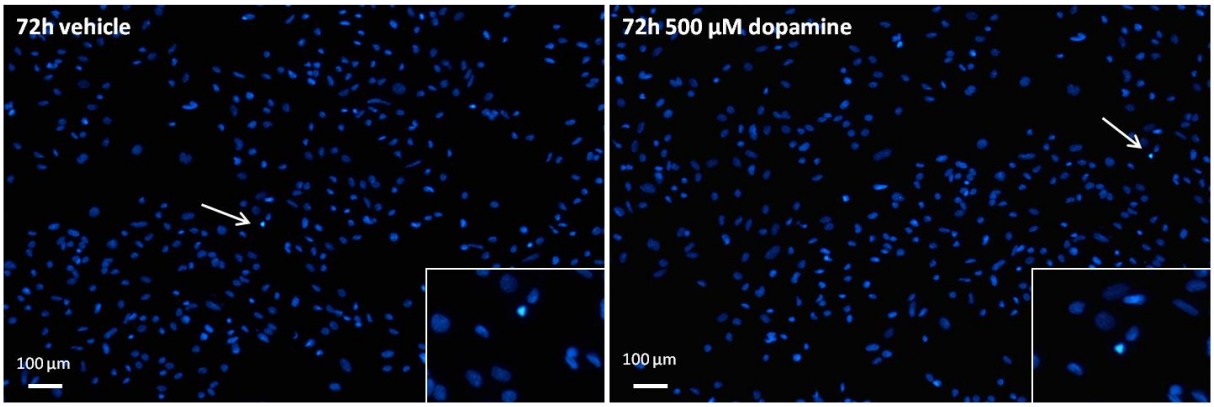

Fig. 3.2_7: Comparison of astrocyte nuclei after 72 hrs of treatment with a vehicle or the highest concentration of dopamine shows the equally low rate of cell death under both conditions

Morphological analyses of GFAP and catalase immunoreactivity show little differences between vehicle-treated controls and cultures incubated with dopamine (Fig. R34). This also indicates that the reactions of astrocytes to dopamine-treatment, as observed in cell cultures with both neurons and astrocytes, are specific to neuron-astrocyte interactions. The only circumstance under which differences could be observed in pure astrocyte cultures were in those samples treated with 200 and 500 µM for 72 hrs. The concentrations of RNA extractable from these preparations were markedly reduced compared to the other cultures.

In immunostainings the same cultures showed a reduction in outgrowing cellular processes, GFAP immunoreactivity and catalase content. It is probable that these cells exhibit a sort of "cellular sickness behavior", during which the entire metabolism is reduced and shifted towards cellular survival at the expense of reduced anabolic activity. This again would be in line with the concept of atypical neurodegeneration.

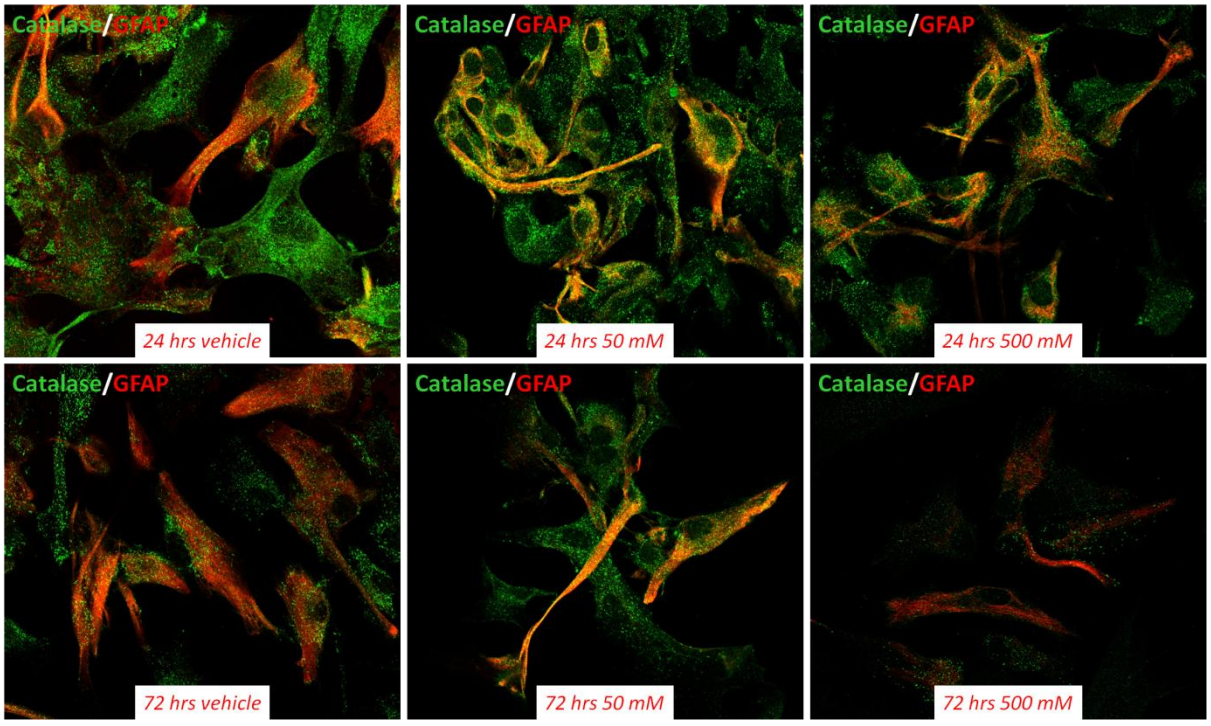

Fig. 3.2_8: Double IF labeling of catalase and GFAP in primary murine astrocytes incubated with a vehicle or different concentrations of dopamine for 24 or 72 hrs

3.2.3.2 Analyses of gene expressions: In order to assess the capacity of the cultivated astrocytes to take up and metabolize the dopamine from the medium, RNA was extracted from untreated cell cultures and RT-PCRs were performed for all known dopamine synthesizing and catabolizing enzymes and the dopamine active transporter (DAT). Results clearly show that all genes encoding for the aforementioned proteins are actively expressed in the cell cultures (Fig. 3.2_9).

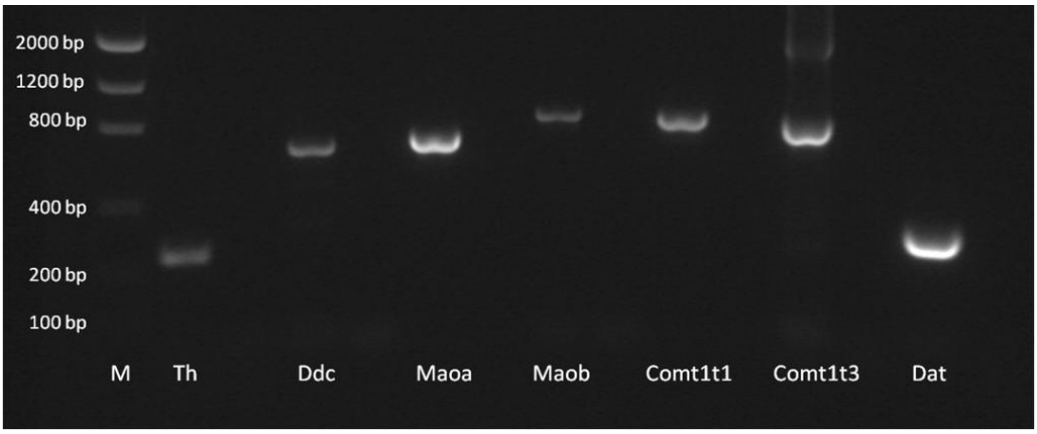

Fig. 3.2_9: RT-PCRs for the dopamine synthesizing and metabolizing enzymes as well as the dopamine active transporter from primary murine astrocytes; *Th: tyrosine hydroxylase, Ddc: DOPA decarboxylase, Mao: monoamino oxidase, Comt: catechol-O-methyl transferase, transcripts 1 & 3*

Additionally, the expression of genes coding for various dopamine receptors was examined. The number of mRNA copies, however, appeared to be very much lower leading to unspecific background amplification. Therefore, in these cases nested PCRs were performed. The results again show that the cultivated astrocytes contain RNAs of all five dopamine receptors, whereby the expression of dopamine receptor D_5 is lower by far than that of the other receptors (Fig. 3.2_10). It can therefore be established that the cultured astrocytes are capable of taking up and metabolizing dopamine as well as that dopamine may bind to dopamine receptors expressed by the astrocytes, thereby leading to the activation or inhibition of intracellular cAMP-dependent metabolic pathways.

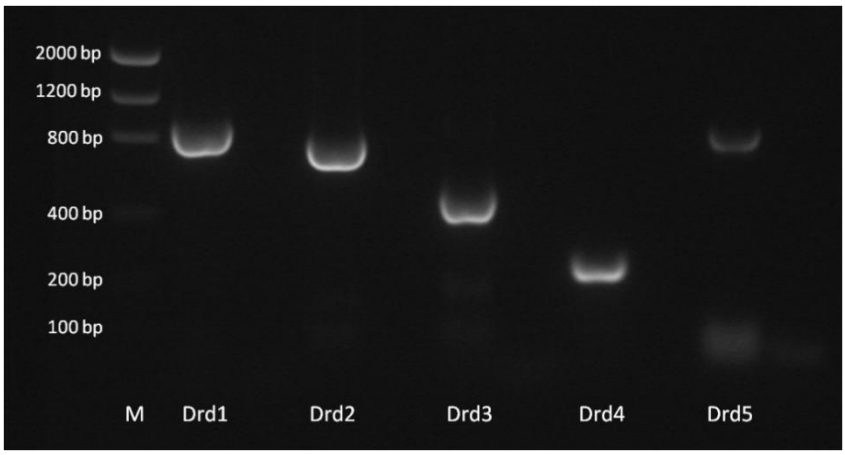

Fig. 3.2_10: Nested RT-PCRs for the dopamine receptors from primary murine astrocytes

RT-PCRs for the mRNA of the 28S rDNA gene functioned as housekeeping controls and show that equal amounts of RNA were used for first strand synthesis as well as that equal amount of amplified cDNA were loaded onto the gel (Fig. 3.2_11).

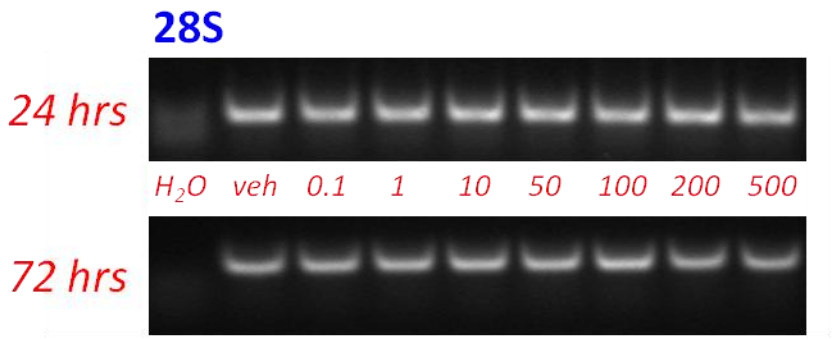

Fig. 3.2_11: RT-PCRs for 28S rDNA (housekeeping gene) from primary murine astrocytes treated with different concentrations of dopamine or a vehicle for 24 or 72 hrs, showing equal amounts of RNA were used for first strand synthesis and equal amounts of amplified cDNA were loaded onto the gel

Expression profiles of the genes coding for the two major dopamine receptors (D_1 and D_2) as well as the dopamine active transporter (DAT) show that incubation with high concentrations of dopamine, even after 72 hrs, does not influence the number of mRNA copies transcribed from these genes in pure astrocyte cultures (Fig. 3.2_12).

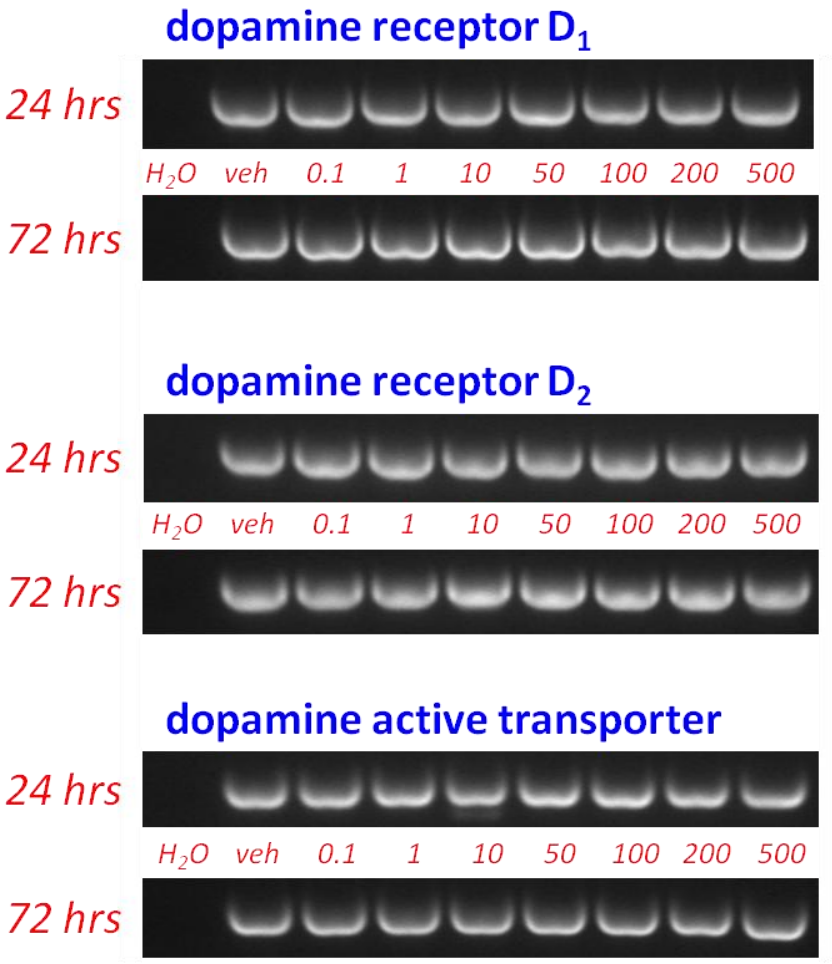

Fig. 3.2_12: RT-PCRs for dopamine receptors D_1 and D_2 as well as the dopamine active transporter from primary murine astrocytes treated with different concentrations of dopamine or a vehicle for 24 or 72 hrs

Dopamine incubation in vitro does also not affect the expression of genes encoding for catabolizing enzymes after 24 hrs or 48 hrs (data not shown here). After 72 hrs, however, MAOA expression still remains unchanged, but a slight increase in mRNA copies for MAOB as well as COMT can be observed in dopamine treated cultures. This increase does not appear to be dose-dependent, with the exception of MAOB expression in the two highest concentrations (200 μM & 500 μM), wherein a reduction of band size can be observed (Fig. 3.2_13). Why this reduction in mRNA copies is not mirrored by MAOA or COMT gene activities is not clear.

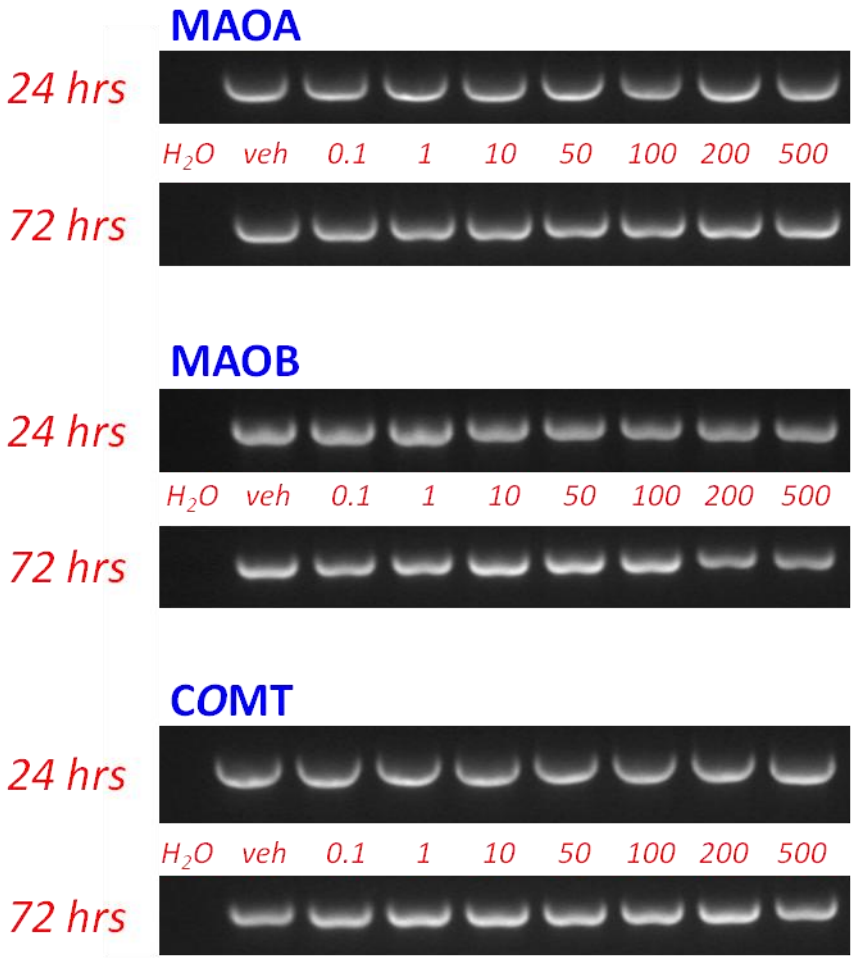

Fig. 3.2_13: RT-PCRs for dopamine metabolizing enzymes from primary murine astrocytes treated with different concentrations of dopamine or a vehicle for 24 or 72 hrs

Expression analyses of selected peroxisomal genes also show no activation differences after 24 hrs of dopamine incubation. While the same goes for the genes encoding for catalase and ABCD3 after 72hrs, the gene number of mRNA copies transcriped from the PEX14 gene increases slightly after 72 hrs in cultures incubated with higher concentrations than 0.1 mM dopamine (Fig. 3.2_14). This shows that peroxisomal proliferation does not automatically

induce the expression of all peroxisomal membrane bound or matrix enzymes, but rather appears to be a differentially regulated process. This is in accordance with findings of peroxisomal heterogeneity within this thesis and also with the results from primary murine neurons cultivated with a peroxisome proliferator for 24 hrs, wherein Pex14p levels increased in a non linear fashion compared to catalase levels. Finally the lack of increase in catalase expression could be indicative of the high efficiency of this enzyme, meaning that the increase in ROS caused by dopamine incubation can still be degraded by the relatively high basal level of catalase already present within the astrocytes.

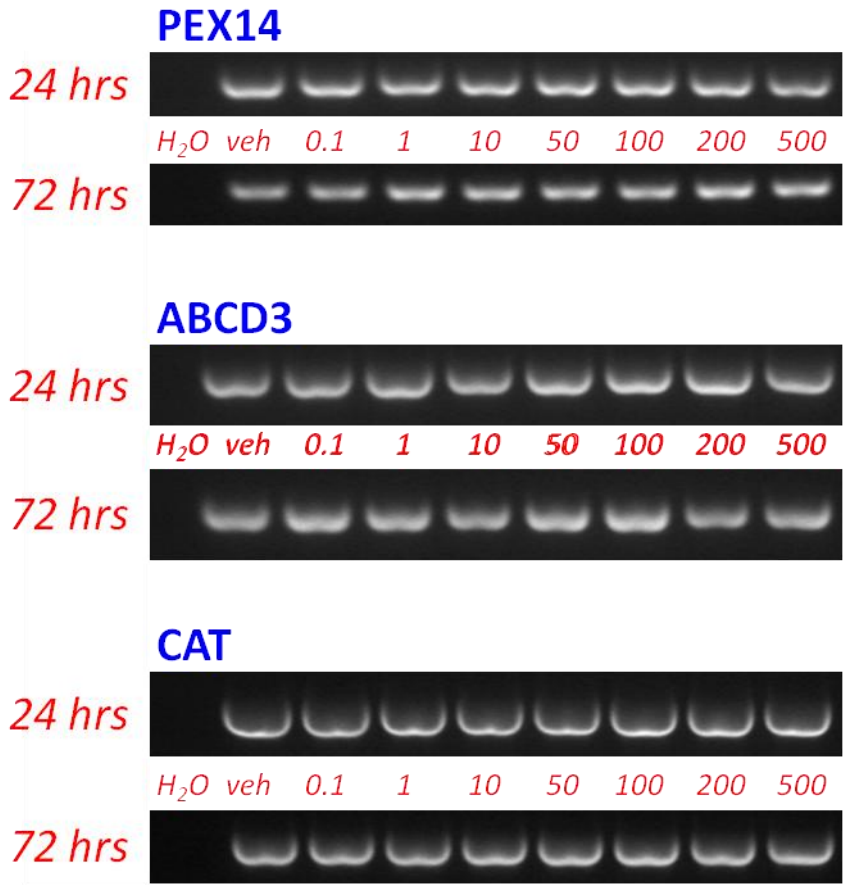

Fig. 3.2_14: RT-PCRs for selected peroxisomal proteins from primary murine astrocytes treated with different concentrations of dopamine or a vehicle for 24 or 72 hrs)

3.2.4 Effects of MK-801-treatment in male pubescent C57Bl/6J mice

To examine the effects of increased mesolimbic dopamine in vivo wildtype animals were injected intraperitoneally with the NMDAR-antagonist MK-801, since it has been shown in literature that this group of drugs leads to an activation of mesolimbic pathways. Excised animal brains were used either for morphological analyses or for the extraction of RNA with subsequent RT-PCR.

3.2.4.1 Analyses of gene expressions: In order to ensure maximum reliability and validity of results from experiments downstream of RNA isolation, the nucleic acid integrity was measured through MOPS/FA gel electrophoresis. With the exception of one sample from the liver of an animal treated for 49 hrs (which was not used for further analyses) the integrity of all RNA samples was considered more than sufficient. An exemplary gel shows clear bands for 18S and 28S rRNAs, whereby the 28S band is larger than the 18S band (Fig. 3.2_15).

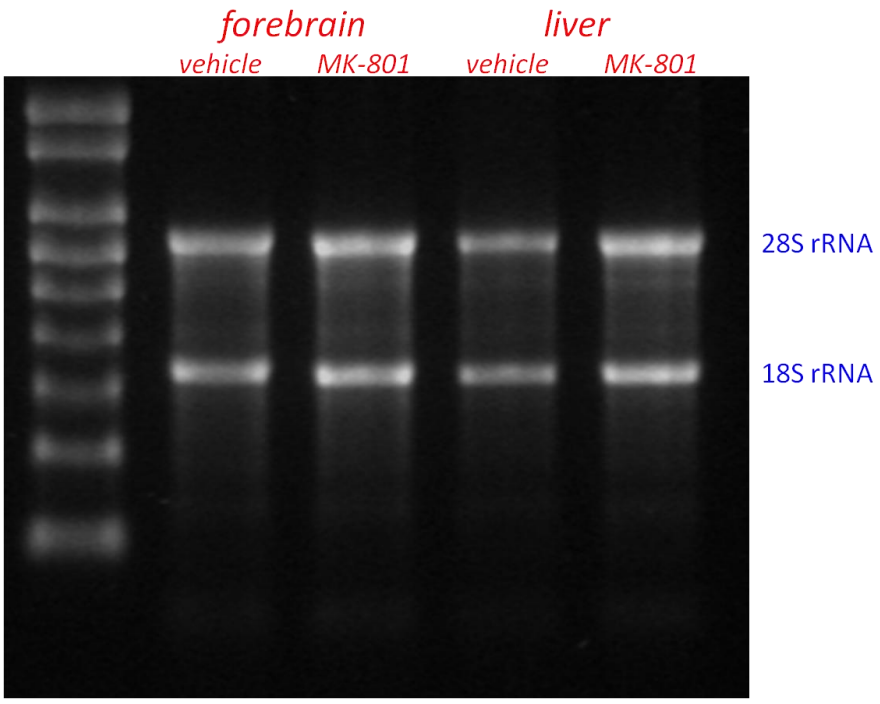

Fig. 3.2_15: Exemplary MOPS/FA gel showing the integrity of extracted RNAs

Since it was not possible to record and quantify parameters of behavior which could identify the development of a schizophrenia-like phenotype (e.g. prepulse inhibition, latent inhibition, vertical activity or rearing behavior), animals were observed by blind raters and could always be accurately identified as control or experimental animals respectively. Additionally, the expression of serine racemase mRNA was examined after 1 hour of treatment as a metabolic internal positive control, since it has been shown that MK-801 leads to an increase in serine racemase expression. Using two different pairs of primers it was shown that animals treated with MK-801 did indeed have a markedly higher expression of serine racemase compared to vehicle-treated controls (Fig. 3.2_16).

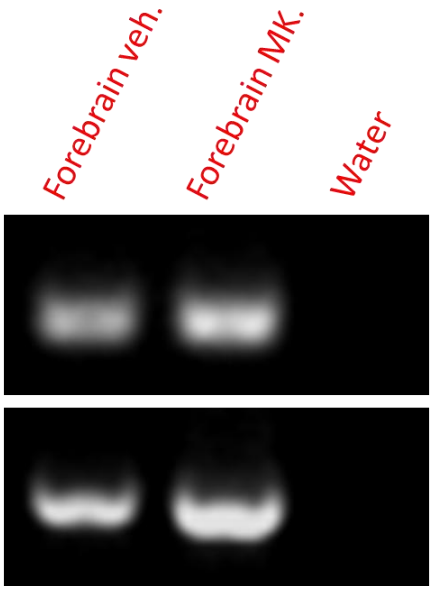

Fig. 3.2_16: RT-PCRs for serine racemase using two different primer pairs as metabolic internal positive control of MK-801 treatment

The application of equal amounts of RNA for first strand synthesis was controlled through parallel analyses of a housekeeping gene, 28S rDNA, which encodes for 28S rRNA.

After 1 hour of treatment with MK-801 increases in gene expression in the forebrain were observed for serine racemase and D-aspartate oxidase and to a small extent for PEX14. Due to the non-quantitative nature of gel electrophoresis, especially the latter finding should be interpreted with care. No differences were observed in catalase, Nrf2 or any of the liver samples (Fig. 3.2_17).

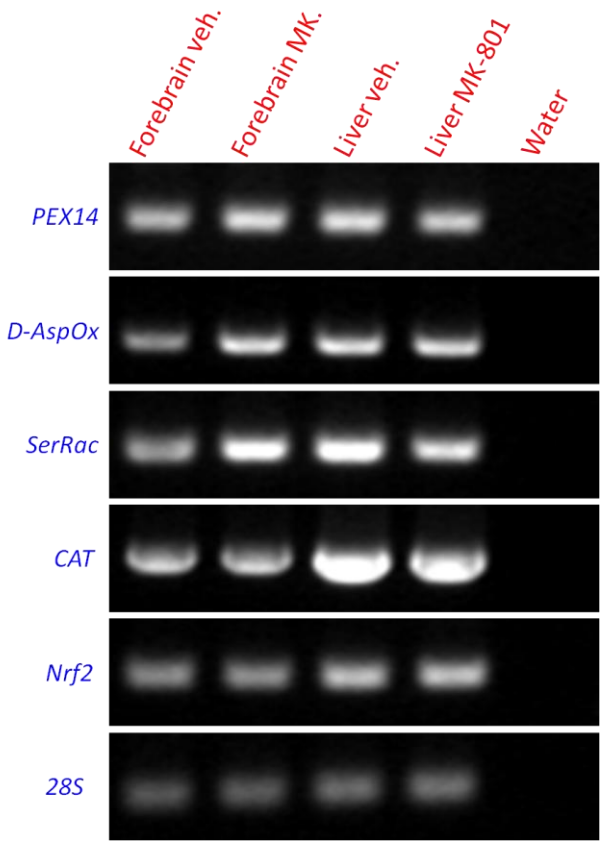

Fig. 3.2_17: RT-PCRs of selected genes from forebrain and liver of animals treated with MK-801 or a vehicle for 1 hour

Housekeeping controls for the expression profile of the 28S rDNA-gene show that equal amounts of RNA were used for first strand synthesis and that subsequently equal amounts of amplified cDNA were loaded onto the gel (Fig. 3.2_18).

Expression profiles of serine racemase are somewhat ambivalent. Even though, as expected, signal intensity is higher after 25 and 73 hrs in the MK-801-treated group, the expression appears to also increase after 49 and 73 hrs in the vehicle-treated animals. Especially after 49 hrs the intensity appears to be higher in the vehicle- rather than the MK-801-treated animals.

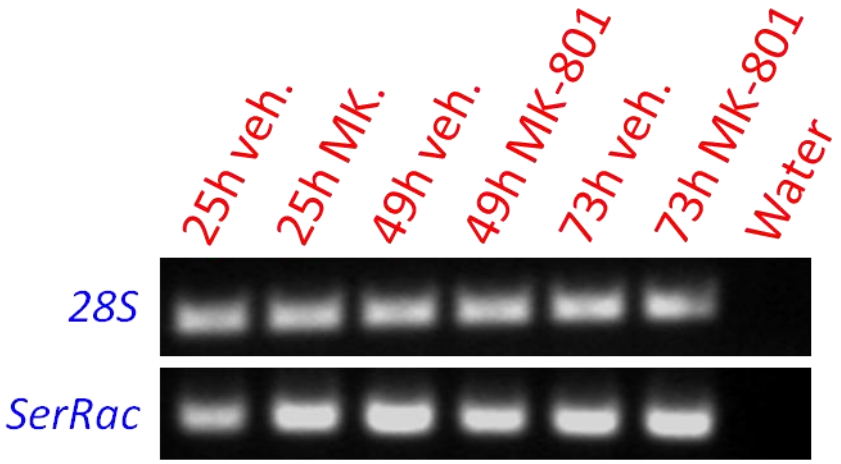

Fig. 3.2_18: RT-PCRs of serine racemase and 28S rDNA (housekeeping gene) from the forebrain of animals treated for 25, 49 or 73 hrs with MK-801 or a vehicle as controls for the MK-801 treatment and the use of equal amounts of RNA for first strand synthesis as well as amplified cDNA for gel loading

Expression profiles of MAOA and C*O*MT genes are similar in that there appears to be a slight decrease in MK-801-treated animals after 25 hrs followed by an upregulation of gene expression after 49 hrs. The major difference between these two genes shows up after 73 hrs, where MAOA expression does not appear to be altered between groups, whereas C*O*MT expression seems slightly decreased. The expression patter of MAOB, however, differs markedly from that of the other two degrading enzymes in that levels decrease in both groups from 25 over 49 to 73 hrs of treatment. Additionally the expression in the MK-801-treated animals is lower in comparison to controls at all given time points.

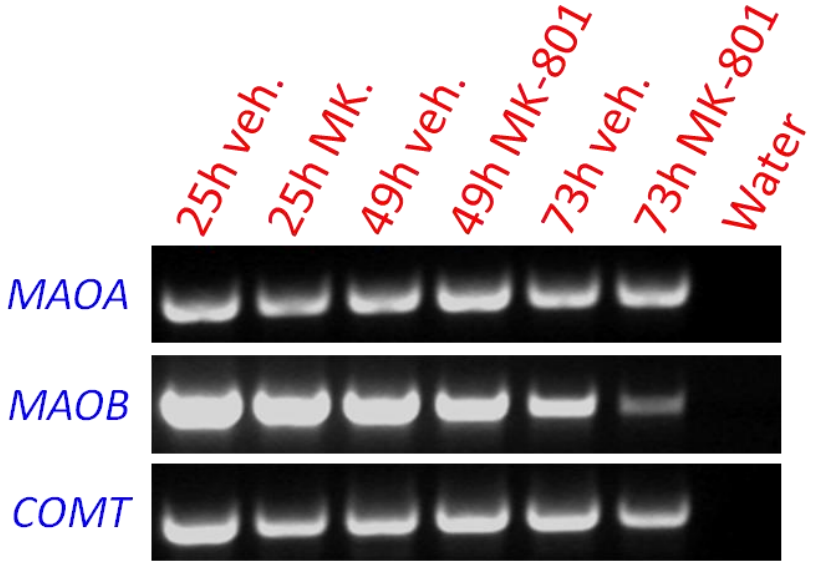

Fig. 3.2_19: RT-PCRs of the genes coding for dopamine metabolizing enzymes from the forebrain of animals treated for 25, 49 or 73 hrs with MK-801 or a vehicle

Both antioxidant enzyme expression levels appear to increase after treatment with MK-801 (Fig. 3.2_20). In the case of catalase there appears to be no difference detectable between vehicle treated groups (25, 49 or 73 hrs), but in the appropriate MK-801 treated brains the signal intensity is always higher, with the most pronounced increase found after 49 hrs. The differences in SOD2 expression levels are more complex. After 25 hrs the difference between control and MK-801 brains is minimal, but after 49 and 73 hrs it becomes apparent that SOD2 expression is induced in animals treated with MK-801. Interestingly, however, the levels in the 73 hrs group are lower both in vehicle and MK-801 treated animals compared to the 49 hrs group, even though the expression is still relatively higher after MK-801 treatment. A possible explanation herefore could be that the increase in expression after 49 hrs creates a surplus of enzyme, wherefore not as many new mRNA copies need to be transcribed. Alternatively the stability of the mRNA could be altered, whereby each strand could serve as template for the translation of relatively more protein copies. In any case, the amount of enzyme present, as examined through immunolabeling, is equal in all vehicle-treated groups and always relatively higher in the MK-801-treated animals (see below). Unfortunately this explanation does not account for the reduction in band intensity in the vehicle treated animals after 73 hrs.

Fig. 3.2_20: RT-PCRs of the genes coding for the antioxidant enzymes catalase and SOD2 from the forebrain of animals treated for 25, 49 or 73 hrs with MK-801 or a vehicle

Marker proteins of peroxisomes (Pex14p) and astrocytes (GFAP) show differential expression patterns. While treatment with MK-801 appears to have little to no effect on the expression of the PEX14 gene it appears to lead to an activation of astrocytes as shown through the rapid increase in GFAP expression after 25 hrs of treatment (Fig. 3.2_21). The

bands of all three vehicle-treated groups are relatively similar, whereas the expression of the gene in the MK-801 groups increases dramatically, but is then reduced in the 49 and 72 hrs groups. Since GFAP is a cytoskeleton protein, which can be seen in higher abundance in MK-801-treated animals in the morphological analyses as well, an increase in gene expression early after treatment with MK-801 would lead to higher protein content in the astrocytes. Therefore an ongoing increased level of expression should not be necessary. The reduction of mRNA copies in the animals treated with MK-801 for 49 and 73 hrs could therefore be explained by the fact that the early increase after 25 hrs might be sufficient over a longer time, thereby negating the necessity for further increases in gene expression.

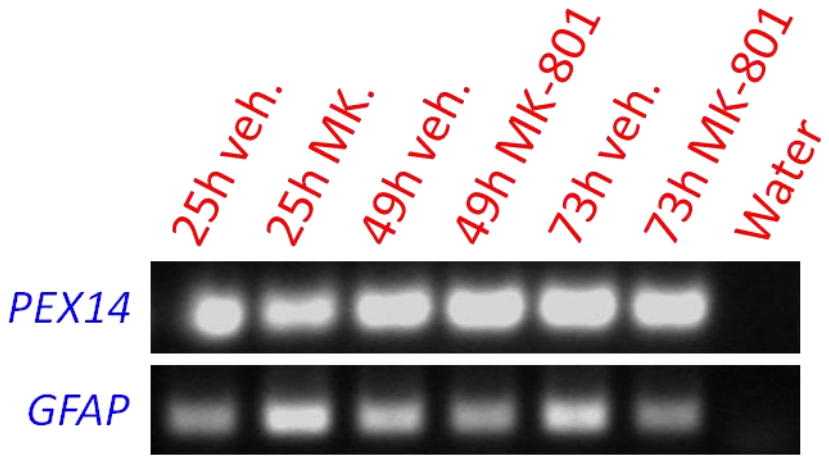

Fig. 3.2_21: RT-PCRs of the genes coding for peroxisomal (PEX14) and astrocyte (GFAP) marker proteins from the forebrain of animals treated for 25, 49 or 73 hrs with MK-801 or a vehicle

3.2.4.2 Morphological analyses: Immunolabeling of catalase in the hippocampus of vehicle- and MK-801-treated animals show shows results concurrent to those found in the expression analyses of the CAT-gene. Whereas the increase in enzymatic catalase cannot be observed in situ after 25 hrs, after 49 hrs the signal intensity is recognizably higher in the MK-801-treated animal compared to the vehicle-treated controls (Fig. 3.2_22). Since catalase is generally not found in high abundance in the mammalian nervous system, the increases are obviously only subtle. Unfortunately results for catalase from the animals treated for 73 hrs could not be obtained.

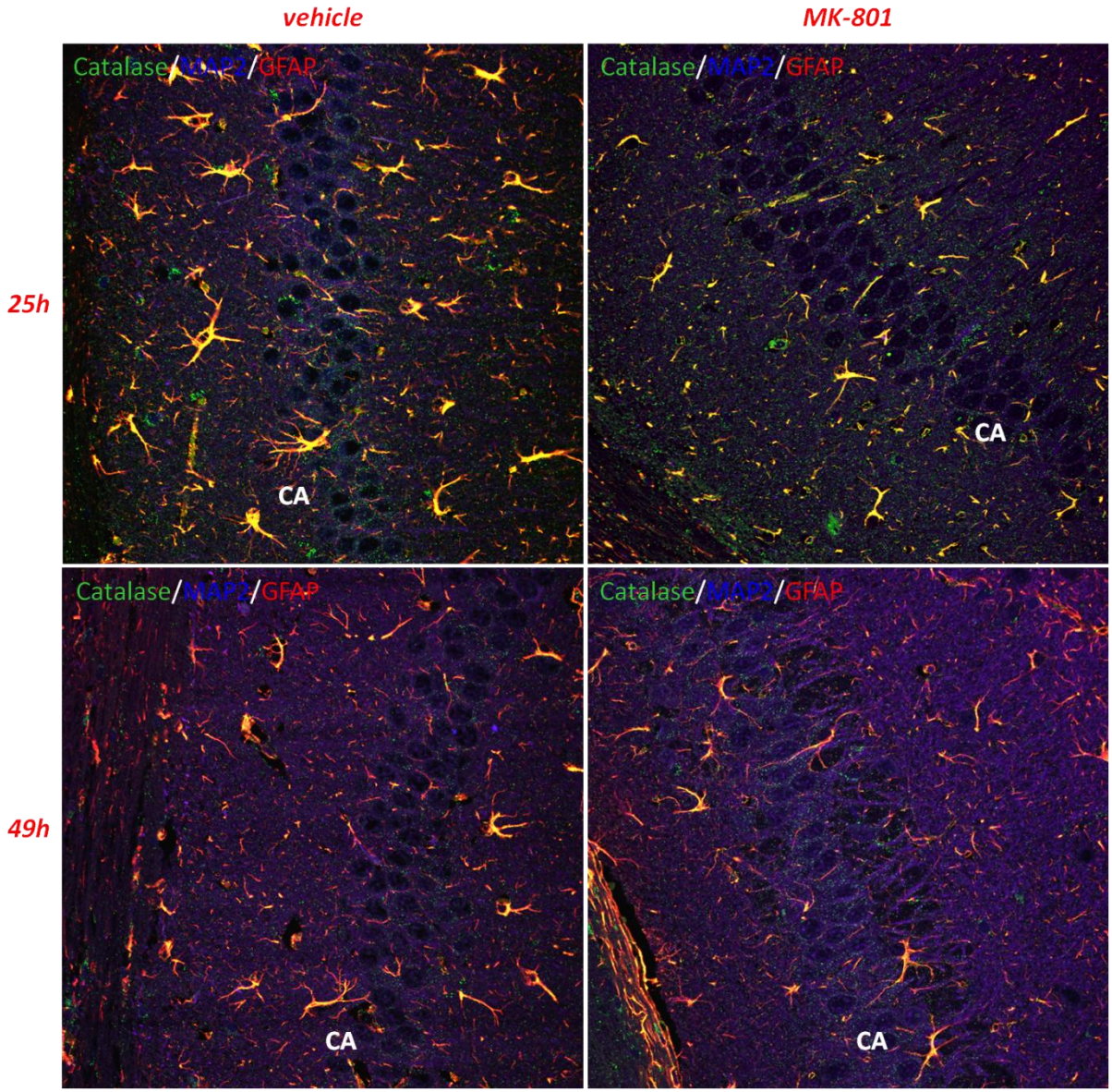

Fig. 3.2_22: Triple IF labeling for catalase, MAP2 and GFAP in the hippocampal formation of animals treated for 25 or 49 hrs with MK-801 or a vehicle

Immunostainings for Pex14p show that even after 73 hrs treatment of animals with MK-801 does not lead to noticeable alterations in peroxisomal abundance or distribution (Fig. 3.2_23). While treatments of primary murine neurons with a peroxisome proliferator as well as with dopamine showed that 24 hrs are sufficient time for both peroxisomal proliferation as well as redistribution from peripheral processes to the larger dendrites and perikarya, it would appear that the intrinsic increase in dopamine within the hippocampus caused by MK-801 is markedly lower than the concentrations used in experiments on cultured cells. Whether an ongoing treatment over the course of several weeks would finally lead to peroxisomal redistribution as found in vitro is presumable, but can only be speculated upon from the data at hand.

Interestingly, however, these sections clearly show an increase in GFAP immunoreactivity, especially in the images taken from animals sacrificed after 25 and 49 hrs. This increase is mirrored by an increase in number of mRNA copies of the GFAP-coding gene, as shown through RT-PCR experiments.

IF staining for mitochondrial manganese superoxide dismutase (SOD2) show a noticeable increase in protein content in all animals treated with MK-801 compared to vehicle-treated controls (Fig 3.2_24). This increase appears to be time-dependent, since SOD2 levels increase with treatment duration. Whereas the protein content at first only rises within the perikarya of the neurons and astroytes (as can be illustrated nicely in the relatively small and densely packed neurons of the dentate gyrus), after 73 hrs there appears to be an increase in immunoreactivity not only in perikarya, but also in the surrounding neuropil.

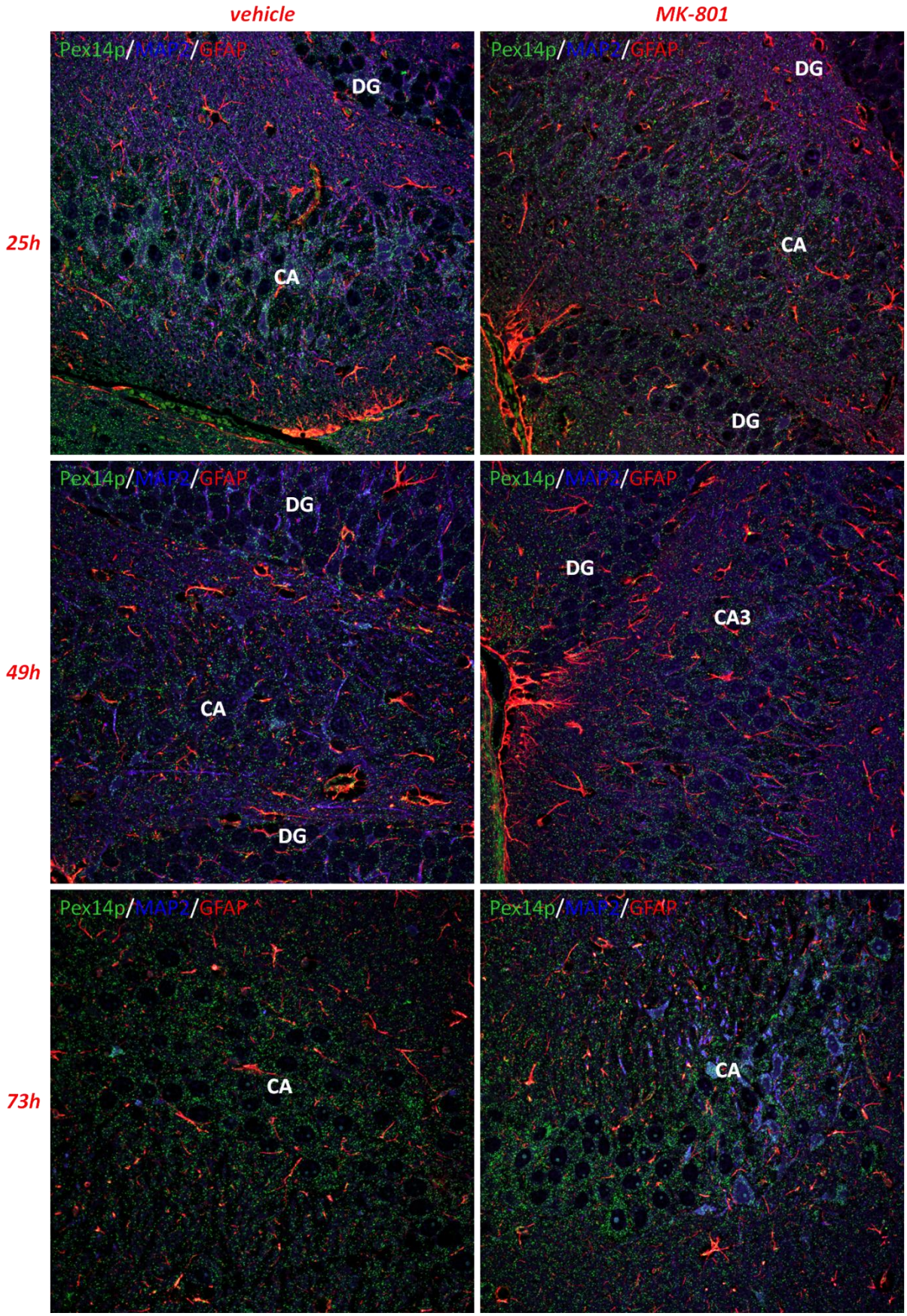

Fig. 3.2_23: Triple IF labeling for Pex14p, MAP2 and GFAP in the hippocampal formation of animals treated for 25, 49 or 73 hrs with MK-801 or a vehicle

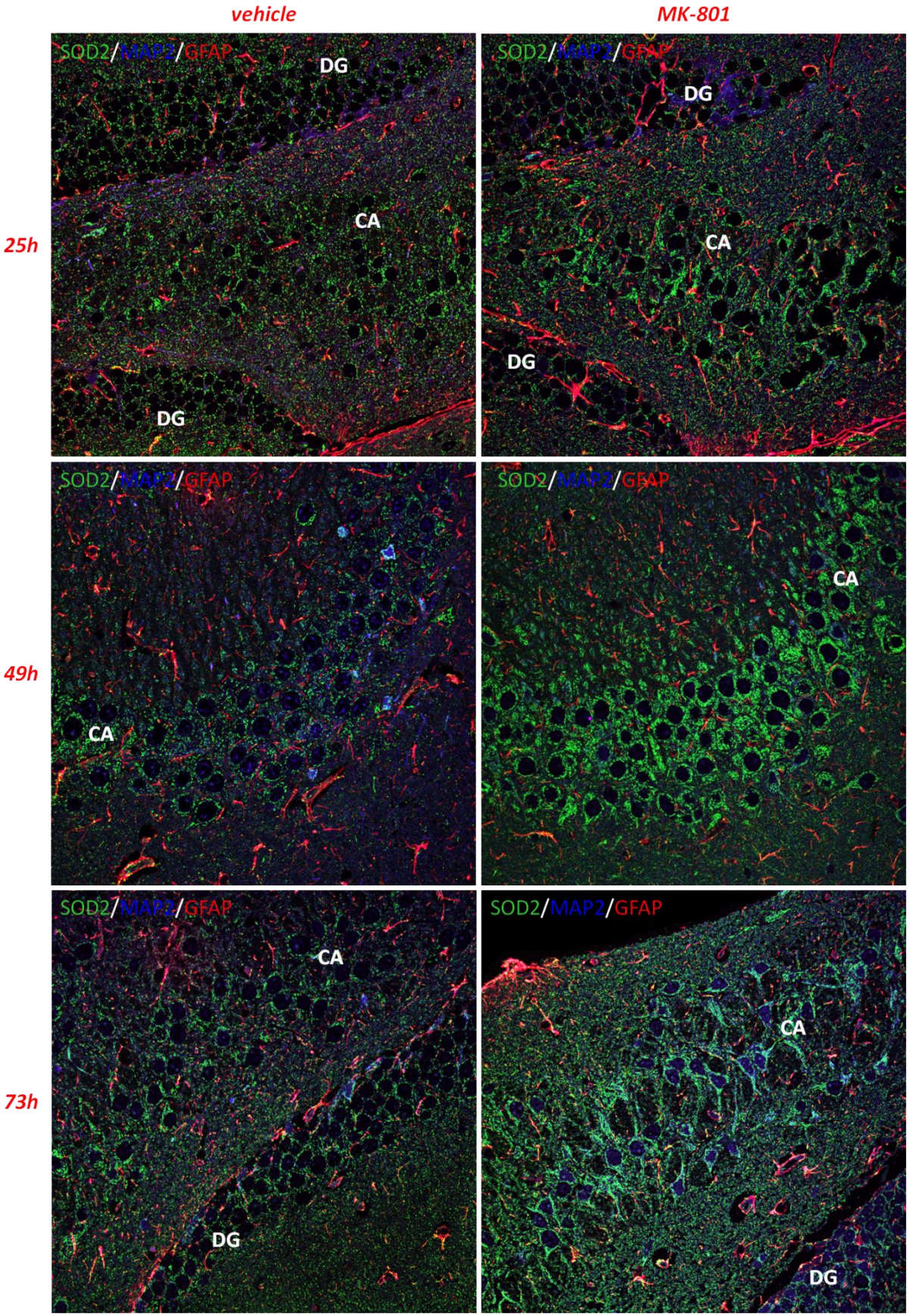

Fig. 3.2_24: Triple IF labeling for SOD2, MAP2 and GFAP in the hippocampal formation of animals treated for 25, 49 or 73 hrs with MK-801 or a vehicle

4. Discussion, summary and conclusions

4.1 Peroxisomal localization with Pex14p as a novel marker protein

It could be shown clearly that peroxisomal protein content is highly variable within as well as between distinct cell types and tissues, especially when comparing the abundance and distribution of proteins involved in specific peroxisomal metabolic function, like catalase or ABCD3, with proteins involved in peroxisomal biogenesis, like peroxins 13 or 14. It could further be illustrated that matrix enzymes like catalase are highly unsuitable for peroxisome marking on comparative morphometry since they are markedly altered by metabolic parameters, whereas peroxins, like Pex14p, give a far superior estimation of true peroxisomal abundance and distribution.

It is therefore necessary to critically reexamine old publications which describe peroxisomal abundance solely on the base of (mainly histochemical) stainings of catalase. It was for example proposed by Arnold and Holtzman (1978) that even though microperoxisomes are abundant in the cells of the developing rat central nervous system they are no longer found in the fully developed adult rat CNS. In 1982 Holtzman published having observed heterogeneity of enzyme content between subgroups of peroxisomes, namely those containing high catalase and low levels of D-amino acid oxidase (DAAO) and those with low catalase, but high DAAO. A metabolically similar enzyme, D-aspartate oxidase (D-AspOx), is shown to be highly abundant in neurons, glial cells as well as the epithelia of the proximal tubules in the kidney in both rat and human samples. D-amino acids are knows to be of modulatory function in N-methyl-D-aspartate glutamate receptors (NMDAR), binding to a specific binding site at the NMDAR. Peroxisomes are described in kidney and liver as the only organelles known to contain D-AspOx (Van Veldhoven et al., 1991; Zaar et al., 1989; Zaar, 1996). In this thesis it was, however, possible to show that peroxisomes can be found both in the adult brain as well as in distal tubules of the kidney, amongst other organs. It is therefore obvious that Pex14p is present in the membrane of different peroxisomal subtypes, as described by Holtzman, making it superior as marker protein compared to functional enzymes like catalase, DAAO or D-AspOx.

The differences in peroxisomal distribution between distinct cells of the submandibular gland as well as within the same cells during the development of the gland

were described by Mooradian and Cutler in 1978 using a cytochemical demonstration of catalase through alkaline DAB. These partially extreme differences are found not only in electron microscopy, but can also be seen in light and fluorescence microscopy using antibodies against catalase (Fig. 3.1_5). It is interesting to note that some cells in the ducts of the submandibular gland show what appears to be physiologically cytoplasmic catalase both in mouse as well as human samples. These findings were interpreted as differences in peroxisomal distribution by Mooradian, but appear to be mainly differences in catalase content of individual peroxisomes, as peroxisomal abundance shown through Pex14p appears relatively homogeneous within the mucous and serous parts of the gland, albeit obviously different between the serous and mucous cells. Finally the interpretation of cytoplasmic catalase is supported through the observation that, albeit that duct cells have slightly more Pex14p compared to primary secretory cells, the amount of Pex14p found within the duct is not nearly as high as that of catalase. This, according to peroxisome ultrastructure, is only possible, if catalase is in fact present outside of the peroxisomal membrane in these cells. Therefore, a membrane protein, like Pex14p, is again superior in its qualities as peroxisomal marker. Due to its role in the docking complex involved in both PTS1- and PTS2-linked matrix protein import, it cannot be found outside of peroxisomes, unlike metabolic enzymes which can leak or be mistargeted. Pex14p is also suitable for the labeling of peroxisomal membrane ghosts, which occur in specific peroxin knockouts, like the PEX5-knockout (Baes et al., 1997).

The first extensive screening of various tissues and organs for peroxisomes (then called microbodies) again made use of the DAB-method for labeling of endogenous catalase (Hruban, et al., 1972). Albeit not necessary to discuss all findings in comparison to new findings within this thesis, some special points of interest may be emphasized. A main difference, which was also analyzed by co-workers (Ahlemeyer et al., 2007) is the abundance of peroxisomes in neural tissue, such as the cerebellar and cerebral cortices or the dorsal root ganglia, both of which are described by Hruban as having “occasional” microbodies with relatively weak DAB reaction. Analyses of the abundance of peroxisomes using Pex14p clearly show that peroxisomal abundance in neurons is relatively high in the somata and dendrites, as it also is in astrocytes, even though these peroxisomes appear to contain only very small amounts of catalase, wherefore they do not appear (strongly) when using the DAB reaction.

Similarly Hruban et al. report a low number of DAB-detectable microbodies in testicular Leydig cells, various cells of the ovary, podocytes of the renal glomerula or

endocrine cells of the adrenal cortex. In all of these organs the results of this thesis show substantially higher numbers of Pex14p-positive peroxisomes compared to those found by others as well as compared to those found when staining for catalase. It would therefore appear that the advantages of Pex14p as peroxisomal marker are found in most organs and tissues and that there are only few organs in which catalase yields higher signal intensities compared to Pex14p. Examples hereof are liver or the corpus luteum.

Online gene expression profile analyses (performed with BioGPS, www.biogps.gnf.org) show that PEX14 is expressed in similar amounts in most organs and cells types unlike ABCD3 and especially CAT which show major differences between different organs and cell types. Furthermore PEX14 appears to be expressed in all analyzed samples, whereas catalase is not (Fig. 4_1).

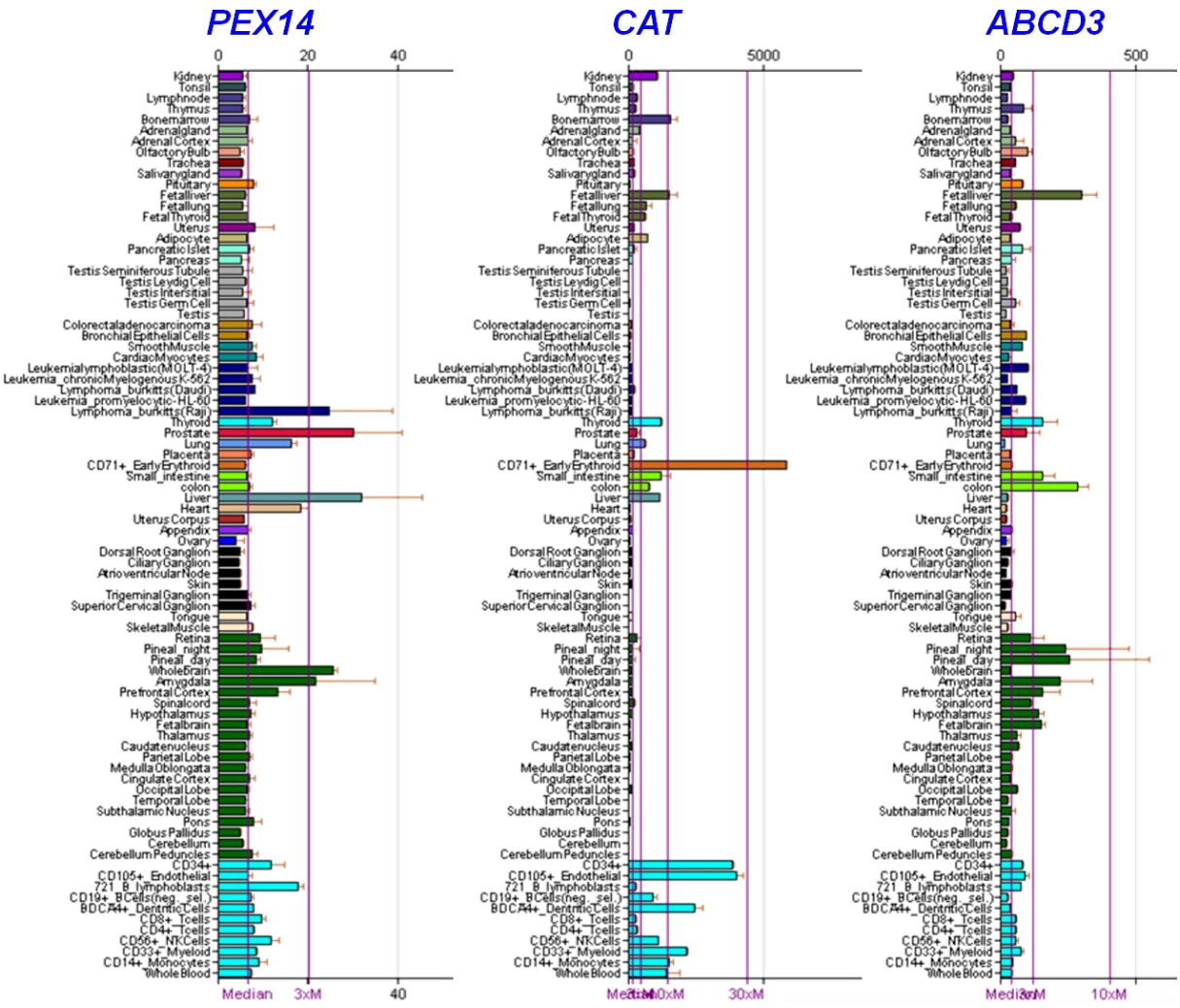

Fig. 4_1: Gene expression charts for PEX14, CAT and ABCD3; performed with BioGPS

The importance of peroxisomes for healthy bodily functions is becoming more evident from year to year. Especially since the discovery that not only functional catalase is necessary

for peroxisomal defense against oxidative stress, as shown in patients suffering from X-ALD (Powers et al., 2005). The absence of the lipid transporter ABCD1 (formerly known as ALDP, adrenoleukodystrophy protein) leads to an accumulation of VLCFA, which in turn causes an imbalance in oxidative homeostasis in various tissues (Fourcade et al., 2008). Similar observations were made in mice after genetic knockout of the transporter ABCD2 (Fourcade et al., 2009). It has been shown under these circumstances that loss of peroxisomal antioxidant capacity, and thereby oxidative stress, is shown through an increase in mitochondrial manganese superoxide dismutase (SOD2). This relationship between peroxisomal and mitochondrial antioxidant defense appears to be vital for the equilibrium of oxidant and antioxidant chemicals within the body. For example, Baumgart et al. (2001) investigated the behavior of mitochondria in the Pex5p-knockout mouse, the first ever mouse model for Zellweger syndrome (Baes et al., 1997), to find proliferation of mitochondria with significant differences in ultrastructure, respiratory chain proteins and enzymes as well as a significant upregulation of mitochondrial SOD2.

Also interestingly, Li et al. (2002) showed that a deficiency in the peroxisomal biogenesis protein PEX11β leads to a pathological picture similar to that found in patients suffering from or in mouse models for Zellweger syndrome (Baes et al., 1997; Faust & Hatten, 1997; Maxwell et al., 2003), the severest form of peroxisomal biogenesis disorders. Upon closer examination, however, it could be shown that peroxisomal function was not significantly altered. Similarly hereto, it was shown that the neuronal migration defects prototypical to Zellweger syndrome were not caused by the inactivation of peroxisomal β-oxidation pathways (Baes et al., 2002). This was evaluated in mice carrying a defect in the gene encoding for multifunctional enzymes MFP1 and MFP2, the second step in peroxisomal β-oxidation. These mice exhibited no noticeable changes in phenotype at birth.

It therefore becomes quite obvious that peroxisomal function and involvement in various pathogenetic mechanisms are highly complex and far less understood than was believed initially. Peroxisomal function is essential as a protector against oxidative stress as well as lipid toxicity in many cell types and tissues. This function is, however, not solely dependent on single enzyme or protein actions, e.g. catalase, ABCD1 or MFP1/MFP2. Furthermore, peroxisomal function is also not solely dependent on functional peroxisomal β-oxidation or lipid import. This can also be shown through the knockout of another peroxisomal biogenesis protein encoding gene, namely PEX13 encoding for the peroxin 13

(Pex13p). Mice lacking the gene PEX13 exhibit a phenotype similar to that found in Zellweger Syndrome (Maxwell et al., 2003), as do mice lacking the gene PEX2 (Faust and Hatten, 1997; Faust et al., 2002 & Faust, 2003).

A possible reason for the usefulness of Pex14p lies in its protein structure and how it is embedded into the peroxisomal membrane. The human orthologue was identified by Will et al. (1999) and analyzed and described in detail by Oliviera et al. (2002). They find major similarities between the Pex14proteins of human, rat and mouse. Overall the protein (in rat) has 377 aminos acids, whereof only the first 130 N-terminal amino acids serve as a true membrane protein. The remainder of the protein including the C-terminus is completely exposed to the cytosol. It is yet unclear, whether the N-terminus of the protein reaches the luminal side of the organelle or is in fact also exposed to the cytosol, as proposed earlier by Shimizu et al. (1999). It can, however, be concluded that since more than two thirds of the Pex14protein are actually cytoplasmic it can easily be accessed and bound to by antibodies against epitopes contained within this part of the amino-acid sequence. This optimal accessibility makes the protein highly suitable as a marker for comparative morphometry.

Additionally it could be suggested that Pex14p would be a marker usable for cells and tissues of many different species, since, additionally to the species shown in this thesis (*Homo sapiens, Mus musculus, Rattus norvegicus, Felis catus,* and *Papio hamadryas*), the PEX14 gene and proteins sequence are also conserved in *Pan troglodytes, Canis lups, Gallus gallus, Danio rerio, Drosophila melanogaster,* and *Anopheles gambiae* (HomoloGene: 37936, NCBI). It is most likely that many more species share sequence homologies for PEX14 as well as Pex14p.

Over all, the key pathogenetic mechanisms underlying most peroxisomal diseases appears to be oxidative stress, defined as a disequilibrium of reactive oxygen species (ROS) and antioxidant capacities of the cell. Both the production of ROS as well as the forms of antioxidant defense are multifaceted, wherefore it can be assumed that differences in peroxisomal content are adaptive mechanisms for combat of different form of oxidative danger. It was therefore important to find a common marker for all peroxisomes, which was found in Pex14p. In doing so, it is now possible to catalogue the distribution of peroxisomes in all tissues and to assess the exact differences in protein and enzyme content by tissue.

The labeling of peroxisomes in morphological studies for example is by its very nature a diagnosis. The usage of a diagnostic tool (in this case a marker protein) for the prediction of

an unknown condition (in this case the existence of peroxisomes) is obviously prone to two kinds of errors (incorrect negative diagnosis and incorrect positive diagnosis) as well as likely to yield two forms of correct results (correct negative diagnosis and correct positive diagnosis). A diagnostic testing of this kind, as is done in every case of organelle-labeling through a marker protein, is therefore assessable in its quality through Bayes' theorem and is dependent on the one hand on the sensitivity of the diagnostic tool (in this case the antibody's capability of binding to the correct antigen) and on the other on its specificity (in this case the capability of the antibody not to bind to other antigens). By respecting the base rate of the diagnostic condition (in this case the amount of specific antigens in the cell or tissue sample) it is possible to estimate the positive (PPP) and negative predictive power (NPP) of the diagnosis, meaning both the validity of the statement that the marker successfully labels all of the respective organelles (PPP) as well as that of the statement that everything which is not labeled is also not the organelle in question (NPP). This theoretical reasoning easily goes to show the value of Pex14p as a marker for peroxisomes: Pex14p is (to date) known to be part of every intact peroxisomal membrane. The Pex14p-antibody has been shown through Western blotting to have a highly specific affinity for its antigen. And finally, the antibody exhibits a high sensitivity for its respective antigen, as shown through studies on partially decayed tissue samples from human body donors to the gross anatomy course (Fig. 3.1_6). One can therefore argue that Pex14p is not only suited best as a marker protein for peroxisomes due to its cell biological properties, but also due to its probabilistic assets, meaning that not only the labeling as such is excellent, but also the validity of the diagnostic conclusion based on this labeling.

These findings provide the possibility for future explorative and morphometric studies on alterations of the peroxisomal compartment in all tissues and cell types und different experimental conditions as well as in various human disorders, like schizophrenia.

4.2 Dopamine neurotoxicity, schizophrenia and peroxisomal metabolism

Although studies analyzing the protein abundance and activity of various peroxisomal enzymes, like catalase, DAAO or D-AspOx, find differences both between schizophrenic patients and controls as well as the result of dopamine neurotoxicity in vitro, no data exists in literature regarding the abundance or distribution of peroxisomes as an organelle in morphological and morphometric analyses. As could be shown in figure 3.2_1 the low amount of catalase in the healthy brain of humans makes the immunohistochemical labeling very difficult and does not allow for comparative morphometric analyses between schizophrenia patients and controls. Stainings for Pex14p, however, open the door to the localization of peroxisomes in the human brain and make more detailed in situ analyses of peroxisomal behavior in schizophrenia possible. The minute differences in peroxisomal size and distribution as shown also in figure 3.2_1 are, however, very subtle and should not be overinterpreted, due to the lack of information regarding the medical histories and case histories of the patients analyzed in these experiments. This holds true not only for the schizophrenia cases, but also for the controls, of whom not more information was available other than that they had never been diagnosed with schizophrenia and did not show any other detectable neuropathological alterations. To investigate the differences regarding peroxisomal abundance and distribution more detailed and especially controlled analyses are necessary. These, however, usually prove hard to accomplish, since sufficient numbers of standardized cases (e.g. first-episode patients or patients treated with known pharmaceuticals for known spans of time etc.) are generally not available.

It was therefore necessary to perform in vitro and animal studies in order to control as many confounding variables as possible.

4.2.1 Effects of dopamine treatment on primary murine neuronal and astrocyte cultures

All analyses were performed under the assumptions mentioned in the chapter on dopamine metabolism, namely that the causal factor underlying the schizophrenia phenotype is mesolimbic hyperdopaminergia, that dopamine is neurotoxic by leading to the formation of ROS and that systemic injections of NMDAR-antagonists (like MK-801) in turn cause mesolimbic hyperdopaminergia. As illustrated also in the aforementioned chapter there is sufficient evidence in literature to support all these assumptions. Unfortunately the complex

interactions known to exists between various bodily functions and organs as well as between functional parts of the brain and systems of neurotransmission make it highly improbable that even the best animal model, be it through drug challenges or knock outs/downs of possible candidate genes, will be able to explain all of the differences found between schizophrenics and healthy controls or the differences within the rather heterogeneous group of phenotypes characterized under the diagnosis of clinical schizophrenia or related disorders. This is exacerbated by the still rather vague knowledge regarding the etiopathogenesis of schizophrenia spectrum disorders. The main advantage of in vitro or animal research, however, is the possibility to perform qualitative research through (relatively) controllable alterations to a cell culture or animal environment, metabolism or genome and use the gathered information to form more precise hypotheses, which can then be translated, operationalized and tested in human samples. The results of the second part of this thesis should therefore be viewed as well as interpreted in this light, namely as qualitative and hypothesis-generating, rather than quantitative and hypothesis-testing.

Incubation of primary murine neuronal cultures with different concentrations of dopamine showed a resulting dose-dependent increase in catalase abundance especially in astrocytes and neuronal perikarya. This allows the conclusion that hyperdopaminergia indeed leads to an increase in H_2O_2-production in both cell types. It also suggests that initially cells are able to activate compensatory antioxidant pathways, which raises the question whether or not these antioxidant defense mechanisms are sufficient to prevent oxidative stress as defined by disequilibrium between ROS production and ROS degradation. Unfortunately it was not possible within this thesis to measure the levels of oxidative damage and compare them to the activation of antioxidant pathways. Additionally the influences on other (peroxisomal, mitochondrial and cytosolic) antioxidant defense mechanisms like the peroxiredoxins, superoxide dismutases or the glutathione system have yet to be examined in this experimental setting. The lack of a major increase in cell death even in the cultures treated with extremely high dopamine concentrations suggests that the effects of dopamine neurotoxicity need to be prolonged in order to influence neuronal survival, as is hypothesized in Parkinson's disease. This is also in line with findings of little cell death and gliosis in post-mortem brains of schizophrenic patients. It is therefore arguable, if dopamine neurotoxicity over a specific time span may lead to neuronal degradation resulting in a Parkinsonian phenotype, that the underlying mechanisms in the schizophrenic brain must be different. This

is further supported by findings on cell death and catalase abundance in primary murine neuronal cultures treated with haloperidol. In these experiments there was also a dose-dependent increase in catalase, which was, however, markedly higher compared to dopamine-treated cultures and was accompanied by an increase in cell death, which was also dose-dependent. Since haloperidol is known to lead to a Parkinsonian phenotype in patients it can therefore be seriously questioned, whether the causal relationship between disorder and oxidative stress reported in literature is the same for schizophrenia and Parkinson's, even though both conditions involve dopamine neurotoxicity. And since oxidative stress is far better established as a causal factor for Parkinson's, it would seem that the relationship in schizophrenia is probably different, likely vice versa, in that schizophrenia is not caused by oxidative stress, but rather that schizophrenia results in oxidative stress.

The influences of ROS production in schizophrenia may, however, play an important role in the maintenance of the disorder and also, in part, the expression of specific symptoms like progressive loss of gray matter volume as well as cognitive decline, even after the cessation of psychosis. The reduction of peripheral processes of both neurons and astrocytes (Fig. 3.2_2) would be in line both with the aforementioned argument and with the findings of atypical neurodegeneration. The novel technique of peroxisomal labeling with Pex14p additionally shows a reduction and redistribution of peroxisomes from the peripheral processes to the perikarya upon treatment with dopamine. It can therefore be argued that, albeit that dopamine does not lead to neuronal death, it probably leads to a reduction of dendritic arborization and synaptic density, thereby influencing the balance between neurotransmitter systems. As mesolimbic pathways project into various areas involved in functions that are attenuated in schizophrenia, like the NAcc, the hippocampus or the prefrontal cortex, and as these regions are known for their glutamate transmission, it is therefore safe to argue that a reduction of synaptic connectivity in these regions will also affect the glutamate system. These results therefore suggest in vitro quite clearly that there probably is a link between "dopaminergic noise and glutamatergic silence" (Bernd Gallhofer, conference statement, 2010). Since both facets are discussed heavily in schizophrenia research, these findings support an integrative model, whereby frontal hyperdopaminergia causes hypoglutamatergia, rather than the idea of two separate concepts in which dopamine and glutamate are independent entities.

Since the observed differences in Pex14p and even more so catalase content were most pronounced in astrocytes and since astrocytes are important cells for the regulation of NMDAR-linked glutamate transmission, the effects of dopamine incubation on pure primary murine astrocyte cultures were examined. This also links back to peroxisomal metabolisms, as two enzymes important for NMDAR-cofactor metabolism, namely DAAO and D-AspOx, are localized solely in peroxisomes and are both shown to be altered in activity and abundance in schizophrenia. The genes encoding these proteins are both considered candidate or risk genes in schizophrenia research. Figures 3.2_5 and 3.2_6 showed that astrocyte cultures were devoid of neurons and that increasing concentrations of dopamine lead to a dose-dependent discoloration of the medium. It can therefore be assumed that there was a chemical reaction caused by dopamine. This does not, however, influence levels of cell death, similar to neuronal cultures, even in markedly higher concentrations and over the course of 24, 48 or 72 hrs of incubation. Since the cultured astrocytes were able to take up dopamine and react with dopamine through receptor binding, it can be assumed that the treatment not only leads to an increase of extracellular, but also intracellular dopamine concentrations as well as metabolic cAMP-dependent pathways. No differences were observed in the expression profiles of dopamine receptors, the dopamine active transporter or dopamine synthesizing enzymes. This can be explained through several possible arguments: Firstly, the reactions of neurons and astrocytes are heavily dependent on each other, whereby astrocytes react to neurotransmitter/cAMP-mediated intracellular increase in Ca^{2+}-levels with a production of signal molecules for the regulation of synaptic transmission (Newman, 2003; Volterra & Meldolesi, 2005). It could therefore be assumed that the lack of cross talk between neurons and astrocytes in these cultures significantly alters the astrocytes' metabolism. This argument is probably especially relevant for dopamine synthesizing enzymes. Since this is not primarily a function of astrocytes it is not surprising that expression levels of this group of enzymes are not altered in cultures without neurons. As is shown in figure 3.2_9 the basal expression levels of both enzymes are relatively low to begin with. Secondly, other experimental setups involving various stimulation or inhibition of different dopamine receptors generally show few to no differences in receptor expression levels, albeit that some studies report differences in receptor protein abundance (Maus et al., 1993; Horiuchi & Felder, 1996; Autelitano & van den Buuse, 1997; Lammers et al., 1999a; 1999b; Unger et al., 2008). It would therefore appear that short-term alterations of dopamine receptor density do not require

alterations of gene expression, but are regulated on the post-transcriptional level. Thirdly, the amount of time necessary for alterations in expression profiles for dopamine receptor genes might be longer than 72 hrs. Finally, Hirrlinger et al. (2002) showed that blocking of dopamine receptors in cultured astrocytes did not influence the oxidation of intracellular GSH to GSSG upon treatment with astrocytes. It could therefore be argued that the detoxification of excess dopamine by astrocytes in vitro is not necessarily dependent on dopamine receptor binding.

In general it has to be emphasized that RT-PCR, as performed in this thesis, is neither a quantitative method nor is it capable of reliably detecting subtle differences between expression levels. For the detection of finer alterations in a more reliable fashion quantitative PCRs or other methods of expression profiling, like microarrays or SAGE (serial analysis of gene expression) need to be performed.

The fact that the expression levels of the three dopamine degrading enzymes are barely changed can be interpreted in different ways. The slight increase shown in MAOB expression, but not in MAOA, taken in light with the initially higher basal expression rate of MAOA, allows for the hypothesis that enzymatic content of the cultured astrocytes is sufficient for the degradation of the increased levels of dopamine. Since detoxification of metabolites of neuronal activity is one of the primary functions of astrocytes it would be necessary for these cells to express all necessary enzymes regularly and in ample quantities. Due to the fact that dopamine is degraded by both MAOs equally, the high basal expression levels of MAOA would therefore only necessitate the observed slender increase in expression of MAOB and C*O*MT. As described above, the chemical interaction between neurons and astrocytes in vivo is known to play an important role in the regulation of astrocytal function. Since these are missing in these in vitro cultures it could be argued that the cells have no reason for a further transcription of the genes in question. The increased dopamine levels obviously do not appear to be life threatening to the cultured cells as can be shown through the lack of increase in cell death even in highest concentrations after 73 hours, although these latter cultures do begin to show signs of reduced over-all metabolic function.

An alternative explanation to lack of necessity to increase numbers of mRNA copies could be again that major alterations to the dopamine degrading system occur on a post-translational level. To examine this hypothesis it would be necessary to examine the stability of the mRNA copies, the enzyme content of the cells as well as the activity of the enzymes

and compare these values between groups. It could be possible that, regardless of relatively little change in gene expression, either or all of these values may still increase.

The effects of dopamine incubation on genes coding for selected peroxisomal proteins are also hardly visible. PEX14 is the only gene that appears to be induced in concentrations of 1 μM dopamine and higher after 72 hrs of incubation, albeit only slightly. Since Pex14p as an integral membrane protein is a part of every peroxisome, the elevation of the expression of the PEX14 gene can be considered as indicative of peroxisomal proliferation in these cultures. The lack of increase in ABCD3 expression shows that peroxisomal proliferation is a selective process, wherein new peroxisomes could cater adaptively to those functions required in a given cell or tissue. Since ABCD3 is a transporter for very long chain fatty acids (VLCFAs) into the peroxisomal matrix, it is not required in cells confronted with an increase in dopamine related ROS production. The expression of the enzyme more relevant in this context, catalase, is, however, also not induced in a detectable fashion. This could be due to the limitations of the method, but could also mean that the level of catalase present in the atrocytes as well as the basal level of catalase are already sufficient for the degradation of the increased levels of ROS expected to be induced by dopamine treatment. Due to the high efficiency of catalase, the latter argument does not appear unlikely. Furthermore, the argument of enzyme activity also needs to be considered, similar to the enzymes involved in degradation of dopamine. To answer this with any given amount of certainty additional enzyme activity assays would need to be performed. Since catalase activity is reduced by almost 75% in the developing mouse cortex between postpartum days 2 and 49 (Ahlemeyer, 2007) it would not be unlikely that initial demands regarding an increase in H_2O_2-degradation could be compensated for by activity increases of catalase rather than an immediate increase in the expression of new protein. Since dopamine was shown to increase the activity of Nrf2 (Shih, Erb & Murphy, 2007), which in turn regulates a variety of antioxidant mechanisms, it would be interesting to compare the expression levels of the CAT-gene to those of other Nrf2-activated genes in order to address the question of selective and differential antioxidant activation. This would then also raise the question on molecular mechanisms of this differential activation, since H_2O_2 is not only an activator of Nrf2, but also the direct substrate of catalase. This differential activation mechanism is not only a possibility for interindividual regulation of various genes within the same cell, but also for intraindividual differences in expression patterns in or without the presence of neurons. This could possibly be regulated through the level of Keap1

(kelch-like ECH-associated protein 1), a major regulator of Nrf2 activity, within the different cultures. Since Nrf2 is expressed constitutively its activity is controlled through degradation by ubiquitylation, which is promoted by Keap1 (Nguyen, Nioi & Pickett, 2009). The increase in catalase as shown in figure 3.2_2 in astrocytes cultivated in the presence of neurons in comparison to pure astrocyte cultures (Fig. 3.2_8) suggests higher levels of H_2O_2 in the first cultivation condition. Whether this comes from neurons via passive diffusion or is produced in the astrocytes at higher levels due to neuronal signaling is unclear, but in any case the increase in H_2O_2 would lead to a higher level of degradation of Keap1, a protein high in cystein residues (Nguyen, Nioi & Pickett, 2009), the thiol moieties of which are prone to oxidation by hydrogen peroxide and other oxidizing agents. Since Keap1 is only expressed in moderate amounts in the brain to begin with, compared to other tissues (online expression pattern analysis performed with BioGPS), it could be assumed that the added degradation of Keap1 through an increase in H_2O_2 in intact neuron-astrocyte interaction would therefore lead to a potent activation of Nrf2. It is therefore a possibility that the differential regulation of catalase expression, or rather the relative lack of regulation in pure astrocyte cultures, could be lead back to reduced enzymatic dopamine degradation or to increased H_2O_2 degradation or the added effects of both in comparison to cultures with neuron-astrocyte interactions. Therefore, interesting aspects would be to research the expression levels of Keap1 in schizophrenic patients and the therapeutic effects of Keap1-inhibitors or Nrf2-agonists as potential palliatives.

In closing, albeit apparent that astrocytes are by far more robust to increased levels of dopamine compared to neurons, incubation with the highest concentrations of dopamine (200 μM & 500 mM) for 72 hrs resulted not only in a decrease of general levels of transcription (data not shown here, see diploma thesis: Fischer, 2011), but also in a reduction of protein content not only for catalase, but also for GFAP (Fig. 3.2_8). Since cellular survival is not decreased in these cultures it could be assumed that the apparent reduction in overall cell activity is due to a kind of “cellular sickness behavior”.

4.2.2 Effects of treatment of male pubescent C57Bl/6J-mice with the NMDAR-antagonist MK-801

1 h after treatment of animals with MK-801 a clear increase in the expression of the gene for serine racemase could be observed (Fig. 3.2_16). This is considered as internal positive control for the effectivity of systemic (i.p.) MK-801 administration in the brain, in addition to the observations of expected phenotypical behavior in the animals by blind independent raters. It can therefore be assumed that MK-801-treatment managed to induce the desired pharmacological schizophrenia phenotype within this set of experiments.

Additional RT-PCRs showed increases in the expression of D-AspOx and to a lesser extent PEX14. Since MK-801 rapidly induces serine racemase expression, the elevated levels of D-serine are likely to lead to an increase in D-amino acid degrading enzymes. This was shown by Yoshikawa et al. (2004b) for D-amino acid oxidase and would also be expected in the case of D-aspartate oxidase, not only due to the fact that both enzymes have synergistic function, but are both also found exclusively in peroxisomes (Zaar et al., 2002). When comparing the time courses of the increases in expression of serine racemase (Yoshiakwa et al., 2004a) and D-amino acid oxidase (Yoshikawa et al., 2004b), the time delay in transcription induction between the two genes (maximum expression in serine racemase after 1 h vs. 4 hrs for D-amino acid oxidase) could also support the hypothesis that DAAO expression is not only induced directly by the increase in dopamine due to the CRE in the promoter and first intron of the DAAO gene (Fukui & Miyake, 1992), but also due to the secondary activation via the aforementioned increase in D-serine. It is therefore probable that similar mechanisms also lead to the increased expression of the D-AspOx gene. The most important aspect is, however, that MK-801 induced hyperdopaminergia leads to an increased expression not only of D-amino acid oxidase, but also of D-AspOx. It can therefore be assumed that the influences between the dopaminergic and glutamatergic systems are bidirectional: NMDAR blockade leads to an increase in mesolimbic dopamine, as is established in literature, while hyperactivity of the mesolimbic dopamine system in turn leads to an increase in enzymes degrading important cofactors of NMDAR-mediated glutamate transmission. This would give rise to a vicious circle in patients whose hyperdopaminergia is not caused by administration of a drug and is therefore not transient. It also gives rise to the question regarding the chicken and the egg: Is it the initial increase in dopamine transmission leading to frontal glutamate deficiency, which in turn exacerbates the underlying hyperdopaminergia? Or is the other way

around, meaning that initial frontal glutamate hypofunction disinhibits mesolimbic dopamine pathways thereby leading to a neurotoxic effect which not only reduces the density of synaptic spines on peripheral dendrites carrying NMDARs, but also reduces the availability of important NMDAR cofactors? More research is necessary to answer this question. It may also be possible that both possibilities could be found in patients, whereby the end-effect would be the same.

The slight increase in PEX14 expression could be due to a rise in dopamine-related ROS levels, but could also be linked to the aforementioned activation of transcription in the genes of the two peroxisomal enzymes D-AspOx and DAAO. As the difference in band size is only slight it should not be overinterpreted. Since neither the expression of Nrf2 nor CAT is induced it is unlikely that ROS levels will have risen substantially 1 h after treatment with MK-801. The constitutive expression of Nrf2 and the primary regulation through Keab1 as described above as well as the high efficiency spectrum of catalase and lack of information regarding changes in the activity of the enzyme, however, do not exclude the possibility of dopamine-related ROS production after MK-801 treatment. It can therefore probably be ascertained that after 1 h there is no oxidative stress, in a sense of disequilibrium between ROS production and cellular ROS defense. Since the time is, however, sufficient to induce a schizophrenia phenotype in the treated animals, the hypothesis found in literature that oxidative stress is a primary cause of schizophrenia, comparable to Parkinson's disease, becomes ever more doubtful.

The lack of markedly changed expression levels in the liver samples after 1h of MK-801 treatment compared to vehicle-treated animals shows that the systemic administration of the drug has differential and specific effects in the brain and does not support a primary mechanism of ROS production of MK-801 itself. Since drugs blocking NMDAR channels are commonly shown to reduce oxidative stress caused by glutamate excitotoxicity it therefore becomes most likely that the proposed ROS production after administration of MK-801 is due to secondary mechanisms like dopamine neurotoxicity.

The inconsistencies in the expression patterns of serine racemase after 25, 49 and 73 hrs in both groups (Fig. 3.2_18) are not easy to interpret. On the one hand Yoshikawa et al. (2004) showed that 8 hrs after MK-801 administration expression levels of the serine racemase genes had returned to baseline, but on the other hand Hashimoto et al. (2007) reported a significant increase in serine racemase expression after chronic treatment (14

days) with MK-801. Since the expression of serine racemase appeared to be highest after 49 hrs in the vehicle-treated group it could be possible that other factors strongly influence the transcription of the gene and mask the effects of the MK-801 treatment. It has been suggested that the protein content of the diet fed to experimental animals could be one such factor with influence on the serine metabolism (Antflick, Baker & Hanson, 2010). Whether this could be relevant regarding the results presented in this paper cannot be excluded, but can also not be ascertained without further research. Another possibility could be an undetected inflammation in one or some of the control animals, as inflammation has also been shown to increase serine racemase expression (Wu & Barger, 2004).

The influences of MK-801 on the expression patterns of dopamine-degrading enzymes are surprising. It would be expected that increase in prosencephalic dopamine through MK-801 would lead to a reactive increase in MAO and C*O*MT transcription, as is found after 49 hrs of treatment (Fig. 3.2_19). After 25 hrs of treatment as well as after 73 hrs (with the exception of MAOA) the numbers of mRNA copies are, however, reduced in the MK-801 treated animals compared to controls. A possible explanation herefore may be levels of plasma glucocorticoids, which have been shown to differentially regulate the expression patterns of all three dopamine degrading enzymes (Edelstein & Breakefield, 1986; Carlo et al., 1996; Lindley, She & Schatzberg, 2005). Although these findings are more than ambiguous they all commonly show major influences of glucocorticoids on both expression and activity of MAOs and C*O*MT and also show that MAOA and MAOB are differentially regulated and do not necessarily follow a parallel course. Since rodents are animals prone to flight it is commonly accepted that the act of catching and immobilizing them during injection will be perceived as extremely stressful and cause high releases of corticosterone, the primary glucocorticoid in rodents, from the adrenals. It is therefore possible that the reduction or lack of induction of dopamine degrading enzymes could be caused by increases in the activity of the hypothalamic-pituitary-adrenal axis. This can be seen especially in the reduction of MAOB expression over time in both the MK-801- as well as the vehicle-treated groups. The reduction in transcription levels in the MK-801 animals at all time points regarding MAOB and after 25hrs in MAOA and C*O*MT as well as after 73 hrs in C*O*MT could therefore be caused by the increase in locomotion activity due to drug treatment, which in turn should raise the glucocorticoid production. Again, as previously mentioned, possible posttranscriptional modifications, e.g. increases in enzyme activity, might also play an important role in the

degradation of increased levels of dopamine. On the whole it would seem that the levels of dopamine are probably not too high after 73 hrs so that massive increases in the expression levels of MAOs and C*O*MT are not (yet) necessary. This would seem to be supported by the fact that no morphological signs of increased neuronal death could be observed in any of the immunolabeling experiments (Figs. 32._22 through 3.2_24), thus one could argue that, although MK-801 leads to a sufficient increase in dopamine to cause a schizophreniform phenotype in the animals, after 73 hrs the levels are not yet high enough to cause marked neurodegeneration. This argument also supports the hypothesis, that neuronal damage caused by oxidative stress is not a primary cause of schizophrenia.

Both the expression patterns (Fig. 3.2_21) as well as the immunolabeling results (Fig. 3.2_23) show little to no increase in PEX14 expression levels or Pex14p abundance. Since results from the differential distribution of Pex14p and catalase in various organs including the brain show that many peroxisomes are present in neuronal tissue which do not contain catalase, it would therefore not be surprising that the slight increases in catalase protein abundance and gene expression (Figs. 3.2_22 & 3.2_20) do not require a proliferation of peroxisomes, since obviously many peroxisomes exists that can be filled with newly synthesized catalase. This again shows the heterogeneity of the peroxisomal compartment. It could, however, be reasonable to assume that chronic elevation of prosencephalic dopamine levels would at some point lead to peroxisome proliferation. Since degradation of H_2O_2 through catalase occurs in peroxisomes, a forced proliferation through treatment with peroxisome proliferators (like PPARγ-agonists; Shintu et al., 2009) might still prove therapeutically relevant in schizophrenia. As catalase has an immense substrate turnover it would therefore be probable that an increase in peroxisomes, even if catalase levels were to remain unchanged, would therefore still lead to a more efficient ROS degradation, if only through an increased capability of sequestering the ROS inside the increased number of peroxisomes, thereby preventing damage to other intracellular proteins, fatty acids and nucleic acids.

The increased expression of GFAP after 25 hrs of MK-801 treatment is expected, since similar findings have been reported both for NMDAR-antagonists (O'Callaghan, 1994; Fix, Wightman & O'Callaghan, 1995) as well as for various substances increasing dopamine levels or dopamine transmission including (meth)amphetamine (Sheng, Cerruti & Cadet, 1994; Armstrong et al., 2004), D2-receptor agonists (Sands & Chronwall, 1996) and MAO-inhibitors

(Revuelta et al., 1997). Since GFAP is an intermediate filament in the astrocyte cytoskeleton and not a functional protein, it is not surprising that an initial increase in expression levels after 25 hrs is sufficient and further increases after 49 and 73 hrs are not required. This can also be seen in the immunolabeling results, where increased protein abundance can still be observed after 49 and 73 hrs, even though expression patterns have fallen back to baseline (Figs. 3.2_23 & 3.2_24).

Finally, the increases in both catalase and SOD2 protein levels (Figs. 3.2_22 & 3.2_24) as well as in the expression levels of the coding genes (Fig. 3.2_20) show that the apparently heightened ROS levels caused by dopamine neurotoxicity are compensated for by antioxidant defense mechanisms. Whether this increase is sufficient to attenuate ROS-mediated cell damage cannot be said, due to the fact that direct ROS measurements or evaluations of peroxidation (by)products could not be performed. It is, however, unlikely that the MK-801-treated animals exhibit significant oxidative stress, since the tissue sections showed no signs of morphological differences that would suggest severe neurodegeneration. It can therefore be assumed that compensatory inductions of antioxidant enzymes are capable of making up for the increase in dopamine-related ROS. In any case, the antioxidant defense mechanisms include many more elements than catalase and SOD2 that have not been assessed within this thesis. It would therefore again appear that animals do not exhibit significant levels of oxidative stress, although they are confronted with increased ROS levels, since they are still capable of activating and increasing antioxidant defense pathways. Most studies on patients regarding oxidative stress and schizophrenia show the opposite findings, namely a decrease in cellular antioxidant defense and an increase in morphological as well as biochemical signs of oxidative damage compared to matched controls.

4.3 Summary, conclusions and implications for further research

It could be shown that Pex14p is the optimal novel marker protein for peroxisomes in comparative as well as experimental morphometry, as it appears to be present in every healthy peroxisome, independently of enzyme content, cell or tissue type. The Pex14p-antibody is highly specific and selective and can be used in IHC, IF, IGL as well as in combination with Qdots®. The epitope also appears to be very well accessible and highly stable even in tissues with progressed autolysis. It can therefore be used not only in experiments performed with freshly perfused animal tissues, but also be used in human tissues with moderately preserved ultrastructure. This is, however limited through other factors specific to aged human tissue, such as the accumulation of lipofuscin granules in the human brain.

Using Pex14p as a marker it was therefore now possible to examine the effects of increased dopamine on the antioxidant defense mechanisms using the peroxisome as model and studying its reaction to dopamine neurotoxicity in more detail. Cell culture experiments showed that dopamine, although not leading to marked increase in cell death, leads to a reduction of peroxisomal abundance in peripheral neuronal and astrocyte processes in line with the concept of atypical neurodegeneration, combined with an increase in catalase content especially in astrocytes. It can therefore be hypothesized that mesolimbic hyperdopaminergia and frontal hypoglutamatergia are not separate entities, but rather causally linked, in that dopamine neurotoxicity caused reduction of dendritic arborization and thereby loss of glutamatergic synapses.

When cultivated in the absence of neurons, however, it was shown that dopamine in concentrations far higher than were used for neurons and over significantly longer time periods has little effect on the cultivated cells. It can therefore be concluded that astrocytes play a decisive role in the protection of neurons against dopamine neurotoxicity and are by far more robust than neurons. For the antioxidant reactions to be induced, however, intact neuron-astrocyte interaction is necessary. This interaction and possible impairments thereof are therefore potent fields of research regarding the antioxidant capacity of the brain as an organ.

Finally, animals treated with the non-competitive NMDAR-antagonist MK-801 for 1, 25, 49 and 73 hrs showed a schizophrenia-like phenotype 10-15’ after systemic injection of

the drug, but no marked differences in PEX14 or CAT expression 1 h after treatment. There was, however, an increase in D-AspOx expression, thereby showing in vivo that MK-801-induced hyperdopaminergia may in turn lead to NMDAR-hypofunction.

Continued treatment with MK-801 over 25, 49 and 73 hrs showed differential effects on the expression on genes coding for dopamine degrading enzymes. A slight increase in gene expression was observed after 49 hrs in MAOA and COMT, while MAOB-levels continuously decreased. This could be interpreted in such a fashion that the increased levels of dopamine can still be degraded by the existing amount of enzymes, whereby increases in enzyme activities are a probable mechanism herefore. Both RT-PCRs and immunolabelings showed no conclusive evidence of peroxisomal proliferation within the aforementioned time frame, although levels of expression and protein abundance for the two antioxidant enzymes catalase and SOD2 increased in the MK-801-treated animals. It can therefore be concluded that antioxidant pathways of the brain are still active and can be adapted to increased ROS production caused by dopamine neurotoxicity, thereby questioning the proposition that oxidative stress is a primary cause of schizophrenia.

In conclusion the preliminary results of the exploratory experiments performed within this thesis suggest that that schizophrenia is a not disorder caused by oxidative stress, a condition in which antioxidant defense mechanisms are relatively hypofunctional, that dopamine hyperfunction and glutamate hypofunction are not separate entities, but may induce and increase each other in vivo and that dopamine induced neurotoxicity plays an important role in the upkeep and exacerbation of the core pathogenic mechanism of schizophrenia on the one hand and on the other via the induction of ROS-production leads to an increase in atypical neurodegeneration which could play an important role in the development and persistence of cognitive symptoms in schizophrenic patients. The results lead to the postulation of an integrative model regarding the etiopathogenesis and upkeep of schizophrenia based on dopamine neurotoxicity and dopamine-glutamate-interactions.

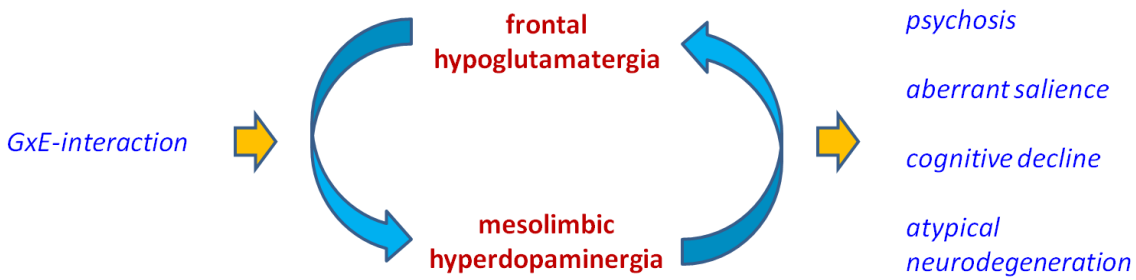

Fig. 4_2: Schematic illustration of the proposed integrative “mesolimbic bottleneck model” of schizophrenia

4.3.1 Implications for further research

In order to further examine the verisimilitude of the aforementioned hypothesis (q.v. Fig. 4_2) the results from this thesis need to be replicated in larger samples. Furthermore the effects of systemic treatment with MK-801 need to be evaluated over longer time spans in order to differentiate between acute and chronic effects of increased activity of the mesolimbic dopamine system. Especially regarding findings of decreased antioxidant defense in patients suffering from schizophrenia, it would be relevant to ascertain if and when the antioxidant defense systems of the brain (which appear to be functional during acute and short-term treatment with MK-801) become hypofunctional when confronted with chronically elevated dopamine levels. In this respect there is also a strong necessity for research into the confounding effects of neuroleptic treatment, since results from this thesis show that haloperidol has a markedly higher potential for (oxidative) damage than dopamine (q.v. section 3.2.2). It is therefore likely that oxidative stress as found in patients is partly caused or at the least exacerbated through treatment with antipsychotic medication, especially typical neuroleptics like haloperidol.

The possibility of palliative treatment of schizophrenia with antioxidant medication is therefore another question worth examining based on the findings of this thesis. The animal research application for this thesis, approved by the regional board for animal protection, incorporates treatment of animals for up to 14 days as well as a second set of experiments in which animals are to be treated with a peroxisome proliferator (rosiglitazone) prior to injections with MK-801. It is therefore planned to expand upon the preliminary research as laid out in this thesis in order to answer some of the aforementioned questions regarding both acute vs. chronic MK-801-treatment as well as palliative treatment with drugs augmenting antioxidant capacity.

Additionally a number of targeted experiments need to be performed using quantitative methods like real-time RT-PCR (qRT-PCR), microarrays, ELISA (enzyme-linked immunosorbent assay) and enzyme-activity assays in larger samples in vivo, in animals and in human patients.

Finally it would be of great interest to examine possible effects of altered dopamine transmission in non-clinical samples. Since, on the genotype level, polymorphisms of candidate genes for schizophrenia that were also analyzed within this thesis, like DAAO (Stefanis et al., 2007) or COMT (Avramopoulos et al., 2002), have also been shown to be

associated with the trait of schizotypy, examinations of the genes' expression patterns could show correlations with self-reported schizotypy levels, especially when other factors, like self-reported life-events or gene methylation patterns would be taken into account additionally. Since Stefanis et al. (2004) report that variations in the COMT Val^{158}Met polymorphism are associated with schizotypy, but not with cognition, the question arises, whether or not atypical neurodegeneration caused by dopamine neurotoxicity might play a role in the transition from subclinical schizotypy to clinical schizophrenia. There is an ongoing dispute on the question, if schizotypy and schizophrenia are represented by the same continuum or if there is a clear dichotomy between the two concepts (conference statement by Gordon Claridge, Oxford). It would therefore be interesting to examine the levels of antioxidant defense, neurotoxicity and atypical neurodegeneration in schizotypy in order to establish, whether these are also continuously distributed and correlated with schizoptypy or whether they make the difference between schizoptypy and schizophrenia in a sense that atypical neurodegeneration only presents in clinical schizophrenia, but is absent in persons with high schizotypy. This would mean that persons high in schizotypy may be prone to develop schizophrenia (e.g. through the experience of negative life-events), but that the latter condition would then involve additional processes leading to manifest damage to the brain. Should this be the case, the question would arise, what the nature of this discontinuity between schizotypy and clinical schizophrenia on the neurophysiological, neurochemical and neuropathological level would be. It is, however, in the opinion of the author more likely that schizotypy and schizophrenia are presented both phenotypically as well as a neuropsychologically on the same continuum, wherefore the research into the neurophysiological and -chemical correlates of schizoptypy could answer many of the open questions in schizophrenia research, but without the additional confounding influences of many of the variables (e.g. antipsychotic medication) commonly associated with clinical schizophrenia.

5. References

Abdalla, D. S., Monteiro, H. P., Oliveira, J. A. & Bechara, E. J. (1986). Activities of superoxide dismutase and glutathione peroxidase in schizophrenic and manic-depressive patients. *Clin Chem, 32* (5): 805-807.

Addington, J., Brooks, B. L. & Addington, D. (2003). Cognitive functioning in first episode psychosis: initial presentation. *Schizophr Res, 62* (1-2): 59-64.

Adler, C. M., Malhotra, A. K., Elman, I., Goldberg, T., Egan, M., Pickar, D. & Breier, A. (1999). Comparison of ketamine-induced thought disorder in healthy volunteers and thought disorder in schizophrenia. *Am J Psychiatry, 156* (10): 1646-1649.

Aebi, H. (1984). Catalase in vitro. *Methods Enzymol, 105*: 121-126.

Ahlemeyer, B., Neubert, I., Kovacs, W. J. & Baumgart-Vogt, E. (2007). Differential expression of peroxisomal matrix and membrane proteins during postnatal development of mouse brain. *J Comp Neurol, 505* (1): 1-17.

Albertini, M., Rehling, P., Erdmann, R., Girzalsky, W., Kiel, J. A., Veenhuis, M. & Kunau, W. H. (1997). Pex14p, a peroxisomal membrane protein binding both receptors of the two PTS-dependent import pathways. *Cell, 89* (1): 83-92.

Allen, N. C., Bagade, S., McQueen, M. B., Ioannidis, J. P., Kavvoura, F. K., Khoury, M. J., . . . Bertram, L. (2008). Systematic meta-analyses and field synopsis of genetic association studies in schizophrenia: the SzGene database. *Nat Genet, 40* (7): 827-834.

Alva, N., Palomeque, J. & Carbonell, T. (2006). Nitric oxide induced by ketamine/xylazine anesthesia maintains hepatic blood flow during hypothermia. *Nitric Oxide, 15* (1): 64-69.

Amaral, D. G. (1978). A Golgi study of cell types in the hilar region of the hippocampus in the rat. *J Comp Neurol, 182* (4 Pt 2): 851-914.

Antflick, J. E., Baker, G. B. & Hampson, D. R. (2010). The effects of a low protein diet on amino acids and enzymes in the serine synthesis pathway in mice. *Amino Acids, 39* (1): 145-153.

APA. (2000). *Diagnostic and Statistical Manual of Mental Disorders, Forth Edition, Text Revision (DSM-IV-TR)* (4th text revised ed.).

Arguello, P. A. & Gogos, J. A. (2006). Modeling madness in mice: one piece at a time. *Neuron, 52* (1): 179-196.

Arnold, G. & Holtzman, E. (1978). Microperoxisomes in the central nervous system of the postnatal rat. *Brain Res, 155* (1): 1-17.

Arnold, S. E., Franz, B. R., Trojanowski, J. Q., Moberg, P. J. & Gur, R. E. (1996). Glial fibrillary acidic protein-immunoreactive astrocytosis in elderly patients with schizophrenia and dementia. *Acta Neuropathol, 91* (3): 269-277.

Austin, J. (2005). Schizophrenia: an update and review. *J Genet Couns, 14* (5): 329-340.

Autelitano, D. J. & van den Buuse, M. (1997). Concomitant up-regulation of proopiomelanocortin and dopamine D2-receptor gene expression in the pituitary intermediate lobe of the spontaneously hypertensive rat. *J Neuroendocrinol, 9* (4): 255-262.

Avramopoulos, D., Stefanis, N. C., Hantoumi, I., Smyrnis, N., Evdokimidis, I. & Stefanis, C. N. (2002). Higher scores of self reported schizotypy in healthy young males carrying the COMT high activity allele. *Mol Psychiatry, 7* (7): 706-711.

Baes, M., Gressens, P., Baumgart, E., Carmeliet, P., Casteels, M., Fransen, M., . . . Mannaerts, G. P. (1997). A mouse model for Zellweger syndrome. *Nat Genet, 17* (1): 49-57.

Baes, M., Gressens, P., Huyghe, S., De, N. K., Qi, C., Jia, Y., . . . Reddy, J. K. (2002). The neuronal migration defect in mice with Zellweger syndrome (Pex5 knockout) is not caused by the inactivity of peroxisomal beta-oxidation. *J Neuropathol Exp Neurol, 61* (4): 368-374.

Baumgart, E. (1997). Application of in situ hybridization, cytochemical and immunocytochemical techniques for the investigation of peroxisomes. A review including novel data. Robert Feulgen Prize Lecture 1997. *Histochem Cell Biol, 108* (3): 185-210.

Baumgart, E., Fahimi, H. D., Steininger, H. & Grabenbauer, M. (2003). A review of morphological techniques for detection of peroxisomal (and mitochondrial) proteins and their

corresponding mRNAs during ontogenesis in mice: application to the PEX5-knockout mouse with Zellweger syndrome. *Microsc Res Tech, 61* (2): 121-138.

Baumgart, E., Vanhorebeek, I., Grabenbauer, M., Borgers, M., Declercq, P. E., Fahimi, H. D. & Baes, M. (2001). Mitochondrial alterations caused by defective peroxisomal biogenesis in a mouse model for Zellweger syndrome (PEX5 knockout mouse). *Am J Pathol, 159* (4): 1477-1494.

Benes, F. M., McSparren, J., Bird, E. D., SanGiovanni, J. P. & Vincent, S. L. (1991). Deficits in small interneurons in prefrontal and cingulate cortices of schizophrenic and schizoaffective patients. *Arch Gen Psychiatry, 48* (11): 996-1001.

Benes, F. M., Sorensen, I. & Bird, E. D. (1991). Reduced neuronal size in posterior hippocampus of schizophrenic patients. *Schizophr Bull, 17* (4): 597-608.

Berridge, K. C. (2007). The debate over dopamine's role in reward: the case for incentive salience. *Psychopharmacology (Berl), 191* (3): 391-431.

Bertler, A. & Rosengren, E. (1959a). Occurrence and distribution of catechol amines in brain. *Acta Physiol Scand, 47*: 350-361.

Bertler, A. & Rosengren, E. (1959b). Occurrence and distribution of dopamine in brain and other tissues. *Experientia, 15* (1): 10-11.

Billino, J., Hennig, J., Gegenfurtner, K. (2011a). Dopaminergic Correlates of the Gap Effect in Reflexive Saccades, *18th Annual Meeting of the Cognitive Neuroscience Society*. San Francisco (California, USA).

Billino, J., Hennig, J., Gegenfurtner, K. (2011b). Genetic Correlates of Anticipatory Smooth Pursuit, *DGPA Spring School 2011 - Genes, Brain & Behavior: From Personality to Psychopathology*. St. Goar (Germany).

Bondy, S. C. & Guo, S. X. (1996). Effect of an NMDA receptor antagonist and a ganglioside GM1 derivative upon ethanol-induced modification of parameters of oxidative stress in several brain regions. *Brain Res, 716* (1-2): 165-170.

Bossong, M. G. & Niesink, R. J. (2010). Adolescent brain maturation, the endogenous cannabinoid system and the neurobiology of cannabis-induced schizophrenia. *Prog Neurobiol, 92* (3): 370-385.

Bowers, M. B., Jr. & Freedman, D. X. (1966). "Psychedelic" experiences in acute psychoses. *Arch Gen Psychiatry, 15* (3): 240-248.

Braff, D. L., Geyer, M. A. & Swerdlow, N. R. (2001). Human studies of prepulse inhibition of startle: normal subjects, patient groups, and pharmacological studies. *Psychopharmacology (Berl), 156* (2-3): 234-258.

Brock, T. D. & Freeze, H. (1969). Thermus aquaticus gen. n. and sp. n., a nonsporulating extreme thermophile. *J Bacteriol, 98* (1): 289-297.

Brown, S., Inskip, H. & Barraclough, B. (2000). Causes of the excess mortality of schizophrenia. *Br J Psychiatry, 177*: 212-217.

Browning, M. D., Dudek, E. M., Rapier, J. L., Leonard, S. & Freedman, R. (1993). Significant reductions in synapsin but not synaptophysin specific activity in the brains of some schizophrenics. *Biol Psychiatry, 34* (8): 529-535.

Bubenikova-Valesova, V., Horacek, J., Vrajova, M. & Hoschl, C. (2008). Models of schizophrenia in humans and animals based on inhibition of NMDA receptors. *Neurosci Biobehav Rev, 32* (5): 1014-1023.

Burnet, P. W., Eastwood, S. L., Bristow, G. C., Godlewska, B. R., Sikka, P., Walker, M. & Harrison, P. J. (2008). D-amino acid oxidase activity and expression are increased in schizophrenia. *Mol Psychiatry, 13* (7): 658-660.

Caldwell, C. B. & Gottesman, II. (1990). Schizophrenics kill themselves too: a review of risk factors for suicide. *Schizophr Bull, 16* (4): 571-589.

Carlo, P., Violani, E., Del Rio, M., Olasmaa, M., Santagati, S., Maggi, A. & Picotti, G. B. (1996). Monoamine oxidase B expression is selectively regulated by dexamethasone in cultured rat astrocytes. *Brain Res, 711* (1-2): 175-183.

Carlsson, A. & Lindqvist, M. (1963). Effect of Chlorpromazine or Haloperidol on Formation of 3methoxytyramine and Normetanephrine in Mouse Brain. *Acta Pharmacol Toxicol (Copenh), 20*: 140-144.

Carlsson, A., Lindqvist, M. & Magnusson, T. (1957). 3,4-Dihydroxyphenylalanine and 5-hydroxytryptophan as reserpine antagonists. *Nature, 180* (4596): 1200.

Carlsson, A., Lindqvist, M., Magnusson, T. & Waldeck, B. (1958). On the presence of 3-hydroxytyramine in brain. *Science, 127* (3296): 471.

Carpenter, W. T. & Koenig, J. I. (2008). The evolution of drug development in schizophrenia: past issues and future opportunities. *Neuropsychopharmacology, 33* (9): 2061-2079.

Castegna, A., Thongboonkerd, V., Klein, J. B., Lynn, B., Markesbery, W. R. & Butterfield, D. A. (2003). Proteomic identification of nitrated proteins in Alzheimer's disease brain. *J Neurochem, 85* (6): 1394-1401.

Castellano, M. A., Liu, L. X., Monsma, F. J., Jr., Sibley, D. R., Kapatos, G. & Chiodo, L. A. (1993). Transfected D2 short dopamine receptors inhibit voltage-dependent potassium current in neuroblastoma x glioma hybrid (NG108-15) cells. *Mol Pharmacol, 44* (3): 649-656.

Chaturvedi, R. K. & Beal, M. F. (2008). PPAR: a therapeutic target in Parkinson's disease. *J Neurochem, 106* (2): 506-518.

Cheng, H. Y., Hsieh, M. T., Wu, C. R., Tsai, F. H., Lu, T. C., Hsieh, C. C., . . . Peng, W. H. (2008). Schizandrin protects primary cultures of rat cortical cells from glutamate-induced excitotoxicity. *J Pharmacol Sci, 107* (1): 21-31.

Chien, A., Edgar, D. B. & Trela, J. M. (1976). Deoxyribonucleic acid polymerase from the extreme thermophile Thermus aquaticus. *J Bacteriol, 127* (3): 1550-1557.

Chinta, S. J. & Andersen, J. K. (2008). Redox imbalance in Parkinson's disease. *Biochim Biophys Acta, 1780* (11): 1362-1367.

Chumakov, I., Blumenfeld, M., Guerassimenko, O., Cavarec, L., Palicio, M., Abderrahim, H., . . . Cohen, D. (2002). Genetic and physiological data implicating the new human gene G72 and the gene for D-amino acid oxidase in schizophrenia. *Proc Natl Acad Sci U S A, 99* (21): 13675-13680.

Civelli, O., Bunzow, J., Albert, P., Van Tol, H. & Grandy, D. (1991). Molecular biology of the dopamine D2 receptor. *NIDA Res Monogr, 111*: 45-53.

Civelli, O., Bunzow, J. R., Grandy, D. K., Zhou, Q. Y. & Van Tol, H. H. (1991). Molecular biology of the dopamine receptors. *Eur J Pharmacol, 207* (4): 277-286.

Clarke, D. D., Solokoff, L. 1999. (Circulation and energy metabolism of the brain). In G. J. Sigel, Agranoff, B. W., Albers, R. W., Fisher, S. K., Uhler, M. D. (Ed.), *Basic neurochemistry: molecular, cellular and medical aspects*: 637-669. Philadelphia: Lippincott-Raven.

Clinton, S. M. & Meador-Woodruff, J. H. (2004). Abnormalities of the NMDA Receptor and Associated Intracellular Molecules in the Thalamus in Schizophrenia and Bipolar Disorder. *Neuropsychopharmacology, 29* (7): 1353-1362.

Coan, E. J., Saywood, W. & Collingridge, G. L. (1987). MK-801 blocks NMDA receptor-mediated synaptic transmission and long term potentiation in rat hippocampal slices. *Neurosci Lett, 80* (1): 111-114.

Collip, D., Myin-Germeys, I. & Van Os, J. (2008). Does the concept of "sensitization" provide a plausible mechanism for the putative link between the environment and schizophrenia? *Schizophr Bull, 34* (2): 220-225.

Creese, I., Burt, D. R. & Snyder, S. H. (1976). Dopamine receptor binding predicts clinical and pharmacological potencies of antischizophrenic drugs. *Science, 192* (4238): 481-483.

Crow, T. J. (1972). A map of the rat mesencephalon for electrical self-stimulation. *Brain Res, 36* (2): 265-273.

da Cunha, A. A., Nunes, F. B., Lunardelli, A., Pauli, V., Amaral, R. H., de Oliveira, L. M., . . . de Oliveira, J. R. (2011). Treatment with N-methyl-D-aspartate receptor antagonist (MK-801) protects against oxidative stress in lipopolysaccharide-induced acute lung injury in the rat. *Int Immunopharmacol, 11* (6): 706-711.

da Silva, F. C., do Carmo de Oliveira Cito, M., da Silva, M. I., Moura, B. A., de Aquino Neto, M. R., Feitosa, M. L., . . . de Sousa, F. C. (2010). Behavioral alterations and pro-oxidant effect of a single ketamine administration to mice. *Brain Res Bull, 83* (1-2): 9-15.

Davidson, C., Gow, A. J., Lee, T. H. & Ellinwood, E. H. (2001). Methamphetamine neurotoxicity: necrotic and apoptotic mechanisms and relevance to human abuse and treatment. *Brain Res Brain Res Rev, 36* (1): 1-22.

Davis, K. L., Kahn, R. S., Ko, G. & Davidson, M. (1991). Dopamine in schizophrenia: a review and reconceptualization. *Am J Psychiatry, 148* (11): 1474-1486.

Davison, G. C., Neale, J. M. (1998). *Abnormal Psychology* (5th German ed.). Weinheim: BeltzPVU.

Daviss, S. R. & Lewis, D. A. (1995). Local circuit neurons of the prefrontal cortex in schizophrenia: selective increase in the density of calbindin-immunoreactive neurons. *Psychiatry Res, 59* (1-2): 81-96.

de Duve, C. (1969). The peroxisome: a new cytoplasmic organelle. *Proc R Soc Lond B Biol Sci, 173* (30): 71-83.

De Duve, C. & Baudhuin, P. (1966). Peroxisomes (microbodies and related particles). *Physiol Rev, 46* (2): 323-357.

de Oliveira, L., Spiazzi, C. M., Bortolin, T., Canever, L., Petronilho, F., Mina, F. G., . . . Zugno, A. I. (2009). Different sub-anesthetic doses of ketamine increase oxidative stress in the brain of rats. *Prog Neuropsychopharmacol Biol Psychiatry, 33* (6): 1003-1008.

del Rio, L. A., Sandalio, L. M., Altomare, D. A. & Zilinskas, B. A. (2003). Mitochondrial and peroxisomal manganese superoxide dismutase: differential expression during leaf senescence. *J Exp Bot, 54* (384): 923-933.

Delay, J., Deniker, P. & Harl, J. M. (1952). [Therapeutic use in psychiatry of phenothiazine of central elective action (4560 RP)]. *Ann Med Psychol (Paris), 110* (2:1): 112-117.

Depue, R. A. & Collins, P. F. (1999). Neurobiology of the structure of personality: dopamine, facilitation of incentive motivation, and extraversion. *Behav Brain Sci, 22* (3): 491-517; discussion 518-469.

Desikan, R., S, A. H.-M., Hancock, J. T. & Neill, S. J. (2001). Regulation of the Arabidopsis transcriptome by oxidative stress. *Plant Physiol, 127* (1): 159-172.

Dhaunsi, G. S., Singh, I. & Hanevold, C. D. (1993). Peroxisomal participation in the cellular response to the oxidative stress of endotoxin. *Mol Cell Biochem, 126* (1): 25-35.

Di Chiara, G., Bassareo, V., Fenu, S., De Luca, M. A., Spina, L., Cadoni, C., . . . Lecca, D. (2004). Dopamine and drug addiction: the nucleus accumbens shell connection. *Neuropharmacology, 47 Suppl 1*: 227-241.

Distel, B., van der Leij, I. & Kos, W. (1996). Peroxisome isolation. *Methods Mol Biol, 53*: 133-138.

Domino, E. F., Luby, E. D. 1981. (Abnormal mental states induced by phencyclidine as a model of schizophrenia). In E. F. Domino (Ed.), *PCP (Phencyclidine): Historical and Current Perspectives*: 400-418. Ann Arbor (MI): NPP Books.

Drenckhahn, D. 2003. (Zellenlehre). In D. Benninghoff (Ed.), *Anatomie*, 16th ed., Vol. 1: 10-91. München Jena: Urban & Fischer.

Drian, M. J., Kamenka, J. M., Pirat, J. L. & Privat, A. (1991). Non-competitive antagonists of N-methyl-D-aspartate prevent spontaneous neuronal death in primary cultures of embryonic rat cortex. *J Neurosci Res, 29* (1): 133-138.

Dringen, R., Pawlowski, P. G. & Hirrlinger, J. (2005). Peroxide detoxification by brain cells. *J Neurosci Res, 79* (1-2): 157-165.

Duhita, N., Le, H. A., Satoshi, S., Kazuo, H., Daisuke, M. & Takao, S. (2010). The origin of peroxisomes: The possibility of an actinobacterial symbiosis. *Gene, 450* (1-2): 18-24.

Edelstein, S. B. & Breakefield, X. O. (1986). Monoamine oxidases A and B are differentially regulated by glucocorticoids and "aging" in human skin fibroblasts. *Cell Mol Neurobiol, 6* (2): 121-150.

Eiden, L. E., Schafer, M. K., Weihe, E. & Schutz, B. (2004). The vesicular amine transporter family (SLC18): amine/proton antiporters required for vesicular accumulation and regulated exocytotic secretion of monoamines and acetylcholine. *Pflugers Arch, 447* (5): 636-640.

Eiden, L. E. & Weihe, E. (2011). VMAT2: a dynamic regulator of brain monoaminergic neuronal function interacting with drugs of abuse. *Ann N Y Acad Sci, 1216*: 86-98.

Eisenhofer, G., Huynh, T. T., Elkahloun, A., Morris, J. C., Bratslavsky, G., Linehan, W. M., . . . Pacak, K. (2008). Differential expression of the regulated catecholamine secretory pathway in different hereditary forms of pheochromocytoma. *Am J Physiol Endocrinol Metab, 295* (5): E1223-1233.

Eisenhofer, G., Kopin, I. J. & Goldstein, D. S. (2004). Catecholamine metabolism: a contemporary view with implications for physiology and medicine. *Pharmacol Rev, 56* (3): 331-349.

Elsworth, J. D. & Roth, R. H. (1997). Dopamine synthesis, uptake, metabolism, and receptors: relevance to gene therapy of Parkinson's disease. *Exp Neurol, 144* (1): 4-9.

Emerit, J., Edeas, M. & Bricaire, F. (2004). Neurodegenerative diseases and oxidative stress. *Biomed Pharmacother, 58* (1): 39-46.

Errico, F., Rossi, S., Napolitano, F., Catuogno, V., Topo, E., Fisone, G., . . . Usiello, A. (2008). D-aspartate prevents corticostriatal long-term depression and attenuates schizophrenia-like symptoms induced by amphetamine and MK-801. *J Neurosci, 28* (41): 10404-10414.

Evins, A. E. & Goff, D. C. (2008). Varenicline treatment for smokers with schizophrenia: a case series. *J Clin Psychiatry, 69* (6): 1016.

Fahimi, H. D. (1968). Cytochemical localization of peroxidase activity in rat hepatic microbodies (peroxisomes). *J Histochem Cytochem, 16* (8): 547-550.

Fahimi, H. D. (1969). Cytochemical localization of peroxidatic activity of catalase in rat hepatic microbodies (peroxisomes). *J Cell Biol, 43* (2): 275-288.

Fahimi, H. D., Gray, B. A. & Herzog, V. K. (1976). Cytochemical localization of catalase and peroxidase in sinusoidal cells of rat liver. *Lab Invest, 34* (2): 192-201.

Faust, P. L. (2003). Abnormal cerebellar histogenesis in PEX2 Zellweger mice reflects multiple neuronal defects induced by peroxisome deficiency. *J Comp Neurol, 461* (3): 394-413.

Faust, P. L. & Hatten, M. E. (1997). Targeted deletion of the PEX2 peroxisome assembly gene in mice provides a model for Zellweger syndrome, a human neuronal migration disorder. *J Cell Biol, 139* (5): 1293-1305.

Faust, P. L., Su, H. M., Moser, A. & Moser, H. W. (2001). The peroxisome deficient PEX2 Zellweger mouse: pathologic and biochemical correlates of lipid dysfunction. *J Mol Neurosci, 16* (2-3): 289-297; discussion 317-221.

Fischer, A. (2010). *Schizophrenie und oxidativer Stress - In-vitro Analyse peroxisomaler Reaktionen auf die Behandlung mit Dopamin in primär-kultivierten murinen Astrozyten*. Unpublished Diploma-Thesis, Justus-Liebig-Universität, Giessen.

Fitzmaurice, P. S., Tong, J., Yazdanpanah, M., Liu, P. P., Kalasinsky, K. S. & Kish, S. J. (2006). Levels of 4-hydroxynonenal and malondialdehyde are increased in brain of human chronic users of methamphetamine. *J Pharmacol Exp Ther, 319* (2): 703-709.

Fix, A. S., Wightman, K. A. & O'Callaghan, J. P. (1995). Reactive gliosis induced by MK-801 in the rat posterior cingulate/retrosplenial cortex: GFAP evaluation by sandwich ELISA and immunocytochemistry. *Neurotoxicology, 16* (2): 229-237.

Fleckenstein, A. E., Volz, T. J., Riddle, E. L., Gibb, J. W. & Hanson, G. R. (2007). New insights into the mechanism of action of amphetamines. *Annu Rev Pharmacol Toxicol, 47*: 681-698.

Fourcade, S., Lopez-Erauskin, J., Galino, J., Duval, C., Naudi, A., Jove, M., . . . Pujol, A. (2008). Early oxidative damage underlying neurodegeneration in X-adrenoleukodystrophy. *Hum Mol Genet, 17* (12): 1762-1773.

Fourcade, S., Ruiz, M., Camps, C., Schluter, A., Houten, S. M., Mooyer, P. A., . . . Pujol, A. (2009). A key role for the peroxisomal ABCD2 transporter in fatty acid homeostasis. *Am J Physiol Endocrinol Metab, 296* (1): E211-221.

Fukui, K. & Miyake, Y. (1992). Molecular cloning and chromosomal localization of a human gene encoding D-amino-acid oxidase. *J Biol Chem, 267* (26): 18631-18638.

Gabaldon, T. & Capella-Gutierrez, S. (2010). Lack of phylogenetic support for a supposed actinobacterial origin of peroxisomes. *Gene, 465* (1-2): 61-65.

Gao, H., Xiang, Y., Sun, N., Zhu, H., Wang, Y., Liu, M., . . . Lei, H. (2007). Metabolic changes in rat prefrontal cortex and hippocampus induced by chronic morphine treatment studied ex vivo by high resolution 1H NMR spectroscopy. *Neurochem Int, 50* (2): 386-394.

Girault, J. A. & Greengard, P. (2004). The neurobiology of dopamine signaling. *Arch Neurol, 61* (5): 641-644.

Glantz, L. A. & Lewis, D. A. (1997). Reduction of synaptophysin immunoreactivity in the prefrontal cortex of subjects with schizophrenia. Regional and diagnostic specificity. *Arch Gen Psychiatry, 54* (7): 660-669.

Glazov, V. A. & Mamtsev, V. P. (1976). [Catalase in the blood and leukocytes of patients with nuclear schizophrenia]. *Zh Nevropatol Psikhiatr Im S S Korsakova, 76* (4): 549-552.

Goldman-Rakic, P. S. & Selemon, L. D. (1997). Functional and anatomical aspects of prefrontal pathology in schizophrenia. *Schizophr Bull, 23* (3): 437-458.

Goldner, E. M., Hsu, L., Waraich, P. & Somers, J. M. (2002). Prevalence and incidence studies of schizophrenic disorders: a systematic review of the literature. *Can J Psychiatry, 47* (9): 833-843.

Golse, B., Debray, Q., Puget, K. & Michelson, A. M. (1978). [Superoxide dismutase 1 and glutathione peroxidase levels in erythrocytes of adult schizophrenics]. *Nouv Presse Med, 7* (23): 2070-2071.

Gottesman, I. I. (1991). Schizophrenia genesis: The origins of madness. *Behavior Genetics, 23* (6): 543-544.

Graham, D. G. (1978). Oxidative pathways for catecholamines in the genesis of neuromelanin and cytotoxic quinones. *Mol Pharmacol, 14* (4): 633-643.

Graham, D. G., Tiffany, S. M., Bell, W. R., Jr. & Gutknecht, W. F. (1978). Autoxidation versus covalent binding of quinones as the mechanism of toxicity of dopamine, 6-hydroxydopamine, and related compounds toward C1300 neuroblastoma cells in vitro. *Mol Pharmacol, 14* (4): 644-653.

Gray, J. A. (1982). *The neuropsychology of anxiety: An enquiry into the functions of the septo-hippocampal system*. Oxford: Oxford University Press.

Gray, J. A. 1987. (The neuropsychology of emotion and personality). In S. M. Stahl, Iversen, S. D., Goodman, E. G. (Ed.), *Cognitive neurochemistry*: 171-190. Oxford: Oxford University Press.

Gray, J. A., McNaughton, N. (2000). *The Neuropsychology of Anxiety: An Enquiry into the Functions of the Septo-Hippocampal System* (2nd ed.). Oxford: Oxford University Press.

Grima, G., Benz, B., Parpura, V., Cuenod, M. & Do, K. Q. (2003). Dopamine-induced oxidative stress in neurons with glutathione deficit: implication for schizophrenia. *Schizophr Res, 62* (3): 213-224.

Haber, S. N., Lynd, E., Klein, C. & Groenewegen, H. J. (1990). Topographic organization of the ventral striatal efferent projections in the rhesus monkey: an anterograde tracing study. *J Comp Neurol, 293* (2): 282-298.

Hafner, H., Maurer, K., Loffler, W. & Riecher-Rossler, A. (1993). The influence of age and sex on the onset and early course of schizophrenia. *Br J Psychiatry, 162*: 80-86.

Halliwell, B. (1992). Reactive oxygen species and the central nervous system. *J Neurochem, 59* (5): 1609-1623.

Halliwell, B. (2006). Oxidative stress and neurodegeneration: where are we now? *J Neurochem, 97* (6): 1634-1658.

Harkany, T., Mulder, J., Sasvari, M., Abraham, I., Konya, C., Zarandi, M., . . . Nyakas, C. (1999). N-Methyl-D-aspartate receptor antagonist MK-801 and radical scavengers protect cholinergic nucleus basalis neurons against beta-amyloid neurotoxicity. *Neurobiol Dis, 6* (2): 109-121.

Hashimoto, A., Yoshikawa, M., Andoh, H., Yano, H., Matsumoto, H., Kawaguchi, M., . . . Kobayashi, H. (2007). Effects of MK-801 on the expression of serine racemase and d-amino acid oxidase mRNAs and on the D-serine levels in rat brain. *Eur J Pharmacol, 555* (1): 17-22.

Hashimoto, K., Engberg, G., Shimizu, E., Nordin, C., Lindstrom, L. H. & Iyo, M. (2005). Reduced D-serine to total serine ratio in the cerebrospinal fluid of drug naive schizophrenic patients. *Prog Neuropsychopharmacol Biol Psychiatry, 29* (5): 767-769.

Hashimoto, K., Fukushima, T., Shimizu, E., Komatsu, N., Watanabe, H., Shinoda, N., . . . Iyo, M. (2003). Decreased serum levels of D-serine in patients with schizophrenia: evidence in support of the N-methyl-D-aspartate receptor hypofunction hypothesis of schizophrenia. *Arch Gen Psychiatry, 60* (6): 572-576.

Hastings, T. G., Lewis, D. A. & Zigmond, M. J. (1996). Role of oxidation in the neurotoxic effects of intrastriatal dopamine injections. *Proc Natl Acad Sci U S A, 93* (5): 1956-1961.

Heresco-Levy, U., Javitt, D. C., Ebstein, R., Vass, A., Lichtenberg, P., Bar, G., . . . Ermilov, M. (2005). D-serine efficacy as add-on pharmacotherapy to risperidone and olanzapine for treatment-refractory schizophrenia. *Biol Psychiatry, 57* (6): 577-585.

Hirrlinger, J., Schulz, J. B. & Dringen, R. (2002). Effects of dopamine on the glutathione metabolism of cultured astroglial cells: implications for Parkinson's disease. *J Neurochem, 82* (3): 458-467.

Hoek, H. W., Brown, A. S. & Susser, E. (1998). The Dutch famine and schizophrenia spectrum disorders. *Soc Psychiatry Psychiatr Epidemiol, 33* (8): 373-379.

Hoepfner, D., Schildknegt, D., Braakman, I., Philippsen, P. & Tabak, H. F. (2005). Contribution of the endoplasmic reticulum to peroxisome formation. *Cell, 122* (1): 85-95.

Holtzman, E. (1982). Peroxisomes in nervous tissue. *Ann N Y Acad Sci, 386*: 523-525.

Horiuchi, A. & Felder, R. A. (1996). High-level expression of rat D1A dopamine receptor cDNA in mouse fibroblast LTK- cells by n-butyrate. *Clin Exp Pharmacol Physiol, 23* (2): 150-154.

Horrobin, D. F., Manku, M. S., Hillman, H., Iain, A. & Glen, M. (1991). Fatty acid levels in the brains of schizophrenics and normal controls. *Biol Psychiatry, 30* (8): 795-805.

Howes, O. D. & Kapur, S. (2009). The dopamine hypothesis of schizophrenia: version III--the final common pathway. *Schizophr Bull, 35* (3): 549-562.

Hruban, Z., Vigil, E. L., Slesers, A. & Hopkins, E. (1972). Microbodies: constituent organelles of animal cells. *Lab Invest, 27* (2): 184-191.

Huttunen, M. O. & Niskanen, P. (1978). Prenatal loss of father and psychiatric disorders. *Arch Gen Psychiatry, 35* (4): 429-431.

Huyghe, S., Mannaerts, G. P., Baes, M. & Van Veldhoven, P. P. (2006). Peroxisomal multifunctional protein-2: the enzyme, the patients and the knockout mouse model. *Biochim Biophys Acta, 1761* (9): 973-994.

Insausti, R., Amaral, D. G. (2004). Hippocampal formation. In G. Paxinos, Mai, J. (Ed.), *The human nervous system*, 2nd ed.: 871-906: Academic Press.

Jakel, R. J., Kern, J. T., Johnson, D. A. & Johnson, J. A. (2005). Induction of the protective antioxidant response element pathway by 6-hydroxydopamine in vivo and in vitro. *Toxicol Sci, 87* (1): 176-186.

Jakobsen, K. D., Frederiksen, J. N., Hansen, T., Jansson, L. B., Parnas, J. & Werge, T. (2005). Reliability of clinical ICD-10 schizophrenia diagnoses. *Nord J Psychiatry, 59* (3): 209-212.

Janssen, A., Gressens, P., Grabenbauer, M., Baumgart, E., Schad, A., Vanhorebeek, I., . . . Baes, M. (2003). Neuronal migration depends on intact peroxisomal function in brain and in extraneuronal tissues. *J Neurosci, 23* (30): 9732-9741.

Javitt, D. C. & Zukin, S. R. (1991). Recent advances in the phencyclidine model of schizophrenia. *Am J Psychiatry, 148* (10): 1301-1308.

Jenner, P. (2005). Istradefylline, a novel adenosine A2A receptor antagonist, for the treatment of Parkinson's disease. *Expert Opin Investig Drugs, 14* (6): 729-738.

Johnson, R. J., Titte, S., Cade, J. R., Rideout, B. A. & Oliver, W. J. (2005). Uric acid, evolution and primitive cultures. *Semin Nephrol, 25* (1): 3-8.

Jomphe, C., Bourque, M. J., Fortin, G. D., St-Gelais, F., Okano, H., Kobayashi, K. & Trudeau, L. E. (2005). Use of TH-EGFP transgenic mice as a source of identified dopaminergic neurons for physiological studies in postnatal cell culture. *J Neurosci Methods, 146* (1): 1-12.

Kalonia, H., Kumar, P., Nehru, B. & Kumar, A. (2009). Neuroprotective effect of MK-801 against intra-striatal quinolinic acid induced behavioral, oxidative stress and cellular alterations in rats. *Indian J Exp Biol, 47* (11): 880-892.

Kamijo, K., Kamijo, T., Ueno, I., Osumi, T. & Hashimoto, T. (1992). Nucleotide sequence of the human 70 kDa peroxisomal membrane protein: a member of ATP-binding cassette transporters. *Biochim Biophys Acta, 1129* (3): 323-327.

Kapur, S. (2003). Psychosis as a state of aberrant salience: a framework linking biology, phenomenology, and pharmacology in schizophrenia. *Am J Psychiatry, 160* (1): 13-23.

Kapur, S., Mizrahi, R. & Li, M. (2005). From dopamine to salience to psychosis--linking biology, pharmacology and phenomenology of psychosis. *Schizophr Res, 79* (1): 59-68.

Karnati, S. & Baumgart-Vogt, E. (2008). Peroxisomes in mouse and human lung: their involvement in pulmonary lipid metabolism. *Histochem Cell Biol, 130* (4): 719-740.

Kegeles, L. S., Abi-Dargham, A., Zea-Ponce, Y., Rodenhiser-Hill, J., Mann, J. J., Van Heertum, R. L., . . . Laruelle, M. (2000). Modulation of amphetamine-induced striatal dopamine release by ketamine in humans: implications for schizophrenia. *Biol Psychiatry, 48* (7): 627-640.

Kim, J. S., Kornhuber, H. H., Schmid-Burgk, W. & Holzmuller, B. (1980). Low cerebrospinal fluid glutamate in schizophrenic patients and a new hypothesis on schizophrenia. *Neurosci Lett, 20* (3): 379-382.

Kim, P. K., Mullen, R. T., Schumann, U. & Lippincott-Schwartz, J. (2006). The origin and maintenance of mammalian peroxisomes involves a de novo PEX16-dependent pathway from the ER. *J Cell Biol, 173* (4): 521-532.

Kira, Y., Sato, E. F. & Inoue, M. (2002). Association of Cu,Zn-type superoxide dismutase with mitochondria and peroxisomes. *Arch Biochem Biophys, 399* (1): 96-102.

Klenow, H. & Henningsen, I. (1970). Selective elimination of the exonuclease activity of the deoxyribonucleic acid polymerase from Escherichia coli B by limited proteolysis. *Proc Natl Acad Sci U S A, 65* (1): 168-175.

Klenow, H. & Overgaard-Hansen, K. (1970). Proteolytic cleavage of DNA polymerase from Escherichia Coli B into an exonuclease unit and a polymerase unit. *FEBS Lett, 6* (1): 25-27.

Knutson, B. & Cooper, J. C. (2005). Functional magnetic resonance imaging of reward prediction. *Curr Opin Neurol, 18* (4): 411-417.

Kobayashi, T., Saito, N., Takemori, N., Iizuka, S., Suzuki, K., Taniguchi, N. & Iizuka, H. (1993). Ultrastructural localization of superoxide dismutase in human skin. *Acta Derm Venereol, 73* (1): 41-45.

Krysko, O., Hulshagen, L., Janssen, A., Schutz, G., Klein, R., De Bruycker, M., . . . Baes, M. (2007). Neocortical and cerebellar developmental abnormalities in conditions of selective elimination of peroxisomes from brain or from liver. *J Neurosci Res, 85* (1): 58-72.

Krystal, J. H., Karper, L. P., Seibyl, J. P., Freeman, G. K., Delaney, R., Bremner, J. D., . . . Charney, D. S. (1994). Subanesthetic effects of the noncompetitive NMDA antagonist, ketamine, in humans. Psychotomimetic, perceptual, cognitive, and neuroendocrine responses. *Arch Gen Psychiatry, 51* (3): 199-214.

Kuhn, H. & Borchert, A. (2002). Regulation of enzymatic lipid peroxidation: the interplay of peroxidizing and peroxide reducing enzymes. *Free Radic Biol Med, 33* (2): 154-172.

Kunugi, H., Nanko, S., Takei, N., Saito, K., Hayashi, N. & Kazamatsuri, H. (1995). Schizophrenia following in utero exposure to the 1957 influenza epidemics in Japan. *Am J Psychiatry, 152* (3): 450-452.

Kuperberg, G. & Heckers, S. (2000). Schizophrenia and cognitive function. *Curr Opin Neurobiol, 10* (2): 205-210.

Kuroki, T., Kawahara, T., Yonezawa, Y. & Tashiro, N. (1999). Effects of the serotonin2A/2C receptor agonist and antagonist on phencyclidine-induced dopamine release in rat medial prefrontal cortex. *Prog Neuropsychopharmacol Biol Psychiatry, 23* (7): 1259-1275.

Kuroki, T., Meltzer, H. Y. & Ichikawa, J. (1999). Effects of antipsychotic drugs on extracellular dopamine levels in rat medial prefrontal cortex and nucleus accumbens. *J Pharmacol Exp Ther, 288* (2): 774-781.

Kuzniak, E. & Sklodowska, M. (2005). Fungal pathogen-induced changes in the antioxidant systems of leaf peroxisomes from infected tomato plants. *Planta, 222* (1): 192-200.

Lahti, A. C., Koffel, B., LaPorte, D. & Tamminga, C. A. (1995). Subanesthetic doses of ketamine stimulate psychosis in schizophrenia. *Neuropsychopharmacology, 13* (1): 9-19.

Lammers, C. H., D'Souza, U., Qin, Z. H., Lee, S. H., Yajima, S. & Mouradian, M. M. (1999a). Regulation of striatal dopamine receptors by estrogen. *Synapse, 34* (3): 222-227.

Lammers, C. H., D'Souza, U. M., Qin, Z. H., Lee, S. H., Yajima, S. & Mouradian, M. M. (1999b). Regulation of striatal dopamine receptors by corticosterone: an in vivo and in vitro study. *Brain Res Mol Brain Res, 69* (2): 281-285.

Laruelle, M., Abi-Dargham, A., van Dyck, C. H., Rosenblatt, W., Zea-Ponce, Y., Zoghbi, S. S., . . . et al. (1995). SPECT imaging of striatal dopamine release after amphetamine challenge. *J Nucl Med, 36* (7): 1182-1190.

Laruelle, M., Kegeles, L. S. & Abi-Dargham, A. (2003). Glutamate, dopamine, and schizophrenia: from pathophysiology to treatment. *Ann N Y Acad Sci, 1003*: 138-158.

Lastres-Becker, I., Molina-Holgado, F., Ramos, J. A., Mechoulam, R. & Fernandez-Ruiz, J. (2005). Cannabinoids provide neuroprotection against 6-hydroxydopamine toxicity in vivo and in vitro: relevance to Parkinson's disease. *Neurobiol Dis, 19* (1-2): 96-107.

Leon, S., Goodman, J. M. & Subramani, S. (2006). Uniqueness of the mechanism of protein import into the peroxisome matrix: transport of folded, co-factor-bound and oligomeric proteins by shuttling receptors. *Biochim Biophys Acta, 1763* (12): 1552-1564.

Lessig, J. & Fuchs, B. (2009). Plasmalogens in biological systems: their role in oxidative processes in biological membranes, their contribution to pathological processes and aging and plasmalogen analysis. *Curr Med Chem, 16* (16): 2021-2041.

Li, H. C., Chen, Q. Z., Ma, Y. & Zhou, J. F. (2006). Imbalanced free radicals and antioxidant defense systems in schizophrenia: a comparative study. *J Zhejiang Univ Sci B, 7* (12): 981-986.

Li, X., Baumgart, E., Morrell, J. C., Jimenez-Sanchez, G., Valle, D. & Gould, S. J. (2002). PEX11 beta deficiency is lethal and impairs neuronal migration but does not abrogate peroxisome function. *Mol Cell Biol, 22* (12): 4358-4365.

Lieberman, J. A. (1999). Is schizophrenia a neurodegenerative disorder? A clinical and neurobiological perspective. *Biol Psychiatry, 46* (6): 729-739.

Lieberman, J. A., Kane, J. M. & Alvir, J. (1987). Provocative tests with psychostimulant drugs in schizophrenia. *Psychopharmacology (Berl), 91* (4): 415-433.

Lindley, S. E., She, X. & Schatzberg, A. F. (2005). Monoamine oxidase and catechol-o-methyltransferase enzyme activity and gene expression in response to sustained glucocorticoids. *Psychoneuroendocrinology, 30* (8): 785-790.

Liou, W., Chang, L. Y., Geuze, H. J., Strous, G. J., Crapo, J. D. & Slot, J. W. (1993). Distribution of CuZn superoxide dismutase in rat liver. *Free Radic Biol Med, 14* (2): 201-207.

Litwin, J. A. & Beier, K. (1988). Immunogold localization of peroxisomal enzymes in Epon-embedded liver tissue. Enhancement of sensitivity by etching with ethanolic sodium hydroxide. *Histochemistry, 88* (2): 193-196.

Liu, X., He, G., Wang, X., Chen, Q., Qian, X., Lin, W., . . . He, L. (2004). Association of DAAO with schizophrenia in the Chinese population. *Neurosci Lett, 369* (3): 228-233.

Lledias, F., Rangel, P. & Hansberg, W. (1998). Oxidation of catalase by singlet oxygen. *J Biol Chem, 273* (17): 10630-10637.

Lodge, D. & Anis, N. A. (1982). Effects of phencyclidine on excitatory amino acid activation of spinal interneurones in the cat. *Eur J Pharmacol, 77* (2-3): 203-204.

Lohr, J. B., Kuczenski, R., Bracha, H. S., Moir, M. & Jeste, D. V. (1990). Increased indices of free radical activity in the cerebrospinal fluid of patients with tardive dyskinesia. *Biol Psychiatry, 28* (6): 535-539.

Long, L. E., Malone, D. T. & Taylor, D. A. (2006). Cannabidiol reverses MK-801-induced disruption of prepulse inhibition in mice. *Neuropsychopharmacology, 31* (4): 795-803.

Lopez-Huertas, E., Charlton, W. L., Johnson, B., Graham, I. A. & Baker, A. (2000). Stress induces peroxisome biogenesis genes. *EMBO J, 19* (24): 6770-6777.

Lorente de No, R. (1934). Studies on the structure of the cerebral cortex II. Continuation of the study of the ammonic system. *J Physiol Neurol, 46*: 179-192.

Loscher, W., Annies, R. & Honack, D. (1991). The N-methyl-D-aspartate receptor antagonist MK-801 induces increases in dopamine and serotonin metabolism in several brain regions of rats. *Neurosci Lett, 128* (2): 191-194.

Luby, E. D., Cohen, B. D., Rosenbaum, G., Gottlieb, J. S. & Kelley, R. (1959). Study of a new schizophrenomimetic drug; sernyl. *AMA Arch Neurol Psychiatry, 81* (3): 363-369.

Luers, G. H., Thiele, S., Schad, A., Volkl, A., Yokota, S. & Seitz, J. (2006). Peroxisomes are present in murine spermatogonia and disappear during the course of spermatogenesis. *Histochem Cell Biol, 125* (6): 693-703.

Lui, S., Deng, W., Huang, X., Jiang, L., Ma, X., Chen, H., . . . Gong, Q. (2009). Association of cerebral deficits with clinical symptoms in antipsychotic-naive first-episode schizophrenia: an optimized voxel-based morphometry and resting state functional connectivity study. *Am J Psychiatry, 166* (2): 196-205.

Madeira, C., Freitas, M. E., Vargas-Lopes, C., Wolosker, H. & Panizzutti, R. (2008). Increased brain D-amino acid oxidase (DAAO) activity in schizophrenia. *Schizophr Res, 101* (1-3): 76-83.

Mahadik, J. S., Mukherjee, S., Correnti, E. E., Scheffer, R. (1995). Elevated levels of lipid peroxidation products in plasma from drug-naive patient at the onset of psychosis. *Schizophr Res, 15*: 66.

Mahadik, S. P., Mukherjee, S., Scheffer, R., Correnti, E. E. & Mahadik, J. S. (1998). Elevated plasma lipid peroxides at the onset of nonaffective psychosis. *Biol Psychiatry, 43* (9): 674-679.

Maier, C. M. & Chan, P. H. (2002). Role of superoxide dismutases in oxidative damage and neurodegenerative disorders. *Neuroscientist, 8* (4): 323-334.

Maker, H. S., Weiss, C., Silides, D. J. & Cohen, G. (1981). Coupling of dopamine oxidation (monoamine oxidase activity) to glutathione oxidation via the generation of hydrogen peroxide in rat brain homogenates. *J Neurochem, 36* (2): 589-593.

Malhotra, A. K., Pinals, D. A., Weingartner, H., Sirocco, K., Missar, C. D., Pickar, D. & Breier, A. (1996). NMDA receptor function and human cognition: the effects of ketamine in healthy volunteers. *Neuropsychopharmacology, 14* (5): 301-307.

Marnett, L. J. (1999a). Chemistry and biology of DNA damage by malondialdehyde. *IARC Sci Publ* (150): 17-27.

Marnett, L. J. (1999b). Lipid peroxidation-DNA damage by malondialdehyde. *Mutat Res, 424* (1-2): 83-95.

Mateos, R. M., Leon, A. M., Sandalio, L. M., Gomez, M., del Rio, L. A. & Palma, J. M. (2003). Peroxisomes from pepper fruits (Capsicum annuum L.): purification, characterisation and antioxidant activity. *J Plant Physiol, 160* (12): 1507-1516.

Mates, J. M. (2000). Effects of antioxidant enzymes in the molecular control of reactive oxygen species toxicology. *Toxicology, 153* (1-3): 83-104.

Mathe, J. M., Nomikos, G. G., Hildebrand, B. E., Hertel, P. & Svensson, T. H. (1996). Prazosin inhibits MK-801-induced hyperlocomotion and dopamine release in the nucleus accumbens. *Eur J Pharmacol, 309* (1): 1-11.

Maus, M., Vernier, P., Valdenaire, O., Homburger, V., Bockaert, J., Glowinski, J. & Mallet, J. (1993). D2-dopaminergic agonist quinpirole and 8-bromo-cAMP have opposite effects on Go alpha GTP-binding protein mRNA without changing D2 dopamine receptor mRNA levels in striatal neurones in primary culture. *J Recept Res, 13* (1-4): 313-328.

Maxwell, M., Bjorkman, J., Nguyen, T., Sharp, P., Finnie, J., Paterson, C., . . . Crane, D. I. (2003). Pex13 inactivation in the mouse disrupts peroxisome biogenesis and leads to a Zellweger syndrome phenotype. *Mol Cell Biol, 23* (16): 5947-5957.

McGhie, A. & Chapman, J. (1961). Disorders of attention and perception in early schizophrenia. *Br J Med Psychol, 34*: 103-116.

McNamara, R. K., Jandacek, R., Rider, T., Tso, P., Hahn, C. G., Richtand, N. M. & Stanford, K. E. (2007). Abnormalities in the fatty acid composition of the postmortem orbitofrontal cortex of schizophrenic patients: gender differences and partial normalization with antipsychotic medications. *Schizophr Res, 91* (1-3): 37-50.

McNaughton, N. & Corr, P. J. (2004). A two-dimensional neuropsychology of defense: fear/anxiety and defensive distance. *Neuroscience and Biobehavioral Reviews*, *28*: 285-305.

Mednick, S. A., Machon, R. A., Huttunen, M. O. & Bonett, D. (1988). Adult schizophrenia following prenatal exposure to an influenza epidemic. *Arch Gen Psychiatry, 45* (2): 189-192.

Menken, M., Munsat, T. L. & Toole, J. F. (2000). The global burden of disease study: implications for neurology. *Arch Neurol, 57* (3): 418-420.

Miyazaki, I. & Asanuma, M. (2008). Dopaminergic neuron-specific oxidative stress caused by dopamine itself. *Acta Med Okayama, 62* (3): 141-150.

Mooradian, B. A. & Cutler, L. S. (1978). Developmental distribution of microperoxisomes in the rat submandibular gland. *J Histochem Cytochem, 26* (11): 989-999.

Moreira, P. I., Honda, K., Liu, Q., Santos, M. S., Oliveira, C. R., Aliev, G., . . . Perry, G. (2005a). Oxidative stress: the old enemy in Alzheimer's disease pathophysiology. *Curr Alzheimer Res, 2* (4): 403-408.

Moreira, P. I., Oliveira, C. R., Santos, M. S., Nunomura, A., Honda, K., Zhu, X., . . . Perry, G. (2005b). A second look into the oxidant mechanisms in Alzheimer's disease. *Curr Neurovasc Res, 2* (2): 179-184.

Moreira, P. I., Siedlak, S. L., Aliev, G., Zhu, X., Cash, A. D., Smith, M. A. & Perry, G. (2005c). Oxidative stress mechanisms and potential therapeutics in Alzheimer disease. *J Neural Transm, 112* (7): 921-932.

Moreira, P. I., Smith, M. A., Zhu, X., Honda, K., Lee, H. G., Aliev, G. & Perry, G. (2005d). Oxidative damage and Alzheimer's disease: are antioxidant therapies useful? *Drug News Perspect, 18* (1): 13-19.

Moron, J. A., Brockington, A., Wise, R. A., Rocha, B. A. & Hope, B. T. (2002). Dopamine uptake through the norepinephrine transporter in brain regions with low levels of the dopamine transporter: evidence from knock-out mouse lines. *J Neurosci, 22* (2): 389-395.

Mosolov, S. N., Smulevich, A. B., Neznanov, N. G., Tochilov, V. A., Andreev, B. V., Avedisova, A. S., . . . Martenyi, F. (2010). [The use of mGlu2/3 receptors as a new approach to treat schizophrenia: results of a randomized double-blind trial]. *Zh Nevrol Psikhiatr Im S S Korsakova, 110* (7): 16-23.

Moszczynska, A., Fitzmaurice, P., Ang, L., Kalasinsky, K. S., Schmunk, G. A., Peretti, F. J., . . . Kish, S. J. (2004). Why is parkinsonism not a feature of human methamphetamine users? *Brain, 127* (Pt 2): 363-370.

Mueser, K. T. & McGurk, S. R. (2004). Schizophrenia. *Lancet, 363* (9426): 2063-2072.

Mukherjee, S., Decina, P., Bocola, V., Saraceni, F. & Scapicchio, P. L. (1996). Diabetes mellitus in schizophrenic patients. *Compr Psychiatry, 37* (1): 68-73.

Mullis, K. B., et al. (1987). Process for amplifying, detecting, and/or cloning nucleic acid sequences using a thermostable enzyme. U.S. Patent 4,965,188.

Mullis, K. B., Ferré, F., Gibbs, R. A. (1994). *The polymerase chain reaction (PCR)*. Basel, Switzerland: Birkhäuser Verlag AG.

Nappi, A. J., Vass, E., Prota, G. & Memoli, S. (1995). The effects of hydroxyl radical attack on dopa, dopamine, 6-hydroxydopa, and 6-hydroxydopamine. *Pigment Cell Res, 8* (6): 283-293.

Narendran, R., Frankle, W. G., Keefe, R., Gil, R., Martinez, D., Slifstein, M., . . . Abi-Dargham, A. (2005). Altered prefrontal dopaminergic function in chronic recreational ketamine users. *Am J Psychiatry, 162* (12): 2352-2359.

Nasr, P., Carbery, T. & Geddes, J. W. (2009). N-methyl-D-aspartate receptor antagonists have variable affect in 3-nitropropionic acid toxicity. *Neurochem Res, 34* (3): 490-498.

Nenicu, A., Luers, G. H., Kovacs, W., David, M., Zimmer, A., Bergmann, M. & Baumgart-Vogt, E. (2007). Peroxisomes in human and mouse testis: differential expression of peroxisomal proteins in germ cells and distinct somatic cell types of the testis. *Biol Reprod, 77* (6): 1060-1072.

Neves, S. R., Ram, P. T. & Iyengar, R. (2002). G protein pathways. *Science, 296* (5573): 1636-1639.

Newman, E. A. (2003). New roles for astrocytes: regulation of synaptic transmission. *Trends Neurosci, 26* (10): 536-542.

Nguyen, T., Nioi, P. & Pickett, C. B. (2009). The Nrf2-antioxidant response element signaling pathway and its activation by oxidative stress. *J Biol Chem, 284* (20): 13291-13295.

Nieuwenhuys, R., Voogd, J., Van Huijzen, C. (2007). *The Human Central Nervous System* (4th ed.): Steinkopff.

Nishijima, K., Kashiwa, A., Hashimoto, A., Iwama, H., Umino, A. & Nishikawa, T. (1996). Differential effects of phencyclidine and methamphetamine on dopamine metabolism in rat frontal cortex and striatum as revealed by in vivo dialysis. *Synapse, 22* (4): 304-312.

Noh, S. J., Lee, S. H., Shin, K. Y., Lee, C. K., Cho, I. H., Kim, H. S. & Suh, Y. H. (2011). SP-8203 reduces oxidative stress via SOD activity and behavioral deficit in cerebral ischemia. *Pharmacol Biochem Behav, 98* (1): 150-154.

Novikoff, A. B. & Goldfischer, S. (1969). Visualization of peroxisomes (microbodies) and mitochondria with diaminobenzidine. *J Histochem Cytochem, 17* (10): 675-680.

O'Callaghan, J. P. (1994). Biochemical analysis of glial fibrillary acidic protein as a quantitative approach to neurotoxicity assessment: advantages, disadvantages and application to the assessment of NMDA receptor antagonist-induced neurotoxicity. *Psychopharmacol Bull, 30* (4): 549-554.

Oda, M., Satta, Y., Takenaka, O. & Takahata, N. (2002). Loss of urate oxidase activity in hominoids and its evolutionary implications. *Mol Biol Evol, 19* (5): 640-653.

Olds, J. & Milner, P. (1954). Positive reinforcement produced by electrical stimulation of septal area and other regions of rat brain. *J Comp Physiol Psychol, 47* (6): 419-427.

Oliveira, M. E., Reguenga, C., Gouveia, A. M., Guimaraes, C. P., Schliebs, W., Kunau, W. H., . . . Azevedo, J. E. (2002). Mammalian Pex14p: membrane topology and characterisation of the Pex14p-Pex14p interaction. *Biochim Biophys Acta, 1567* (1-2): 13-22.

Ongur, D., Cullen, T. J., Wolf, D. H., Rohan, M., Barreira, P., Zalesak, M. & Heckers, S. (2006). The neural basis of relational memory deficits in schizophrenia. *Arch Gen Psychiatry, 63* (4): 356-365.

Oye, I., Paulsen, O. & Maurset, A. (1992). Effects of ketamine on sensory perception: evidence for a role of N-methyl-D-aspartate receptors. *J Pharmacol Exp Ther, 260* (3): 1209-1213.

Ozyurt, B., Ozyurt, H., Akpolat, N., Erdogan, H. & Sarsilmaz, M. (2007a). Oxidative stress in prefrontal cortex of rat exposed to MK-801 and protective effects of CAPE. *Prog Neuropsychopharmacol Biol Psychiatry, 31* (4): 832-838.

Ozyurt, B., Sarsilmaz, M., Akpolat, N., Ozyurt, H., Akyol, O., Herken, H. & Kus, I. (2007b). The protective effects of omega-3 fatty acids against MK-801-induced neurotoxicity in prefrontal cortex of rat. *Neurochem Int, 50* (1): 196-202.

Pall, H. S., Williams, A. C., Blake, D. R. & Lunec, J. (1987). Evidence of enhanced lipid peroxidation in the cerebrospinal fluid of patients taking phenothiazines. *Lancet, 2* (8559): 596-599.

Patil, S. T., Zhang, L., Martenyi, F., Lowe, S. L., Jackson, K. A., Andreev, B. V., . . . Schoepp, D. D. (2007). Activation of mGlu2/3 receptors as a new approach to treat schizophrenia: a randomized Phase 2 clinical trial. *Nat Med, 13* (9): 1102-1107.

Pechnick, R. N., Bresee, C. J. & Poland, R. E. (2006). The role of antagonism of NMDA receptor-mediated neurotransmission and inhibition of the dopamine reuptake in the neuroendocrine effects of phencyclidine. *Life Sci, 78* (17): 2006-2011.

Peet, M., Laugharne, J., Rangarajan, N. & Reynolds, G. P. (1993). Tardive dyskinesia, lipid peroxidation, and sustained amelioration with vitamin E treatment. *Int Clin Psychopharmacol, 8* (3): 151-153.

Perrone-Bizzozero, N. I., Sower, A. C., Bird, E. D., Benowitz, L. I., Ivins, K. J. & Neve, R. L. (1996). Levels of the growth-associated protein GAP-43 are selectively increased in association cortices in schizophrenia. *Proc Natl Acad Sci U S A, 93* (24): 14182-14187.

Picchioni, M. M. & Murray, R. M. (2007). Schizophrenia. *BMJ, 335* (7610): 91-95.

Pickering, A. D., Gray, J. A. 2001. (Dopamine, appetitive reinforcement, and the neuropsychology of human learning: An individual differences approach). In A. Eliasz, Angleitner, A. (Ed.), *Advances in individual differences research*. Germany: PABST Science Publishers.

Pilowsky, L. S., Bressan, R. A., Stone, J. M., Erlandsson, K., Mulligan, R. S., Krystal, J. H. & Ell, P. J. (2006). First in vivo evidence of an NMDA receptor deficit in medication-free schizophrenic patients. *Mol Psychiatry, 11* (2): 118-119.

Powers, J. M. (1985). Adreno-leukodystrophy (adreno-testiculo-leukomyelo-neuropathic-complex). *Clin Neuropathol, 4* (5): 181-199.

Powers, J. M., Pei, Z., Heinzer, A. K., Deering, R., Moser, A. B., Moser, H. W., . . . Smith, K. D. (2005). Adreno-leukodystrophy: oxidative stress of mice and men. *J Neuropathol Exp Neurol, 64* (12): 1067-1079.

Prilipko, L. L. 1984. (Activation of lipid peroxidation under stress and in schizophrenia). In M. P. V. Kemali D., Toffano G. (Ed.), *New Research Strategies in Biological Psychiatry. Biological sychiatry-New Perspectives: 3*. London: John Libbey.

Radomsky, E. D., Haas, G. L., Mann, J. J. & Sweeney, J. A. (1999). Suicidal behavior in patients with schizophrenia and other psychotic disorders. *Am J Psychiatry, 156* (10): 1590-1595.

Radonjic, N. V., Knezevic, I. D., Vilimanovich, U., Kravic-Stevovic, T., Marina, L. V., Nikolic, T., . . . Petronijevic, N. D. (2010). Decreased glutathione levels and altered antioxidant defense in an animal model of schizophrenia: long-term effects of perinatal phencyclidine administration. *Neuropharmacology, 58* (4-5): 739-745.

Rajdev, S., Fix, A. S. & Sharp, F. R. (1998). Acute phencyclidine neurotoxicity in rat forebrain: induction of haem oxygenase-1 and attenuation by the antioxidant dimethylthiourea. *Eur J Neurosci, 10* (12): 3840-3852.

Rajkowska, G., Selemon, L. D. & Goldman-Rakic, P. S. (1998). Neuronal and glial somal size in the prefrontal cortex: a postmortem morphometric study of schizophrenia and Huntington disease. *Arch Gen Psychiatry, 55* (3): 215-224.

Ranjekar, P. K., Hinge, A., Hegde, M. V., Ghate, M., Kale, A., Sitasawad, S., . . . Mahadik, S. P. (2003). Decreased antioxidant enzymes and membrane essential polyunsaturated fatty acids in schizophrenic and bipolar mood disorder patients. *Psychiatry Res, 121* (2): 109-122.

Reddy, R., Sahebarao, M. P., Mukherjee, S. & Murthy, J. N. (1991). Enzymes of the antioxidant defense system in chronic schizophrenic patients. *Biol Psychiatry, 30* (4): 409-412.

Reddy, R. D. & Yao, J. K. (1996). Free radical pathology in schizophrenia: a review. *Prostaglandins Leukot Essent Fatty Acids, 55* (1-2): 33-43.

Revuelta, M., Venero, J. L., Machado, A. & Cano, J. (1997). Deprenyl induces GFAP immunoreactivity in the intact and injured dopaminergic nigrostriatal system but fails to counteract axotomy-induced degenerative changes. *Glia, 21* (2): 204-216.

Rhodin, J. (1954). *Correlation of ultrastructural organization and function in normal and experimentally changed proximal tubule cells of the mouse kidney*. Unpublished Doctorate Thesis, Stockholm.

Riddle, E. L., Fleckenstein, A. E. & Hanson, G. R. (2006). Mechanisms of methamphetamine-induced dopaminergic neurotoxicity. *AAPS J, 8* (2): E413-418.

Rodriguez-Serrano, M., Romero-Puertas, M. C., Pastori, G. M., Corpas, F. J., Sandalio, L. M., del Rio, L. A. & Palma, J. M. (2007). Peroxisomal membrane manganese superoxide dismutase: characterization of the isozyme from watermelon (Citrullus lanatus Schrad.) cotyledons. *J Exp Bot, 58* (10): 2417-2427.

Rowe, D. (1994). *The limits of family influence: Genes, experience, and behavior*. New York: The Guilford Press; 1 edition (August 2, 1995).

Rudnick, G. & Clark, J. (1993). From synapse to vesicle: the reuptake and storage of biogenic amine neurotransmitters. *Biochim Biophys Acta, 1144* (3): 249-263.

Salamone, J. D. (1994). The involvement of nucleus accumbens dopamine in appetitive and aversive motivation. *Behav Brain Res, 61* (2): 117-133.

Sandalio, L. M., Lopez-Huertas, E., Bueno, P. & Del Rio, L. A. (1997). Immunocytochemical localization of copper,zinc superoxide dismutase in peroxisomes from watermelon (Citrullus vulgaris Schrad.) cotyledons. *Free Radic Res, 26* (3): 187-194.

Sands, S. A. & Chronwall, B. M. (1996). GFAP expression induced by dopamine D(2) receptor agonists in the rat pituitary intermediate lobe. *Endocrine, 4* (1): 35-42.

Schenck, J. F. & Zimmerman, E. A. (2004). High-field magnetic resonance imaging of brain iron: birth of a biomarker? *NMR Biomed, 17* (7): 433-445.

Schintu, N., Frau, L., Ibba, M., Caboni, P., Garau, A., Carboni, E. & Carta, A. R. (2009). PPAR-gamma-mediated neuroprotection in a chronic mouse model of Parkinson's disease. *Eur J Neurosci, 29* (5): 954-963.

Schmitz, S. (2007). *Der Experimentator: Zellkultur*. Munich: Spektrum.

Schnell, S. A., Staines, W. A. & Wessendorf, M. W. (1999). Reduction of lipofuscin-like autofluorescence in fluorescently labeled tissue. *J Histochem Cytochem, 47* (6): 719-730.

Schrader, M. & Fahimi, H. D. (2004). Mammalian peroxisomes and reactive oxygen species. *Histochem Cell Biol, 122* (4): 383-393.

Schrader, M. & Fahimi, H. D. (2006). Peroxisomes and oxidative stress. *Biochim Biophys Acta, 1763* (12): 1755-1766.

Schrader, M. & Fahimi, H. D. (2008). The peroxisome: Still a mysterious organelle. *Histochem Cell Biol, 129* (4): 421-440.

Schrader, M., Wodopia, R. & Fahimi, H. D. (1999). Induction of tubular peroxisomes by UV irradiation and reactive oxygen species in HepG2 cells. *J Histochem Cytochem, 47* (9): 1141-1148.

Schultz, W., Dayan, P. & Montague, P. R. (1997). A neural substrate of prediction and reward. *Science, 275* (5306): 1593-1599.

Schumacher, J., Jamra, R. A., Freudenberg, J., Becker, T., Ohlraun, S., Otte, A. C., . . . Cichon, S. (2004). Examination of G72 and D-amino-acid oxidase as genetic risk factors for schizophrenia and bipolar affective disorder. *Mol Psychiatry, 9* (2): 203-207.

Seeman, P. & Lee, T. (1975). Antipsychotic drugs: direct correlation between clinical potency and presynaptic action on dopamine neurons. *Science, 188* (4194): 1217-1219.

Seeman, P., Lee, T., Chau-Wong, M. & Wong, K. (1976). Antipsychotic drug doses and neuroleptic/dopamine receptors. *Nature, 261* (5562): 717-719.

Selakovic, V., Janac, B. & Radenovic, L. (2010). MK-801 effect on regional cerebral oxidative stress rate induced by different duration of global ischemia in gerbils. *Mol Cell Biochem, 342* (1-2): 35-50.

Selemon, L. D., Rajkowska, G. & Goldman-Rakic, P. S. (1995). Abnormally high neuronal density in the schizophrenic cortex. A morphometric analysis of prefrontal area 9 and occipital area 17. *Arch Gen Psychiatry, 52* (10): 805-818; discussion 819-820.

Sham, P. C., O'Callaghan, E., Takei, N., Murray, G. K., Hare, E. H. & Murray, R. M. (1992). Schizophrenia following pre-natal exposure to influenza epidemics between 1939 and 1960. *Br J Psychiatry, 160*: 461-466.

Sharma, U., Roberts, E. S., Kent, U. M., Owens, S. M. & Hollenberg, P. F. (1997). Metabolic inactivation of cytochrome P4502B1 by phencyclidine: immunochemical and radiochemical analyses of the protective effects of glutathione. *Drug Metab Dispos, 25* (2): 243-250.

Sheng, P., Cerruti, C. & Cadet, J. L. (1994). Methamphetamine (METH) causes reactive gliosis in vitro: attenuation by the ADP-ribosylation (ADPR) inhibitor, benzamide. *Life Sci, 55* (3): PL51-54.

Shih, A. Y., Erb, H. & Murphy, T. H. (2007). Dopamine activates Nrf2-regulated neuroprotective pathways in astrocytes and meningeal cells. *J Neurochem, 101* (1): 109-119.

Shimizu, N., Itoh, R., Hirono, Y., Otera, H., Ghaedi, K., Tateishi, K., . . . Fujiki, Y. (1999). The peroxin Pex14p. cDNA cloning by functional complementation on a Chinese hamster ovary cell mutant, characterization, and functional analysis. *J Biol Chem, 274* (18): 12593-12604.

Snyder, S. H. (1976). The dopamine hypothesis of schizophrenia: focus on the dopamine receptor. *Am J Psychiatry, 133* (2): 197-202.

South, S. T. & Gould, S. J. (1999). Peroxisome synthesis in the absence of preexisting peroxisomes. *J Cell Biol, 144* (2): 255-266.

St Clair, D., Xu, M., Wang, P., Yu, Y., Fang, Y., Zhang, F., . . . He, L. (2005). Rates of adult schizophrenia following prenatal exposure to the Chinese famine of 1959-1961. *JAMA, 294* (5): 557-562.

Standring, S. (2008). *Gray's Anatomy: The Anatomical Basis of Clinical Practice* (40th ed.): Churchill Livingstone Elsevier.

Stefanis, N. C., Trikalinos, T. A., Avramopoulos, D., Smyrnis, N., Evdokimidis, I., Ntzani, E. E., . . . Stefanis, C. N. (2007). Impact of schizophrenia candidate genes on schizotypy and cognitive endophenotypes at the population level. *Biol Psychiatry, 62* (7): 784-792.

Stefanis, N. C., Van Os, J., Avramopoulos, D., Smyrnis, N., Evdokimidis, I., Hantoumi, I. & Stefanis, C. N. (2004). Variation in catechol-o-methyltransferase val158 met genotype associated with schizotypy but not cognition: a population study in 543 young men. *Biol Psychiatry, 56* (7): 510-515.

Steinberg, S. J., Dodt, G., Raymond, G. V., Braverman, N. E., Moser, A. B. & Moser, H. W. (2006). Peroxisome biogenesis disorders. *Biochim Biophys Acta, 1763* (12): 1733-1748.

Stokes, A. H., Hastings, T. G. & Vrana, K. E. (1999). Cytotoxic and genotoxic potential of dopamine. *J Neurosci Res, 55* (6): 659-665.

Sulzer, D. & Rayport, S. (1990). Amphetamine and other psychostimulants reduce pH gradients in midbrain dopaminergic neurons and chromaffin granules: a mechanism of action. *Neuron, 5* (6): 797-808.

Sulzer, D., Secca, L. (1999). Intraneuronal Dopamine-Quinone Synthesis: A Review. *Neurotoxicity Research, 1*: 181-195.

Sun, Z. W., Zhang, L., Zhu, S. J., Chen, W. C. & Mei, B. (2010). Excitotoxicity effects of glutamate on human neuroblastoma SH-SY5Y cells via oxidative damage. *Neurosci Bull, 26* (1): 8-16.

Susser, E., Neugebauer, R., Hoek, H. W., Brown, A. S., Lin, S., Labovitz, D. & Gorman, J. M. (1996). Schizophrenia after prenatal famine. Further evidence. *Arch Gen Psychiatry, 53* (1): 25-31.

Susser, E. S. & Lin, S. P. (1992). Schizophrenia after prenatal exposure to the Dutch Hunger Winter of 1944-1945. *Arch Gen Psychiatry, 49* (12): 983-988.

Suzuki, M., Zhou, S. Y., Hagino, H., Niu, L., Takahashi, T., Kawasaki, Y., . . . Kurachi, M. (2005). Morphological brain changes associated with Schneider's first-rank symptoms in schizophrenia: a MRI study. *Psychol Med, 35* (4): 549-560.

Takahashi, S., Horikomi, K. & Kato, T. (2001). MS-377, a novel selective sigma(1) receptor ligand, reverses phencyclidine-induced release of dopamine and serotonin in rat brain. *Eur J Pharmacol, 427* (3): 211-219.

Tandon, R. (2005). Suicidal behavior in schizophrenia. *Expert Rev Neurother, 5* (1): 95-99.

Titorenko, V. I. & Mullen, R. T. (2006). Peroxisome biogenesis: the peroxisomal endomembrane system and the role of the ER. *J Cell Biol, 174* (1): 11-17.

Tokuyasu, K. T. (1997). Immuno-cytochemistry on ultrathin cryosections. In Spector, D. L., Goodman, R. D. & Leinwand, L. A.: *Cells, a laboratory manual, Vol. 3, Subcellular localization of genes and their products*: 131.1-131.27. Cold Spring Harbor Laboratory Press.

Tsai, G., Passani, L. A., Slusher, B. S., Carter, R., Baer, L., Kleinman, J. E. & Coyle, J. T. (1995). Abnormal excitatory neurotransmitter metabolism in schizophrenic brains. *Arch Gen Psychiatry, 52* (10): 829-836.

Tsai, G., Yang, P., Chung, L. C., Lange, N. & Coyle, J. T. (1998). D-serine added to antipsychotics for the treatment of schizophrenia. *Biol Psychiatry, 44* (11): 1081-1089.

Tsuang, M. T., Vandermey, R. (1980). *Genes and the mind*. Oxford: Oxford University Press.

Umeda, K., Suemaru, K., Todo, N., Egashira, N., Mishima, K., Iwasaki, K., . . . Araki, H. (2006). Effects of mood stabilizers on the disruption of prepulse inhibition induced by apomorphine or dizocilpine in mice. *Eur J Pharmacol, 553* (1-3): 157-162.

Unger, E. L., Wiesinger, J. A., Hao, L. & Beard, J. L. (2008). Dopamine D2 receptor expression is altered by changes in cellular iron levels in PC12 cells and rat brain tissue. *J Nutr, 138* (12): 2487-2494.

Ustun, T. B. (1999). The global burden of mental disorders. *Am J Public Health, 89* (9): 1315-1318.

Van den Heuvel, D. M. & Pasterkamp, R. J. (2008). Getting connected in the dopamine system. *Prog Neurobiol, 85* (1): 75-93.

van der Valk, P., Gille, J. J., Oostra, A. B., Roubos, E. W., Sminia, T. & Joenje, H. (1985). Characterization of an oxygen-tolerant cell line derived from Chinese hamster ovary. Antioxygenic enzyme levels and ultrastructural morphometry of peroxisomes and mitochondria. *Cell Tissue Res, 239* (1): 61-68.

van Os, J. & Kapur, S. (2009). Schizophrenia. *Lancet, 374* (9690): 635-645.

van Os, J., Kenis, G. & Rutten, B. P. (2010). The environment and schizophrenia. *Nature, 468* (7321): 203-212.

Van Veldhoven, P. P., Brees, C. & Mannaerts, G. P. (1991). D-aspartate oxidase, a peroxisomal enzyme in liver of rat and man. *Biochim Biophys Acta, 1073* (1): 203-208.

Vinogradov, S. (2003). Book Review on Sharma, T. & Harvey, P. (Eds.) (2000). Cognition in Schizophrenia - Impairments, Importance, and Treatment Strategies. *Am J Psychiatry, 160* (2): 404-405.

Volterra, A. & Meldolesi, J. (2005). Astrocytes, from brain glue to communication elements: the revolution continues. *Nat Rev Neurosci, 6* (8): 626-640.

Vucetic, Z., Totoki, K., Schoch, H., Whitaker, K. W., Hill-Smith, T., Lucki, I. & Reyes, T. M. (2010). Early life protein restriction alters dopamine circuitry. *Neuroscience, 168* (2): 359-370.

Wanders, R. J. & Denis, S. (1992). Identification of superoxide dismutase in rat liver peroxisomes. *Biochim Biophys Acta, 1115* (3): 259-262.

Wanders, R. J. & Waterham, H. R. (2006). Peroxisomal disorders: the single peroxisomal enzyme deficiencies. *Biochim Biophys Acta, 1763* (12): 1707-1720.

Wang, Y., Denisova, J. V., Kang, K. S., Fontes, J. D., Zhu, B. T. & Belousov, A. B. (2010). Neuronal gap junctions are required for NMDA receptor-mediated excitotoxicity: implications in ischemic stroke. *J Neurophysiol, 104* (6): 3551-3556.

Wentworth, P., Jr., McDunn, J. E., Wentworth, A. D., Takeuchi, C., Nieva, J., Jones, T., . . . Lerner, R. A. (2002). Evidence for antibody-catalyzed ozone formation in bacterial killing and inflammation. *Science, 298* (5601): 2195-2199.

WHO. (2007). *The ICD-10 Classification of Mental and Behavioural Disorders - Clinical Descriptions and Diagnostic Guidelines*.

WHO. (2008). The Global Burden of Disease - 2004 Update.

Wicks, S., Hjern, A., Gunnell, D., Lewis, G. & Dalman, C. (2005). Social adversity in childhood and the risk of developing psychosis: a national cohort study. *Am J Psychiatry, 162* (9): 1652-1657.

Will, G. K., Soukupova, M., Hong, X., Erdmann, K. S., Kiel, J. A., Dodt, G., . . . Erdmann, R. (1999). Identification and characterization of the human orthologue of yeast Pex14p. *Mol Cell Biol, 19* (3): 2265-2277.

Willis, C. L. & Ray, D. E. (2007). Antioxidants attenuate MK-801-induced cortical neurotoxicity in the rat. *Neurotoxicology, 28* (1): 161-167.

Wilson, J. M., Kalasinsky, K. S., Levey, A. I., Bergeron, C., Reiber, G., Anthony, R. M., . . . Kish, S. J. (1996). Striatal dopamine nerve terminal markers in human, chronic methamphetamine users. *Nat Med, 2* (6): 699-703.

Wolf, M. E., Xue, C. J., White, F. J. & Dahlin, S. L. (1994). MK-801 does not prevent acute stimulatory effects of amphetamine or cocaine on locomotor activity or extracellular dopamine levels in rat nucleus accumbens. *Brain Res, 666* (2): 223-231.

Wood, L. S., Pickering, E. H. & Dechairo, B. M. (2007). Significant support for DAO as a schizophrenia susceptibility locus: examination of five genes putatively associated with schizophrenia. *Biol Psychiatry, 61* (10): 1195-1199.

Woodberry, K. A., Giuliano, A. J. & Seidman, L. J. (2008). Premorbid IQ in schizophrenia: a meta-analytic review. *Am J Psychiatry, 165* (5): 579-587.

Wu, S. & Barger, S. W. (2004). Induction of serine racemase by inflammatory stimuli is dependent on AP-1. *Ann N Y Acad Sci, 1035*: 133-146.

Xu, M. Q., Sun, W. S., Liu, B. X., Feng, G. Y., Yu, L., Yang, L., . . . He, L. (2009). Prenatal malnutrition and adult schizophrenia: further evidence from the 1959-1961 Chinese famine. *Schizophr Bull, 35* (3): 568-576.

Xu, P., LaVallee, P. & Hoidal, J. R. (2000). Repressed expression of the human xanthine oxidoreductase gene. E-box and TATA-like elements restrict ground state transcriptional activity. *J Biol Chem, 275* (8): 5918-5926.

Yao, J. K., Leonard, S. & Reddy, R. (2006). Altered glutathione redox state in schizophrenia. *Dis Markers, 22* (1-2): 83-93.

Yao, J. K., Leonard, S. & Reddy, R. D. (2000). Membrane phospholipid abnormalities in postmortem brains from schizophrenic patients. *Schizophr Res, 42* (1): 7-17.

Yao, J. K., Leonard, S. & Reddy, R. D. (2004). Increased nitric oxide radicals in postmortem brain from patients with schizophrenia. *Schizophr Bull, 30* (4): 923-934.

Yoshikawa, M., Kobayashi, T., Oka, T., Kawaguchi, M. & Hashimoto, A. (2004). Distribution and MK-801-induced expression of serine racemase mRNA in rat brain by real-time quantitative PCR. *Brain Res Mol Brain Res, 128* (1): 90-94.

Yoshikawa, M., Oka, T., Kawaguchi, M. & Hashimoto, A. (2004). MK-801 upregulates the expression of d-amino acid oxidase mRNA in rat brain. *Brain Res Mol Brain Res, 131* (1-2): 141-144.

Young, K. A., Gobrogge, K. L. & Wang, Z. (2011). The role of mesocorticolimbic dopamine in regulating interactions between drugs of abuse and social behavior. *Neurosci Biobehav Rev, 35* (3): 498-515.

Yui, K., Goto, K., Ikemoto, S., Ishiguro, T., Angrist, B., Duncan, G. E., . . . Ali, S. F. (1999a). Neurobiological basis of relapse prediction in stimulant-induced psychosis and schizophrenia: the role of sensitization. *Mol Psychiatry, 4* (6): 512-523.

Yui, K., Goto, K., Ikemoto, S., Ishiguro, T. & Kamada, Y. (1999b). Increased sensitivity to stress and episode recurrence in spontaneous recurrence of methamphetamine psychosis. *Psychopharmacology (Berl), 145* (3): 267-272.

Yui, K., Ishiguro, T., Goto, K., Ikemoto, S. & Kamata, Y. (1999c). Spontaneous recurrence of methampetamine psychosis: increased sensitivity to stress associated with noradrenergic hyperactivity and dopaminergic change. *Eur Arch Psychiatry Clin Neurosci, 249* (2): 103-111.

Zaar, K. (1996). Light and electron microscopic localization of D-aspartate oxidase in peroxisomes of bovine kidney and liver: an immunocytochemical study. *J Histochem Cytochem, 44* (9): 1013-1019.

Zaar, K., Kost, H. P., Schad, A., Volkl, A., Baumgart, E. & Fahimi, H. D. (2002). Cellular and subcellular distribution of D-aspartate oxidase in human and rat brain. *J Comp Neurol, 450* (3): 272-282.

Zaar, K., Volkl, A. & Fahimi, H. D. (1989). D-aspartate oxidase in rat, bovine and sheep kidney cortex is localized in peroxisomes. *Biochem J, 261* (1): 233-238.

Zaidel, D. W., Esiri, M. M. & Harrison, P. J. (1997). The hippocampus in schizophrenia: lateralized increase in neuronal density and altered cytoarchitectural asymmetry. *Psychol Med, 27* (3): 703-713.

Zellweger, H. (1988). Peroxisomes and peroxisomal disorders. *Ala J Med Sci, 25* (1): 54-58.

Zhang, X. Y., Tan, Y. L., Cao, L. Y., Wu, G. Y., Xu, Q., Shen, Y. & Zhou, D. F. (2006). Antioxidant enzymes and lipid peroxidation in different forms of schizophrenia treated with typical and atypical antipsychotics. *Schizophr Res, 81* (2-3): 291-300.

Zuo, D. Y., Wu, Y. L., Yao, W. X., Cao, Y., Wu, C. F. & Tanaka, M. (2007). Effect of MK-801 and ketamine on hydroxyl radical generation in the posterior cingulate and retrosplenial cortex of free-moving mice, as determined by in vivo microdialysis. *Pharmacol Biochem Behav, 86* (1): 1-7.

5.1 Figure references

Fig. 1.1_1: modified from Hafner, H., Maurer, K., Loffler, W. & Riecher-Rossler, A. (1993). The influence of age and sex on the onset and early course of schizophrenia. *Br J Psychiatry, 162*: 80-86.

Fig. 1.1_3: modified from van Os, J., Kenis, G. & Rutten, B. P. (2010). The environment and schizophrenia. *Nature, 468* (7321): 203-212.

Fig. 1.1_4: based on Collip, D., Myin-Germeys, I. & Van Os, J. (2008). Does the concept of "sensitization" provide a plausible mechanism for the putative link between the environment and schizophrenia? *Schizophr Bull, 34* (2): 220-225.

Fig. 1.1_5: modified from Vucetic, Z., Totoki, K., Schoch, H., Whitaker, K. W., Hill-Smith, T., Lucki, I. & Reyes, T. M. (2010). Early life protein restriction alters dopamine circuitry. *Neuroscience, 168* (2): 359-370.

Fig. 1.1_6: modified from Javitt, D. C. (2006). Glutamate Involvement in Schizophrenia: Focus on N-methyl-D-aspartate Receptors. *Primary Psychiatry, 13* (10): 38-46.

Fig.1.1_7: modified from Yoshikawa, M., Kobayashi, T., Oka, T., Kawaguchi, M. & Hashimoto, A. (2004). Distribution and MK-801-induced expression of serine racemase mRNA in rat brain by real-time quantitative PCR. *Brain Res Mol Brain Res, 128* (1): 90-94.

Fig. 1.2_1: modified from http://media.web.britannica.com/eb-media/04/96904-003-D868D39B.gif

Fig. 1.2_2: modified from Stokes, A. H., Hastings, T. G. & Vrana, K. E. (1999). Cytotoxic and genotoxic potential of dopamine. *J Neurosci Res, 55* (6): 659-665.

Fig. 1.2_4: modified from Dringen, R., Pawlowski, P. G. & Hirrlinger, J. (2005). Peroxide detoxification by brain cells. *J Neurosci Res, 79* (1-2): 157-165.

Fig. 1.2_5: adapted from Bellance, N., Lestienne, P. & Rossignol, R. (2009). Mitochondria: from bioenergetics to the metabolic regulation of carcinogenesis. *Front Biosci, 14*: 4015-4034.

Fig. 1.2_6: modified from Dringen, R., Pawlowski, P. G. & Hirrlinger, J. (2005). Peroxide detoxification by brain cells. *J Neurosci Res, 79* (1-2): 157-165.

Fig.1.3_3: modified from Nieuwenhuys, R., Voogd, J., Van Huijzen, C. (2007). *The Human Central Nervous System* (4th ed.): Steinkopff.

Fig.1.3_5: modified from Stokes, A. H., Hastings, T. G. & Vrana, K. E. (1999). Cytotoxic and genotoxic potential of dopamine. *J Neurosci Res, 55* (6): 659-665.

Fig. 1.4_1: modified from Titorenko, V. I. & Mullen, R. T. (2006). Peroxisome biogenesis: the peroxisomal endomembrane system and the role of the ER. *J Cell Biol, 174* (1): 11-17.

Fig. 1.4_2: adapted from South, S. T. & Gould, S. J. (1999). Peroxisome synthesis in the absence of preexisting peroxisomes. *J Cell Biol, 144* (2): 255-266.

Fig. 1.4_3: modified from Schrader, M. & Fahimi, H. D. (2008). The peroxisome: Still a mysterious organelle. *Histochem Cell Biol, 129* (4): 421-440.

Fig. 1.4_5: adapted from Schrader, M. & Fahimi, H. D. (2006). Peroxisomes and oxidative stress. *Biochim Biophys Acta, 1763* (12): 1755-1766.

Fig. 1.4_6: adapted from Johnson, R. J., Titte, S., Cade, J. R., Rideout, B. A. & Oliver, W. J. (2005). Uric acid, evolution and primitive cultures. *Semin Nephrol, 25* (1): 3-8.

Fig. 1.4_7: modified from Zaar, K., Kost, H. P., Schad, A., Volkl, A., Baumgart, E. & Fahimi, H. D. (2002). Cellular and subcellular distribution of D-aspartate oxidase in human and rat brain. *J Comp Neurol, 450* (3): 272-282.

Fig. 1.4_8: modified from Ahlemeyer, B., Neubert, I., Kovacs, W. J. & Baumgart-Vogt, E. (2007). Differential expression of peroxisomal matrix and membrane proteins during postnatal development of mouse brain. *J Comp Neurol, 505* (1): 1-17.

Fig. 1.4_9: modified from Ahlemeyer, B., Neubert, I., Kovacs, W. J. & Baumgart-Vogt, E. (2007). Differential expression of peroxisomal matrix and membrane proteins during postnatal development of mouse brain. *J Comp Neurol, 505* (1): 1-17.

Fig. 1.4_10: modified from Baes, M., Gressens, P., Baumgart, E., Carmeliet, P., Casteels, M., Fransen, M., . . . Mannaerts, G. P. (1997). A mouse model for Zellweger syndrome. *Nat Genet, 17* (1): 49-57.
Fig. 4_1: Expression profiles from www.biogps.gnf.org
Fig. A.2_1: modified from www.di.uq.edu.au/indirectif
Fig. A.2_2: modified from Hoffman, G. E., Le, W. W. & Sita, L. V. (2008). The importance of titrating antibodies for immunocytochemical methods. *Curr Protoc Neurosci, Chapter 2*: Unit 2 12.
Fig. A.2_3: modified from http://www.nanoprobes.com/newsletters/Vol10_Iss6.html
Fig. A.2_4: modified from http://www.nanoprobes.com/newsletters/Vol10_Iss6.html
Fig. A.2_5: adapted from www.invitrogen.com
Fig. A.3_1: modified from Kendall, L. V. & Riley, L. K. (2000). Reverse transcriptase polymerase chain reaction (RT-PCR). *Contemp Top Lab Anim Sci, 39* (1): 42.

5.2 Online references

Duncker, H.-R. (1999). *Die Kulturfähigkeit des Menschen und ihre evolutionsbiologischen Grundlagen*. http://www2.uni-jena.de/journal/unidez99/essay.htm
Goodsell, D. (2004). *Catalase - September 2004 Molecule of the Month.* http://dx.doi.org/10.2210/rcsb_pdb/mom_2004_9
Taylor, A., Taylor, S., Markham, J. & Koenig, J. (2009). *Animal Models of Schizophrenia.* http://www.schizophreniaforum.org/res/models/Animal_Models_04_09.pdf
www.biogps.gnf.org
www.dsm5.org
www.ncbi.nlm.nih.gov/gene
www.ncbi.nlm.nih.gov/tools/primer-blast
www.psychogenics.com/pdf/Psychosis.pdf
www.szgene.org

Appendix A – Materials and methods: Detailed descriptions

A.1 Cell culture

A.1.1 Mixed primary murine neuronal cultures

Briefly, the cortices were digested for 20' with 0.1% papain. Afterwards, the sedimented tissue sample was gently triturated three times with Pasteur pipettes of subsequently smaller opening sizes. The supernatants were removed, transferred to neurobasal medium containing 1% trypsin inhibitor and 1% BSA and then centrifuged at 200 *g* for 10' at room temperature (RT). Cell pellets were gently resuspended and the cells were seeded onto 35 mm poly-L-lysine-coated Petri dishes containing a coverslip at a density of 3 x 10^5 cells. Neurons were cultured in neurobasal medium plus B27 supplement for 6 days before experiments.

A.1.2 Primary astrocytes cultures

Each culture was taken from an entire litter of newborn C57Bl/6J mice. Animals were sacrificed through decapitation, after which the brains were excised and the cerebella, bulbi olfactorii as well as all non-neuronal tissue was removed. Cortices were digested in a water bath for 20' at 37°C in samples of two or three in 2 ml of 0.1% Papain (Sigma) in neurobasal medium (neuronal base medium, PAA) with 0.02% bovine serum albumin (BSA). After 20' the papain solution was removed by pipetting and 1 ml warm medium was added to the pellet and the sedimented tissue sample was gently triturated eight times each with three Pasteur pipettes of subsequently smaller opening sizes. The supernatants were removed, transferred to neurobasal medium containing 1% trypsin inhibitor and 1% BSA and then centrifuged at 200 *g* for 10 min at room temperature (RT). The supernatant was removed through pipetting and 5ml warm medium were added. The samples were triturated several times and pipette into a glass beaker, mixed again by pipetting and decanted into an uncoated Falcon^{TM}-culture flask (75 cm^2), which already contained 10 ml medium (final volume was 25 ml).

Cells were cultured in Dulbecco's modified Eagle's medium (DMEM) Low Glucose (1g/l) with L-glutamine at 37°C in a Hera Cell 240 incubator (Heraeus) with 5% CO_2. 10%

(vol/vol) fetal calf serum (FCS), 1% penicillin-streptomycin (100x, PAA) and 1% sodium pyruvate (100 mM, PAA) were added to the medium to achieve optimal concentrations of amino acids, vitamins and ATP-generation substrates and germicides for the astrocytes in the culture. This treatment along with the lack of coating of the culture flask did not allow other cells like neurons, oligodendrocytes, microglia, endothelial cells or smooth muscle cells from vessels to survive. This method of cultivation along with the length of cultivation did, however, allow for the common contamination (Schmitz, 2007) with fibroblasts.

The medium was changed on the first day after preparation. Between removal of old and addition of new medium (25 ml) cells were washed with 25 ml cold (4°C) PBS (pH 7.4). Hereafter cells were cultured for 8-11 days until reaching confluence with medium changes every 2-3 days, however, with the omission of the PBS-washing step. Upon reaching confluence cells were passaged into Petri dishes (20 cm^2). Here for 3 ml of Hank's Balanced Salt Solution (HBSS, PAA) containing 0.05% porcine trypsin were added for 30'', removed by pipetting and another 1 ml 0.05% porcine trypsin in HBSS was added and incubated for 3'. 10 ml warm medium were added and the entire contents were pipetted into a glass beaker and mixed by pipetting. Cells were seeded with $2x10^4$ cells per cm^2. To achieve this seeding density cells were counted in a Neubauer Improved Counting Chamber and the necessary amount of medium was added to allow for the intended seeding concentration. 6 ml were pipetted into each Petri dish and the remainder of the suspension in the beaker was mixed through pipetting prior to each seeding. Petri dishes intended for subsequent indirect immunofluorescence labeling contained an additional uncoated cover slip. Cells were cultivated for another 3 days after passaging with a medium change as described above (including a washing step in PBS) on the first day after passaging. After the third day medium was changed once again (without the PBS washing step) and a defined amount of dopamine was added (see section 2.2.2.2 on dopamine treatment).

A.2 Morphological staining techniques

A.2.1 Histological staining

A.2.1.1 Modified Kluver-Barrera staining: Sections were incubated over night at 60°C followed by 3 changes of xylene (5' each) to remove the paraffin. Afterwards sections were rehydrated through a descending series of ethanol (2 x 99%, 1 x 96°; 5' each) and then

incubated in a sealed cuvette in luxol fast blue for 1.5-2 hrs at 60°C. After a brief wash in ethanol (96%) sections were hydrated in ultrapure water for 5' and then differentiated in 0.1% NaOH (aq) for 20-30''. The differentiation was stopped by placing the sections in ultrapure water and controlled under the microscope. Nuclei and Nissl bodies (rough endoplasmic reticulum, rER) were counterstained with acidophilic cresyl violet at room temperature for 8-15', followed by a short rinse in ultrapure water. Sections were then dehydrated in an ascending graded ethanol series (70 %, 99%, 1 x 3' each) and then transferred to a 50:50 solution of 99% ethanol and xylene, followed by three changes of pure xylene (3 x 3'). Sections were then mounted in DePeX. Kluver-Barrera stains myelin sheaths blue, nuclei, nucleoli and Nissl bodies (rER) violet and neuropil cyan.

A.2.2 Indirect Immunohistochemistry (IHC), Immunofluorescence (IF) and ImmunoGoldLabeling (IGL)

A.2.2.1 Principle of indirect immunolabeling: Immunolabeling techniques are based on the binding of antibodies (immunoglobins, usually IgG) to specific protein sequences (epitopes) in situ within biological materials. Antibodies are raised by treating animals with specific antigens of interest. The variety of possible epitopes within an antigens protein sequence leads to the creation of multiple antibodies from different parent immunocytes with the capacity of recognizing the protein of interest (antiserum containing various polyclonal antibodies) within the host animal. These antisera can either be used directly for immunobeling procedures or can alternatively be purified further through various methods (mostly forms of chromatography and/or precipitation) to include only antibodies against a single epitope. Since these antibodies are made in the host animal by clones of one unique parent cell, they are referred to as monoclonal antibodies. These antibodies are then labeled with either enzymes that catalyze color producing reactions, organic fluorescent dyes (fluorochromes) or electron-dense metals (usually gold particles) and therefore be visualized. Since the antibody binding to the specific epitope of the target protein is directly labeled, this method is referred to as "direct immunolabeling".

In indirect immunolabeling techniques a secondary antibody is introduced, which does not bind to the protein of interest, but to the Fc (fragment crystallizable) domain of the primary antibody. In this case not the primary, but the secondary antibody is labeled as described above. This method increases the sensitivity of labeling compared to direct

immunolabeling, since more than one secondary antibody can bind to each primary antibody, thereby intensifying the signal yield and ideally reducing the signal to noise ratio. For this method it is therefore important that the secondary antibody is raised against the species-specific Fc domain of the primary antibody. E.g.: If the primary antibody is raised in rabbit (the most commonly used species for these purposes), then the secondary antibody must firstly be raised in any species other than rabbit and must secondly be of anti-rabbit binding capacity. In some cases the secondary antibody is not a complete Ig-molecule, but consists only of labeled IgG-Fab (fragment antigen-binding)-domains.

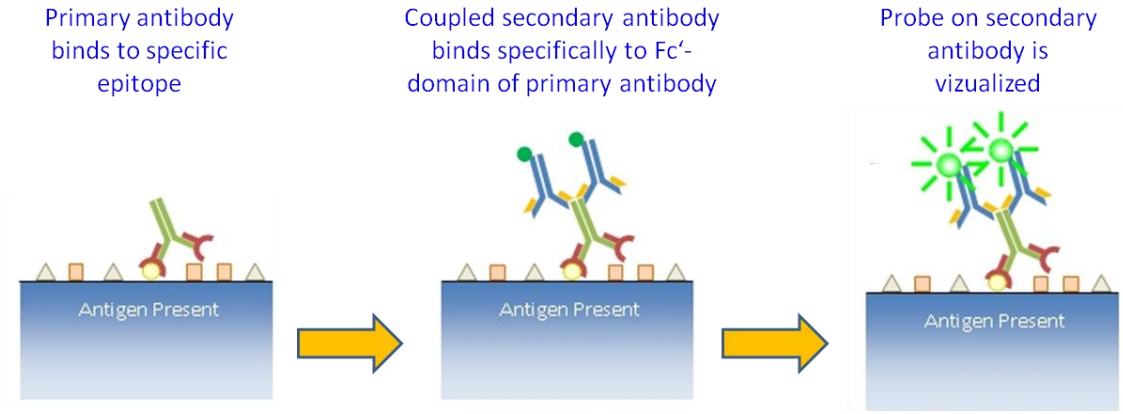

Fig. A.2_1: Principle of indirect immunolabeling (*modified from www.di.uq.edu.au/indirectif*)

The most commonly used methods of visualizing labeled antibodies as mentioned above shall be explained briefly, since they were all used within this thesis.

Enzyme linked immunolabeling techniques (e.g. enzyme linked immunosorbent assays (ELISA) or immunohistochemistry) involve the catalyzation of a color reaction through an enzyme bound to the (secondary) antibody. The most commonly used enzymes are alkaline phosphatase or horseradish peroxidase. This method is often slightly modified for the purpose of additional signal amplification. Hereby the enzyme is not directly bound to the antibody, but rather both the secondary antibodies as well as the enzyme are biotinylated and bound to each other using (strept)avidin. The resulting avidin-biotin complex (ABC) is known for its high affinity interaction, thereby making it ideal for utilization in scientific research. In a final step a specific organic dye is introduced (e.g. 3,3'-diaminobenzidine, DAB), which is then converted by the enzyme resulting in a color reaction. In the case of DAB the color reaction is brown, but can be intensified by nickel ammonium sulfate to form a black product.

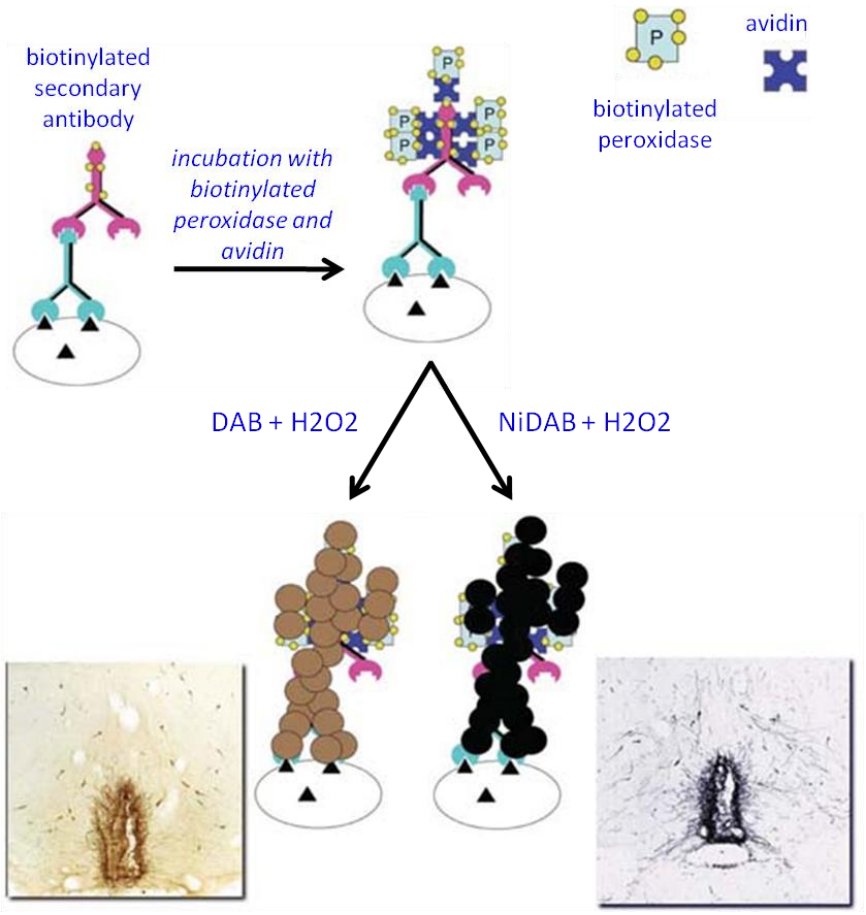

Fig. A.2_2: Indirect immunohistochemistry principle using the ABC system with DAB or DAB with nickel (NiDAB) intensification as reaction substrates (*modified from Hoffman, Le & Sita, 2008*)

Immunofluorescence and immunogold staining both involve direct visualization of agents bound to the secondary antibody (or Fab-domains of secondary antibodies). Fluorescent agents (mostly organic fluorochromes or alternatively crystalline semiconductors/quantum dots) are excited by photons of a specific wavelength. These photons are absorbed by orbital electrons leading to an increase in quantum state of the excited electrons. When these fall back into their ground state another photon is released (usually of longer wavelength than the absorbed photon) leading to a fluorescent signal.

Using primary antibodies (against different proteins) raised in different species and secondary antibodies labeled with fluorescent markers of different emission spectra it is possible to perform multiplex immunostainings.

Finally, immunogold labeling works upon the same principle as in immunofluorescence with the difference of electron dense colloidal gold particles conjugated to secondary antibodies rather than fluorescent materials (quantum dots can be used both in both immunofluorescence a well as in immuno-electron microscopy).

Depending on the size of the gold particles they can either by visualized directly or be enhanced using silver or gold ions which are reduced to metallic silver/gold in a reaction catalyzed by the colloidal gold particles. This leads to an increase in size of the colloidal gold particles (q.v. Fig. A.2_2).

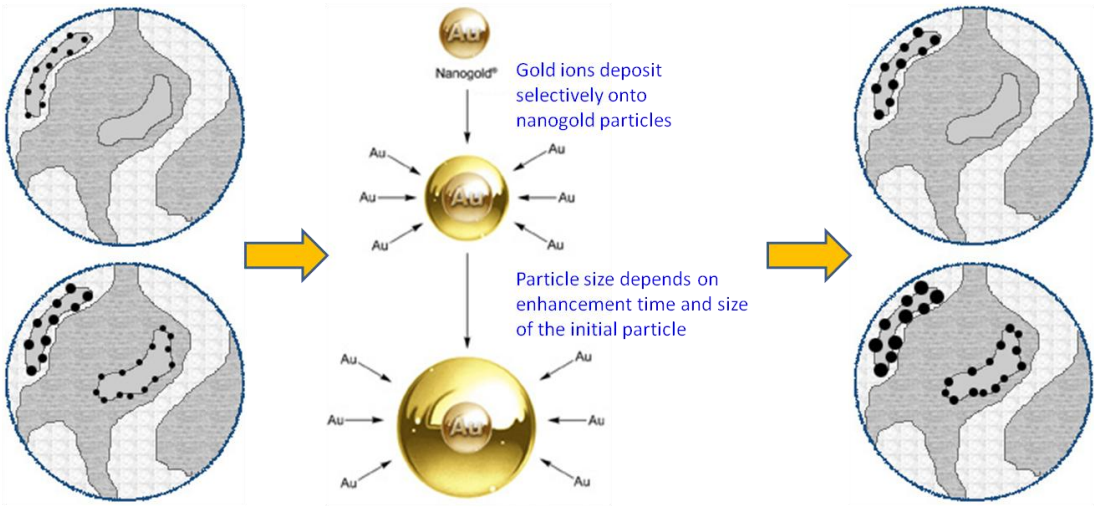

Fig. A.2_3: Principle of gold enhancement. Using nanogold particles of different initial size allows for multiplex IGL-stainings (*modified from nanoprobes.com*)

This technique is used in cases where larger colloidal gold particles infringe upon the ability of the labeled antibody to penetrate into the ultracut section (see Fig. A.2_4). Using smaller particles (nanogold), which can then be enlarged during gold/silver enhancement solves this problem. During examination under the electron microscope electron dense materials like gold, silver or heavy metals (osmium, uranium or lead) deflect the electron beam leading to lack of excitation of these areas of the electron-detecting membrane, which shows as black signals.

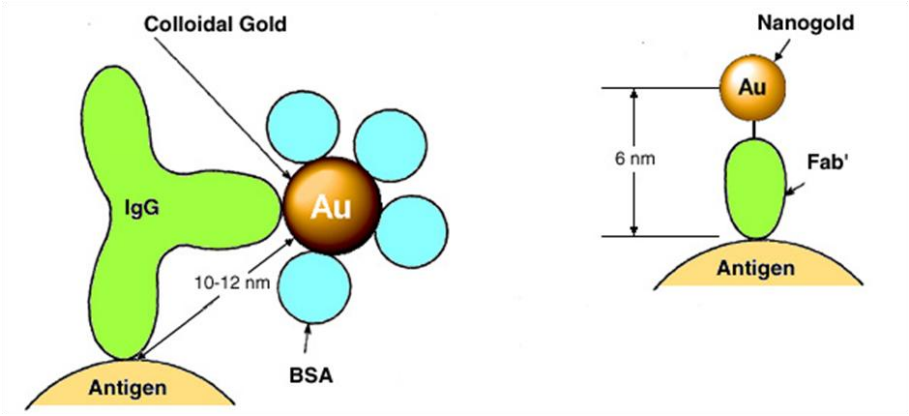

Fig. A.2_4: Size comparison between conventional IgG-coupled colloidal gold particle (left) and a nanogold-Fab'-probe (right) (*modified from nanoprobes.com*)

A.2.2.2 IHC on paraffin-embedded tissue sections: Paraffin was removed from the tissue by over-night incubation at 60°C followed by xylene (3x5'), after which the sections were rehydrated through a descending graded ethanol series (2x99%, 1x96%, 90%, 80%, 70%, 50% and ultrapure water for 5' each). Stainings for Pex14p, catalase, ABCD3 as well as mitochondrial Mn-superoxide dismutase (SOD2) were carried out according to a standardized protocol for indirect immunofluorescence on formalin-fixed paraffin-embedded (FFPE) tissues (based on Grabenbauer et al., 2001 and Baumgart et al., 2003). Antigen retrieval was carried out through digestion with freshly prepared 0.01% trypsin solution (10' at 37°C) followed by microwave irradiation (3x5') at 800W in 10mM citrate buffer (pH 6.0) and subsequent cooling back to room temperature (30'-40'). Hereafter the sections were incubated with freshly prepared 3% H_2O_2 (in ultrapure water; for quenching of endogenous peroxidases). Washing buffer was 1xPBS (pH 7.4). Non-specific binding sites were blocked with 4% bovine serum albumin in PBS (PBSA, pH7.4) with 0.05% Tween 20 (Sigma) and additional avidin. Primary antibodies were all raised in rabbit and diluted 1:1000 in 1% PBSA with 0.05% Tween 20 and additional biotin. Antibodies against catalase and Pex14p were self-created by Denis Crane (SBPS, Griffith University Brisbane, Australia). The antibody against ABCD3 was a kind gift from Alfred Völkl (Dept. of Anatomy and Cell Biology II, Ruprecht-Karls-University, Heidelberg). The SOD2- antibody was acquired from Biozol Diagnostica GmbH, Germany.

The secondary antibody against rabbit was biotinylated and visualized through an ABC (avidin-biotin-complex)-protocol with the substrates being either Vector®NovaRED™ or DAB with nickel enhancement. Nuclei were counterstained with hematoxylin, after which slides were dehydrated through a graded series of ascending ethanols and mounted in DePeX.

A.2.2.3 Multiplex IF on human and murine brain tissue sections: Main steps were the same as described above. During primary antibody incubation three antibodies were used, whereof one was raised in rabbit against either Pex14p, catalase or SOD2 (see above). The other were an antibody against microtubule associated protein 2 (MAP2, raised in chicken, Novus Biologials) and an antibody against glial fibrillary acidic protein (GFAP, raised in mouse, Chemicon). MAP2 is expressed in the perikarya and dendrites of most neurons, whereas GFAP is expressed exclusively in astrocytes. These antibodies therefore served as

cell markers. Secondary antibodies were donkey anti-rabbit AlexaFlour 488 (green emission, Molecular Probes), horse anti-mouse Texas Red (orange-red emission, Vector) and anti-chicken AlexaFlour 633 (deep red emission, Molecular Probes). Cells were only counterstained with Hoechst 33258/33342 solution, since TOTO-3 iodide has a similar emission wavelength to AlexaFlour 633. Antibodies against Pex14p and catalase were diluted 1:2000, the antibody against SOD2 was diluted 1:1000. Secondary antibodies were all diluted 1:300.

A.2.2.4 Multiplex IF on murine primary neuronal and astrocyte cultures: Medium was removed from the Petri dishes by pipetting, whereupon cells were washed briefly with three changes of warm (37°C) PBS prior to fixing in 4% PFA in PBS for 20'. The fixing solution was then removed and cells were washed 3x5' with PBS. After this cells were incubated for 10' with 1% glycin (Roth) in PBS to assure quenching of unsaturated aldehydes through possibly repolymerized PFA. Cells were then permeabilized for 10' with 0.3% Triton X-100 (Sigma) in PBS with 1% glycin, followed by washing 3x5' in PBS. After removal of PBS the cover slips in the Petri dishes were encircled with a PAP-pen (Super PAP Pen IM 35800, Beckman-Coulter) to assure that following incubation solutions remain in place over the cells. Blocking solution (1% PBSA with 0.05% Tween 20) was added and Petri dishes were incubated at room temperature in a humind chamber for 30', where after blocking solution was removed by pipetting and substituted with primary antibody incubation solution. Primary antibodies were against Pex14p or catalase, MAP2 and GFAP (see above) and incubated in a humid chamber at room temperature for 1h, followed by 3x5' washing in PBS and subsequent incubation with secondary antibodies (see above) for 30'. Hereafter cells were washed again 3x5' prior to counterstaining of nuclei with Hoechst 33258/33342 solution (1:750 in PBS). After a final 3x5' washing in PBS cover slips were removed from the Petri dishes with a tweezer and mounted onto SuperFrost Plus microscope slides using two parts Mowiol 4-88 and one part n-propyl gallate.

A.2.2.5 IF using QuantumDots® on mouse and human hepatoma cells: The steps up to and including the incubation with the primary antibody against Pex14p are identical to those described above in the IF protocol for cell cultures. QuantumDots (QDots, Invitrogen) fluorescence was, however, found to be highly dependent on pH of washing buffers and

mounting media. Therefore several different modifications of the IF protocol for cell cultures were performed and subsequently changed stepwise in order to achieve the final optimal protocol for IF using QDots (data not shown here). Since QDot fluorescence was strongest in a hydrophobic medium (DePeX) and relatively poor in most aqueous media (including Mowiol 4-88 and various buffered glycerol solutions of different pH, with the exception of carbonate buffered glycerol, pH > 10) these modifications included the addition of several dehydration steps in order to allow for mounting in a hydrophobic medium. The incubation with the primary antibody was therefore followed only by a single washing step with PBS, where after the pH had to be adjusted to that of the optimal QDot incubation buffer (see below). The cells were therefore washed twice in 50mM borate buffer (pH 8.3). QDots were diluted 1:500 in 1% bovine serum albumin in 50mM borate buffer with 0.05% Tween 20 (final optimal QDot incubation buffer). After 30' of incubation with QDots cells were washed several times in borate buffer and then dehydrated and washed (simple dehydration proved insufficient for removing unbound QDots) further in a graded ascending ethanol series and finally cleared in three changes of xylene prior to mounting onto object slides using DePeX mounting medium. QDots are optimally excited by UV-light, wherefore no nuclear counterstaining was performed, so as not to outshine the QDots' signals.

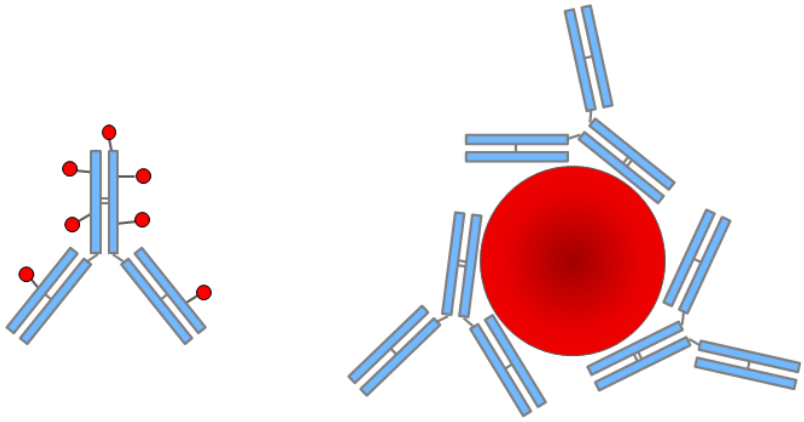

Fig. A.2_5: Size comparison between organic fluorophore (left) and Qdot ® (right) antibody conjugates (*adapted from invitrogen.com*)

A.2.2.6 IGL for electron microscopy: All washing and incubation steps were performed on drops pipetted onto a specially cast rubber panel. Grids with cryo-ultrathin section were washed 3 times in 1xPBS to remove the pick-up solution (2.3M sucrose and 2% methyl cellulose). After this all grids were washed in 1xPBS with 0.1% glycin to quench the aldehydes from the fixation. Blocking of non-specific binding sites as well as dilution of both

primary and secondary antibodies was achieved with 1% BSA-c (Aurion) in normal donkey serum without the addition of any detergents. Primary antibodies against Pex14p and catalase were diluted 1:2000 (twice as strongly as for light microscopy to reduce unspecific background). The secondary antibody against rabbit was coupled with AlexaFour 488 fluorogold and diluted 1:200. The reaction was fixed after incubation with 1% glutardialdehyde (GDA) in PBS for 10mins and the aldehydes were again quenched with washes in PBS with 1% glycine. Fluorogold particles were intensified with a silver enhancement kits (Nanoprobes, NY, USA; Aurion, Netherlands) and grids were then washed thoroughly with deionized water. Resin grids were then contrasted with a saturated aqueous solution of uranyl acetate, washed in water and left to dry, whereas cryo-grids were conveyed onto two successive drops of nine parts 2% methyl cellulose and one part saturated aqueous uranyl acetate. On the second drop the grids were contrasted for 5’ and then looped out on a sheet of filter paper and left to dry.

A.3 Reverse transcription polymerase chain reaction (RT-PCR)

A.3.1 Pinciple of RT-PCR

The basic principle of Polymerase Chain Reaction (PCR) is taken from in vivo DNA (deoxyribonucleic acid) duplication during mitotic division of a parent cell into two daughter cells. This process, however, depends not only on the activity of DNA-dependent polymerases, but also requires the involvement of primarily three other enzymes, namely helicase, primase and topoisomerase. Helicase is important for the unwinding of the DNA double helix, thereby leading to the formation of the replication fork. Primase is an RNA (ribonucleic acid) polymerase which builds short strands of RNA complementary to the origin sites of replication. In this context a fourth enzyme, DNA ligase, becomes important, since DNA replication, which always goes from 3’ to 5’, on the lagging strand leads to the formation of short amplicons (Okazaki fragments) which need to be spliced together to form a complete strand of daughter DNA. After replication topoisomerase cuts the parent DNA strand and “unwinds” physical stresses which evolve during denaturation of the parent DNA by helicase, so that both strands may reanneal to each other without breaking.

In vitro two of these enzymes (primase and topoisomerase) are not necessary, since primers are designed specifically not to bind to origins, but rather to encompass a sequence

of the DNA of interest, which is to be amplified. These primers are therefore not synthesized during the amplification reaction, but in separate reactions (usually performed by service providers). Topoisomerase is also not necessary, since DNA breakage due to physical stress may still occur, but unlike in vivo does not pose any further risk to the host. The simplest in vitro method of DNA amplification is therefore called helicase dependent amplification (HDA), a process involving only parent DNA, site-specific primers and the two enzymes DNA-polymerase and helicase. HDA is therefore, unlike PCR, an isothermal reaction.

An alternative to enzyme-dependent separation of DNA strands was found in physical denaturation through elevation of the temperature to >90°C. This method was described in theory without any evidence of practical application by Kjell Kleppe in 1971, but the invention of the actual PCR-method is generally accredited to Kary Mullis in 1983 (described in Mullis, Ferré & Gibbs, 1994). First experiments did not, however, involve thermostable DNA polymerase, but the Klenow fragment of DNA polymerase I from *Escherichia coli* (lacking nuclease activity compared to the entire enzyme) (Klenow & Henningsen, 1970; Klenow & Overgaard-Hansen, 1970). Since the Klenow fragment is also inactivated through the temperature elevation necessary for denaturation of DNA, this method involved adding new polymerase in each cycle in order to achieve exponential amplification. This problem was also solved (and a patent was filed by Mullis and coworkers in 1987) by using a thermostable DNA polymerase which had been isolated just over a decade ago (Chien, Edgar & Trela, 1976) from the thermophile *Thermus aquaticus* (Brock & Freeze, 1969). The enzyme is therefore commonly known as Thermus aquaticus polymerase (Taq).

PCR using Taq consists of repetitive cycling between three steps which occur at different temperatures. The first steps is the denaturing of the parental DNA strands and occurs at >90°C. In many PCR-designs (like in this thesis) an additional single denaturation step is included before the first cycle. Within the cycles, denaturation is followed by cooling of the reaction mix to optimal primer annealing temperature (depending on primer-melting temperature as a function of C/G vs. A/T content of the primer). The final step is the actual elongation and thereby duplication of the amplicon at optimal activity temperature of the Taq used. These cycles are repeated (usually between 30 and 45 times) and followed by a single final elongation step, after which the reaction is terminated by cooling the reaction mix to 4°C.

In each cycle the amount of amplicons is doubled, leading to fast exponential growths of the number of template copied. Due to this, the name polymerase **chain** reaction was chosen. Albeit that chain reaction normally involve the generation of reaction products which in turn lead to further reactions of themselves, as is not the case in PCR, each reaction product becomes an integral part of the next reaction cycle, wherefore the term chain reaction is applicable. Furthermore, due to the fact that amplicons of parental DNA lack sequences outside of the primer range (apart from the first amplicons, which are elongated beyond the 5'-end of the sequence complementary to the second primer binding region), the majority of PCR products have identical number of base pairs (bps) and can therefore be analyzed and compared to amplicons of different sizes by means of gel electrophoresis.

Reverse transcription polymerase chain reaction (RT-PCR; not to be mistaken for Real Time PCR) is also taken from in vitro metabolic processes. Normal transcription involves the generation of a complementary strand of ribonucleic acid (in most cases messenger RNA, mRNA) by RNA polymerase. During this process the aforementioned enzyme binds to specific response elements (or promoters) of genomic DNA and transcribes it, this being the first (and in cases of non-coding RNAs also the last) step of gene expression. In retroviridae, however, this process also works in reverse, whereby the RNA-containing virus uses an RNA-dependent polymerase (so-called reverse transcriptase) to synthesize a complementary single stranded DNA (cDNA) out of an RNA template. The most commonly known retroviridae are the human immunodeficiency virus (HIV), the hepatitis B virus (HBV) and several strands of leukaemia viridae or other oncoviridae.

RT-PCR uses these enzymes (mostly mutations of reverse transcriptases isolated from Moloney murine leukaemia virus [MMLV] or avian myeloblastosis virus [AMV]) to analyze the number of mRNA copies of specific gene, thereby giving an indication of the amount of expression of the gene(s) in question. After extraction of RNA, the first step of RT-PCR is the incubation with reverse transcriptase to form complementary strands of cDNA (first strand synthesis, FSS), which can then be introduced into and amplified in standard PCR reactions. Many forms of reverse transcriptase have an additional RNase H-activity, which selectively degrades RNAs only in RNA/DNA-hybrids, thereby increasing the purity of the cDNA.

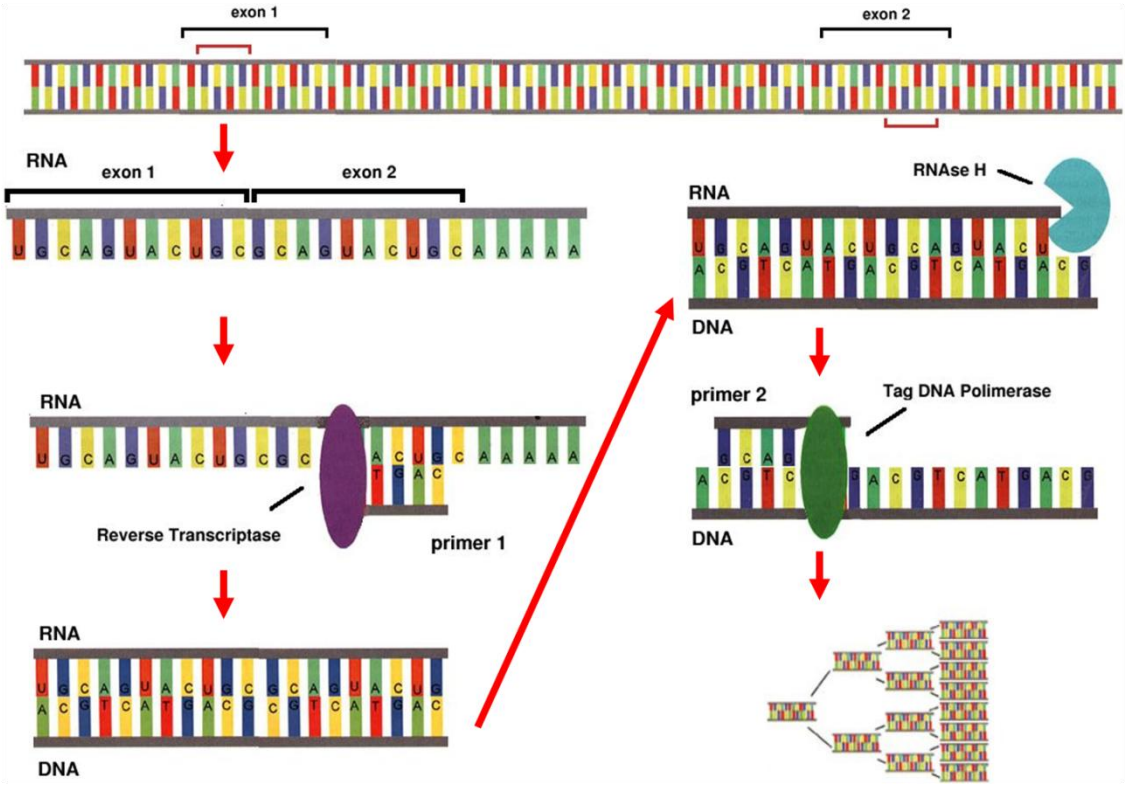

Fig. A.3_1: Principle of RT-PCR (*modified from Kendall & Riley; 2000*)

Apart from this, reverse transcriptases also differ regarding their optimal activity temperature. Generally, enzymes with a higher temperature optimum perform better during FSS, since RNAs (unlike DNA) possess complex secondary and tertiary structures, which may not be fully denatured at lower temperatures. A final point of differentiation between FSS-reactions depends on the choice of priming. As in DNA polymerases, reverse transcriptase also requires a short nucleotide sequence complementary to the origins (primer). Commonly two varieties of primers are used during FSS: Olido(dT)-primers, which anneal selectively to poly(A)-tails of mRNAs, and random polymer (often hexa-, octa- or nonamers) primers, which bind to any complementary sequence of the RNA, thereby not only being limited to mRNAs. The enzyme used in this thesis, SuperScript® II Reverse Transcriptase (Invitrogen), is an in vitro mutation of MMLV and possesses reduced RNase H-activity, a temperature optimum of 42°C and was primed using oligo(dT)-primers.

General remarks: Prior to RNA extraction all surfaces and gloves were treated with chaotropic agents (RNaseZap, Sigma) to avoid RNase contamination. Metal tools (scissors, tweezers and scalpels) were incubated for 60’ in 70% ethanol. RNA extraction were performed using appropriate kits from Qiagen (RNeasy Mini Kit for cells and tissues; RNeasy

Protect Animal Blood Kit for blood samples), wherefore buffer compositions cannot be described. Buffer names are those given by Qiagen.

A.3.2 RNA extraction protocols

A.3.2.1 RNA extraction from animal tissues: After animals were sacrificed through cervical dislocation livers and brains were excised. Brains were cut between mesencephalon and diencephalon resulting in two samples: Brain stem and forebrain. Samples were rapidly placed into a stabilizing agent (*RNA later*, Qiagen), quick frozen in liquid nitrogen and stored at -80°C. On the day of extraction tissues were thawed and the *RNA later* was removed by pipetting, where after tissues were incubated for 30' at room temperature with 600 µl buffer RLT + 6 µl β-mercaptoethanol (β-ME) in order to lyse the tissue and reduce protein disulfide bonds. The tissue was homogenizes in a two-step process. The first step was manual homogenization through a needle and syringe method, using 19 *G* needles for the livers and 21 *G* needles for the brain samples. For the second step 300 µl of the pre-homogenate were respectively mixed with 600 µl buffer RLT + 6 µl β-ME and centrifuged in a QIAshredder homogenization column at max. speed for 2'. The lysate was centrifuged for 3' at max. speed, where after the supernatant was removed carefully through pipetting and 600 µl ethanol (in RNase-free water) were added and mixed. 700 µl of the sample were pipetted onto an RNeasy spin column and centrifuged for 15'' at >8000 *g*. The flow-through was discarded and the remainder of the sample was pipetted onto the column and centrifuged for 15'' at >8000 *g*. 700 µl buffer RW 1 were added to wash the column and centrifuged for 15'' at >8000 *g*. The flow-through and collection tube were discarded and the column was transferred into a new collection tube. 500 µl buffer RPE were pipetted onto the column to wash it, followed by 15'' centrifugation at >8000 *g*. The flow through was discarded and another 500 µl of buffer RPE were added, where after the column was centrifuged for 2' at >8000 *g* with open lid to dry the silica membrane. The RNA was eluted using 50 ml RNase-free water in the first and 30 ml RNase-free water in the second centrifugation step (each 1' at >8000 G). RNA was stored at -80°C.

A.3.2.2 RNA extraction from animal whole blood: Blood was collected from the animals after cervical dislocation by introducing a syringe into the aorta. 100 µl of blood were pipetted into 300 µl RNA Protect Animal Blood Reagent (Qiagen), inverted 10 times and incubated for 2 hrs at room temperature prior to quick freezing in liquid nitrogen. On the

day of the extraction samples were thawed and samples from the same animal were pooled into 1.5 ml RNase-free reaction tubes. Tubes were centrifuged at 5000 *g* for 3', the supernatant was decanted and 1 ml RNase-free water was added. The tubes were vortexed until the pellet was clearly dissolved and centrifuged at 5000 *g* for another 3'. The supernatant was removed by decanting and 240 µl buffer RSB were added and the tube was again vortexed until the pellet had dissolved. The sample was pipetted into a new tube along with 200 µl buffer RBT and 20 µl proteinase K, vortexed shortly and incubated on a thermo-shaker (set at 600 rpm) at 55°C for 10' to allow for proteinase digestion. The sample was then pipetted onto a QIAshredder spin column and centrifuged for 3' at 19.999 *g*. The supernatant of the flow-through was mixed with 240 µl ethanol (absolute) in a new tube, mixed by vortexing and then pipetted onto an RNeasy MinElute spin column and centrifuged for 1' at >8000g. The flow-through was discarded and the column was washed with 350 µl buffer RW1 by centrifugation at >8000 *g* for 15''. For on column DNase digestion 80 µl of DNase I incubation mix (prepared freshly from 10 µl DNase I stock solution and 70 µl buffer RDD) was pipetted onto the silica membrane and incubated at room temperature for 15'. Hereafter the column was washed again with 350 µl buffer RW1 by centrifugation for 15'' at > 8000 *g*. Membrane bound RNA was washed from residual guanidinium-isothiocyanate salts using 500 µl buffer RPE (which had previously been diluted in ethanol as described by the provider) by centrifugation for 15'' at > 8000 *g*, followed by adding 500 µl ethanol (80% in RNase-free water) onto the membrane and centrifugation for 2' at >8000 *g*. The silica membrane was dried by placing the column into a new collection tube and centrifugation for 2' at 19.900g with open lids. RNA was eluted with 30 µl of elution buffer REB for 1' at >8000 *g*.

A.3.3 RNA denaturation, quantification and quality control

All RNA eluates were denatured through incubation for 5' at 65°C. RNA was quantified using a spectrophotometer (BioRad Smart Spec™ 3000). RNA was diluted in RNase-free water (1:50 for tissue RNA; 1:25 for whole blood RNA), which was also used for blanking the spectrophotometer. An appropriate volume of the RNA eluate (containing 1 mg of RNA) was mixed with 0.5 µl RNA loading dye (see appendix B) and run through a denaturing agarose-MOPS/FA-gel electrophoresis. Here for 1 g agarose was dissolved in 100 ml RNase-free MOPS-buffer (20 mM 3-(N-morpholino)propanesulfonic acid (MOPS), 5 mM

sodium acetate, 1 mM ethylenediaminetetraacetic acid (EDTA), pH 7.0) and boiled briefly twice in a microwave at max. power. 1 µl ethidium bromide (EtBr) was added and the gel was allowed to polymerize in an RNase-free tray with an RNase-free 15-well spacer. The gel was run for 30-45' at 80 V in an RNase-free electrophoresis chamber containing 1x RNase-free FA/MOPS gel running buffer (2.5 M formaldehyde (FA), 20mM MOPS, 5 mM sodium acetate, 1 mM EDTA, pH 7.0). Gels were analyzed in a BioRad Gel Doc 2000 using the QuantityOne® (Version 4.3.0, BioRad) software. RNA-integrity was considered sufficient if both the 18S and 28S rRNA bands were clearly visible, the 28S rRNA band was roughly twice as strong as the 18S rRNA band and there was little smearing between the bands from other RNAs.

A.3.3.1 DNase digestion: Since the RNeasy Protect Animal Blood System includes on column DNase digestion, post hoc DNase digestion was only carried out for RNA extracted from cells and tissue samples.

3 µg RNA were mixed by pipetting in an RNase-free reaction tube with 3 µl DNase I (Amp Grade, 1 U/µl, Qiagen), 3 µl 10x DNase incubation buffer (Qiagen) and an appropriate volume of RNase-free water to reach a reaction volume of 30 µl. The mixture was incubated at room temperature for 15' and the reaction was terminated by adding of 3 µl EDTA (25 mM) and heating to 65°C for 10'.

A.3.4 First Strand Synthesis (FSS) with SuperScript™ II reverse transcriptase

30 ml of the DNase digested sample were mixed by pipetting in an RNase-free reaction tube with 3 µl oligo$(dT)_{12\text{-}18}$-primers (oligo thymidine, 500 µg/ml; bind to poly(A) tails of mRNA) and 3 µl dNTPs (deoxyribonucleotide triphosphates, 10 mM of each) and incubated for 5' at 65°C. The reaction tubes were then chilled on crushed ice and 12 µl 5x first strand buffer, 6 µl DTT (dithiothreitol, Cleland's reagent, 01 M) and 3 µl RNaseOUT™ RNase-inhibitor (40 U/µl) were added and the reaction mix was incubated for 2' at 42°C. Subsequently 3 µl of the SuperScript™ II reaction mix (Invitrogen) were added and the first strand synthesis was run for 50' at 42°C. The reaction was terminated through heat inactivation of the enzyme at 70°C for 15'. The resulting single stranded cDNA was stored at -80°C.

A.3.5 Polymerase Chain Reaction (PCR)

PCRs were pipetted and run in DNase-free PCR-softstrips (0.2 ml, Biozym). Pipetting steps were all carried out either on crushed ice or PCR cool blocks. PCRs were run in an iCycler thermal cycler (BioRad).

PCR single reaction volume was 25 μl, consisting of 5.2 μl master mix, 1 μg (0.5 μg for samples taken from whole blood) cDNA (X μl) and an appropriate volume of AAI (19.8-X μl). For each primer pair a control samples was run containing just 5.2 μl master mix and 19.8 μl of AAI with the omission of cDNA.

The reaction master mix consisted (per sample) of 2.5 μl 10x PCR buffer (Taq Buffer advanced with Mg^{2+}, 5-Prime), 0.5 μl dNTPs (10 mM each, 5-Prime), 1 μl forward and reverse primers respectively (see above) and 0.2 μl Taq DNA-polymerase (5 U/ml, 5-Prime).

The PCR protocol began with a single denaturing step at 94°C for 1' 30''. Repetitive PCR cycles consisted of denaturing at 94°C for 30'', annealing at optimal temperature (see appendix B) for 30'' and elongation at 72°C for 2'. The protocol ended with a single extension step at 72°C for 7'. PCRs were run with optimal number of cycles regarding template and primer pair (see appendix B).

A.3.5.1 Agarose-Gel Electrophoresis: PCR amplification products were mixed with 2ml DNA loading dye (Blue/Orange 6x loading dye, Promega) and analyzed through agarose-gel electrophoresis. 1 g of agarose (2 g for cell culture experiments) was dissolved in 100 ml 1x TAE (tris acetate EDTA) buffer and boiled twice briefly in a microwave at maximum power, where after 1ml EtBr was added and the gel was allowed to polymerize in a gel tray with an appropriate spacer. The gel was run for 30-60' at 120 V in 1x TAE buffer. Each gel contained at least one lane filled with a 1kb DNA ladder (Promega).

Appendix B - Recipes and Primers

B.1 Recipes

Borate buffer, 50 mM

19.07 g sodium tetraborate (borax)

3,09 g boric acid

fill to 1 l with ultrapure water

adjust to pH 8.3 with boric acid

Citrate buffer

stock solution A (1mM citric acid monohydrate; 2.1010 g/100 ml ultrapure water)

stock solution B (50mM trisodium citrate dehydrate; 14.705 g/500 ml ultrapure water)

15 ml stock solution A

85 ml stock solution B

fill to 1l with ultrapure water

adjust pH to 6.0 and store at 4°C

Cresyl violet solution (0.1%)

dissolve 0.5 g cresyl violet in 500 ml acetic acid (1%)

DAB stock solution

dissolve 1 g DAB (Sigma, D5637) in 44.4 ml PB (0.1M, pH 7.4)

filter and store in aliquots (1 ml, 22.5 ml DAB) in the dark at -20°C

DNA ladder mix

40 µl DNA ladder (1kb DNA Ladder, Invitrogen)

20 µl Blue/Orange 6x Loading Dye (Invitrogen)

40 µl aqua ad iniectabilia (Braun)

store in 10 µl aliquots at -20°C

Formvar solution (for coating of grids)

rinse an Erlenmeyer flask with chloroform and add 1.2 g Formvar (Sigma F-6146)

slowly add 80 ml chloroform while stirring until Formvar is dissolved completely

fill to 100 ml with chloroform, seal and store in the dark

Glycine solution (1%)

dissolve 0.5 g glycin**e** (!) in 50 ml 1x PBS (pH 7.4)

prepare freshly

Hematoxylin nuclear counterstaining solution

dissolve 1 g Mayer's hemalaun in 1l ultrapure water

0.2 g sodium iodate

50 g potassium alum

50 g chloral hydrate

1 g citric acid

solution is ready to use

Hoechst 33258/33342 (Sigma) nuclear counterstaining stock solution

dissolve 50 mg bis-benzimide (Hoechst 33258 or 33342) in 100 ml ultrapure water

store at -20°C

Luxol fast blue solution (0.1%)

dissolve 1 g Luxol fast blue, MBS, in 1 l ethanol (96%)

add 5 ml acetic acid (10%)

Methyl cellulose solution (for ultracryo microtomy)

heat 196 ml ultrapure water to 90°C

add 4 g methyl cellulose and stir

chill on ice to 10°C

seal container and stir over night at 4°C

mature solution (without stirring) for 3 days at 4°C

centrifuge at 100 000 x *g* for 95'

Methyl cellulose/uranyl acetate solution (for ultracryo microtomy)

mix saturated, freshly filtered uranyl acetate solution with the methyl cellulose solution (ratio 1:10)

always prepare uranyl acetate and final solution freshly

10x MOPS (3-(N-morpholino)propanesulfonic acid) gel buffer

200mM MOPS (41.9 g/l)

50mM sodium acetate (6.8 g/l)

10mM EDTA (20 ml 0.5M EDTA/l, pH 8.0)

fill to 1 l with RNase-free H2O

pH titrated to 7.0 with NaOH (aq)

1x MOPS gel buffer

100 ml 10x MOPS gel buffer

900 ml RNase-free H2O

1x MOPS/FA running buffer

100 ml 10x MOPS gel buffer

20 ml formaldehyde (37%)

880 ml RNase-free H2O

Mowiol 4-88 mounting medium

add 20 g Mowiol 4-88 (Polysciences) to 80 ml 1x PBS, pH 7.4

stir over night

add 40 ml glycerol and stir over night

centrifuge at 15 000 x *g* for 1 hour

withdraw supernatant and store at 4°C or -20°C

NaOH solution (0.1%) for modified Kluver-Barrera differentiation

0.5 ml NaOH (50%)

fill to 250 ml with ultrapure water

always prepare freshly

Nickel/DAB solution

45 ml PB (0.1M, pH 7.4)

100 µl freshly prepared ammonium chloride solution (18 mg/100 µl PB)

900 µl 0.05M nickel sulphate solution

900 µl glucose solution (10%)

1 ml DAB stock solution

stir and filter

before use add 150 µl freshly prepared glucose oxidase solution (0.18 mg/150 µl PB)

n-propyl gallate solution (anti-fading agent)

add 2.5 g n-propyl gallate (Sigma) to 50 ml PBS, pH 7.4

stir for 1 hour

add 50 ml glycerol and stir over night

store at 4°C

1x PB (phosphate buffer), 0.2M

stock solution A (sodium dihydrogen phosphate, 27.6 g/l)

stock solution B (disodium hydrogen phosphate, 35.7 g/l)

mix 19.0 ml of solution A and 81.0 ml of solution B

store at 4°C

10x PBS (phosphate buffered saline)

87.6 g sodium chloride

22.8 g dipotassium hydrogen phosphate

6.8 g potassium dihydrogen phosphate

fill to 1 l with ultrapure water

1x PBS

dilute 10x PBS in ultrapure water, adjust pH to 7.4 with NaOH(aq)/NaCl(aq) and store at 4°C

1% PBSA (for ICH/IF)

2 g (BSA)

100 µl Tween 20

fill to 200 ml with 1x PBS (pH 7.4)

store at -20°C

1% PBSA (for IGL)

1 g BSA

fill to 100 ml with 1x PBS (pH 7.4)

store at -20°C

4% PFA (paraformaldehyde) in PBS

dissolve 12 g PFA in 100 ml ultrapure water (ca. 60°C) and clear with NaOH(aq)

add 6 g sucrose and 30 ml 10x PBS

fill to 250 ml with ultrapure water and adjust pH to 7.4 with NaOH(aq)/NaCl(aq)

fill to 300 ml with ultrapure water

store at -20°C

QDot incubation buffer

1 g bovine serum albumin (BSA)

50 µl Tween 20

fill to 100 ml with 50mM borate buffer (pH 8.3)

store at -20°C

RNA loading dye

16 µl saturated aqueous bromophenol blue

80 µl 0.5M EDTA, pH 8.0

720 µl formaldehyde (37%)

3084 µl 10x MOPS gel buffer

2 ml glycerol (100%)

fill to 10 ml with RNase-free H2O

Rüdeberg staining for semithin sections

0.1 g methylene blue

0.1 g thionin**e** (!)

1.78 g disodium hydrogen phosphate

fill to 70 ml ultrapure water and add 30 ml glycerol

pipette onto semithin section and stain on heating plate (70°C) for 1-10’

Sucrose solution, 2.3M (infiltration solution for ultracryo microtomy)

80 g sucrose

fill to 100 ml with 0.1M PB

stir over night until all sucrose is dissolved

Sudan Black B (0.1%)

1 g Sudan black B

add 100 ml ethanol (70%) and boil to dissolve Sudan black B

cool and filter

50x TAE (Tris-acetate-EDTA) buffer

242 g tris(hydroxymethyl)aminomethane (Tris, Merck)

57.1 ml glacial acetic acid

100 ml ethylenediaminetetraacetate (EDTA; 0.5M, pH 8.0; Fluka)

fill to 1l with ultrapure water and adjust pH to 8.0

1x TAE buffer

dilute stock solution 50:1 with ultrapure water

final concentrations: 40mM Tris, 20mM acetic acid, 1mM EDTA

store at 4°C

Trypsin solution (0.01%)

add 0.01 g trypsin to 100 ml 1x PBS (pH 7.4)

prepare freshly before use

Uranyl acetate solution (saturated, aqueous)

dissolve 4% uranyl acetate in ultrapure water

filter before use

always prepare freshly

B.2 Primers

Table B_1: Final selection of primer pairs and respective PCR conditions. Primers were chosen from a number of primers designed for each template and analysed regarding optimal temperature and number of cycles (q.v. section 2.5.4).

Template	Forward primer	Reverse primer	Annealing temperature	Number of cycles
28S (tissue samples)	CGAAATGCAAGCACGGAGAGT	CTGGGTCAGTGGAGAGTGTCTCA	61°C	35
28S (astrocytes)	AAAGCGGGTGGTAAACTCCA	GGTTTCACGCCCTCTTGAAC	62°C	43
CAT	ATGGTCTGGGACTTCTGGAGTCTTC	GTTTCCTCTCCTCCTCGTTCAACAC	65°C	35
COMT1t1	CATTCTGGCCCATAAATGCT	GGGGGTCAGAGTGAGTGTGT	62°C	35
COMT1t3	TTGGACCTGCCTCCTCTAAA	CTCATCAGGCTGAGTGGTCA	52°C	35
D-AspOx	CGTTGGAGCTGGCGTGATAGG	TCCAGCCACGGGAGGTAGGC	66°C	35
DAT	CATGCTGCTCACTCTGGGTA	GACAGAGGCTTCTTTGTGGC	62°C	35
DDC	ATCATGGAAAAGCTGGTTGC	TGTGCAAATTTCAAAGCGAG	54°C	43
DRD1	AGAGGGACTTCTCCTTTCGC	AATAATGGGGTTCAGGGAGG	62°C	35
DRD1 nested	AGAGGGACTTCTCCTTTCGCATCCT	AGGGAGGAATTCGCCCAGCCA	68°C	30
DRD2	GATGTGCACAGCAAGCATCT	ACACACCAAGAACAATGGCA	62°C	35
DRD2 nested	TGCACAGCAAGCATCTTGAACCTGT	ACACACCAAGAACAATGGCAAGCA	66°C	30
DRD3	TCCCTCAGCAGTCTTCCTGT	CGTGAGTCAAGAAGAAGGGC	52°C	35
DRD3 nested	CCCTCAGCAGTCTTCCTGTCTGC	GTCAAGAAGAAGGGCAGCCAAC	66°C	30
DRD4	TGTCGGACCCTACTCAGGGT	AACTACCACCGGCAGGACTC	68°C	30
DRD4 nested	CCCTACTCAGGGTCCCTTCTTCCC	ACCGGCAGGACTCTCATTGCCT	68°C	30
DRD5	ACCAAGACACGGTCTTCCAC	ATTTCCTCAAGGCCCTTTGT	52°C	35
DRD5 nested	CCAAGACACGGTCTTCCACAGGG	GGCCCTTTGTTCTGCGAGTTCCC	66°C	30
GFAP	GAGGAGTGGTATCGGTCTAAGTTTG	GCCGCTCTAGGGACTCGTT	61°C	35
MAOA	ACCAGAGCTTCCACCTGAGA	TGAAAACTTCAGGACTGGGG	62°C	35

Table B_1 (continued)

MAOB	GAGCAACAAAAGCGATGTGA	AACTGAACCCAAAGGCACAC	61°C	35
Nrf2	CCACTGGTTTAGCCATCTCTCC	GTGGACATTAGCCCTTCCAAAC	66°C	35
PEX14	CACTGGCCTCTGTCCAAGAGCTA	CTGACAGGGGAGATGTCACTGCT	56°C	36
SerRac1	TCAAATAGCAGGGCGCAATCT	GGTAAGGAGCTGGCCGTTCA	56°C	35
SerRac2	CCTGCAGTGATAGCTGGACA	AAGCCAATGCTGGATTTGAC	56°C	35
SOD2	ATGCAGCTGCACCACAGCAA	ACTTCAGTGCAGGCTGAAGAG	62°C	35
TH	CCACGGTGTACTGGTTCACT	GGCATAGTTCCTGAGCTTGT	62°C	43

Ich erkläre: Ich habe die vorgelegte Dissertation selbständig und ohne unerlaubte fremde Hilfe und nur mit den Hilfen angefertigt, die ich in der Dissertation angegeben habe. Alle Textstellen, die wörtlich oder sinngemäß aus veröffentlichten Schriften entnommen sind, und alle Angaben, die auf mündlichen Auskünften beruhen, sind als solche kenntlich gemacht. Bei den von mir durchgeführten und in der Dissertation erwähnten Untersuchungen habe ich die Grundsätze guter wissenschaftlicher Praxis, wie sie in der „Satzung der Justus-Liebig-Universität Gießen zur Sicherung guter wissenschaftlicher Praxis“ niedergelegt sind, eingehalten.

Gießen, den 13.8.2011 _____

(Phillip Grant, Dipl. Psych.)